foods

Special Issue Reprint

Advanced Research in Inactivation Technologies of Foodborne Microorganisms

Edited by
Sara Spilimbergo

mdpi.com/journal/foods

MDPI

Advanced Research in Inactivation Technologies of Foodborne Microorganisms

Advanced Research in Inactivation Technologies of Foodborne Microorganisms

Guest Editor

Sara Spilimbergo

MDPI

Basel • Beijing • Wuhan • Barcelona • Belgrade • Novi Sad • Cluj • Manchester

Guest Editor
Sara Spilimbergo
Department of Industrial
Engineering
University of Padova
Padova
Italy

Editorial Office
MDPI AG
Grosspeteranlage 5
4052 Basel, Switzerland

This is a reprint of the Special Issue, published open access by the journal *Foods* (ISSN 2304-8158), freely accessible at: https://www.mdpi.com/journal/foods/special_issues/Inactivation_Foodborne_Microorganisms.

For citation purposes, cite each article independently as indicated on the article page online and as indicated below:

Lastname, A.A.; Lastname, B.B. Article Title. *Journal Name* **Year**, *Volume Number*, Page Range.

ISBN 978-3-7258-4343-5 (Hbk)
ISBN 978-3-7258-4344-2 (PDF)
https://doi.org/10.3390/books978-3-7258-4344-2

Contents

About the Editor

Sara Spilimbergo

Sara Spilimbergo is an Ordinary Professor in the Department of Industrial Engineering at the University of Padova, Italy. Her main research interests comprise innovative technologies at low temperature for the treatment of food and biomedical matrices, in particular by the use of supercritical carbon dioxide for food pasteurization and drying. She served as a coordinator and project leader of different national and international research projects, some of which were in collaboration with food and pharmaceutical industries. She is the author or co-author of more than 130 peer-reviewed papers, book chapters, conference proceedings. She owns three patents.

foods

MDPI

Article

Sequential Pulsed Light and Ultrasound Treatments for the Inactivation of *Saccharomyces cerevisiae* and PPO and the Retention of Bioactive Compounds in Sweet Lime Juice

Lubna Shaik [1,2] and Snehasis Chakraborty [1,*]

[1] Department of Food Engineering and Technology, Institute of Chemical Technology, Matunga, Mumbai 400019, India; lubna.shaik@dypiu.ac.in
[2] School of Biosciences and Bioengineering, D Y Patil International University, Akurdi, Pune 411044, India
* Correspondence: sc.chakraborty@ictmumbai.edu.in

Abstract: Designing a pasteurization con dition for sweet lime juice while ensuring microbial safety, enzymatic stability, and high nutritional quality is crucial for satisfying stakeholder demands. The present research investigates the effects of matrix pH, ultrasound treatments, and sequential pulsed light on the microbial population, enzyme activity, and bioactive chemicals in sweet lime juice. The sequential pulsed light (PL: 0.6–0.84 J/cm^2) and ultrasound (US: 0.2–0.4 W/cm^3) treatments for sweet lime juice were optimized using response surface methodology (RSM). A three-factor full factorial design was used for this purpose. The independent variables encompassed pH (X_1), PL effective fluence (X_2, J/cm^2), and US intensity (X_3, W/cm^3). The responses assessed included the inactivation of *Saccharomyces cerevisiae* (Y_1, log cfu/mL) and polyphenol oxidase (PPO: Y_2 in %) and the retention of vitamin C (Y_3, %). The polynomial models were optimized using numerical optimization to attain the maximum desirability value (0.89). The optimized PL + US sample (0.8 J/cm^2 + 0.4 W/cm^3, respectively) at pH 3.5 resulted in a 5-log cycle reduction in *S. cerevisiae* count and a 90% inactivation in PPO activity and retained 95% of its vitamin C content. This optimized sample underwent further analysis, including phenolic profiling, assessment of microbial cell morphology, and examination of enzyme conformational changes. After sequential pulsed-light (0.8 J/cm^2) and ultrasound (0.4 W/cm^3) treatments, yeast cells showed unusual structural changes, indicating additional targets besides membranes. Following PL + US treatment, the PPO composition changed to 2.7 ± 0.1% α-helix, 33.9 ± 0.3% β-sheet, 1.4 ± 0.2% β-turn, and 62 ± 0.7% random coil. Impressively, the optimized PL + US sample maintained a sensory acceptance level similar to that of the untreated sample.

Keywords: flavor compounds; microbial structure; vitamin C; *Saccharomyces cerevisiae*; polyphenol oxidase

1. Introduction

Sweet lime (*Citrus limetta*), also called mosambi, is rich in antioxidants, phenolics, and vitamin C. The consumption of sweet lime juice is renowned for its potential to treat scurvy, diabetes, dehydration, and skin diseases [1]. It is preferred for its mild flavor and unique aroma. However, this juice is susceptible to both microbial and enzymatic spoilages, negatively affecting its quality and limiting its shelf life. Pectin methylesterase (PME) is the enzyme responsible for cloud loss in sweet lime juice. To ensure microbial safety in fruit juice, the U.S. Food and Drug Administration recommends a 5-log$_{10}$ cycle reduction in the pathogen population [2]. Furthermore, the extent of microbial inactivation in a matrix is regulated by its pH [3]. Depending on maturity, sweet lime juice has a pH range from 3.5 to 4.5, and total soluble solids (TSS) vary between 7 and 12 °Brix [4]. The batch thermal pasteurization condition for the sweet lime juice is reported for 10 min at

80 °C [5]. Unfortunately, this severe thermal treatment condition also degrades heat-sensitive vitamins and other components in the juice, thus reducing its freshness. To address these needs, researchers across the world have started exploring the application of nonthermal processing technologies, for example, ultrasonication, plasma, pulsed electric field (PEF), high-intensity pulsed light (HIPL), high-pressure processing (HPP), and membrane filtration (MF). Recent studies revealed that nonthermal processing technologies, such as pulsed light (PL) and ultrasound (US) treatments, can preserve bioactive components in fruit juice while attaining food safety.

Pulsed light (PL) represents a nonthermal technology featuring white light generated by an inert gas lamp, ideally xenon. This light spectrum typically spans from 200 to 1100 nm in wavelength [6]. It can inactivate bacteria and enzymes while retaining nutrients [7]. PL is an excellent alternative for surface disinfection. In addition, the restricted light penetration in opaque juices, such as sweet lime juice, restricts the trials of scaling them up [7]. Likewise, ultrasound (US) is another nonthermal technique utilizing sound waves above the audible 20 kHz range. The US is generated through the conversion of electrical pulses into sound energy by transducers with the required frequency and intensity. As these US waves traverse through a medium, they create compressions and rarefactions, leading to a substantial increase in energy and mass transmission rate. Ultrasound's cavitation impacts bacteria and enzymes in fruit juice [8]. Future research is required to develop automated, cost-effective, and energy-efficient commercial ultrasound systems while ensuring the maximum production of high-value and microbiologically safe juice. Microbiological safety, enzyme stability, and nutrient retention in PL or US-treated strawberry, orange, pear, and apple juices were already examined [9–11].

Several studies suggest that pH impacts microbial or enzyme inactivation during nonthermal treatments. There is not very much information available on thermal and nonthermal treatments of sweet lime juice. Pellicer et al. [12] explored the influence of matrix pH on the inactivation of PPO under pulsed light exposure. The authors concluded that the extent of PPO inactivation was faster at a low pH, and it has a significant impact on the unfolding of enzyme conformation. Namala et al. [13] examined the UV and thermal processing of sweet lime juice. Khandpur et al. [5] examined the degradation of nutrients in sweet lime juice after ultrasonication. Shaik and Chakraborty [14,15] explored how matrix pH affected the microbiological, enzyme, and qualitative features of PL- and US-treated sweet lime juice individually.

It is evidenced that various hurdle technologies work in synergy to inactivate microorganisms [16]. Ramírez-Corona et al. [17] conducted a study to determine the effect of US, UVC, and combined treatment targeting the inactivation of mold, yeast, and total aerobic mesophilic bacteria (TAMB) in samples of orange juice and mango nectar. It was concluded that the combined US + UVC treatment improved the log microbial reductions as compared to the samples that were individually treated with US or UVC. Sequential nonthermal processing inactivates bacteria and enzymes, but limits nutrition loss in the food. There is no research exploring how sequential nonthermal processing and matrix pH affect sweet lime juice-quality attributes. To explore it, a well-spaced experimental design and modeling are needed to optimize and statistically validate answers and understand how independent process characteristics (factors) affect them. Response surface methodology (RSM) is a common and reliable method for systematic experimental design and optimization. Using a simple quantitative optimization procedure, RSM helps us understand how factors affect responses and provides quick optimum outcomes [18]. This study examines how sequential pulsed light, ultrasound treatments, and matrix pH affect sweet lime juice's microbial population, enzyme activity, and bioactive compounds. The conditions were fine-tuned through a combination of RSM and numerical optimization techniques. The hypothesis is that combining two or more hurdles (such as PL and US along with a reduction in matrix pH) can produce microbially safe and enzymatically stable juice at lower intensities of either treatment. Moreover, the attributes of equivalent thermally pasteurized sweet lime juice were analyzed for comparison. Quantifying the influence of matrix pH on sequential

PL and US treatments' lethality can help the juice processing industry identify the optimum pH–optimal fruit harvesting conditions.

2. Materials and Methods

2.1. Materials and Chemicals

Fresh sweet limes (*Citrus limetta*) were purchased from Matunga in Mumbai, India. The sweet lime variety with a TSS of 11.7–12.2 °Brix was considered. The microorganism strains were provided by NCL in Pune, India. Media agars were purchased from HiMedia Labs in Mumbai, India. Furthermore, chemicals such as anhydrous sodium carbonate, gallic acid, methanol, and 2,2-diphenylpicrylhydrazyl were provided by HiMedia Labs and Research-Lab Fine Chem Companies in Mumbai, India. The enzyme tyrosinase (PPO) [T3824-25KU] was purchased from Sigma-Aldrich in Bangalore, India.

2.2. Extraction of Sweet Lime Juice

After being peeled, sweet limes were processed into juice using a centrifugal juicer (HR 1863/20 Philips, Chennai, India) at a speed of 5360× *g* and subsequently filtered through a 100-micron mesh. A detailed extraction flowsheet for sweet lime juice is presented in Figure 1. Citric acid and sodium bicarbonate solutions were employed to adjust the pH of the juice to 3.5, 4.0, and 4.5.

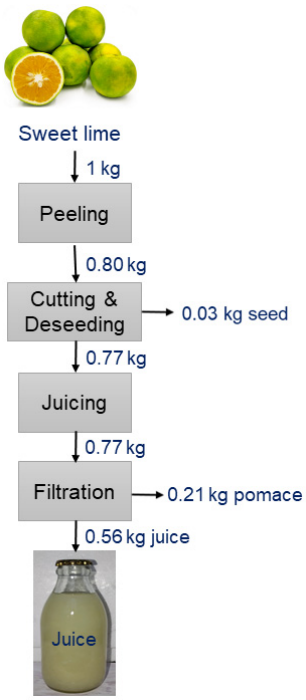

Figure 1. A detailed flowsheet for the extraction of sweet lime juice.

2.3. Experimental Design

The optimization of the sequential PL and US process was achieved through RSM. The experimental design utilized a three-factor–three-level (3^3) full factorial design, with the three independent variables being pH (X_1), PL effective fluence (X_2, J/cm^2), and US intensity (X_3, W/cm^3); the responses analyzed were inactivation of *Saccharomyces cerevisiae* (Y_1, log cfu/mL), inactivation of PPO (Y_2, %), and retention of vitamin C (Y_3, %). Shaik and Chakraborty [14] reported that *S. cerevisiae* was the most resistant microorganism, even more so than *Escherichia coli*, *Listeria monocytogenes*, and natural microbiota, such as aerobic mesophiles and yeasts and mold. The trend was also true for the ultrasound treatment of the juice [15]. Both studies confirmed that, among the spoilage enzymes, polyphenol oxidase (PPO) was the most resistant to PL and US intensity, and vitamin C was the most

sensitive bioactive component among other phytochemicals present in sweet lime juice. Therefore, regarding microbial safety, the survival count for *S. cerevisiae* was taken, and a >90% inactivation of PPO was desired to achieve the enzymatic stability of the juice. Moreover, ensuring a 5-log reduction in *S. cerevisiae* will also ensure a >5-log reduction in *E. coli*, *Listeria monocytogenes*, aerobic mesophiles, and yeasts and molds. The thermal pasteurization process, equivalent in efficacy, was conducted within a thermostatic water bath (AI-7981, I-therm, Mumbai, India) at a temperature of 95 °C for a duration of 5 min.

The independent variables (X_i) were transformed into dimensionless coded values (x_i) using Equation (1), where X_{max} and X_{min} denote the maximum and minimum values of X_i, respectively.

$$x_i = \frac{X_i - \frac{X_{max}+X_{min}}{2}}{X_{max} - \frac{X_{max}+X_{min}}{2}} \quad (1)$$

The boundary values of the experimental domain, which were determined through preliminary experiments and the referenced literature, were established. Specifically, the coded value domain ranged from −1 to +1 for pH (X_1), PL effective fluence (X_2), and US intensity (X_3), with respective ranges of 3.5–4.5, 0.6–0.84 J/cm^2, and 0.2–0.4 W/cm^3. For each independent variable, three equidistant levels (x_i = −1, 0, and 1) were considered, resulting in a total of 3^3 experimental runs (including factorial points) to explore the entire domain. Additionally, five experiments were replicated at the center point of the domain (coded as 0, 0, 0) to assess the lack of fit. In addition, separate PL (0.6, 0.72, and 0.84 J/cm^2 without any US treatment) and US treatments (0.2, 0.3, and 0.4 W/cm^3 without any PL treatment) were performed at all three matrix pH levels (3.5, 4.0, and 4.5).

2.4. Response Surface Methodology

A quadratic polynomial model (Equation (2)) was developed for each response, depicting its relationship with the independent variables in their coded forms.

$$Y_i = \beta_0 + \beta_1 x_1 + \beta_2 x_2 + \beta_3 x_3 + \beta_4 x_1 x_2 + \beta_5 x_1 x_3 + \beta_6 x_2 x_3 + \beta_7 {x_1}^2 + \beta_8 {x_2}^2 + \beta_9 {x_3}^2 \quad (2)$$

In this context, Y_i (where i = 1 or 3) represents the actual response value. The model's regression coefficients are denoted as follows: β_0 (constant term), β_1, β_2, and β_3 (coefficients for linear terms of x_1, x_2, and x_3, respectively); β_4, β_5, and β_6 (coefficients for interaction terms); and β_7, β_8, and β_9 (coefficients for quadratic terms). Here, x_1, x_2, and x_3 refer to the coded values of pH, PL fluence, and US intensity, respectively. The adequacy of the model fit was assessed using metrics such as the coefficient of determination (R^2), adjusted R^2, F-value, and p-value, along with evaluating the non-significant lack of fit (p_{lof}). Additionally, response surface analysis was employed to visually represent the combined or interactive effects between any two parameters among pH, PL effective fluence, and US intensity on the experimental responses.

2.5. Numerical Optimization

For optimizing the processing conditions, the log cycle reduction in *S. cerevisiae* count, inactivation of PPO, and vitamin C retention were maximized. A minimum 5-log cycle reduction in the *S. cerevisiae* population and 90% inactivation in PPO activity was set as a target during optimization. The desirability of individual responses was correlated with the process parameters according to Equation (3).

$$d_i = \frac{Y_i - L_i}{U_i - L_i} \quad (3)$$

In this context, d_i represents the desirability index for Y_i, where L_i and U_i are the lower and upper limits for Y_i, respectively. To consolidate these desirability values, an overall desirability index (D) was computed using Equation (4).

$$D = [\, {d_1}^{r_1} \times {d_2}^{r_2} \times {d_3}^{r_3}]^{\frac{1}{r_1+r_2+r_3}} \quad (4)$$

Additionally, r_1, r_2, and r_3 denote the relative importance (rated on a scale of 1 to 5) of Y_1, Y_2, and Y_3, respectively. A numerical optimization technique was employed to maximize the value of D, which falls within the range of 0 to 1 (with 1 being the most desirable) at any given combination of X_1, X_2, and X_3 within the defined domain. The process conditions yielding the maximum D-value were considered the optimized conditions. Subsequently, these optimized conditions were validated through actual experimental trials.

2.6. Processing of Sweet Lime Juice

2.6.1. Pulsed-Light Processing

Pulsed-light (PL) processing of sweet lime juice was conducted on a benchtop X-1100 System, according to Shaik and Chakraborty [14]. Throughout the PL treatment, a J-type thermocouple recorded the sample temperature (pencil type, length of 1 inch, diameter of 6.35 mm, Thermonic, Gujarat, India). The effective fluence of the PL treatment was maintained at 0.60, 0.72, and 0.84 J/cm^2 by performing experiments at 2.8 kV/160 s, 2.9 kV/180 s, and 2.4 kV/240 s, respectively. The spectral distribution of flash lamps was 21% ultraviolet, 36% visible light, and 43% infrared. The pulse frequency was 1 Hz, and the ON/OFF duration (pulse width) was 400 µs. To measure the amount of fluence received by the sample, a pyroelectric energy sensor (PE-50C Ophir Optronics Solutions Ltd., Jerusalem, Israel) at the equivalent elevation was placed below the lamp house. The dosimetry for PL treatment was calculated as per the method suggested by Gómez-López and Bolton [19] (Table 1). The effective fluence (F_e, J/cm^2) per pulse is the fluence rate times pulse width. The fluence rate values for 0.60, 0.72, and 0.84 J/cm^2 were 9.36 ± 0.05, 10.06 ± 0.02, and 8.74 ± 0.01 W/cm^2, respectively (Table 1). When the PL treatment was conducted at 0.80 J/cm^2, the condition was 2.7 kV/225 s with a fluence rate of 8.88 ± 0.02 W/cm^2. Further on in this manuscript, the PL treatment has been recognized by its respective effective fluence (F_e, J/cm^2) value.

Table 1. Dosimetry of the pulsed-light treatments employed for sweet lime juice.

Voltage (kV)	Average Fluence Rate [#] (W/cm^2)	Treatment Time [§] (s)	Number of Pulses *	Pulse Width (µs)	Effective Fluence * (F_e, J/cm^2) [¥]
2.8	9.36 ± 0.05	160	160	400	0.60
2.9	10.06 ± 0.02	180	180	400	0.72
2.4	8.74 ± 0.01	240	240	400	0.84
2.7	8.88 ± 0.02	225	225	400	0.80

* The pulse frequency was 1 Hz (1 pulse per second); the ON and OFF times were set at 400 µs. [#] Total fluence = average fluence per pulse × number of pulses. [§] Fluence rate = total fluence/treatment time. [¥] Effective fluence (F_e, J/cm^2) = fluence rate × pulse width × number of pulses.

2.6.2. Ultrasound Processing

A 250 W ultrasonic homogenizer (Model ATP-250, Probe sonicator, Athena Technologies, Mumbai, India) with a 9 mm probe was used for sonication. The interval between pulsed light and ultrasound treatments was one minute. Then, 50 mL juice samples were processed at 20 kHz. Extrinsic control parameters of US intensity at 0.2–0.4 W/cm^3 (150–190 W) were varied by 6 s ON/3 s OFF pulses. The ultrasonic probe was placed 20 mm from the beaker's bottom (4.8 cm beaker diameter and 3.4 cm height of the juice). The intensity for the US treatment was maintained at 0.2, 0.3, and 0.4 W/cm^3 by performing experiments at radiofrequency power outputs of 150, 170, and 190 W, respectively.

2.6.3. Selection of Sequence for Pulsed Light (PL) and Ultrasound (US) Treatments

For the selection of the sequence, the experiments were conducted at the four possible combinations of extreme levels of PL effective fluence and US power intensity (Table 2). Therefore, the experiments were PL (0.60 J/cm^2) + US (0.2 W/cm^3); PL (0.84 J/cm^2) + US (0.4 W/cm^3); US (0.2 W/cm^3) + PL (0.60 J/cm^2); and US (0.4 W/cm^3) + PL (0.84 J/cm^2) (Table 2). The pH of the juice was fixed at mid-pH 4.0. The same three responses, such as the survival count of *S. cerevisiae* (Y_1, log cfu/mL), inactivation of PPO (Y_2, %), and retention of vitamin C (Y_3, %) in the juice, were determined after the sequential treatment.

Table 2. Effect of PL and US treatment sequence on inactivation of *S. cerevisiae*, PPO, and vitamin C in sweet lime juice at pH 4.0.

Sequence	Treatment Conditions				*S. cerevisiae* Inactivation (log cfu/mL)	PPO Inactivation (%)	Vitamin C Retention (%)
PL + US	0.60	J/cm^2	0.2	W/cm^3	3.7 ± 0.1^{a}	36.3 ± 0.4^{a}	94.4 ± 0.5^{a}
	0.84		0.4		6.0 ± 0.2^{b}	97.2 ± 0.3^{b}	91.6 ± 0.5^{b}
US + PL	0.2	W/cm^3	0.60	J/cm^2	3.7 ± 0.3^{a}	36.5 ± 0.4^{a}	94.2 ± 0.5^{a}
	0.4		0.84		5.9 ± 0.2^{b}	97.0 ± 0.5^{b}	91.4 ± 0.6^{b}

PL, pulsed light; US, ultrasound; PPO, polyphenol oxidase. The values are presented as mean ± standard error. The different alphabets above each bar denote that the corresponding values differ significantly at a 95% confidence interval of the mean.

2.7. Characterization of Optimized Sequential PL- and US-Treated Sweet Lime Juice

Various quality attributes of optimally sequential PL- and US-treated and thermally pasteurized juice samples were analyzed as discussed below. The attributes include microbial enumeration, determination of enzyme activity, and estimation of acidity, soluble solids, viscosity, color profile, total phenolics, antioxidant activity, and vitamin C content in the juice, together with its sensory acceptance. After the sequential PL + US treatment, the samples were cooled to 2 °C and analyzed for various attributes within 3 h.

2.7.1. Microbial Enumeration

The maintenance of microbial stock cultures (*Escherichia coli* ATCC 43888, *Listeria monocytogenes* ATCC 13932, and *Saccharomyces cerevisiae* ATCC 9763), inoculum preparation, and inoculation in the juice were performed following the protocol described by Shaik and Chakraborty [14]. A total of 5 mL of the microbial cell suspension was inoculated in a 50 mL juice sample to attain the desired concentration of 7.0 ± 0.5 log cfu/mL. According to Guerrouj et al. [20], the detection of aerobic mesophiles (AM) and yeast and molds (YM) was carried out. In total, 10 cfu/mL of juice was chosen as the microbiological detection limit.

2.7.2. Enzyme Assay

Polyphenol oxidase (PPO) and peroxidase (POD) activity in sweet lime juice were determined following the method outlined by Shaik and Chakraborty [14]. Specifically, PPO activity was assessed at 420 nm, while POD activity was measured at 470 nm. Likewise, pectin methyl esterase (PME) was extracted, and its activity was quantified using 0.05% apple pectin as the substrate, following the procedure detailed by Sahoo and Chakraborty [21]. The protein concentration in the extract was determined using bovine serum albumin. PME activity, expressed as a single unit (U), represented the amount of crude extract required to produce one micromole of carboxylic group per minute per mL of the sample.

2.7.3. Measurement of Physicochemical Properties

The total soluble solids (TSS) and titratable acidity (TA) of the juice samples were analyzed using a handheld refractometer (Erma Inc., Tokyo, Japan) and standard titration methods, respectively, according to Shaik and Chakraborty [14]. A pH meter was used to measure the pH of sweet lime juice. The Brookfield viscometer (AMETEK Brookfield India Centre of Excellence, Mumbai, Maharashtra, India) was used to measure the viscosity of

the juice [22]. A sweet lime juice concentration of 100 mL was placed in a glass beaker, and the temperature was set at 25 °C. The torque was adjusted by selecting a specific spindle (RV-02) and its rotational speed of 60 rpm for a certain juice sample.

The color characteristics of the juice sample were analyzed using a Hunter-Lab colorimeter (LabScan-XE LX17375, Reston, VA, USA) in the CIE format, which represents the $L^*a^*b^*$ color space. The calculations of the total color change (ΔE^*) and browning index (BI) involved the application of the following formulas, as per Shaik and Chakraborty [15]: Equation (5) for ΔE^* and Equation (6) for BI.

$$\Delta E^* = \sqrt{(L_t^* - L_u^*)^2 + (a_t^* - a_u^*)^2 + (b_t^* - b_u^*)^2} \quad (5)$$

$$BI = \frac{31}{0.172}\left[\frac{a^* + 1.75\,L^*}{5.645L^* + a^* - 3.012\,b^*}\right] \quad (6)$$

In Equation (5), the 't' and 'u' suffixes represent the respective indices for treated and untreated juice.

2.7.4. Total Phenolic Content, Antioxidant Capacity, and Vitamin C

The assessments of vitamin C, total phenolic content (TPC), and antioxidant capacity (AOX) in the juice were carried out through spectrophotometric techniques, following the procedures detailed in the work of Shaik and Chakraborty [14]. Vitamin C content was expressed as grams of ascorbic acid (AA) per milliliter (mL) of juice, using L-AA as the reference compound. TPC was determined as grams of gallic acid equivalent (GAE) per mL of juice, with gallic acid serving as the reference compound. AOX, measured in grams of gallic acid equivalent antioxidant capacity (GAEAC) per mL of the sample, was quantified for each 1 mL of the sample. The percentage decrease in bioactive compounds in the treated sample was evaluated by comparing it to the untreated sample.

2.7.5. Sensory Analysis

Sensory evaluation was conducted on juices that demonstrated enzymatic stability and microbial safety. The assessment involved a partially trained panel comprising 25 members, including 16 males and 9 females, aged between 23 and 35 years old, affiliated with the Institute of Chemical Technology in Mumbai. This panel evaluated the juices based on six sensory attributes: aroma, taste, color, consistency, mouthfeel, and aftertaste. The semi-trained panelists, who were not professional sensory experts, underwent a comprehensive 10 h training program spread over two weeks. This training covered various attributes and scales until their evaluations were consistently aligned. Each panelist assigned a hedonic score (S) to the juices on a scale ranging from 1 (dislike extremely) to 9 (like extremely). Additionally, they indicated the importance (I) of each sensory attribute, using a scale from 1 to 5, representing 'not at all important', 'somewhat important', 'important', 'very important', and 'extremely important', respectively. To determine the overall acceptability (OA) of each juice sample, Equation (7) was utilized, where 'n_a' denotes the number of attributes, 'S' represents the hedonic score on the 1 to 9 scale, and 'I' indicates the corresponding importance score on the 1 to 5 scale.

$$OA = \frac{1}{n_a} \times \frac{\sum(S \times I)}{\sum I} \quad (7)$$

OA represents the weighted average of the product of hedonic scores and importance. It nullifies the person's individual bias to judge a sample based on a certain attribute. On the other hand, each sensory attribute cannot have the same importance during evaluation, as it varies from panelist to panelist. Therefore, OA combines all the scores for all six attributes and corresponding importance and provides a single value out of 9, making the comparison easier.

2.7.6. Phenolic Profile Using LC-DAD-ESI-MS/MS

The methodology developed by Rodriguez-Rivera et al. [23] was employed to extract phenolic compounds from sweet lime juice. After diluting the juice with an equal volume of 80% methanol (v/v), the resulting mixture was centrifuged at 7155× g for 5 min at a temperature of 6 °C. Prior to injection into the LC-MS/MS system (Agilent 1260 HPLC system; Agilent Technologies, Palo Alto, CA, USA), the extracts were filtered using a membrane filter with a pore size of 0.45 microns (manufactured by Whatman Inc., Clinton, NJ, USA). The HPLC equipment comprised a diode array detector, an autosampler (G1367 E, 1260 HIP ALS), a binary pump (G1312 B), a degasser (G1322), and another binary pump (G1312 B) (G1351D 1260 DAD VL). Phenomenex Luna reversed-phase C-18 column (4.6 mm 250 mm, 5 m) was employed (Torrance, CA, USA). Two solvents, solvent A, water/formic acid (99:1; v/v), and solvent B, acetonitrile/solvent A (60:40; v/v), made up the mobile phase. The procedure outlined by Kelebek et al. [24] was used to elute phenolic chemicals. In addition to exact reference compounds, the calibration of chemically similar substances was used for some instances while accounting for the molecular weight adjustment factor.

2.7.7. Morphology of *Saccharomyces cerevisiae*

To observe alterations in the morphology of *S. cerevisiae* cells following sequential treatment under optimized conditions, scanning electron microscopy (SEM) was employed. Initially, a culture of *S. cerevisiae* containing 7.1 $\log_{10}$ cfu/mL was mixed with 40 mL of citrate phosphate buffer at pH 4 and allowed to acclimate for 1 h. The control group consisted of untreated samples, while the treated *S. cerevisiae* cells in buffer at pH 4.0 were exposed to conditions including 0.80 J/cm^2 (PL treatment only), 0.4 W/cm^3 (US treatment only), and a combination of 0.80 J/cm^2 and 0.4 W/cm^3 (sequential PL + US treatment). Subsequent to the pulsed light treatment, the cells were recovered via centrifugation at 3913× g for 10 min at 20 °C. The retrieved cells were then subjected to fixation, dehydration, and freeze-fracturing following the protocol outlined by Kaláb et al. [25]. The fixation involved incubating the microbial cells with 2% glutaraldehyde for 18 h to serve as a fixative agent. Excess cells were rinsed with a 0.1 M sodium cacodylate solution for 5 min. Dehydration was carried out using a graded ethanol series (70%, 85%, and 100% (v/v)) to displace air spaces within the tissues. Lastly, liquid nitrogen was utilized for freeze-fracturing. The specimen was stored in a 50% (v/v) glycerol solution at 4 °C until SEM analysis was conducted. The imaging of freeze-fractured cells was performed using a low-vacuum scanning electron microscope (FEI™ Quanta 200, FEI Company, Hillsboro, OR, USA), with SEM images of both untreated and pulsed-light-treated *S. cerevisiae* cells acquired at 4000× and 2000× magnifications, respectively.

2.7.8. Circular Dichroism Analysis of PPO

The PPO sample for circular dichroism (CD) analysis was prepared by dissolving it in a pH 6.5 SSP buffer solution, resulting in a final protein concentration of 1.98 µmol/L. Circular dichroism spectra were obtained using a JASCO J-720 CD spectropolarimeter (Japan Spectroscopic Company, Tokyo, Japan) equipped with a 1 mm optical path length quartz cuvette at a room temperature of 25 ± 1 °C. CD spectra were scanned in the far UV range (250–200 nm) with four replicates, utilizing a scanning rate of 50 nm/min and a 1 nm bandwidth. The CD data were expressed in terms of the mean residue ellipticity, [θ], in deg cm^2 dmol^{-1}, as computed using Equation (8).

$$[\theta] = (0.1 \times \theta \times \mathrm{MRW})/(\mathrm{E} \times \mathrm{d}) \quad (8)$$

where d represents the path length in cm, E denotes the PPO concentration (mg/mL), and θ signifies the ellipticity (mdeg). MRW stands for the mean residue weight, calculated as the protein's mean weight (in atomic mass units or Da) divided by the number of residues in the protein. The molecular weight of PPO was considered as 119 kDa and the mean amino acid residue weight (MRW) for PPO was taken as 113.7 Da [26]. The secondary structure

components were analyzed using DichroWeb: online analysis for protein circular dichroism spectra website (https://dichroweb.cryst.bbk.ac.uk/home.shtml (accessed on 25 April 2023)). The fundamentals and algorithm for DichroWeb analysis have been detailed by Miles et al. [27]. The K2D method, when combined with DichroWeb, was utilized to process circular dichroism spectra as the input and generate an estimation of the secondary structure composition (namely alpha helix and beta strand) for the corresponding protein [28]. K2D, a neural network, functions by linking neurons from an input layer to an output layer. The output layer, representing secondary structure, is derived from the input layer's CD data through weighted connections to each neuron. During training, these weights are initially randomized. Both layers are supplied with extensive CD and structural data, similar to reference proteins. Through iterative adjustments, the weights are fine-tuned until an accurate secondary structure profile is achieved.

2.8. Statistical Analysis

Each run was conducted thrice, and each treatment was replicated three times, resulting in a total of nine data points for each treatment condition. Six data sets were collected for each PL + US condition for the microbial counts. The results are presented as mean values along with their respective standard deviations. To assess the significance of any changes in these mean values, a one-way analysis of variance (ANOVA) followed by Tukey's HSD test with a 95% confidence interval was employed. Microsoft Office Excel (Microsoft Corporation, Redmond, WA, USA, 2016) was utilized for the purposes of response surface methodology (RSM) and numerical optimization.

3. Results and Discussions

3.1. Selection of Sequence for Pulsed Light (PL) and Ultrasound (US) Treatments

It is clear from Table 2 that the influence of the sequence of PL and US intensities has no statistically significant effect ($p > 0.1$) on its microbial and enzymatic lethality. For instance, after PL (0.84 J/cm^2) + US (0.4 W/cm^3), the log reduction in the *S. cerevisiae* population was 6.0, whereas a 5.9 log cycle reduction was obtained after a US (0.4 W/cm^3) + PL (0.84 J/cm^2) treatment. Therefore, for the optimization, juice samples were treated at the desired fluence level of PL followed by a specific US intensity.

3.2. Effect of Sequential Pulsed Light (PL) and Ultrasonication (US) Treatments on S. cerevisiae, PPO, and Vitamin C

The intensity of sequential pulsed-light (PL) and ultrasonication (US) treatment had a significant influence on the inactivation of *S. cerevisiae* (Y_1, log cfu/mL) and PPO (Y_2, %). The initial population of *S. cerevisiae* in the juice was 7.1 log cfu/mL. The inactivation of *S. cerevisiae* ranged between 3.6 and 6.1 log cfu/mL when the sequential PL + US treatments were considered (Table 3). The PPO inactivation ranged between 36.1 and 100%. A microbially safe (>5 log cycle reduction in *S. cerevisiae* population) and enzymatically stable (>90% inactivation of PPO activity) juice was produced within the PL (0.60–0.84 J/cm^2) + US (0.2–0.4 W/cm^3) domain, where the vitamin C retention (Y_3, %) varied in the range of 92–100% (Table 3). Overall, a higher microbial and enzyme inactivation was obtained at a lower pH when the PL and US intensities were the same. As expected, more PL exposure or an intense US treatment resulted in higher lethality toward *S. cerevisiae* and PPO in the juice of the same pH. An increase in voltages during PL treatment yielded increased fluence rates, which in turn impacted the total fluence since it is the fluence rate times the treatment time. In terms of response, only the total effective fluence has been considered. In individual PL and US conditions, the *S. cerevisiae* population decreased by a maximum of 5.5 and 2.9 $\log_{10}$ cycles at 0.84 J/cm^2 and 0.4 W/cm^3, respectively, when the juice pH was 3.5. In the case of sequential treatments, the corresponding yeast inactivation of 6.1 $\log_{10}$ cycles was achieved when juice samples were treated at 0.60 J/cm^2 + 0.4 W/cm^3 (pH 3.5). The sample temperature was 15 °C before the PL + US treatment,

with a maximum temperature rise of 14.1 °C after the PL treatment and 11.1 °C after the US treatment, as summarized in Table 3.

Table 3. Sequential pulsed-light and ultrasound processing conditions and corresponding responses for the sweet lime juice.

Independent Parameters (Coded Value)			Maximum Temperature Rise (ΔT, °C)		Dependent Variables or Responses ($Y_{1–3}$)		
pH	PL Fluence (J/cm^2)	US Intensity (W/cm^3)	After PL (J/cm^2)	After US (W/cm^3)	Inactivation of *S. cerevisiae* (Y_1, log cfu/mL)	Inactivation of PPO (Y_2, %)	Retention in Vitamin C (Y_3, %)
3.5 (−1)	0.60 (−1)	0.2 (−1)	1.3 ± 0.1	1.0 ± 0.1	3.9 ± 0.3 ^{j}	36.8 ± 0.8 ^{ef}	96.2 ± 0.4 ^{e}
3.5 (−1)	0.60 (−1)	0.3 (0)	2.1 ± 0.2	1.6 ± 0.2	4.6 ± 0.2 ^{k}	43.9 ± 1.1 ^{g}	95.9 ± 0.6 ^{de}
3.5 (−1)	0.60 (−1)	0.4 (+1)	3.5 ± 0.1	2.7 ± 0.1	5.5 ± 0.2 ^{l}	50.7 ± 1.0 ^{h}	95.5 ± 1.0 ^{d}
3.5 (−1)	0.72 (0)	0.2 (−1)	5.6 ± 0.3	4.3 ± 0.1	4.5 ± 0.2 ^{k}	47.6 ± 0.9 ^{gh}	95.9 ± 0.6 ^{de}
3.5 (−1)	0.72 (0)	0.3 (0)	8.9 ± 0.1	6.6 ± 0.2	5.4 ± 0.1 ^{ll}	62.5 ± 1.5 ^{ij}	95.5 ± 0.8 ^{d}
3.5 (−1)	0.72 (0)	0.4 (+1)	10.6 ± 0.1	8.2 ± 0.1	6.0 ± 0.2 ^{m}	76.3 ± 1.3 ^{j}	95.5 ± 1.2 ^{d}
3.5 (−1)	0.84 (+1)	0.2 (−1)	11.4 ± 0.1	8.7 ± 0.2	5.2 ± 0.1 ^{kl}	79.9 ± 1.0 ^{jk}	95.5 ± 0.7 ^{d}
3.5 (−1)	0.84 (+1)	0.3 (0)	13.1 ± 0.1	10.2 ± 0.2	6.0 ± 0.2 ^{m}	97.7 ± 0.9 ^{kl}	95.5 ± 0.9 ^{d}
3.5 (−1)	0.84 (+1)	0.4 (+1)	14.1 ± 0.2	10.9 ± 0.2	6.1 ± 0.1 ^{n}	100.0 ± 0.3 ^{l}	95.1 ± 1.2 ^{d}
4 (0)	0.60 (−1)	0.2 (−1)	1.3 ± 0.1	1.0 ± 0.1	3.7 ± 0.1 ^{j}	36.3 ± 0.4 ^{ef}	94.4 ± 0.5 ^{cd}
4 (0)	0.60 (−1)	0.3 (0)	2.0 ± 0.2	1.6 ± 0.1	4.4 ± 0.1 ^{k}	43.6 ± 0.5 ^{g}	93.7 ± 0.7 ^{cd}
4 (0)	0.60 (−1)	0.4 (+1)	3.8 ± 0.1	2.9 ± 0.1	5.4 ± 0.2 ^{l}	50.5 ± 0.6 ^{h}	93.0 ± 0.8 ^{c}
4 (0)	0.72 (0)	0.2 (−1)	5.7 ± 0.2	4.3 ± 0.1	4.3 ± 0.2 ^{jk}	47.3 ± 0.5 ^{gh}	94.1 ± 0.9 ^{cd}
4 (0)	0.72 (0)	0.3 (0)	8.6 ± 0.1	6.6 ± 0.2	5.2 ± 0.1 ^{kl}	62.2 ± 0.4 ^{ij}	93.4 ± 1.0 ^{cd}
4 (0)	0.72 (0)	0.4 (+1)	10.5 ± 0.2	8.0 ± 0.1	6.0 ± 0.2 ^{m}	76.1 ± 0.5 ^{j}	92.3 ± 0.9 ^{c}
4 (0)	0.84 (+1)	0.2 (−1)	11.5 ± 0.1	8.8 ± 0.1	5.0 ± 0.1 ^{jk}	59.9 ± 0.4 ^{i}	93.7 ± 0.8 ^{cd}
4 (0)	0.84 (+1)	0.3 (0)	13.1 ± 0.1	10.1± 0.2	6.0 ± 0.2 ^{m}	79.6 ± 0.5 ^{jk}	93.0 ± 0.7 ^{c}
4 (0)	0.84 (+1)	0.4 (+1)	14.0 ± 0.2	10.8 ± 0.1	6.0 ± 0.2 ^{m}	97.2 ± 0.3 ^{kl}	91.6 ± 0.5 ^{ab}
4.5 (+1)	0.60 (−1)	0.2 (−1)	1.3 ± 0.4	1.0 ± 0.2	3.6 ± 0.1 ^{j}	36.1 ± 0.4 ^{f}	92.7 ± 0.6 ^{b}
4.5 (+1)	0.60 (−1)	0.3 (0)	2.0 ± 0.3	1.6 ± 0.3	4.3 ± 0.2 ^{k}	43.3 ± 0.5 ^{g}	91.2 ± 0.7 ^{ab}
4.5 (+1)	0.60 (−1)	0.4 (+1)	3.8 ± 0.2	2.9 ± 0.1	5.3 ± 0.2 ^{l}	50.2 ± 0.3 ^{h}	90.5 ± 0.5 ^{ab}
4.5 (+1)	0.72 (0)	0.2 (−1)	5.8 ± 0.2	4.4 ± 0.2	4.2 ± 0.1 ^{jk}	47.1 ± 0.4 ^{gh}	92.3 ± 0.5 ^{b}
4.5 (+1)	0.72 (0)	0.3 (0)	8.4 ± 0.4	6.5 ± 0.3	5.1 ± 0.1 ^{kl}	61.8 ± 0.3 ^{ij}	90.9 ± 0.6 ^{ab}
4.5 (+1)	0.72 (0)	0.4 (+1)	10.4 ± 0.2	8.0 ± 0.2	6.0 ± 0.2 ^{m}	75.9 ± 0.7 ^{j}	89.8 ± 0.5 ^{a}
4.5 (+1)	0.84 (+1)	0.2 (−1)	11.7 ± 0.1	8.7 ± 0.1	4.8 ± 0.2 ^{kl}	59.7 ± 0.4 ^{i}	92.0 ± 0.5 ^{b}
4.5 (+1)	0.84 (+1)	0.3 (0)	13.0 ± 0.2	10.3 ± 0.2	6.0 ± 0.1 ^{m}	79.3 ± 0.5 ^{jk}	90.2 ± 0.7 ^{ab}
4.5 (+1)	0.84 (+1)	0.4 (+1)	13.9 ± 0.2	11.0 ± 0.1	6.0 ± 0.2 ^{m}	95.5 ± 0.5 ^{k}	89.1 ± 0.4 ^{a}
3.5 (−1)	0.60 (−1)	0 (−3)	1.3 ± 0.1	NA	1.9 ± 0.3 ^{b}	26.3 ± 0.3 ^{de}	95.1 ± 0.5 ^{d}
4 (0)	0.60 (−1)	0 (−3)	1.3 ± 0.1	NA	1.6 ± 0.2 ^{ab}	25.9 ± 0.4 ^{d}	94.0 ± 0.6 ^{cd}
4.5 (+1)	0.60 (−1)	0 (−3)	1.3 ± 0.4	NA	1.4 ± 0.2 ^{a}	25.8 ± 0.4 ^{d}	93.7 ± 0.7 ^{cd}
3.5 (−1)	0.72 (0)	0 (−3)	5.6 ± 0.3	NA	3.7 ± 0.2 ^{g}	34.0 ± 0.3 ^{e}	94.2 ± 0.6 ^{cd}
4 (0)	0.72 (0)	0 (−3)	5.7 ± 0.2	NA	3.4 ± 0.2 ^{f}	33.8 ± 0.2 ^{e}	93.6 ± 0.5 ^{c}
4.5 (+1)	0.72 (0)	0 (−3)	5.8 ± 0.2	NA	3.2 ± 0.3 ^{ef}	33.6 ± 0.2 ^{e}	93.1 ± 0.5 ^{c}
3.5 (−1)	0.84 (+1)	0 (−3)	11.4 ± 0.1	NA	5.5 ± 0.2 ^{i}	40.2 ± 0.3 ^{g}	93.9 ± 0.4 ^{cd}
4 (0)	0.84 (+1)	0 (−3)	11.5 ± 0.1	NA	5.3 ± 0.3 ^{hi}	38.6 ± 0.2 ^{f}	93.4 ± 0.5 ^{c}
4.5 (+1)	0.84 (+1)	0 (−3)	11.7 ± 0.1	NA	5.1 ± 0.1 ^{h}	42.6 ± 0.3 ^{g}	93.0 ± 0.5 ^{c}
3.5 (−1)	0 (−6)	0.2 (−1)	NA	1.0 ± 0.1	1.6 ± 0.3 ^{ab}	10.5 ± 0.3 ^{a}	95.5 ± 0.6 ^{d}
4 (0)	0 (−6)	0.2 (−1)	NA	1.0 ± 0.1	1.5 ± 0.3 ^{a}	10.4 ± 0.2 ^{a}	95.5 ± 0.5 ^{d}
4.5 (+1)	0 (−6)	0.2 (−1)	NA	1.1 ± 0.2	1.3 ± 0.2 ^{a}	10.3 ± 0.2 ^{a}	95.6 ± 0.3 ^{d}
3.5 (−1)	0 (−6)	0.3 (0)	NA	6.6 ± 0.2	2.4 ± 0.2 ^{d}	13.6 ± 0.2 ^{b}	96.7 ± 0.6 ^{de}
4 (0)	0 (−6)	0.3 (0)	NA	6.5 ± 0.2	1.8 ± 0.3 ^{b}	13.5 ± 0.1 ^{b}	96.4 ± 0.4 ^{e}
4.5 (+1)	0 (−6)	0.3 (0)	NA	6.7 ± 0.2	1.7 ± 0.2 ^{ab}	13.5 ± 0.2 ^{b}	95.6 ± 0.3 ^{d}
3.5 (−1)	0 (−6)	0.4 (+1)	NA	10.9 ± 0.2	2.9 ± 0.2 ^{e}	20.1 ± 0.2 ^{c}	97.8 ± 0.7 ^{f}
4 (0)	0 (−6)	0.4 (+1)	NA	10.8 ± 0.4	2.5 ± 0.2 ^{d}	21.3 ± 0.2 ^{c}	97.4 ± 0.4 ^{f}
4.5 (+1)	0 (−6)	0.4 (+1)	NA	11.1 ± 0.3	2.0 ± 0.1 ^{cd}	17.1 ± 0.1 ^{bc}	96.7 ± 0.3 ^{de}

PL, pulsed light; US, ultrasound; PPO, polyphenol oxidase; NA, not applicable. Coded values are dimensionless. The values are presented as mean ± standard error. The different alphabets above each bar denote that the corresponding values differ significantly at a 95% confidence interval of the mean. The temperature was measured at the surface of the juice after each individual treatment. The temperature of the juice before treatment was 15 °C.

3.2.1. Response Surface Models

Response surface methodology (RSM) is employed to establish a connection between independent and response variables with the aim of pinpointing an optimal condition. In

our experimental design matrix, the data were fitted to various polynomial models, and it was found that the quadratic polynomial (Equation (2)) provided the best fit, as evidenced by high R^2 (>0.9), adjusted R^2 values (>0.9), and an insignificant lack of fit ($p_{lof} > 0.1$). Consequently, a quadratic polynomial model was developed to illustrate the impact of pH and PL + US process parameters on the dependent variables. Table 4 presents a summary of the regression coefficients and other parameters used for model fitting across all responses. The R^2 values for the polynomial model, representing the inactivation of *S. cerevisiae* (Y_1), PPO inactivation (Y_2), and retention of vitamin C (Y_3), were 0.93, 0.97, and 0.97, respectively, with corresponding adjusted R^2 values of 0.91, 0.96, and 0.96. These values indicate a strong fit of the data to the model for each response. Additionally, the model *p*-values for all responses were significantly lower than 0.0001, accompanied by higher *F*-values (51.9, 133.6, and 122.4 for Y_1, Y_2, and Y_3, respectively). An insignificant lack of fit (*p*-value > 0.15) suggests that the variations in responses are primarily influenced by process variables rather than random noise. In conclusion, the generated equation demonstrates a robust fit and reliability, facilitating the understanding of the relative impact of process variables (linear terms) and various combined effects between variables (quadratic and interaction terms) during the juice processing.

Table 4. Coefficients of polynomial models and corresponding ANOVA data describing the effect of different matrix pH and process parameters on the responses in sweet lime juice during sequential PL and US treatments.

Model Terms	Responses		
	Inactivation of *S. cerevisiae* (Y_1, log cfu/mL)	**Inactivation of PPO (Y_2, %)**	**Retention in Vitamin C (Y_3, %)**
	Coefficient ± CI	**Coefficient ± CI**	**Coefficient ± CI**
Constant	5.07 ± 0.14	60.13 ± 1.48	93.36 ± 0.12
x_1	−0.11 ± 0.11 **	−2.47 ± 1.09	−2.27 ± 0.09
x_2	0.84 ± 0.10	18.13 ± 1.01	−0.57 ± 0.08
x_3	0.56 ± 0.11	13.11 ± 1.08	−0.67 ± 0.09
$x_1 \times x_2$	0.03 ± 0.04 **	−0.46 ± 0.36 **	−0.30 ± 0.03
$x_1 \times x_3$	0.03 ± 0.06 **	−0.51 ± 0.64 **	−0.54 ± 0.05
$x_3 \times x_2$	−0.06 ± 0.03	1.97 ± 0.33	−0.21 ± 0.02
$x_1 \times x_1$	0.03 ± 0.15 **	1.38 ± 1.53 **	0.04 ± 0.12 **
$x_2 \times x_2$	0.05 ± 0.02	1.71 ± 0.18	−0.01 ± 0.01 **
$x_3 \times x_3$	0.00 ± 0.01 **	1.15 ± 0.44	−0.17 ± 0.03
p_{lof}	0.155	0.251	0.347
p_{model}	<0.0001	<0.0001	<0.0001
F value	51.9	133.6	122.4
R^2	0.93	0.97	0.97
Adj R^2	0.91	0.96	0.96

PPO, polyphenol oxidase; lof: lack of fit; Adj: adjusted; CI, 95% confidence interval; x_1, x_2, and x_3 are the dimensionless coded forms of pH, pulsed light fluence, and ultrasound intensity, respectively. All terms are significant at $p < 0.05$, otherwise marked as **. ** $p > 0.10$.

Linear Terms

The linear terms (x_1, x_2, and x_3) within the quadratic model have demonstrated significance ($p < 0.05$), indicating their notable contribution to the observed variations in the three responses, as illustrated in Table 4. It is worth noting, however, that the linear term associated with pH did not exhibit significance ($p > 0.1$) in the context of *S. cerevisiae* inactivation. The effective fluence of PL exposure is found to have the largest effect on *S. cerevisiae* and PPO inactivation when the coefficients for these linear terms are examined. Moreso than PL effective fluence, ultrasound intensity affects vitamin C retention. With the exception of pH, PL effective fluence and US intensity both favorably influence *S. cerevisiae* and PPO inactivation. A positive influence in this case means that a higher response value results by an increase in the independent variable's magnitude. On the other hand,

S. cerevisiae inactivation, PPO, and vitamin C retention are adversely affected by the pH of the matrix. This suggests that increasing the juice's pH might decrease vitamin C retention and minimize the inactivation of *S. cerevisiae* and PPO. The three linear terms (x_1, x_2, and x_3) all have a negative effect on the retention of vitamin C. Gomez-Lopez et al. [7] found that UV-induced DNA damage causes PL-induced microbial inactivation, while sonic waves break cell membranes in US inactivation. Changing inactivation methods may increase their levels. PPO accelerates the oxidation of the polyphenols in the juice, contributing to the nutritional and sensorial quality [29]. Both the duration and intensity of the ultrasound treatment had significant effects on enzyme inactivation. Enzymes may lose function if US waves alter their secondary and tertiary structures. Sonochemical processes during US treatment generate free radicals that may accelerate ascorbic acid oxidation [30].

Square Terms

Several square terms present in the polynomial models contribute to providing insight into the overall relationship between process variables and responses. In the case of the inactivation of *S. cerevisiae*, only the square term of PL effective fluence (coefficient = 0.053) is significant (Table 4). For PPO inactivation, all three square terms contribute; moreover, the square term for PL fluence is 1.71. However, the coefficients for pH and US intensities are 1.32 and 1.15, respectively. The only square term significant for vitamin C retention is US intensity, with a coefficient of -0.17. When the variable increases up to a maximum, a negative square term indicates that the response value increases and then trends in the opposite direction. Conversely, a positive square term indicates that an increase in the variable will initially compromise the response value; however, after the behavior reaches the optima, the opposite behavior becomes dominant.

Interaction Terms

The interaction term (-0.06) between PL effective fluence (x_2) and US intensity (x_3) influencing the inactivation of *S. cerevisiae* is significant at $p < 0.1$. A negative interaction coefficient reflects that PL effective fluence and US intensity are acting antagonistically to a minimal extent (Table 4). There may be chances of US intensity protecting the inactivation of *S. cerevisiae*. The slight concave nature of the Y_1 contours between PL fluence and US intensity at different pH levels reflects the same in Figure 2. On the other hand, the PL effective fluence and US intensity behave synergistically (coefficient 1.97) for PPO inactivation (Figure 3). This means an increase in the PL effective fluence and US intensities leads to a higher PPO inactivation. For vitamin C retention, the interactions of pH-PL, pH-US, and PL-US showed an antagonistic (negative coefficients) trend toward the response. An increase in pH-PL, pH-US, and PL-US would lead to greater vitamin C loss (Figure 4). Ferrario et al. [31] observed that 60 s PL at 71.4 J/cm^2 followed by 30 min US reduced *S. cerevisiae* by 6.4 and 5.8 log cycles in commercial and natural apple juice, respectively. Combining US and PL with natural apple juice reduced *E. coli* survival by 5.4 logs. In another case, US (600 W, 20 kHz, 30 min, and beginning temperature: 44 °C) and PL (0.73 J/cm^2, 155 mL/min, and temperature build-up from 44 to 56 °C) reduced *S. cerevisiae* cells by 6.4 and 5.8 log cycles in commercial and natural apple juice, respectively [32]. This demonstrated heat-induced inactivation. Wang et al. [29] found US-UV at 10 min, 600 W inactivated mango juice PPO, POD, and PME. Enzyme inactivation is caused by structural changes to enzyme proteins, typically in the tertiary structure. Unfolding, aggregation, protein backbone cleavage, or the all-or-nothing approach to these processes may cause these changes [33]. Fonteles et al. [34] found that ultrasound and ozone synergistically improved cashew apple juice independent of order. Parameters such as oxygen, pressure, temperature, metal ions, and pH contribute to vitamin C degradation [35].

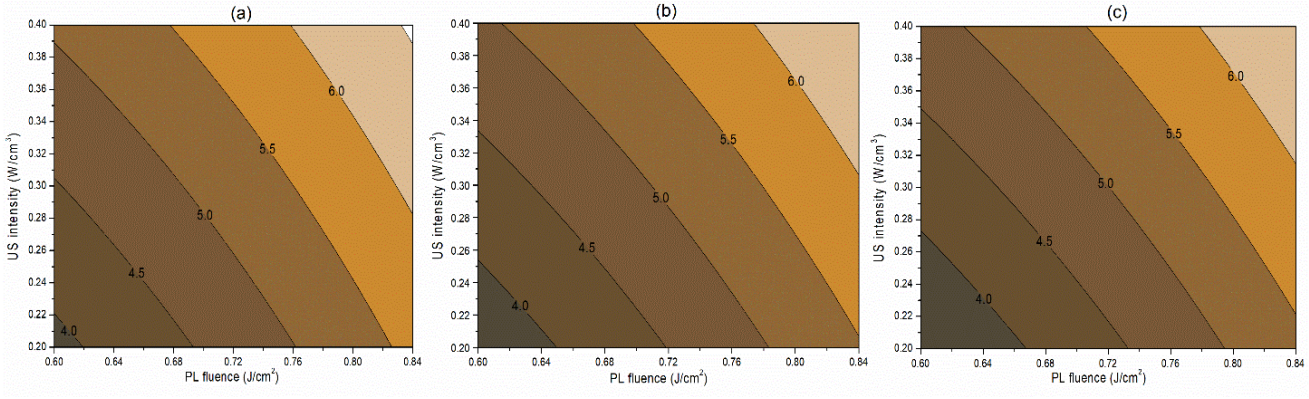

Figure 2. Contour plots showing the influence of pulsed light (PL) and ultrasound (US) conditions on the inactivation of *S. cerevisiae* (log cfu/mL) in the juice. (**a**) Matrix pH 3.5, (**b**) matrix pH 4.0, and (**c**) matrix pH 4.5.

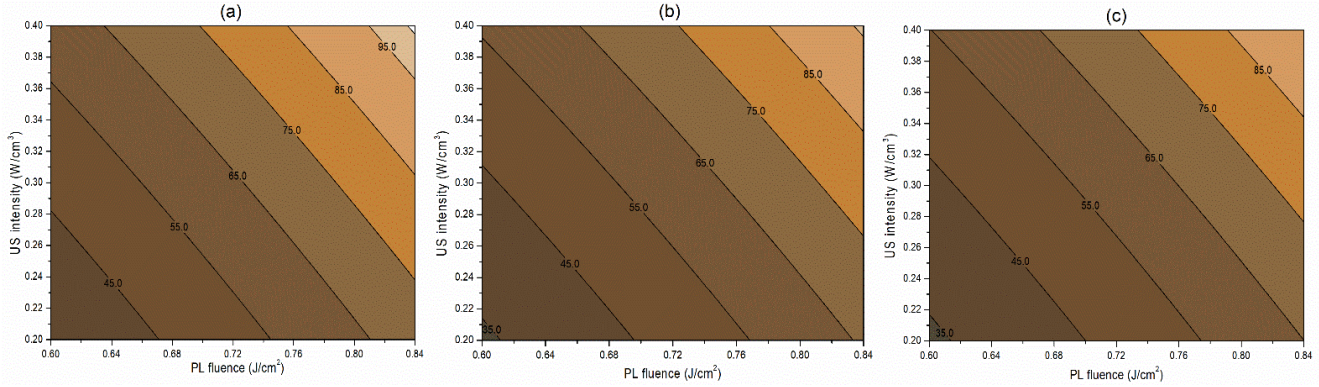

Figure 3. Contour plots showing the influence of pulsed light (PL) and ultrasound (US) conditions on the inactivation of PPO (%) in the juice. (**a**) Matrix pH 3.5, (**b**) matrix pH 4.0, and (**c**) matrix pH 4.5.

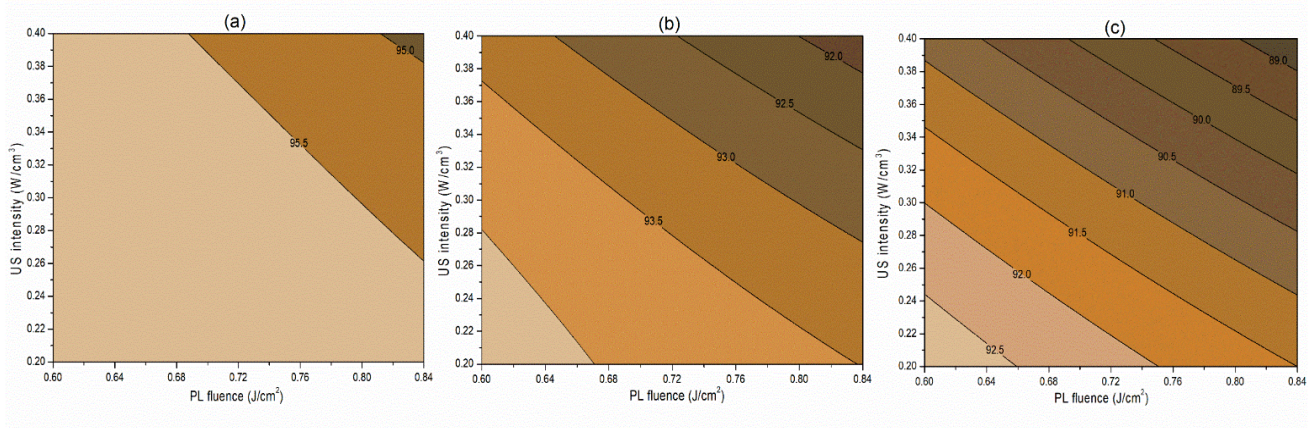

Figure 4. Contour plots showing the influence of pulsed-light and ultrasound conditions on the retention of vitamin C (%) in the juice. (**a**) Matrix pH 3.5, (**b**) matrix pH 4.0, and (**c**) matrix pH 4.5.

3.2.2. Numerical Optimization

In the pursuit of ensuring the safety, stability, and quality of the juice, our objective was to optimize the inactivation of *S. cerevisiae*, PPO, and vitamin C retention through numerical optimization. To prioritize these objectives, the relative importance (r_i) was assigned on a scale of 1 to 5, with 5 signifying the highest importance. Vitamin C retention and PPO inactivation received a significant priority rating of 4 out of 5, underscoring their importance. Meanwhile, *S. cerevisiae* inactivation was accorded the utmost significance,

with the highest relative importance (r_i) score of 5, reflecting our primary concern for microbial safety (Table 5). The numerical optimization suggested that sweet lime juice with pH 3.5 treated at PL effective fluence of 0.80 J/cm^2 followed by US intensity of 0.4 W/cm^3 would achieve 6.2 log cycles inactivation of *S. cerevisiae*, 90.1% PPO inactivation, and 95.0% retention of vitamin C, with an overall desirability of 0.89. The validation experiment was conducted at juice pH 3.5/0.80 J·cm^{-2}/0.4 W·cm^{-3}. The observed value of *S. cerevisiae* inactivation was 6.1 ± 0.2 log cfu/mL with a 90.5% inactivation of PPO and 95% retention of vitamin C (Table 6). The predicted and actual values are almost similar, thus validating the numerical optimization.

Table 5. The set of constraints for different parameters targeting high-quality sweet lime juice obtained through sequential pulsed-light and ultrasound processing.

Parameters	Goal	Lower Limit (L_i)	Upper Limit (U_i)	Importance (r_i)	Optimized Value at D = 0.89	Actual Value
pH (-)	In range	3.5	4.5	-	3.5	3.5
PL fluence (J/cm^2)	In range	0.60	0.84	-	0.80	0.80
US intensity (W/cm^3)	In range	0.2	0.4	-	0.4	0.4
Inactivation of *S. cerevisiae* (Y_1, log cfu/mL)	Maximize	1.3	6.2	5	6.2	6.1 ± 0.2
Inactivation of PPO (Y_2, %)	Maximize	10.3	100	4	90.1	90.5 ± 1.3
Retention in vitamin C (Y_3, %)	Maximize	89.1	97.8	4	95.2	95.0 ± 0.8

PPO, polyphenol oxidase; PL, pulsed light; US, ultrasound; D, overall desirability.

Table 6. Changes in biochemical attributes of microbially safe and enzymatically stable sweet lime juice (pH 3.5) during optimized PL and US treatment conditions.

Attributes	Sample Treated at Various Conditions				
	Untreated	PL (F_e = 0.8 J·cm^{-2}) + US (0.4 W·cm^{-3})	PL (F_e = 1.2 J·cm^{-2}) [14]	US (0.69 W·cm^{-3}) [15]	Thermal Treatment (95 °C/5 min)
	S1	S2	S3	S4	S5
Aerobic mesophilic count (log cfu/mL)	6.0 ± 0.2	<DL	<DL	<DL	<DL
Yeast and molds count (log cfu/mL)	6.3 ± 0.2	<DL	<DL	<DL	<DL
E. coli population (log cfu/mL)	7.0 ± 0.1	<DL	<DL	<DL	<DL
L. monocytogenes population (log cfu/mL)	7.0 ± 0.3	<DL	<DL	<DL	<DL
S. cerevisiae population (log cfu/mL)	7.1 ± 0.2	<DL	<DL	<DL	<DL
Inactivation of PPO (%)	0 ^{d}	90.5 ± 1.1 ^{b}	99.9 ± 0.2 ^{c}	60.0 ± 1.2 ^{a}	99.0 ± 0.3 ^{c}
Inactivation of POD (%)	0 ^{c}	95.3 ± 1.3 ^{a}	99.9 ± 0.1 ^{b}	95.5 ± 0.9 ^{a}	100 ± 0.1 ^{b}
Inactivation of PME (%)	0 ^{c}	97.6 ± 0.6 ^{a}	99.9 ± 0.1 ^{b}	99.8 ± 0.1 ^{b}	100 ± 0.1 ^{cd}
pH (-)	3.5 ± 0.1 ^{a}	3.5 ± 0.1 ^{a}	3.5 ± 0.2 ^{a}	3.51 ± 0.1 ^{a}	3.49 ± 0.2 ^{a}
TSS (°Brix)	11.7 ± 0.1 ^{a}	11.8 ± 0.2 ^{a}	11.7 ± 0.1 ^{a}	11.9 ± 0.3 ^{a}	11.78 ± 0.3 ^{a}
Titratable acidity (% citric acid)	2.1 ± 0.1 ^{a}	2.1 ± 0.2 ^{a}	2.1 ± 0.1 ^{a}	2.1 ± 0.1 ^{a}	2.1 ± 0.2 ^{a}
Viscosity (cp)	12.25 ± 0.3 ^{a}	12.05 ± 0.2 ^{a}	N.D.	N.D.	12.17 ± 0.3 ^{a}
Total phenolic content (g GAE/L)	26.4 ± 0.3 ^{c}	25.3 ± 0.2 ^{ab}	24.6 ± 0.2 ^{a}	30.8 ± 0.3 ^{d}	16.2 ± 0.3 ^{a}
Antioxidant capacity (g GAEAC/L)	22.7 ± 0.3 ^{c}	21.8 ± 0.3 ^{b}	20.8 ± 0.2 ^{a}	24.9 ± 0.3 ^{d}	13.1 ± 0.2 ^{a}
Ascorbic acid (g/L)	2.82 ± 0.2 ^{c}	2.68 ± 0.4 ^{b}	2.19 ± 0.2 ^{a}	3.24 ± 0.3 ^{d}	1.64 ± 0.3 ^{a}
Browning Index (*BI*)	63.8 ± 0.2 ^{a}	64.7 ± 0.3 ^{b}	67.1 ± 0.1 ^{c}	64.0 ± 0.1 ^{a}	72.6 ± 0.4 ^{d}
Total color change (ΔE^*)	-	1.7 ± 0.3 ^{a}	7.8 ± 0.4 ^{c}	2.6 ± 0.2 ^{b}	12.4 ± 0.4 ^{d}
Overall acceptability (out of 9)	8.1 ± 0.2 ^{c}	7.7 ± 0.2 ^{b}	7.2 ± 0.3 ^{a}	7.5 ± 0.2 ^{ab}	6.9 ± 0.2 ^{a}
Flavor (out of 9)	7.8 ± 0.1 ^{d}	7.5 ± 0.2 ^{c}	6.9 ± 0.1 ^{b}	7.1 ± 0.1 ^{bc}	6.3 ± 0.3 ^{a}
Mouthfeel (out of 9)	7.9 ± 0.2 ^{d}	7.4 ± 0.3 ^{c}	7.0 ± 0.2 ^{b}	7.3 ± 0.2 ^{c}	6.1 ± 0.2 ^{a}
Aroma (out of 9)	8.2 ± 0.1 ^{d}	7.5 ± 0.2 ^{bc}	7.1 ± 0.3 ^{b}	7.2 ± 0.2 ^{b}	6.4 ± 0.3 ^{a}

The alphabets in small letters (a, b, c, and d) in the superscripts denote that the mean values are statistically different across the columns at $p < 0.05$. Values are presented as mean ± standard error. PL, pulsed light; US, ultrasound; GAE, gallic acid equivalent; GAEAC, gallic acid equivalent antioxidant capacity; DL, detection limit of 1 log cfu/mL; N.D., not determined.

3.3. Quality Attributes of the Optimized PL + US Treated Sweet Lime Juice

The characteristics that define the quality of the chosen juice samples, including untreated juice (S1), optimally pulsed-light + ultrasound-treated juice (0.80 J/cm^{-2} + 0.4 W cm^{-3}) (S2), PL-treated juice (effective fluence of 1.2 J/cm^2) (S3) [14], US-treated juice (0.7 W/cm^3) (S4) [15], and thermally treated juice (95 °C/5 min) (S5) are summarized in Table 6.

3.3.1. Microbial Inactivation

Compared to the untreated juice (S1), the complete inactivation of aerobic mesophiles, yeasts and molds, *E. coli*, *L. monocytogenes,* and *S. cerevisiae* was achieved in the S2, S3, and S4 samples. After thermal pasteurization (95 °C/5 min), the juice (S5) was microbially safe, with no AM, YM, *E. coli*, *L. monocytogenes*, or *S. cerevisiae* detected (Table 6). Several authors have reported similar findings. For example, Alabdali et al. [36] discovered that a 50 °C, 3.5 L/min flow rate, 5.1 mW/cm^2 UV dosage, and 10 min US (200 W) reduced the microbial population to below detection limits. There is evidence of applying sequential nonthermal hurdles to achieve microbial inactivation in food matrices. For instance, Ferrario et al. [37] discovered that 60 s of PL at 71.4 J/cm^2, followed by 30 min of US, reduced *S. cerevisiae* by 6.4 and 5.8 log cycles, respectively, in commercial and natural apple juice. According to Gomez-Lopez et al. [7], UV-induced DNA damage (photochemical effect) is the primary cause of PL-induced microbial inactivation. In contrast, US inactivation is caused by sonic waves physically destroying cell membranes.

3.3.2. Enzyme Inactivation

The percentages of PPO inactivation were 90.5%, 99.9%, 60%, and 99% in S2, S3, S4, and S5, respectively. The values pertaining to the inactivation of peroxidase (POD) were 95.3%, 99.9%, 95.5%, and 100% in samples S2, S3, S4, and S5, respectively. Similarly, the percentages for PME inactivation were 97.6%, 99.9%, 99.8%, and 100% in S2, S3, S4, and S5, correspondingly (Table 6). Spoilage enzyme activity (PPO, POD, and PME) in the pasteurized juice was less than 0.5%, ensuring enzymatic stability. Similar pasteurization conditions have been recommended in prior studies for achieving microbial and enzymatic stability in fruit beverages. According to Iqbal et al. [38], structural changes to enzyme proteins, particularly in the tertiary conformation, cause enzyme inactivation. These alterations are probably a result of processes like unfolding, aggregation, cleavage of the protein backbone, or a sudden transition to complete unfolding and aggregation.

3.3.3. Physicochemical Attributes

There is no significant change in pH, TSS, and TA after S2, S3, S4, and S5, respectively. Regarding physicochemical properties, Ferrario et al. [9] discovered similar trends in apple juice. The sequential PL and US intensities were insufficient to cause the pH and TA to change significantly. PL + US energy levels and processing time were most likely insufficient to disrupt chemical bonds between dietary components. TSS may not have changed significantly after PL and US treatments [39].

3.3.4. Bioactive Compounds

The total phenolic content decreased by 4.1% and 6.8% in the S2 and S3 samples, respectively. In comparison, a 16.6% increase in phenolic content and a 9.6% increase in antioxidant capacity were reported in the S4 sample. The antioxidant capacity decreased by 3.9% and 8.35 in the S2 and S3 samples, respectively. The vitamin C content decreased by 4.9% and 22.3% in the S2 and S3 samples, respectively. In comparison, an increase of 14.8% was observed in the S4 sample. Thermal pasteurization did not significantly impact the TSS but resulted in a 38.6% reduction in total phenolic content, a 42.2% loss in antioxidant capacity, and a 42.3% degradation in vitamin C content in the sample (S5). In previous studies, ultraviolet light and ultrasound were reported to preserve the antioxidants in mango juice [30]. Another explanation for the antioxidant capacity of juice is PL exposure and cavitation-produced hydroxyl radicals, which may add a second hydroxyl group to a phenolic molecule's benzoic ring [40]. Fonteles et al. [34] discovered that applying ultrasound and ozone in any order had a synergistic effect on microbial inactivation of cashew apple juice. The degradation of vitamin C can be influenced by various factors, such as oxygen, elevated temperature, pressure, metal ions, and pH. Additionally, the UV-C wavelength emitted by PL induces photo-oxidation, thereby diminishing the quality of

juice treated with PL [35]. To conclude, sequential PL and US processing could be a better alternative, considering the safety, stability, and nutrient retention in sweet lime juice.

3.3.5. Color Profile and Bioactive Compounds

The untreated juice sample showed the color values of L^* = 65.02 ± 0.03, a^* = − 4.12 ± 0.05, and b^* = 10.93 ± 0.06, while the sequentially treated sample (S2) had color values of L^* = 63.61 ± 0.02, a^* = − 4.95 ± 0.03, and b^* = 10.64 ± 0.04. The browning index values were 63.8, 64.7, 67.1, 64.0, and 72.6 in S1, S2, S3, S4, and S5, respectively. The total color change values were 1.7, 7.8, 2.6, and 12.4 for S2, S3, S4, and S5, respectively. The thermally pasteurized juice showed a darker color (increased ΔE^* and reduced L^* value) and greater redness (increased a* value), possibly due to phenolic isomerization or decomposition. The alteration in color was clearly discernible, signifying the adverse influence of intense thermal processing on color integrity. Additionally, thermal pasteurization led to the loss of vitamin C and total phenolics in various citrus juices, as reported in previous studies. Compared to thermally pasteurized juice, PL-, US-, and PL + US-pasteurized juices retained more phenolics, antioxidants, and vitamin C, in line with earlier research [13,14]. The thermal pasteurization procedure could potentially trigger thermal degradation, acid-catalyzed degradation, and/or the Maillard reaction, resulting in a decline in the phytochemical content in the citrus juice. Caminiti et al. [41] discovered a 4.51 overall color shift in orange and carrot juice following PL and manothermosonication. The color of sweet lime juice may change due to ultrasound cavitation and photo-oxidation. These processes can result in physical, chemical, and biological phenomena like increased diffusivities, particle breakdown, and carotenoid conformational change, which results in colorless pigments [42].

3.3.6. Viscosity

The viscosity of fresh sweet lime juice was 12.25 ± 0.3 cP, which is low compared to other fruit beverages, such as mango juice, banana juice, papaya juice, sapota juice, etc. The viscosities of untreated, sequential PL + US, and thermally treated sweet lime juice are 12.25 ± 0.3, 12.05 ± 0.2, and 12.17 ± 0.3 cP, respectively. The viscosity of sweet lime juice did not change with respect to sequentially pulsed light + ultrasound and thermal treatments. Sweet lime juice's viscosity is almost near the viscosity of distilled water (~10.00 cP) [43].

3.3.7. Overall Sensory Acceptability

The sensorial overall acceptability values are 8.1, 7.7, 7.2, 7.5, and 6.9 out of 9 in S1, S2, S3, S4, and S5, respectively. To be more specific, the flavor, mouthfeel, and aroma of the optimized PL + US sample were more comparable to those of untreated sample. For instance, the flavor, mouthfeel, and aroma of the optimized PL + US sample were 7.5 ± 0.2, 7.4 ± 0.3, and 7.5 ± 0.2, while the corresponding values for the untreated sample were 7.8 ± 0.1, 7.9 ± 0.2, and 8.2 ± 0.1 respectively. In contrast, when compared to the traditional thermal pasteurization method, the citrus juice subjected to sequential PL + US treatment received a higher hedonic rating. The reduced overall acceptability of the thermally treated sample can be attributed to browning, which arises from the copolymerization of organic acids. Anjaly et al. [44] stated the combination of ultrasound treatment (33 kHz) for 22.95 min and ultraviolet dosage of 1.577 J/cm^2 was found to retain the organoleptic quality close to that of fresh pineapple juice.

3.4. Characterization of Optimized PL + US Treated Sweet Lime Juice

3.4.1. Phenolic Profiling of Sweet Lime Juice

HRLC-MS of the optimally treated juice identified 15 phenolic compounds (Table 7) in sweet lime juice by comparing mass spectrometry data with characteristic fragment ions. Phenolic compounds, such as 3beta, 6beta-dihydroxynortropane (RT: 1.107), dihydrocaffeic acid 3-O-glucuronide (RT: 1.341), naringenin (RT: 4.978), isocitrate (RT: 1.483), dalpanin (RT: 8.973), and kuwanon Z (RT: 4.701), were identified in both the untreated

and PL + US-treated samples (0.8 J/cm^2 + 0.4 W/cm^3). Vinyl caffeate (RT: 4.616) and 2-(2,5-dimethoxyphenyl)-5,6,7,8-tetramethoxy-4H-1-benzopyran-4-one (RT: 10.235) were the other compounds that were detected in only the treated sample. PL + US treatment degraded 1,2-dihydrostilbene (RT: 3.284), isomyristicin (RT: 4.641), biorobin (RT: 4.717), and 7b-hydroxy-3-oxo-5b-cholanoic acid (RT: 19.317). PL + US forms the following compounds: 3beta,6beta-dihydroxynortropane, a tropane alkaloid; dihydrocaffeic acid 3-O-glucuronide, a powerful antioxidant; naringenin, a flavonoid with strong anti-inflammatory and antioxidant properties; isocitrate, an isomer of citric acid; dalpanin, a flavonoid; kuwanon Z, a flavan; and vinyl caffeate, an antioxidant. 2-(2,5-dimethoxyphenyl)-5,6,7,8-tetramethoxy-4H-1-benzopyran-4-one is a methoxyflavone with methoxy groups at 5, 6, 7, 8, 3′, and 5′ [45]. The enhanced preservation of these phenolic components can be attributed to the transformation of insoluble, bound phenolic compounds into soluble, free phenolic compounds induced by pulsed light and ultrasound. Furthermore, this preservation results from the inactivation of PPO and the removal of obstructive oxygen from the sample during ultrasound treatment [30]. In the course of PL + US processes, the hydroxyl radical may hydroxylate the ortho-, meta-, and para-positions of phenolic aromatic rings, thereby altering the composition of the sample [39].

Table 7. Flavor compounds identified in the untreated and the optimized PL + US treated (0.8 J/cm^2 + 0.4 W/cm^3) sweet lime juice.

No.	Compound Identified	Untreated Juice (S1)	PL + US-Treated Juice (S2)	RT	Mass	Formula	Description
1	3beta,6beta-Dihydroxynortropane	Present	Present	1.107	143.0956	$C_7H_{13}NO_2$	Tropane alkaloid
2	Dihydrocaffeic acid 3-O-glucuronide	Present	Present	1.341	358.0912	$C_{15}H_{18}O_{10}$	Antioxidants
3	1,2-dihydrostilbene	Present	Absent	3.284	182.109	C_{14} H_{14}	Provides protection against chronic diseases
4	Isomyristicin	Present	Absent	4.641	192.0799	$C_{11}H_{12}O_3$	Has anti-cholinergic, antibacterial, and hepatoprotective effects
5	Biorobin	Present	Absent	4.717	594.1595	$C_{27}H_{30}O_{15}$	Flavones and flavonols
6	Naringenin	Present	Present	4.978	272.0696	$C_{15}H_{12}O_5$	Flavonoids and strong anti-inflammatory and antioxidant activities
7	Hesperetin	Present	Present	6.366	302.08	$C_{16}H_{14}O_6$	Antioxidant and anti-inflammatory properties
8	Ononin	Present	Present	6.438	430.1279	$C_{22}H_{22}O_9$	Isoflavone glycoside
9	Vinyl Cafeate	Absent	Present	4.616	206.0591	$C_{11}H_{10}O_4$	Antioxidant
10	2-(2,5-Dimethoxyphenyl)-5,6,7,8-tetramethoxy-4H-1-benzopyran-4-one	Absent	Present	10.235	402.133	$C_{21}H_{22}O_8$	A methoxy flavone that is flavone substituted by methoxy groups at positions 5, 6, 7, 8, 3′, and 5′
11	N-Hexadecanoylpyrrolidine	Absent	Present	18.837	309.3044	$C_{20}H_{39}NO$	Byproduct of the Maillard reaction
12	Isocitrate	Present	Present	1.483	192.027	$C_6H_8O_7$	Commonly used as a marker to detect the authenticity and quality of fruit products, most often in citrus juices
13	Dalpanin	Present	Present	8.973	534.1754	$C_{26}H_{30}O_{12}$	Flavonoid
14	7b-Hydroxy-3-oxo-5b-cholanoic acid	Present	Absent	19.317	390.2793	$C_{24}H_{38}O_4$	Bile acid
15	Kuwanon Z	Present	Present	4.701	594.1548	$C_{34}H_{26}O_{10}$	Flavans that feature a C5-isoprenoid substituent at the 3-position. This could make kuwanon-Z a potential biomarker for consuming these foods

PL, pulsed light; US, ultrasound; RT, retention time. PL + US-treated juice is optimally processed at a PL fluence of 0.8 J/cm^2, followed by a US intensity at 0.4 W/cm^3.

3.4.2. Influence of PL + US Treatment on the Morphology of *Saccharomyces cerevisiae*

Saccharomyces cerevisiae is the most resistant microorganism in the juice when compared to *E. coli* and *L. monocytogenes*. Therefore, the juice sample treated with sequential pulsed-light (0.60 J/cm^2 of effective fluence) and ultrasound (intensity of 0.4 W/cm^3) treatments (condition at which the inactivation of >5 log cfu/mL was achieved) was studied by SEM to explore possible structural damage in yeast cells. Figure 5 shows the morphology of untreated and PL + US-treated *Saccharomyces cerevisiae* ATCC 9763 cells in sweet lime juice. Regarding untreated *S. cerevisiae* cells (Figure 5A), they exhibited an ellipsoidal shape with intact membranes, organelles, and cell walls. Individual PL treatment (0.84 J/cm^2) (condition at which a >5-log cycle reduction was achieved) showed pores on the cell layers, while individual US treatment (0.4 W/cm^3) (highest US condition explored in this study)

ruptured the cell wall. PL + US (0.8 J/cm^2 + 0.4 W/cm^3) caused a fragmented lumen, punctured cell walls, and cytoplasmatic membrane discontinuities (Figure 5D). Cytoplasmic membrane shrinkage may have reduced semi-permeability, upsetting the osmotic equilibrium. Cell shape alterations, membrane distortion, and vacuolization may have resulted from irregular high-intensity pulses. Leaking cytoplasm triggers cell death [46]. Takeshita et al. [47] reported rounded cells, plasma membrane deformation, and vacuole expansion after PL exposure of *S. cerevisiae* IFO2347 cells in model medium (1.421 J/cm^2 and batch mode). In a PL-treated model solution (5 s, 4.95 J/cm^2, 12 mL, and batch mode), Krishnamurthy et al. [48] observed *S. aureus* ATCC 25,923 cell wall disintegration and cell content leaking. They also noticed plasmalemma breakdown and shrinkage. After sequential pulsed-light (0.8 J/cm^2) and ultrasound (0.4 W/cm^3) treatments, yeast cells showed unusual structural changes, indicating additional targets besides membranes.

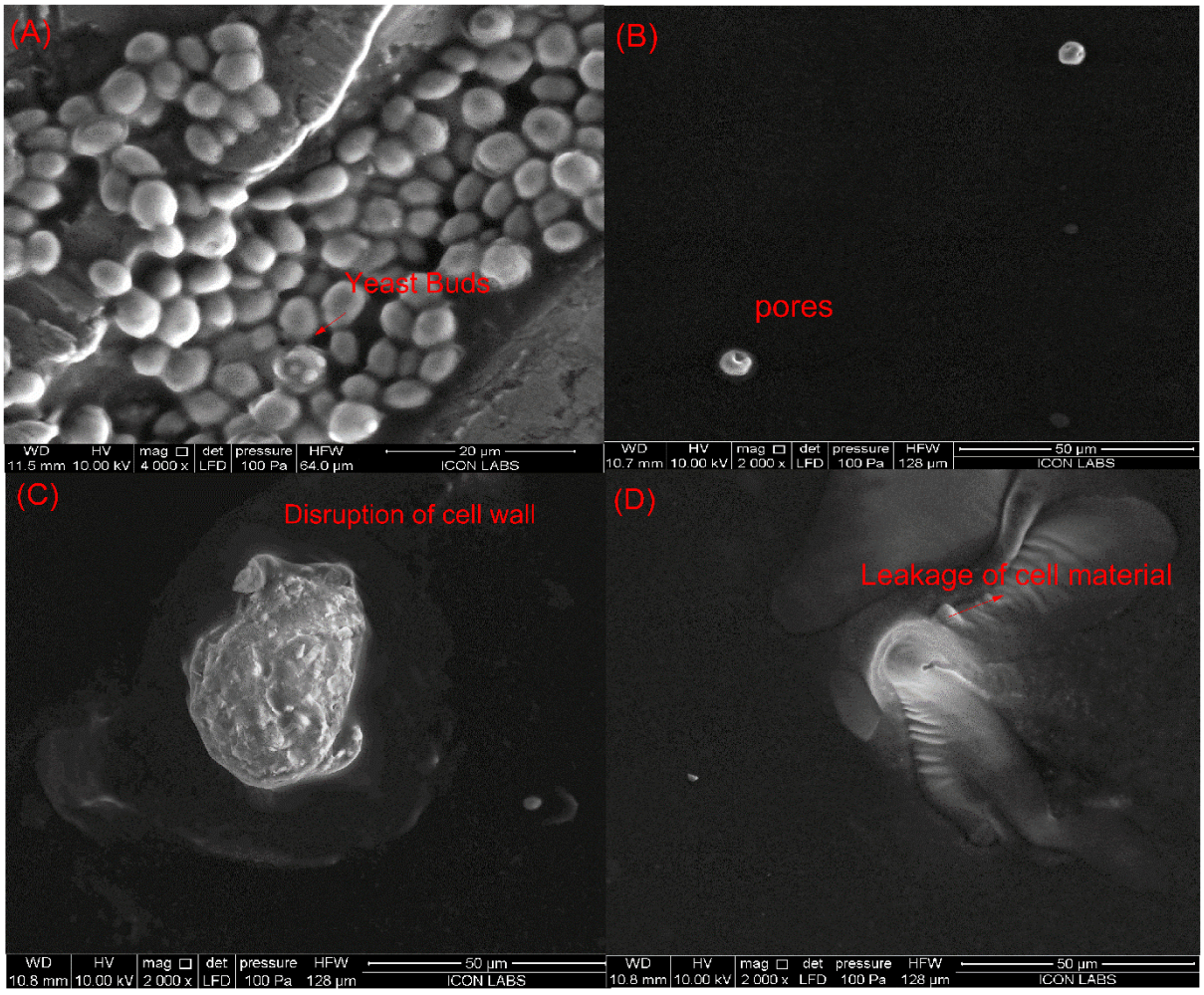

Figure 5. Influence of individual and sequential treatments on the morphology of the *Saccharomyces cerevisiae* (**A**) untreated sample; (**B**) pulsed light sample (0.84 J/cm^2); (**C**) ultrasound sample (0.4 W/cm^3); (**D**) PL + US (0.60 J/cm^2 + 0.4 W/cm^3).

3.4.3. Conformational Change in PPO after Sequential PL + US Treatment

Circular dichroism (CD) analysis revealed the secondary structure (α-helix, β-turn, β-sheet, and random coil) of both untreated and PL + US-treated PPO enzymes (Figure 6). PPO was the most resistant enzyme to the pulsed light domain among all PPO, POD, and PME in the juice. Therefore, as a target enzyme, it is crucial to explore the conformational change in the structure of PPO after sequential PL and US treatment, as well as its individual effect. Sequential pulsed light (0.80 J/cm^2) and ultrasound (0.4 W/cm^3) (condition at which

a >90% inactivation in the PPO enzyme was achieved) treatments altered the secondary structure. The α-helix structural characteristic absorption peaks at 208 and 222 nm in untreated PPO were negative [49]. Native PPO has a secondary constellation α-helix alignment. Liu et al. [50] found mushroom PPO activity centers had four α-helices crucial to enzyme activity. PL + US processing decreased α-helix content and increased disordered structure, increasing CD spectra negative ellipticity. After PL + US treatment, CD spectra showed an increase in PPO β-sheet concentration at 214 nm. Table 8 compares untreated and PL + US-treated PPO secondary structures. The untreated PPO sample consisted of a 7.7 ± 0.2% α-helix, 37.7 ± 0.4% β-sheet, 6.9 ± 0.2% β-turn, and 47.7 ± 0.5% random coil. Following PL + US treatment, the PPO composition changed to a 2.7 ± 0.1% α-helix, 33.9 ± 0.3% β-sheet, 1.4 ± 0.2% β-turn, and 62 ± 0.7% random coil. PPO's most critical structural constituent is the α-helix [29]. PL + US treatment inactivates the PPO enzyme, reducing helixes. PL + US increased the random coil ratio in the range of 47.7–62% in PPO. Zhou et al. [51] found a 38.3% α-helix, 12.7% β-sheet, 25.1% β-turn, and 23.9% random coil in a characteristic mushroom PPO. Yi et al. [52] found that the mushroom PPO's catalytic activity depended on α-helix concentration. These modifications are likely the result of unfolding, aggregation, protein backbone cleavage, or a sudden transition to complete unfolding and aggregation. Enzymes may lose their functionality if US waves alter their secondary and tertiary structures.

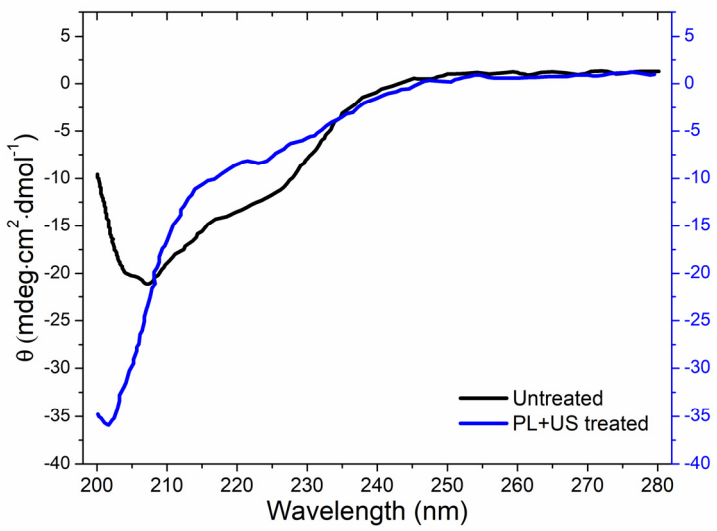

Figure 6. Effect of sequential PL + US (0.8 J/cm^2 + 0.4 W/cm^3) on the secondary structure of PPO.

Table 8. Secondary structure contents of untreated and sequential PL + US-treated (0.8 J/cm^2 + 0.4 W/cm^3) polyphenol oxidase enzyme.

Sample	α-Helix (%)	ß Sheet (%)	ß Turn (%)	Random Coil (%)
Untreated (S1)	7.7 ± 0.2	37.7 ± 0.4	6.9 ± 0.2	47.7 ± 0.5
PL + US (S2)	2.7 ± 0.1	33.9 ± 0.3	1.4 ± 0.2	62 ± 0.7

PL, pulsed light; US, ultrasound.

4. Conclusions

A sequential pulsed light (0.80 J/cm^2) and ultrasound (0.4 W/cm^3) treatment can reduce the *S. cerevisiae* population by 6.2 log cycles along with a 90% inactivation of PPO activity and 95% retention of vitamin C in sweet lime juice at pH 3.5. This satisfies the microbial safety aspect (>5-log reduction), enzymatic stability (90% inactivation in resistant enzyme), and nutrient retention (maximal retention of vitamin C) criteria for processing the juice. The total phenolic content and antioxidant activity reduced by 4.1 and 3.9% in the optimized PL + US treated sample, respectively. The viscosity of sweet lime juice did

not change with respect to sequentially PL + US and thermal treatments. The sensory acceptability of the optimally PL + US-treated juice (acceptability of 7.7 out of 9) was on par with the untreated one (acceptability of 8.1 out of 9). The optimal PL + US treatment led to fragmented lumens, punctured cell walls, and disruptions in the cytoplasmic membrane of *S. cerevisiae* cells. HRLC-MS confirms that 15 phenolic compounds are retained after PL + US treatment. Inactivation of PPO by PL + US treatment includes losses in α and β helixes and increased disordered structure. Shelf-life stability following PL + US juice processing needs to be explored.

Author Contributions: L.S.: methodology, formal analysis, investigation, validation, resources, writing—original draft preparation, reviewing, and editing; S.C.: conceptualization, supervision, writing—review and editing, and visualization. All authors have read and agreed to the published version of the manuscript.

Funding: This research received no external funding.

Institutional Review Board Statement: There was no coercion to participate in the sensory evaluation, there was a full disclosure of study requirements and risks, written or verbal consent of participants was provided, there was no release of participant data without their knowledge, and they had the ability to withdraw from the study at any time.

Data Availability Statement: The original contributions presented in the study are included in the article, further inquiries can be directed to the corresponding author.

Acknowledgments: Lubna Shaik wishes to express her gratitude to the All India Council for Technical Education (AICTE) for sponsoring her Ph.D. studies via the National Doctoral Fellowship (NDF) 2019–2020 program.

Conflicts of Interest: The authors declare no conflicts of interest.

References

1. Kehinde, B.A.; Nayik, G.A.; Rafiq, S. *Muntingia calabura. Antioxidants in Fruits: Properties and Health Benefits*; Springer: Berlin/Heidelberg, Germany, 2020; pp. 251–270.
2. Kashtock, M.E. *Guidance for Industry: Juice Hazard Analysis Critical Control Point Hazards and Controls Guidance*, 1st ed.; FDA Guid. Doc. no. 2; Centre for Food Safety and Applied Nutrition: College Park, MD, USA, 2004; pp. 1–52.
3. Aneja, K.R.; Dhiman, R.; Aggarwal, N.K.; Kumar, V.; Kaur, M. Microbes associated with freshly prepared juices of citrus and carrots. *Int. J. Food Sci.* **2014**, *2014*, 408085. [CrossRef] [PubMed]
4. Aleem, S.; Ramteke, P.W. Sensory and Nutritional study of locally available fresh and processed Fruit and Vegetable juices in Allahabad City. *Pharma Innov.* **2017**, *6*, 380–386.
5. Khandpur, P.; Gogate, P.R. Effect of novel ultrasound-based processing on the nutrition quality of different fruit and vegetable juices. *Ultrason. Sonochem.* **2015**, *27*, 125–136. [CrossRef]
6. Chacha, J.S.; Zhang, L.; Ofoedu, C.E.; Suleiman, R.A.; Dotto, J.M.; Roobab, U.; Agunbiade, A.O.; Duguma, H.T.; Mkojera, B.T.; Hossaini, S.M.; et al. Revisiting nonthermal food processing and preservation methods—Action mechanisms, pros and cons: A technological update (2016–2021). *Foods* **2021**, *10*, 1430. [CrossRef] [PubMed]
7. Gómez-López, V.M.; Ragaert, P.; Debevere, J.; Devlieghere, F. Pulsed light for food decontamination: A review. *Trends Food Sci. Technol.* **2007**, *18*, 464–473. [CrossRef]
8. Illera, A.E.; Sanz, M.T.; Benito-Román, O.; Varona, S.; Beltrán, S.; Melgosa, R.; Solaesa, A.G. Effect of thermosonication batch treatment on enzyme inactivation kinetics and other quality parameters of cloudy apple juice. *Innov. Food Sci. Emerg. Technol.* **2018**, *47*, 71–80. [CrossRef]
9. Ferrario, M.; Alzamora, S.M.; Guerrero, S. Study of pulsed light inactivation and growth dynamics during storage of *Escherichia coli* ATCC 35218, *Listeria innocua* ATCC 33090, *Salmonella Enteritidis* MA44 and *Saccharomyces cerevisiae* KE162 and native flora in apple, orange and strawberry juices. *Int. J. Food Sci. Technol.* **2015**, *50*, 2498–2507. [CrossRef]
10. Char, C.D.; Mitilinaki, E.; Guerrero, S.N.; Alzamora, S.M. Use of High-Intensity Ultrasound and UV-C Light to Inactivate Some Microorganisms in Fruit Juices. *Food Bioprocess Technol.* **2010**, *3*, 797–803. [CrossRef]
11. Pataro, G.; Muñoz, A.; Palgan, I.; Noci, F.; Ferrari, G.; Lyng, J.G. Bacterial inactivation in fruit juices using a continuous flow Pulsed Light (PL) system. *Food Res. Int.* **2011**, *44*, 1642–1648. [CrossRef]
12. Pellicer, J.A.; Gabaldón, J.A.; Gómez-López, V.M. Effect of pH on pulsed light inactivation of polyphenol oxidase. *Enzym. Microb. Technol.* **2021**, *148*, 109812. [CrossRef]
13. Namala, B.; Reddy, P.Y. Design, development and fabrication of batch type continuous UV-C light system for food products. *J. Pharmacogn. Phytochem.* **2017**, *6*, 2078–2081.

14. Shaik, L.; Chakraborty, S. Effect of pH and total fluence on microbial and enzyme inactivation in sweet lime (*Citrus limetta*) juice during pulsed light treatment. *J. Food Process. Preserv.* **2022**, *46*, e16749. [CrossRef]
15. Shaik, L.; Chakraborty, S. Ultrasound processing of sweet lime juice: Effect of matrix pH on microbial inactivation, enzyme stability, and bioactive retention. *J. Food Process Eng.* **2023**, *46*, e14231. [CrossRef]
16. Putnik, P.; Pavlić, B.; Šojić, B.; Zavadlav, S.; Žuntar, I.; Kao, L.; Kitonić, D.; Kovačević, D.B. Innovative hurdle technologies for the preservation of functional fruit juices. *Foods* **2020**, *9*, 699. [CrossRef] [PubMed]
17. Ramírez-Corona, N.; García, N.A.; Martínez, M.J.; López-Malo, A.; Mani-López, E. Effect of combining ultrasound and UVC treatments for processing orange juice and mango nectar on their microbiological, physicochemical, and sensory characteristics. *Innov. Food Sci. Emerg. Technol.* **2024**, *94*, 103686. [CrossRef]
18. Hasani, M.; Chudyk, J.; Murray, K.; Lim, L.T.; Lubitz, D.; Warriner, K. Inactivation of Salmonella, Listeria monocytogenes, Aspergillus and Penicillium on lemons using advanced oxidation process optimized through response surface methodology. *Innov. Food Sci. Emerg. Technol.* **2019**, *54*, 182–191. [CrossRef]
19. Gómez-López, V.M.; Bolton, J.R. An Approach to Standardize Methods for Fluence Determination in Bench-Scale Pulsed Light Experiments. *Food Bioprocess Technol.* **2016**, *9*, 1040–1048. [CrossRef]
20. Guerrouj, K.; Sánchez-Rubio, M.; Taboada-Rodríguez, A.; Cava-Roda, R.M.; Marín-Iniesta, F. Sonication at mild temperatures enhances bioactive compounds and microbiological quality of orange juice. *Food Bioprod. Process.* **2016**, *99*, 20–28. [CrossRef]
21. Sahoo, P.; Chakraborty, S. Influence of Pulsed Light, Ultrasound, and Series Treatments on Quality Attributes, Pectin Methyl Esterase, and Native Flora Inactivation in Sweet Orange Juice (*Citrus sinensis* L. Osbeck). *Food Bioprocess Technol.* **2023**, *16*, 2095–2112. [CrossRef]
22. Dak, M.; Verma, R.C.; Jaaffrey, S.N.A. Effect of temperature and concentration on Rheological properties of 'Kesar' mango juice. *J. Food Eng.* **2007**, *80*, 1011–1015. [CrossRef]
23. Rodríguez-Rivera, M.P.; Lugo-Cervantes, E.; Winterhalter, P.; Jerz, G. Metabolite profiling of polyphenols in peels of *Citrus limetta* Risso by combination of preparative high-speed countercurrent chromatography and LC-ESI-MS/MS. *Food Chem.* **2014**, *158*, 139–152. [CrossRef] [PubMed]
24. Kelebek, H.; Selli, S.; Kola, O. Quantitative determination of phenolic compounds using LC-DAD-ESI-MS/MS in cv. Ayvalik olive oils as affected by harvest time. *J. Food Meas. Charact.* **2017**, *11*, 226–235. [CrossRef]
25. Kaláb, M.; Yang, A.-F.; Chabot, D. Conventional Scanning Electron Microscopy of Bacteria. *Infocus Mag.* **2008**, *10*, 42–61. [CrossRef]
26. Dhar, R.; Chakraborty, S. Effect of continuous microwave processing on enzymes and quality attributes of bael beverage. *Food Chem.* **2024**, *453*, 139621. [CrossRef] [PubMed]
27. Miles, A.J.; Ramalli, S.G.; Wallace, B.A. DichroWeb, a website for calculating protein secondary structure from circular dichroism spectroscopic data. *Protein Sci.* **2022**, *31*, 37–46. [CrossRef]
28. Andrade, M.A.; Chacon, P.; Merelo, J.J.; Morán, F. Evaluation of secondary structure of proteins from UV circular dichroism spectra using an unsupervised learning neural network. *Protein Eng. Des. Sel.* **1993**, *6*, 383–390. [CrossRef]
29. Zhang, J.; Yu, X.; Xu, B.; Yagoub, A.E.A.; Mustapha, A.T.; Zhou, C. Effect of intensive pulsed light on the activity, structure, physico-chemical properties and surface topography of polyphenol oxidase from mushroom. *Innov. Food Sci. Emerg. Technol.* **2021**, *72*, 102741. [CrossRef]
30. Wang, J.; Liu, Q.; Xie, B.; Sun, Z. Effect of ultrasound combined with ultraviolet treatment on microbial inactivation and quality properties of mango juice. *Ultrason. Sonochem.* **2019**, *64*, 105000. [CrossRef]
31. Ferrario, M.; Guerrero, S. Impact of a combined processing technology involving ultrasound and pulsed light on structural and physiological changes of *Saccharomyces cerevisiae* KE 162 in apple juice. *Food Microbiol.* **2017**, *65*, 83–94. [CrossRef]
32. Ferrario, M.; Alzamora, S.M.; Guerrero, S. Study of the inactivation of spoilage microorganisms in apple juice by pulsed light and ultrasound. *Food Microbiol.* **2015**, *46*, 635–642. [CrossRef]
33. Raso, J.; Barbosa-Cánovas, G.V. Nonthermal Preservation of Foods Using Combined Processing Techniques. *Crit. Rev. Food Sci. Nutr.* **2003**, *43*, 265–285. [CrossRef]
34. Fonteles, T.V.; Barroso, M.K.D.A.; Alves Filho, E.D.G.; Fernandes, F.A.N.; Rodrigues, S. Ultrasound and ozone processing of cashew apple juice: Effects of single and combined processing on the juice quality and microbial stability. *Processes* **2021**, *9*, 2243. [CrossRef]
35. Vollmer, K.; Chakraborty, S.; Bhalerao, P.P.; Carle, R.; Frank, J.; Steingass, C.B. Effect of Pulsed Light Treatment on Natural Microbiota, Enzyme Activity, and Phytochemical Composition of Pineapple (*Ananas comosus* [L.] Merr.) juice. *Food Bioprocess Technol.* **2020**, *13*, 1095–1109. [CrossRef]
36. Alabdali, T.A.; Icyer, N.C.; Ucak Ozkaya, G.; Durak, M.Z. Effect of Stand-Alone and Combined Ultraviolet and Ultrasound Treatments on Physicochemical and Microbial Characteristics of Pomegranate Juice. *Appl. Sci.* **2020**, *10*, 5458. [CrossRef]
37. Ferrario, M.; Alzamora, S.M.; Guerrero, S. Inactivation kinetics of some microorganisms in apple, melon, orange and strawberry juices by high-intensity light pulses. *J. Food Eng.* **2013**, *118*, 302–311. [CrossRef]
38. Iqbal, A.; Murtaza, A.; Hu, W.; Ahmad, I.; Ahmed, A.; Xu, X. Activation and inactivation mechanisms of polyphenol oxidase during thermal and nonthermal methods of food processing. *Food Bioprod. Process.* **2019**, *117*, 170–182. [CrossRef]
39. Ordóñez-Santos, L.E.; Martínez-Girón, J.; Arias-Jaramillo, M.E. Effect of ultrasound treatment on visual color, vitamin C, total phenols, and carotenoids content in *Cape gooseberry* juice. *Food Chem.* **2017**, *233*, 96–100. [CrossRef] [PubMed]

40. Masuzawa, N.; Ohdaira, E.; Ide, M. Effects of ultrasonic irradiation on phenolic compounds in wine. *Jpn. J. Appl. Phys.* **2000**, *39*, 2979. [CrossRef]
41. Caminiti, I.M.; Noci, F.; Morgan, D.J.; Cronin, D.A.; Lyng, J.G. The effect of pulsed electric fields, ultraviolet light or high intensity light pulses in combination with manothermosonication on selected physico-chemical and sensory attributes of an orange and carrot juice blend. *Food Bioprod. Process.* **2012**, *90*, 442–448. [CrossRef]
42. Rodriguez-Concepcion, M.; Daròs, J.A. Transient expression systems to rewire plant carotenoid metabolism. *Curr. Opin. Plant Biol.* **2022**, *66*, 102190. [CrossRef]
43. Momin, S.M.I. Analysis of Viscosity of Orange Fruit Juice to Ensure the Suitability of Processing Applications. *Int. J. Pure Appl. Biosci.* **2015**, *3*, 223–225. [CrossRef]
44. Anjaly, M.G.; Prince, M.V.; Warrier, A.S.; Lal, A.N.; Mahanti, N.K.; Pandiselvam, R.; Thirumdas, R.; Sreeja, R.; Rusu, A.V.; Trif, M.; et al. Design consideration and modelling studies of ultrasound and ultraviolet combined approach for shelf-life enhancement of pine apple juice. *Ultrason. Sonochem.* **2022**, *90*, 106166. [CrossRef] [PubMed]
45. Vilas-Boas, A.A.; Magalhães, D.; Campos, D.A.; Porretta, S.; Dellapina, G.; Poli, G.; Istanbullu, Y.; Demir, S.; San Martín, Á.M.; García-Gómez, P.; et al. Innovative Processing Technologies to Develop a New Segment of Functional Citrus-Based Beverages: Current and Future Trends. *Foods* **2022**, *11*, 3859. [CrossRef] [PubMed]
46. Niu, L.; Liu, J.; Wang, X.; Wu, Z.; Xiang, Q.; Bai, Y. Effect of Combined Treatment with Cinnamon Oil and petit-High Pressure CO_2 against Saccharomyces cerevisiae. *Foods* **2022**, *11*, 3474. [CrossRef] [PubMed]
47. Takeshita, K.; Shibato, J.; Sameshima, T.; Fukunaga, S.; Isobe, S.; Arihara, K.; Itoh, M. Damage of yeast cells induced by pulsed light irradiation. *Int. J. Food Microbiol.* **2003**, *85*, 151–158. [CrossRef] [PubMed]
48. Krishnamurthy, K.; Demirci, A.; Irudayaraj, J. Inactivation of Staphylococcus aureus in milk and milk foam by pulsed UV-light treatment and surface response modeling. *Trans. ASABE* **2008**, *51*, 2083–2090.
49. Kuznetsova, I.M.; Stepanenko, O.V.; Turoverov, K.K.; Zhu, L.; Zhou, J.M.; Fink, A.L.; Uversky, V.N. Unraveling multistate unfolding of rabbit muscle creatine kinase. *Biochim. Biophys. Acta Protein Struct. Mol. Enzymol.* **2002**, *1596*, 138–155. [CrossRef] [PubMed]
50. Liu, W.; Liu, J.; Liu, C.; Zhong, Y.; Liu, W.; Wan, J. Activation and conformational changes of mushroom polyphenoloxidase by high pressure microfluidization treatment. *Innov. Food Sci. Emerg. Technol.* **2009**, *10*, 142–147. [CrossRef]
51. Zhou, L.; Liu, W.; Xiong, Z.; Zou, L.; Liu, J.; Zhong, J.; Chen, J. Effect of ultrasound combined with malic acid on the activity and conformation of mushroom (*Agaricus bisporus*) polyphenoloxidase. *Enzym. Microb. Technol.* **2016**, *90*, 61–68. [CrossRef]
52. Yi, J.; Yi, J.; Dong, P.; Liao, X.; Hu, X.; Zhang, Y. Effect of high-hydrostatic-pressure on molecular microstructure of mushroom (*Agaricus bisporus*) polyphenoloxidase. *LWT Food Sci. Technol.* **2015**, *60*, 890–898. [CrossRef]

foods

MDPI

Article

Microbial Inhibition by UV Radiation Combined with Nisin and Shelf-Life Extension of Tangerine Juice during Refrigerated Storage

Isaya Kijpatanasilp [1,2], Khursheed Ahmad Shiekh [1], Saeid Jafari [1], Randy W. Worobo [2] and Kitipong Assatarakul [1,*]

[1] Department of Food Technology, Faculty of Science, Chulalongkorn University, Bangkok 10330, Thailand; ykijpat@gmail.com (I.K.); khursheedahmad.s@chula.ac.th (K.A.S.); saeid.j@chula.ac.th (S.J.)
[2] Department of Food Science, College of Agriculture and Life Sciences, Cornell University, Ithaca, NY 14853, USA; rww8@cornell.edu
* Correspondence: kitipong.a@chula.ac.th; Tel.: +662-218-5328

Abstract: This study evaluated the efficiency of UV radiation doses (4.68–149.76 J/cm^2) and nisin (50–200 ppm) and their combination in comparison with thermal pasteurization on the microbial inhibition kinetics and physicochemical properties of tangerine juice. It was noted that UV-149.76 J/cm^2 and nisin (NS) at 200 ppm in conjunction exhibited the highest log reduction in spoilage and pathogenic microbes including *Escherichia coli*, *Lactiplantibacillus plantarum*, and *Saccharomyces cerevisiae*, yeast and molds, and total plate count in tangerine juice. Additionally, the first-order kinetic model provides a better fit for spoilage and pathogenic strains compared with the zero-order model (higher coefficient of determination, R^2), particularly for *E. coli*. UV and NS showed insignificant effects ($p > 0.05$) on pH, TSS, and TA values compared with pasteurization. However, there were notable differences observed in color analysis, total phenolic compound, total flavonoid content, vitamin C, carotenoid content, and antioxidant activity using DPPH and FRAP assays. The optimized UV + NS samples were subjected to refrigerated storage for 21 days. The results revealed that during the entire storage period, the pH values and the TSS values slightly decreased, and the TA values increased in the treated samples. The UV + NS treatment insignificantly impacted the color properties. The total phenolic, total flavonoid, and carotenoid contents, and vitamin C decreased over time for all sample treatments, whereas the antioxidant properties exhibited varying outcomes, compared with an untreated control and pasteurization. Therefore, UV radiation and nisin (UV-149.76 J/cm^2 + NS-200 ppm) in combination could serve as a viable alternative to traditional heat pasteurization of fruit juice during cold storage.

Keywords: bacteriocin; cold storage; fruit juice; hurdle concept; microorganisms; quality

1. Introduction

As people become more health-conscious, there has been a surge in demand for food and beverages that are both healthy and functional. This trend has led to a rise in the popularity and availability of fresh juices and beverages in supermarkets [1]. Tangerine juice is a well-liked beverage that has several health advantages. It contains significant amounts of vitamin C, which supports a healthy immune system and guards against illnesses and infections. Antioxidants, which are included in orange juice, may aid in preventing cell damage and lowering the risk of chronic illnesses like cancer and heart disease [2]. Therefore, consuming tangerine juice often as part of a balanced diet might be an effective way to enhance general health and wellbeing. However, tangerine juice is a perishable product that is vulnerable to oxidation and microbial growth, which can lead to a decrease in its nutritional content and potential health benefits during storage.

Pasteurization is a preservation method that helps to make the liquid safer for consumption by reducing the risk of spoilage. However, this process can also result in a loss of certain heat-sensitive nutrients and enzymes in the liquid as well as some negative impacts on the sensory qualities of the juice. On the other hand, nonthermal technology is a type of processing using techniques other than heat to preserve foods, including fruit juice. Some of the benefits of nonthermal processing of fruit juice include retention of nutrients, improved flavor and sensory characteristics, and extended shelf life [3]. In order to improve the sensory quality of the finished product while still maintaining microbial safety, ultraviolet irradiation has been researched and developed as a substitute for thermal treatment [4]. In our recent study, we demonstrated that UV treatment of longan juice at a dose of 74.88 J/cm^2 reduced microbial loads, improved quality characteristics, and extended its shelf life during cold storage [3]. Furthermore, when combined with other hurdle technologies, such as the use of chemicals, high-pressure processing, pulsed electric fields, or ozone treatment, the benefits of UV treatment are magnified. Overall, the combination of UV treatment with other hurdle technologies can offer a comprehensive approach to fruit juice processing, resulting in a safer, higher-quality, and longer-lasting product. Nisin is also a naturally occurring antimicrobial peptide produced by *Lactococcus lactis*. It is a peptide known to inhibit bacterial growth, and is widely used in the food industry. It can also be used in combination with UV treatment for fruit juice processing [5]. Verma et al. [6] concluded that bacteriocins such as nisin are more promising preservatives in food products than their chemical counterparts. The previous study reported that UV-C radiation and nisin could significantly reduce microbial contamination on shrimp without significantly affecting quality parameters of the shrimp such as texture or lipid oxidation [7]. However, their effects on tangerine juice have not been elaborated on yet.

This study examined a new processing approach (hurdle concept) for tangerine juice that combines UV irradiation and nisin treatment, and compares it with conventional pasteurization methods. Kinetic modeling was used to analyze the inhibition of spoilage and pathogenic microorganisms by UV treatment, and the effects of UV + nisin treatment on the physical and chemical properties of tangerine juice were also explored. In addition, changes in quality of UV + nisin treated samples were investigated during refrigerated storage.

2. Materials and Methods

2.1. Tangerine Juice Preparation

Tangerines were obtained from a retail market in Bangkok, Thailand. The tangerines were peeled and processed using an Electrolux EMB3500S (Stockholm, Sweden) juice extractor. The resulting pulp was filtered through cheesecloth to eliminate the suspended particles and to further remove any remaining pulp.

2.2. Nisin, Chemicals, and Microbial Media

Nisin (Glenham Life Science Ltd., Corsham, UK) was dissolved in 0.02 mol/L of hydrochloric acid (HCl) and filtered through a 0.22 μm membrane [8]. All the chemicals and microbial media used in this study were of analytical grade.

2.3. Microbial Cultures and Inoculation in Tangerine Juice

Escherichia coli TISTR 117, *Saccharomyces cerevisiae* TISTR 5004, and *Lactiplantibacillus plantarum* TISTR 2365 were obtained from the Thailand Institute of Scientific and Technological Research (TISTR). The microbial strains were added to 10 mL of nutrient broth (NB), yeast malt broth (YMB), and MRS broth, respectively. *Escherichia coli* and *Lactiplantibacillus plantarum* tubes were incubated at 37 °C and shaken at 200 rpm for 24 h, whereas *Saccharomyces cerevisiae* tubes were incubated at 30 °C and shaken at 200 rpm for 24 h to increase the number of microorganisms (approximately 10^7–10^8 CFU/mL). Then, 0.1 mL was transferred into 5 mL of each broth, incubated and shaken for 24 h before being added into tangerine juice at the ratio of 1:100 (v/v). The tangerine juice had initial

microbial content of approximately 10^5–10^6 CFU/mL. The tangerine juice was incubated at room temperature for 24 h to increase the number of microorganisms (for total plate count and yeast and mold count experiments) in the juice. The initial microbial load was approximately 10^5–10^6 CFU/mL.

2.4. UV Sterilization, Nisin Treatment, and Pasteurization of Tangerine Juice

The method of UV irradiation in tangerine juice at various doses, including 4.68, 9.36, 18.72, 37.44, 74.88, and 149.76 J/cm^2, was previously described by Kijpatanasilp et al. [3]. The tangerine juice samples consisted of samples treated with different doses of nisin (50, 100, 150, and 200 ppm). For the pasteurization process, glass bottles containing the samples were placed in a water bath and heated to a temperature of 95 ± 1 °C for 1 min [9]. Control samples of tangerine juice without UV, nisin, and pasteurization treatment were also included.

2.5. UV-Irradiated Tangerine Juice for Analysis of Microbial Growth Inhibition Kinetics

The microbial analysis of the tangerine juice samples was conducted as previously described [3]. In summary, the samples were diluted with 0.1% (*w*/*v*) sterile peptone water and then subjected to microbial analysis. The results were expressed as colony-forming units per milliliter (CFU/mL) and analyzed in triplicates. The analysis utilized both zero-order and first-order kinetic models, as outlined previously by Kijpatanasilp et al. [3]. Bacterial and total microbial plates were incubated at 37 °C for 48 h, whereas yeast and mold plates were incubated at 30 °C for 48 h. Microbial calculation was conducted based on the colony counts on the media plates with the reference range of 30–300 colonies [10].

2.6. Physicochemical Properties of Nisin- and UV-Treated and Pasteurized Tangerine Juice

The pH values and the total soluble solid (TSS) content were measured using a pH meter (Inobab, Tetra Con 325, Adelsdorf, Germany) and using a digital handheld refractometer (Atago No. 3840, Atago, Tokyo, Japan), respectively. Color values were assessed based on the CIE system (L*, a*, and b*), using a colorimeter (Konica Minolta, model CR-400, Tokyo, Japan). The analysis of vitamin C content involved the preparation of a standard solution of ascorbic acid (0.1%) and dichlorophenol indophenol (0.1%). The analysis of carotenoid content using solvent extraction was modified according to Jafari et al. [11,12]. Titratable acidity was analyzed following the method described by Jafari et al. in 2021 [11,12]. The Folin–Ciocalteu method was employed to determine the total phenolic compound (TPC). The TPC values were expressed in milligrams of gallic acid equivalents per liter (mg GAE/L) [11]. For the determination of the total flavonoid content (TFC), the aluminum chloride colorimetric method was used [12].

The measurement of antioxidant activity was conducted using 2,2-diphenyl-1-picryl-hydrazyl (DPPH). To do so, 250 µL of the sample was mixed with 4.75 mL of DPPH methanol solution. The absorbances of both the DPPH solution and the samples were then measured at 515 nm using a spectrophotometer [13]. For the assessment of antioxidant activity using ferric reducing antioxidant power (FRAP), 4.75 mL of FRAP solution was vortex-mixed with 250 µL of the sample. The mixture was subsequently analyzed using a spectrophotometer (GENE-SYSTM 20 Visible, Thermo Fisher Scientific, Waltham, MA, USA) to measure the absorbance at 593 nm for both the FRAP solution and the samples.

2.7. Analysis of Microbial and Physicochemical Characterization during Storage at 4 °C

The samples consisted of various treatments, including a control sample with no treatment, UV radiation at 149.76 J/cm^2, nisin at 200 ppm, a combined treatment with UV radiation at 149.76 J/cm^2 and 200 ppm nisin, and a pasteurized sample treated at 95 ± 1 °C for 1 min. These samples were packaged in sealed 100 mL glass bottles and stored at a temperature of 4 °C. The physicochemical quality of the samples was assessed by measuring changes in pH, total soluble solid (TSS), titratable acidity (TA), color values, total plate count, total fungal count, and functional properties at regular intervals throughout

the refrigerated storage period, as mentioned in the previous sections. The shelf life of the tangerine juice was determined by ensuring that the yeast and mold count remained below 6 log CFU/mL during storage.

2.8. Statistical Analysis

All experiments were carried out in triplicate and results were reported as the average ± standard deviation (SD). The data were analyzed using the analysis of variance (ANOVA) technique, utilizing the Statistical Package for Social Sciences (SPSS Version 23, USA). To assess the mean differences, Duncan's multiple range test was applied at a significance level of $p \leq 0.05$.

3. Results and Discussion

3.1. Impact of UV Radiation on the Microbial Growth and Inhibition Kinetics in Tangerine Juice

The UV treatments applied to tangerine juice for microbial inhibition are summarized in Table S1 (Supplementary Data File). Increasing the UV dose to 149.76 J/cm^2 resulted in decreases in the total plate count and yeast and mold count to 4.26 ± 0.05 and 2.56 ± 0.04 log CFU/mL, respectively, indicating the effective reduction in microorganisms in the sample (Table S1). The populations of *E. coli*, *L. plantarum*, and *S. cerevisiae* decreased to 4.94 ± 0.02, 4.16 ± 0.03, and 4.23 ± 0.05 log CFU/mL, respectively, at the highest UV dose of 149.76 J/cm^2. These log reduction values demonstrate the efficacy of UV treatment against the tested microorganisms. Figure 1 illustrates the inhibition kinetic plots for the total plate count (A), yeast and mold count (B), *Saccharomyces cerevisiae* (C), *Escherichia coli* (D), and *Lactiplantibacillus plantarum* (E) in tangerine juice samples exposed to various UV doses. The quantities of microorganisms in CFU/mL and in ln CFU/mL are depicted on the *y*-axis based on zero-order and first-order kinetics, respectively, while the UV dose is shown on the *x*-axis.

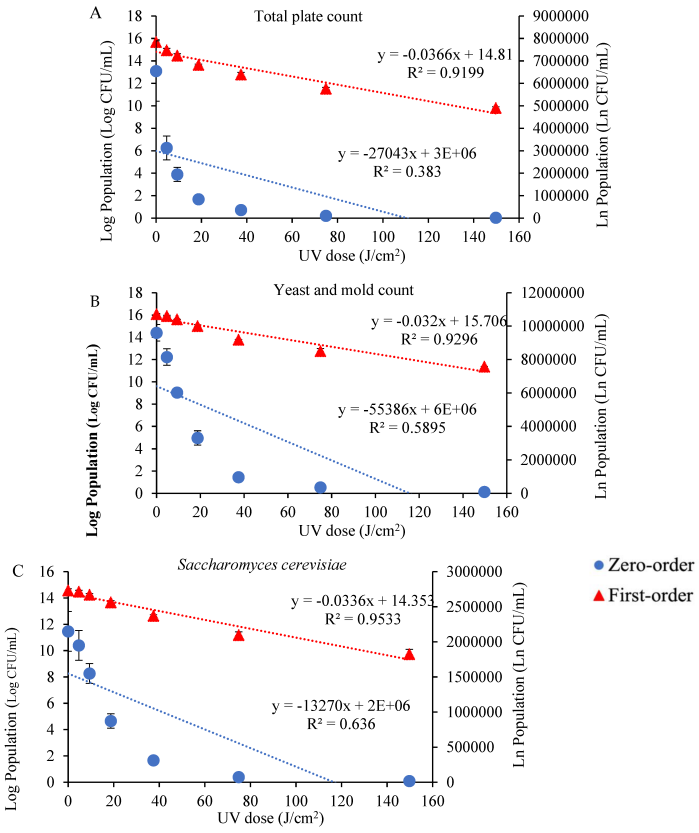

Figure 1. *Cont.*

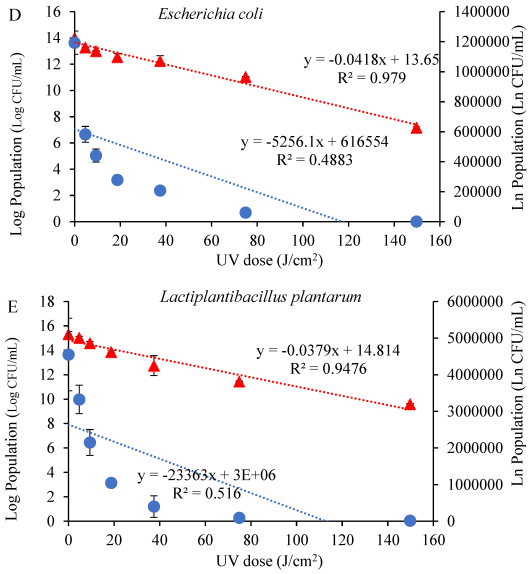

Figure 1. Kinetic modeling plots describing zero-order (blue circle) and first-order (red triangle) inactivation of total plate count (**A**), yeast and mold count (**B**), *Saccharomyces cerevisiae* (**C**), *Escherichia coli* (**D**), and *Lactiplantibacillus plantarum* (**E**) treated with ultraviolet radiation.

Table 1 presents the rate constants (k) and coefficients of determination (R^2) for both the zero-order and first-order kinetic models applied to the total plate count, yeast and mold count, *E. coli*, *L. plantarum*, and *S. cerevisiae*. The findings indicate that the first-order model provides a relatively good fit to the experimental data, with better fitting results observed for *E. coli* compared with the other microorganisms. The rate constant values for the first-order kinetic model range from 0.0320 for yeast and mold count to 0.0418 for *E. coli*. These results suggest that the first-order model adequately describes the experimental data, with better fitting results observed for *E. coli* compared with the other microorganisms. Furthermore, the results indicate that the first-order kinetic model offers a superior fit to the experimental data when compared with the zero-order model, particularly for *E. coli*, where the first-order model exhibits a higher coefficient of determination (R^2) and a higher rate constant (k) compared with the zero-order model.

Table 1. Rate constant and coefficient of determination of zero-order and first-order kinetic inhibition models of microbial proliferation using UV radiation in tangerine juice.

Microorganisms	Zero-Order		First-Order	
	Rate Constant (k)	Coefficient of Determination (R^2)	Rate Constant (k)	Coefficient of Determination (R^2)
Total plate count	27,043	0.3830	0.0366	0.9199
Yeast and mold count	55,386	0.5895	0.0320	0.9296
E. coli	52,561	0.4883	0.0418	0.9790
L. plantarum	23,363	0.516	0.0379	0.9476
S. cerevisiae	13,270	0.6360	0.0336	0.9533

The UV radiation induces structural changes in the genetic material, disrupting the replication and transcription processes essential for microbial growth and survival [14]. The presence of pyrimidine dimers in DNA interferes with DNA polymerase to hinder the separation of DNA strands and the accurate synthesis of new DNA strands, thereby inhibiting microbial reproduction and colony formation [15]. Initially, UV light was primarily utilized for decontaminating water and other transparent fluids. However, UV as nonthermal hurdle technology has since been shown to be effective in decontaminating a

variety of liquid foods, including fruit and vegetable juices, milk, tea, coffee, liquid egg, wine, and sugar syrup [16,17].

3.2. Efficacy of Nisin at Different Concentrations on the Spoilage and Pathogenic Microbial Load of Tangerine Juice

The results of different concentrations (50–200 ppm) of nisin on the populations of different microorganisms, and their log reductions (log CFU/ mL), are presented in Table S2. The increase in the nisin concentration from 150 to 200 ppm reduced the microbial population of tangerine juice samples due to higher log reduction in the total plate count by 2.12 ± 0.05 log CFU/mL, yeast and mold count by 0.23 ± 0.06 log CFU/mL, *E. coli* by 1.55 ± 0.11 log CFU/mL, *L. plantarum* by 3.05 ± 0.07 log CFU/mL, and *S. cerevisiae* by 0.18 ± 0.04 log CFU/mL ($p \leq 0.05$), compared with 50–100 ppm treatments with nisin. Generally, nisin had a greater effect on the populations of *L. plantarum* compared with the other microorganisms tested. Higher concentrations of nisin at 200 ppm showed greater log reductions in all microorganisms [18]. The mechanism of action of nisin involves several key steps that lead to microbial inhibition. In the cell wall components, nisin initially binds in the presence of certain divalent cations, such as calcium ions to the lipid II molecule, which is an essential precursor for the synthesis of peptidoglycan, a major component of the bacterial cell wall. After binding to lipid II, nisin inserts itself into the bacterial cell membrane, and it causes alterations in the lipid bilayer structure, leading to the formation of pores or ion channels to disrupt the membrane integrity of microbes [19]. The pores formed by nisin allow the uncontrolled leakage of essential intracellular components, such as ions, metabolites, and macromolecules, from the bacterial cell. This disruption of membrane integrity and loss of intracellular contents severely impairs bacterial viability. In addition, nisin also induces membrane depolarization by dissipating the electrochemical gradient across the cell membrane that potentially affects various essential cellular processes, including nutrient uptake and energy production, further compromising bacterial survival [14]. Nisin, at a concentration of 100 IU/mL in fresh apple–kale blend juice, was reported to inactivate *E. coli* K12 and *Listeria innocua* by 1.0 and 2.6 log CFU/mL, respectively [20].

3.3. Combined Effects of UV Irradiation and Nisin on the Spoilage and Pathogenic Microbial Load of Tangerine Juice

Table 2 displays the findings of total microbial and yeast and mold counts, as well as other microbial counts, for tangerine juice samples treated with combinations of UV radiation and nisin. The untreated control and pasteurized samples were compared with the UV, NS, and UV + NS samples. The control sample, which did not undergo any treatment, exhibited the highest total plate count (6.75 ± 0.27 log CFU/mL) among all the tested microorganisms. Furthermore, the UV and NS treatments resulted in lower microbial loads compared with the untreated control sample ($p \leq 0.05$). However, the combined UV and nisin treatments showed the lowest total plate count (1.89 ± 0.02 log CFU/mL) and yeast and mold count (4.86 ± 0.02 log CFU/mL) compared with the UV, NS, and control samples ($p \leq 0.05$). The pasteurization sample achieved complete log reduction with no growth of the tested microorganisms ($p \leq 0.05$). The longan juice samples that were pasteurized and subjected to a UV dose of 149.8 J/cm^2 exhibited greater log reduction values for total microbial, yeast/mold, and *E. coli* counts, in comparison with the untreated control and other low doses of UV radiation [21]. The combined use of UV irradiation and fumaric acid (FA) was found to be highly effective in killing *Escherichia coli* O157:H7, *Salmonella enterica* serovar Typhimurium, and *Listeria monocytogenes* in apple juice. This combined approach resulted in greater inhibition of bacterial growth in apple juice compared with using either UV or FA alone [22]. The combination of UV-C (2.52 kJ/m^2) at 3 min of exposure time and nisin (15.62 μg/mL) potentially reduces *Alicyclobacillus acidoterrestris* spores and preserves ascorbic acid in orange juice [8].

Table 2. Total plate count, yeast and mold count, and microbial counts of tangerine juice samples subjected to UV radiation, nisin, combined treatments with UV radiation and nisin, and pasteurization.

Sample Treatments	Total Plate Count (log CFU/mL)		Yeast and Mold Count (log CFU/mL)		*E. coli* (log CFU/mL)		*L. plantarum* (log CFU/mL)		*S. cerevisiae* (log CFU/mL)	
	Population	Log Reduction	Population	Log Reduction	Population	Log Reduction	Population	Log Reduction	Population	Log Reduction
Control	6.75 ± 0.27^{a}	0.00 ± 0.00	6.86 ± 0.09^{a}	0.00 ± 0.00	7.59 ± 0.02^{a}	0.00 ± 0.00	7.85 ± 0.06^{a}	0.00 ± 0.0	7.02 ± 0.03^{a}	0.00 ± 0.00
UV	4.21 ± 0.05^{b}	2.54 ± 0.04	4.84 ± 0.001^{b}	2.02 ± 0.02	4.58 ± 0.02^{b}	3.01 ± 0.07	5.36 ± 0.03^{b}	2.49 ± 0.06	4.94 ± 0.16^{c}	2.08 ± 0.05
NS	3.68 ± 0.16^{c}	2.07 ± 0.05	6.66 ± 0.04^{c}	0.20 ± 0.08	6.08 ± 0.30^{c}	1.51 ± 0.09	4.81 ± 0.20^{c}	3.04 ± 0.02	6.84 ± 0.07^{b}	0.18 ± 0.01
UV + NS	1.89 ± 0.02^{d}	4.86 ± 0.02	4.49 ± 0.01^{d}	2.37 ± 0.04	2.79 ± 0.07^{d}	4.80 ± 0.10	1.81 ± 0.01^{b}	6.04 ± 0.15	4.73 ± 0.03^{d}	2.29 ± 0.02
Pasteurization	0.74 ± 0.00^{e}	6.07 ± 0.09	0.73 ± 0.01^{e}	6.25 ± 0.02	-	6.60 ± 0.10	-	6.08 ± 0.03	-	6.02 ± 0.06

The values in the table represent the mean ± standard deviation of UV-, nisin-UV+NS, and heat-treated tangerine juice obtained from the 3 replicates. a–e indicate significant differences in each column ($p \leq 0.05$) of the microbial experiment. Control: tangerine juice without any treatment; UV: 149.76 J/cm^2 ultraviolet radiation dose; NS: 200 ppm of nisin; Pasteurization: tangerine juice pasteurized for 1 min at 95 ± 1 °C (come-up time was 1 min 50 s).

3.4. Combined Effects of UV Irradiation and Nisin Concentrations on the Physicochemical Properties of Tangerine Juice

The effects of UV treatments (4.68–149.76 J/cm^2) and nisin concentrations (50–200 ppm) on the physicochemical properties of tangerine juice samples are presented in Table S3. The results indicate that different doses of UV and nisin did not significantly affect the pH, TSS, TA, and color values of the tangerine juice samples ($p > 0.05$). However, significant changes were observed in the TPC, TFC, total carotenoid content, and antioxidant activity (DPPH and FRAP assays) of the tangerine juice samples treated with a UV dose of 149.76 J/cm^2 compared with the samples treated with 50–200 ppm nisin ($p \leq 0.05$). Subsequently, the optimized UV treatment (149.76 J/cm^2), 200 ppm nisin (NS), and UV combined with nisin (UV + NS) were compared, as shown in Table 3. The pH values of all the treatments were similar, ranging from 3.85 to 3.87, indicating that the treatments had no significant effect on the pH of the tangerine juice ($p > 0.05$). Similarly, the TSS and TA values were similar among all treatments, suggesting that the sweetness and acidity of the juice were not negatively impacted by any of the treatments ($p > 0.05$).

Table 3. Physiochemical characteristics of tangerine juice subjected to single and combined treatments with UV radiation, nisin, and pasteurization.

Properties	Control	UV	NS	UV + NS	Pasteurization
pH	3.87 ± 0.01^{a}	3.87 ± 0.01^{a}	3.86 ± 0.01^{a}	3.85 ± 0.07^{a}	3.87 ± 0.07^{a}
TSS	9.0 ± 0.04^{a}	8.9 ± 0.14^{a}	8.9 ± 0.04^{a}	8.9 ± 0.04^{a}	9.0 ± 0.01^{a}
TA	0.44 ± 0.01^{a}	0.42 ± 0.01^{a}	0.44 ± 0.01^{a}	0.44 ± 0.01^{a}	0.42 ± 0.01^{a}
L*	71.90 ± 0.07^{ab}	71.81 ± 0.06^{ab}	71.94 ± 0.02^{a}	71.76 ± 0.035^{b}	70.95 ± 0.06^{c}
a*	11.62 ± 0.04^{c}	12.11 ± 0.12^{b}	11.82 ± 0.10^{bc}	11.91 ± 0.018^{bc}	12.53 ± 0.10^{a}
b*	74.73 ± 0.11^{a}	73.70 ± 0.28^{c}	74.26 ± 0.03^{bc}	73.92 ± 0.046^{b}	72.95 ± 0.12^{d}
TPC	203.75 ± 6.38^{a}	148.33 ± 2.70^{b}	197.35 ± 4.62^{a}	139.00 ± 1.57^{b}	101.61 ± 13.01^{c}
TFC	185.90 ± 0.78^{a}	169.23 ± 3.77^{b}	181.88 ± 4.93^{a}	163.79 ± 3.85^{b}	156.45 ± 2.95^{c}
Vitamin C	41.61 ± 0.71^{a}	36.00 ± 0.60^{b}	41.11 ± 0.41^{a}	35.83 ± 0.71^{b}	19.80 ± 0.94^{c}
Carotenoid	17.36 ± 0.38^{a}	12.00 ± 0.30^{b}	15.95 ± 0.11^{a}	11.32 ± 1.94^{c}	4.76 ± 0.11^{d}
DPPH	344.09 ± 8.61^{a}	328.36 ± 2.31^{ab}	339.00 ± 9.26^{ab}	322.00 ± 5.40^{b}	292.00 ± 8.74^{c}
FRAP	348.19 ± 3.85^{a}	322.00 ± 3.60^{b}	343.11 ± 1.36^{a}	317.40 ± 3.47^{b}	285.12 ± 6.95^{c}

The values in the table represent the mean ± standard deviation of UV-, nisin-, and heat-treated tangerine juice obtained from the 3 replicates. a–d indicate significant differences in each row ($p \leq 0.05$) of the physicochemical experiment. Control: tangerine juice without any treatment; UV: 149.76 J/cm^2 ultraviolet radiation dose; NS: 200 ppm of nisin; Pasteurization: tangerine juice pasteurized for 1 min at 95 ± 1 °C (come-up time was 1 min 50 s). TSS: total soluble solid (°Brix); TA: titratable acidity (% malic acid); TPC: total phenolic compound (mg GAE/L); TFC: total flavonoid content (mg QE/L); total carotenoid content (μg/100 mL); DPPH assay (mM TE/100 mL); FRAP assay (mM TE/100 mL).

Regarding color analysis, the L* values were significantly different among the treatments, with the pasteurization treatment showing the lowest L* value. The UV and NS treatments had similar L* values to the control sample ($p > 0.05$). The a* and b* values also showed significant differences among the treatments ($p \leq 0.05$), with the UV + NS sample having the highest a* value and the pasteurization treatment having the lowest b* value. The TPC was highest in the control and UV-treated tangerine juice samples, while the pasteurized juice had the lowest TPC. Similar trends were observed for TFC, vitamin C,

carotenoid content, and antioxidant activity. Overall, the UV and NS treatments, as well as the UV + NS treatment, showed insignificant effects ($p > 0.05$). In contrast, pasteurization resulted in significant reductions in TPC, TFC, vitamin C, carotenoid content, and antioxidant activity ($p \leq 0.05$).

Antioxidant compounds have been shown to have natural protective effects against oxidative damage, commonly found in fruits, vegetables, and whole grains [23]. Pasteurization has been reported to eliminate quality-degrading microbes; however, antioxidant compounds were found to be severely affected in pineapple, mango, and watermelon juice [24]. Nisin was reported to show no notable changes to the physical and chemical properties, especially in antioxidant compounds [25]. Additionally, UV as a nonthermal treatment was reported to have less impact on the bioactive compounds that exhibit antioxidant properties in longan juice than thermal pasteurization, which led to their significant degradation [26]. Thus, optimum doses of UV (149.76 J/cm^2), NS (200 ppm), and their combination were chosen for the storage study under refrigerated storage for 21 days.

3.5. Combined Effects of UV Radiation and Nisin on the Spoilage Microbial Load of Tangerine Juice during Storage at 4 °C

The control samples, which were not treated, had an initial total plate count of 3.08 ± 0.02 log CFU/mL and showed the highest increase in microbial count, reaching 9.49 ± 0.05 log CFU/mL after 21 days of storage (Table 4). Similarly, the total plate count increased over time in all samples up to 21 days, except for in the UV + NS and pasteurized samples, which showed evidence of microbial growth after day 9 and day 6 of refrigerated storage, respectively. The samples treated with UV radiation and NS alone had lower microbial counts. However, the combined treatment with UV + NS resulted in even lower microbial counts than the control, UV, and NS samples at all storage times, ranging from 0.55 ± 0.03 to 2.28 ± 0.02 log CFU/mL. Pasteurization consistently showed the lowest total microbial count throughout the storage period, ranging from 0.74 ± 0.01 to 3.11 ± 0.03 log CFU/mL.

In addition, the total microbial load obtained in the pasteurization treatment was higher compared with the UV + NS sample (21 days). The combination effect of UV and nisin treatment reported <1.7 log CFU/mL of total microbial count in tangerine juice [16]. UV treatments have been successful in deactivating spoilage microorganisms and pathogenic strains in large-scale applications for liquid foods, including juices and beverages with color and turbidity [3]. The combination of UV and nisin (UV + NS) in tangerine juice showed a synergistic effect, preserving its quality while ensuring the total plate count remained within safe consumption limits. Due to its low pH and high content of sugars and organic acids [27], the shelf life of tangerine juice was determined by its yeast and mold content not exceeding 6 log CFU/mL [28]. The yeast and mold count in the control was highest, in the range of 3.46 ± 0.04 log CFU/mL to 9.32 ± 0.13 log CFU/mL during 21 days of storage. The UV + NS combination showed a lower yeast and mold count in comparison with the untreated control tangerine juice during storage, while the NS sample exhibited a higher yeast and mold count, ranging from 3.21 ± 0.05 log CFU/mL to 9.25 ± 0.11 log CFU/mL, than that of the UV + NS treatment. Moreover, yeast and mold growth was not detected in the pasteurization treatment; however, UV + NS could be an excellent substitute to safeguard the color and bioactive properties of tangerine juice and extend shelf life for up to 9 days, while ensuring the total plate count remains within safe consumption limits. Yeast and mold are microorganisms that can grow in fruit juices and can cause spoilage by producing off-flavors, odors, and a fuzzy or cloudy appearance [20]. Refrigeration can slow down their growth; however, it has been reported that yeast and mold even showed growth in lychee juice treated with UV radiation after 35 days of storage [21]. As a result, it is important to maintain a low yeast and mold count in fruit juices to ensure their quality and safety.

3.6. Combined Effects of UV Radiation and Nisin on the Physicochemical Quality Changes in Tangerine Juice during Storage at 4 °C

The pH values of the control, UV, NS, UV + NS, and pasteurized tangerine juice ranged from 3.50 ± 0.01 to 3.88 ± 0.01 for all treatments during 21 days of storage at 4 °C, as shown in Table 5. The pH values slightly decreased during the entire storage period for all treatments. On day 21 of storage, the control sample exhibited the lowest pH, whereas the samples subjected to UV + NS and pasteurization treatments demonstrated the highest pH values. Total soluble solid (°Brix) values tended to decrease slightly during storage for all treatments during 21 days of storage, which was consistent with our previous study on mango and passion fruit smoothies subjected to dimethyl dicarbonate [12]. Additionally, the control sample had the lowest values of TSS, while the samples treated with UV + NS and the pasteurization sample showed the highest values on day 21 of refrigerated storage.

The titratable acidity (TA%) values slightly increased in the control, UV-, and NS-treated tangerine juice samples after 12 days of storage. The combined UV radiation and nisin treatment, along with the pasteurization treatment, showed lower TA values with insignificant differences ($p > 0.05$) compared with the other samples until the end of the storage period. The combined treatment with UV radiation and nisin showed a marked effect on maintaining the chemical quality of tangerine juice during storage at 4 °C. The L* values, which represent lightness, exhibited slight variations between the control and treated samples throughout the storage period of 0 to 21 days (Table 6). This indicates that the UV and NS treatments did not significantly affect the lightness of the tangerine juice. However, pasteurization did affect the L* values of the tangerine juice, although no significant differences were observed during the 21-day storage period. Regarding the a* values, which indicate the degree of redness or greenness, the control sample showed an initial measurement of 11.60 ± 0.12 on day 0, which increased to 12.08 ± 0.08 on day 21. The UV, UV + NS, and pasteurization treatments showed similar results, with slight increases throughout the refrigerated storage period. The NS treatment alone showed insignificant differences across all storage intervals.

In terms of the b* values, which represent the degree of yellowness or blueness, insignificant differences were observed between the control and treated samples during the entire storage period. This suggests that the treatments did not have a significant effect on the yellowness of the tangerine juice. However, a slight increase in b* values was observed in the control tangerine juice after 18 days of storage. In general, the results indicate that the combination of UV radiation and nisin treatment did not have a significant effect on the color properties of the tangerine juice samples during 21 days of cold storage.

The total phenolic compound (TPC) of the tangerine juice decreased over time for all treatments, as shown in Table 7. Among the treatments, the most significant decrease in TPC was observed in the pasteurization treatment. The TPC decreased from 97.39 ± 1.75 mg GAE/L on day 0 to 53.54 ± 1.16 mg GAE/L on day 21. Similarly, the total flavonoid content (TFC) of the tangerine juice decreased over time for all treatments. The pasteurization treatment also showed a significant decrease in TFC, from 147.55 ± 1.01 mg QE/L on day 0 to 88.84 ± 0.74 mg QE/L on day 21. The total carotenoid content of the tangerine juice decreased over time for all treatments. The untreated control had the highest total carotenoid content of 16.6 ± 0.96 μg/100 mL on day 0, which decreased to 12.08 ± 1.28 μg/100 mL on day 21. The pasteurization sample exhibited a decrease in total carotenoid content, starting from 7.64 ± 1.06 μg/100 mL on day 0 and reaching the lowest value of 3.56 ± 0.92 μg/100 mL on day 21. In terms of vitamin C content, the combination of UV and NS treatment resulted in the most stable content during storage, with a value of 17.62 ± 1.77 mg/100 mL on day 21. In comparison, the pasteurization sample had a final value of 12.01 ± 0.75 mg/100 mL on day 21. Regarding antioxidant activity, the combination of UV + NS treatment showed a slower decrease in DPPH antioxidant activity compared with the pasteurization treatment. For the FRAP values, the UV + NS treatment exhibited higher antioxidant activity throughout the 21-day refrigerated storage period compared with the pasteurized sample.

Table 4. Total plate count and yeast and mold count of tangerine juice subjected to optimized treatments with UV radiation, nisin and UV + NS during storage (4 °C).

Storage Time (Days)	Total Plate Count (log CFU/mL)					Yeast and Mold Count (log CFU/mL)				
	Control	UV	NS	UV + NS	Pasteurization	Control	UV	NS	UV + NS	Pasteurization
0	3.08 ± 0.02	0.29 ± 0.16	0.99 ± 0.06	-	-	3.46 ± 0.04	0.99 ± 0.06	3.21 ± 0.05	0.72 ± 0.03	-
3	4.36 ± 0.05	1.09 ± 0.13	2.21 ± 0.10	-	-	4.65 ± 0.27	1.54 ± 0.09	4.52 ± 0.14	1.20 ± 0.05	-
6	6.07 ± 0.09	1.93 ± 0.07	3.68 ± 0.08	-	0.74 ± 0.01	6.24 ± 0.64	3.68 ± 0.14	6.87 ± 0.14	3.03 ± 0.01	-
9	7.26 ± 0.05	3.83 ± 0.18	4.78 ± 0.10	0.55 ± 0.03	0.93 ± 0.03	7.85 ± 0.07	4.86 ± 0.17	7.96 ± 0.05	4.43 ± 0.02	-
12	7.60 ± 0.27	5.71 ± 0.12	6.68 ± 0.17	0.91 ± 0.01	1.54 ± 0.01	8.73 ± 0.08	6.03 ± 0.13	8.49 ± 0.02	5.71 ± 0.01	-
15	7.95 ± 0.04	6.52 ± 0.46	6.98 ± 0.04	1.44 ± 0.02	1.91 ± 0.03	9.21 ± 0.07	7.27 ± 0.041	9.04 ± 0.03	7.09 ± 0.05	-
18	8.28 ± 0.03	6.77 ± 0.23	7.66 ± 0.01	1.95 ± 0.04	2.64 ± 0.01	9.32 ± 0.13	7.96 ± 0.002	9.14 ± 0.11	7.73 ± 0.06	-
21	9.49 ± 0.05	7.24 ± 0.19	7.88 ± 0.08	2.28 ± 0.02	3.11 ± 0.03	8.99 ± 0.03	9.20 ± 0.038	9.25 ± 0.11	8.98 ± 0.02	-

The values in the table represent the mean ± standard deviation of UV-, nisin-, and heat-treated tangerine juice obtained from the 3 replicates. Control: tangerine juice without any treatment; UV: 149.76 J/cm^2 ultraviolet radiation dose; NS: 200 ppm of nisin; Pasteurization: tangerine juice pasteurized for 1 min at 95 ± 1 °C (come-up time was 1 min 50 s).

Table 5. Chemical quality of tangerine juice samples subjected to combined treatments with UV radiation and nisin during storage (4°C).

Storage Time (Days)	pH					Total Soluble Solid (Brix)					Titratable Acidity (TA % Malic Acid)				
	Control	UV	NS	UV + NS	Pasteurization	Control	UV	NS	UV + NS	Pasteurization	Control	UV	NS	UV + NS	Pasteurization
0	3.88 ± 0.025	3.88 ± 0.018	3.88 ± 0.021	3.88 ± 0.001	3.88 ± 0.005	8.51 ± 0.05	9.30 ± 0.14	8.75 ± 0.01	9.30 ± 0.07	9.38 ± 0.04	0.42 ± 0.029	0.42 ± 0.029	0.42 ± 0.029	0.42 ± 0.032	0.42 ± 0.029
3	3.82 ± 0.021	3.86 ± 0.021	3.85 ± 0.025	3.86 ± 0.005	3.87 ± 0.005	8.34 ± 0.05	9.00 ± 0.01	8.60 ± 0.01	9.15 ± 0.01	9.30 ± 0.01	0.44 ± 0.011	0.43 ± 0.016	0.44 ± 0.034	0.41 ± 0.005	0.40 ± 0.001
6	3.77 ± 0.004	3.86 ± 0.032	3.83 ± 0.046	3.85 ± 0.010	3.87 ± 0.001	8.23 ± 0.04	8.70 ± 0.21	8.48 ± 0.04	8.85 ± 0.01	9.20 ± 0.01	0.49 ± 0.027	0.44 ± 0.018	0.46 ± 0.02	0.42 ± 0.005	0.40 ± 0.001
9	3.68 ± 0.007	3.85 ± 0.032	3.78 ± 0.007	3.85 ± 0.001	3.87 ± 0.005	8.05 ± 0.01	8.50 ± 0.21	8.35 ± 0.14	8.75 ± 0.01	9.05 ± 0.01	0.52 ± 0.032	0.47 ± 0.014	0.5 ± 0.029	0.44 ± 0.016	0.40 ± 0.001
12	3.59 ± 0.032	3.82 ± 0.039	3.76 ± 0.014	3.84 ± 0.005	3.87 ± 0.001	7.70 ± 0.21	8.40 ± 0.35	8.23 ± 0.25	8.65 ± 0.01	8.95 ± 0.01	0.58 ± 0.027	0.5 ± 0.007	0.53 ± 0.018	0.45 ± 0.009	0.40 ± 0.001
15	3.54 ± 0.011	3.78 ± 0.060	3.66 ± 0.011	3.81 ± 0.005	3.87 ± 0.005	7.45 ± 0.28	8.25 ± 0.35	7.95 ± 0.28	8.50 ± 0.01	8.85 ± 0.01	0.61 ± 0.036	0.52 ± 0.011	0.55 ± 0.009	0.46 ± 0.011	0.40 ± 0.001
18	3.52 ± 0.011	3.70 ± 0.021	3.62 ± 0.018	3.78 ± 0.005	3.86 ± 0.005	7.18 ± 0.18	8.03 ± 0.25	7.68 ± 0.18	8.30 ± 0.01	8.85 ± 0.01	0.63 ± 0.016	0.55 ± 0.009	0.58 ± 0.014	0.47 ± 0.009	0.4010.001
21	3.50 ± 0.011	3.66 ± 0.025	3.56 ± 0.007	3.72 ± 0.005	3.86 ± 0.001	7.11 ± 0.05	9.30 ± 0.14	8.75 ± 0.01	9.30 ± 0.07	9.38 ± 0.04	0.66 ± 0.007	0.57 ± 0.014	0.61 ± 0.018	0.49 ± 0.009	0.41 ± 0.001

The values in the table represent the mean ± standard deviation of UV-, nisin-, and heat-treated tangerine juice during refrigerated storage obtained from the 3 replicates. Control: tangerine juice without any treatment; UV: 149.76 J/cm^2 ultraviolet radiation dose; NS: 200 ppm of nisin; Pasteurization: tangerine juice pasteurized for 1 min at 95 ± 1 °C (come-up time was 1 min 50 s).

Table 6. Color properties of tangerine juice samples subjected to single and combined treatments with UV radiation and nisin during storage (4°C).

Storage Time (Days)	L* Values					a* Values					b* Values				
	Control	UV	NS	UV + NS	Pasteurization	Control	UV	NS	UV + NS	Pasteurization	Control	UV	NS	UV + NS	Pasteurization
0	71.3 ± 0.04	71.0 ± 0.05	71.2 ± 0.00	71.0 ± 0.01	70.28 ± 0.09	11.6 ± 0.12	12.0 ± 0.01	11.5 ± 0.06	12.0 ± 0.01	12.5 ± 0.05	74.2 ± 0.04	73.9 ± 0.1	74.0 ± 0.02	74.0 ± 0.03	73.0 ± 0.03
3	71.4 ± 0.26	71.0 ± 0.01	71.2 ± 0.01	71.1 ± 0.03	70.12 ± 0.14	11.5 ± 0.01	12.0 ± 0.01	11.5 ± 0.01	12.1 ± 0.04	12.5 ± 0.07	74.2 ± 0.03	73.9 ± 0.2	74.1 ± 0.05	74.0 ± 0.00	73.0 ± 0.11
6	71.4 ± 0.04	71.1 ± 0.00	71.2 ± 0.18	71.1 ± 0.01	70.22 ± 0.04	11.5 ± 0.02	12.1 ± 0.01	11.6 ± 0.05	12.1 ± 0.01	12.5 ± 0.06	74.3 ± 0.00	74.1 ± 0.1	74.2 ± 0.05	74.1 ± 0.01	73.0 ± 0.01
9	71.5 ± 0.07	71.1 ± 0.05	71.4 ± 0.10	71.1 ± 0.01	70.30 ± 0.08	11.6 ± 0.15	12.1 ± 0.01	11.6 ± 0.07	12.1 ± 0.01	12.6 ± 0.09	74.5 ± 0.07	74.1 ± 0.1	74.3 ± 0.07	74.1 ± 0.01	73.1 ± 0.01
12	71.7 ± 0.11	71.2 ± 0.04	71.5 ± 0.07	71.1 ± 0.01	70.32 ± 0.07	11.9 ± 0.01	12.1 ± 0.03	11.7 ± 0.06	12.1 ± 0.03	12.6 ± 0.08	74.7 ± 0.07	74.1 ± 0.1	74.4 ± 0.11	74.1 ± 0.04	73.1 ± 0.01
15	71.7 ± 0.21	71.2 ± 0.03	71.7 ± 0.07	71.1 ± 0.01	70.33 ± 0.06	12.0 ± 0.04	12.2 ± 0.03	11.7 ± 0.03	12.1 ± 0.01	12.6 ± 0.09	74.8 ± 0.14	74.2 ± 0.1	74.6 ± 0.11	74.1 ± 0.01	73.1 ± 0.03
18	71.9 ± 0.12	71.2 ± 0.01	71.8 ± 0.04	71.1 ± 0.02	70.36 ± 0.04	12.0 ± 0.05	12.2 ± 0.02	11.8 ± 0.04	12.2 ± 0.02	12.6 ± 0.10	75.0 ± 0.07	74.3 ± 0.01	74.8 ± 0.07	74.2 ± 0.06	73.1 ± 0.04
21	72.0 ± 0.16	71.3 ± 0.04	71.9 ± 0.01	71.2 ± 0.01	70.40 ± 0.10	12.1 ± 0.08	12.2 ± 0.07	11.9 ± 0.05	12.2 ± 0.03	12.7 ± 0.07	75.4 ± 0.07	74.4 ± 0.0	75.0 ± 0.09	74.2 ± 0.01	73.2 ± 0.04

The values in the table represent the mean ± standard deviation of UV-, nisin-, and heat-treated tangerine juice during refrigerated storage obtained from the 3 replicates. Control: tangerine juice without any treatment; UV: 149.76 J/cm^2 ultraviolet radiation dose; NS: 200 ppm of nisin; Pasteurization: tangerine juice pasteurized for 1 min at 95 ± 1 °C (come-up time was 1 min 50 s).

Table 7. Effects of UV radiation, nisin, UV + nisin, and pasteurization on antioxidant properties of tangerine juice during storage (4 °C).

Antioxidant Properties	Storage Time (Days)							
	0	3	6	9	12	15	18	21
TPC (mg GAE/L)								
Control	213.14 ± 3.40	203.04 ± 9.31	193.18 ± 8.85	189.15 ± 8.93	181.92 ± 15.01	173.29 ± 8.91	165.79 ± 14.92	160.06 ± 15.68
UV	136.53 ± 5.45	123.37 ± 11.34	114.93 ± 10.47	110.77 ± 11.34	107.45 ± 10.63	102.11 ± 6.15	95.22 ± 1.75	90.24 ± 5.34
NS	212.64 ± 2.43	196.86 ± 15.73	187.30 ± 10.80	185.31 ± 11.93	182.64 ± 10.80	176.84 ± 8.10	169.59 ± 10.80	166.38 ± 10.80
UV + NS	135.16 ± 11.61	124.74 ± 9.18	118.81 ± 5.42	109.76 ± 10.28	105.69 ± 11.88	102.98 ± 12.68	98.1 ± 13.49	86.69 ± 5.78
Pasteurization	97.39 ± 1.75	85.90 ± 4.78	76.9 ± 1.86	76.55 ± 3.7	74.70 ± 2.21	71.23 ± 1.40	60.45 ± 3.75	53.54 ± 1.16
Total Flavonoid Content (mg QE/L)								
Control	183.18 ± 2.68	176.67 ± 1.24	166.45 ± 0.78	165.38 ± 1.59	162.08 ± 1.52	151.07 ± 4.58	139.23 ± 0.66	129.45 ± 7.11
UV	170.19 ± 2.33	161.56 ± 0.08	156.48 ± 0.66	149.34 ± 1.2	141.53 ± 0.58	134.14 ± 1.94	123.26 ± 5.44	104.01 ± 4.78
NS	179.80 ± 0.78	171.12 ± 1.55	169.97 ± 1.17	168.76 ± 0.78	161.29 ± 1.94	142.25 ± 0.12	136.29 ± 0.39	133.40 ± 2.37
UV + NS	166.26 ± 3.15	161.48 ± 1.13	153.43 ± 2.33	147.41 ± 4.47	144.20 ± 0.47	133.15 ± 7.23	127.11 ± 7.77	99.42 ± 1.55
Pasteurization	147.55 ± 1.01	146.18 ± 0.16	144.61 ± 0.51	133.98 ± 0.62	125.71 ± 4.47	117.03 ± 1.59	106.09 ± 1.75	88.84 ± 0.74
Total Carotenoid Content (μg/100 mL)								
Control	16.6 ± 0.96	16.05 ± 1.01	15.18 ± 1.18	14.33 ± 2.11	13.96 ± 1.91	13.13 ± 1.57	12.8 ± 1.51	12.08 ± 1.28
UV	13.82 ± 0.98	13.13 ± 0.78	12.44 ± 1.14	11.62 ± 1.09	11.19 ± 1.14	10.31 ± 0.82	9.20 ± 0.49	8.67 ± 0.38
NS	16.22 ± 0.24	15.86 ± 0.39	14.86 ± 0.06	14.41 ± 0.28	13.9 ± 0.39	13.31 ± 0.26	12.49 ± 0.2	11.73 ± 0.10
UV + NS	14.16 ± 1.27	13.67 ± 0.84	12.66 ± 1.05	12.09 ± 0.76	11.52 ± 0.66	10.67 ± 0.09	10.04 ± 0.28	8.82 ± 0.55
Pasteurization	7.64 ± 1.06	7.04 ± 1.21	6.49 ± 1.17	6.00 ± 1.11	5.50 ± 0.98	4.65 ± 0.93	4.07 ± 1.08	3.56 ± 0.92
Vitamin C (mg/100 mL)								
Control	46.32 ± 2.63	42.06 ± 2.26	41.05 ± 2.26	36.48 ± 2.26	33.9 ± 0.11	32.36 ± 0.64	30.95 ± 0.38	28.77 ± 0.30
UV	35.15 ± 1.88	33.77 ± 1.28	31.32 ± 2.03	26.37 ± 1.50	24.27 ± 1.62	22.06 ± 2.26	19.96 ± 3.27	17.99 ± 1.62
NS	47.25 ± 0.94	43.02 ± 2.11	40.71 ± 1.77	36.90 ± 0.15	34.4 ± 1.05	30.31 ± 0.75	29.03 ± 0.75	26.45 ± 1.47
UV + NS	36.05 ± 1.50	34.62 ± 0.15	32.84 ± 0.04	27.97 ± 1.05	25.31 ± 1.28	21.74 ± 1.20	20.55 ± 2.29	17.62 ± 1.77
Pasteurization	28.37 ± 1.84	26.08 ± 1.02	24.56 ± 1.73	22.81 ± 0.60	18.45 ± 0.75	16.27 ± 0.75	15.31 ± 0.75	12.01 ± 0.75

Table 7. *Cont.*

Antioxidant Properties	Storage Time (Days)							
	0	3	6	9	12	15	18	21
DPPH (mM Trolox/100 mL)								
Control	392.18 ± 3.64	361.45 ± 1.82	355.18 ± 3.09	340.45 ± 7.82	323.55 ± 7.82	297.09 ± 5.45	290.82 ± 18.36	256.00 ± 1.09
UV	347.82 ± 2.31	332.91 ± 21.86	302.27 ± 1.16	278.82 ± 1.41	263.91 ± 5.01	260.45 ± 3.73	248.18 ± 1.54	226.09 ± 3.99
NS	381.27 ± 7.97	353.45 ± 3.60	347.73 ± 3.99	328.55 ± 3.60	303.64 ± 2.57	292.91 ± 3.34	283.82 ± 3.34	249.27 ± 6.43
UV + NS	333.27 ± 5.66	317.00 ± 7.07	307.45 ± 29.31	265.09 ± 7.71	254.00 ± 4.37	248.00 ± 3.60	236.82 ± 1.93	227.82 ± 5.40
Pasteurization	292.18 ± 4.37	287.09 ± 3.34	282.00 ± 5.14	233.45 ± 9.77	224.55 ± 2.57	211.82 ± 2.57	202.55 ± 4.37	170.64 ± 4.24
FRAP (mM Trolox/100 mL)								
Control	367.75 ± 3.51	331.09 ± 12.63	322.49 ± 0.35	304.25 ± 3.16	295.04 ± 1.23	289.68 ± 0.35	283.28 ± 0.53	272.4 ± 2.28
UV	325.65 ± 0.50	303.11 ± 2.61	296.70 ± 0.99	280.47 ± 1.12	268.19 ± 1.12	263.46 ± 2.61	255.21 ± 4.84	239.33 ± 6.2
NS	358.81 ± 2.23	331.96 ± 3.97	319.51 ± 11.91	310.74 ± 9.68	287.32 ± 3.6	280.21 ± 6.45	275.21 ± 10.3	265.21 ± 9.06
UV + NS	320.47 ± 3.10	316.61 ± 2.61	292.05 ± 2.61	273.28 ± 5.09	263.81 ± 0.37	268.19 ± 25.18	253.89 ± 11.66	226.79 ± 1.61
Pasteurization	290.56 ± 3.23	274.51 ± 6.57	268.19 ± 3.6	249.16 ± 3.47	244.33 ± 3.85	223.81 ± 5.58	220.56 ± 6.45	207.23 ± 2.48

The values in the table represent the mean ± standard deviation of UV-, nisin-, and heat-treated tangerine juice during refrigerated storage obtained from the 3 replicates. Control: tangerine juice without any treatment; UV: 149.76 J/cm^2 ultraviolet radiation dose; NS: 200 ppm of nisin; Pasteurization: tangerine juice pasteurized for 1 min at 95 ± 1 °C (come-up time was 1 min 50 s).

The ascorbic acid content of the juice decreased by up to 40% during a 24-day storage period at both 4 °C and 20 °C. The storage of watermelon juice, which underwent pasteurization for 15 min, for more than 9 days had adverse effects on its color, total phenolic content, and antioxidant capacities, as reported in a study by Mandha et al. [29]. In another finding, the vitamin C content of unpasteurized mango juice decreased during storage. Furthermore, according to a study by de Oliveira Junior et al. in 2015 [23], nisin remained stable in various juices for at least 30 days at room or refrigerated temperature.

4. Conclusions

The log reductions demonstrate the efficacy of UV radiation at 149.76 J/cm^2 and pasteurization in the tested microorganisms. The first-order kinetic model inhibited microbial growth compared with the zero-order model and was more efficient. Both UV treatment and the addition of nisin significantly reduced the microbial population in tangerine juice. When UV and nisin were combined (UV + NS), no significant changes were observed in the pH, TSS, and TA values. However, notable distinctions were noted in color analysis, total phenolic compound, total flavonoid content, vitamin C and carotenoid content, as well as antioxidant activity according to DPPH and FRAP values. These results (high in functionality) have many health implications, such as helping stop or limit the damage caused by free radicals in the body and preventing them from causing damage to other cells. During storage at 4 °C, the UV + NS sample exhibited the lowest microbial load among all the samples. Furthermore, the UV + NS combination did not noticeably affect the color properties of the tangerine juice during the 21-day refrigerated storage period. While the physicochemical properties changed over time for all treatments, the antioxidant properties scored better compared with thermal pasteurization. In conclusion, the combination of UV and nisin (UV + NS) holds the potential to preserve the quality of tangerine juice during 9 days of storage at 4 °C.

Supplementary Materials: The following supporting information can be downloaded at https://www.mdpi.com/article/10.3390/foods12142725/s1. Table S1. Total plate counts, yeast and mold counts, and selected microbial counts of orange juice samples subjected to different doses of UV-radiation. Table S2. Total microbial and yeast and mold counts, and pathogenic microbial counts of orange juice samples subjected to different levels of nisin. Table S3. Physiochemical characteristics of orange juice subjected to different doses of UV-radiation and nisin.

Author Contributions: Conceptualization, K.A. and I.K.; methodology, K.A., I.K., K.A.S. and S.J.; formal analysis, I.K. and K.A.S.; investigation, I.K. and K.A.S.; data curation, I.K.; writing—original draft preparation, K.A., I.K., K.A.S. and S.J.; writing—review and editing, R.W.W.; supervision, K.A.; project administration, K.A.; funding acquisition, K.A. All authors have read and agreed to the published version of the manuscript.

Funding: This research was funded by the 90th Anniversary of Chulalongkorn University Scholarship under the Ratchadaphisek Somphot Fund, Overseas Research Experience Scholarship for Graduate Student, Graduate School, Chulalongkorn University and the Faculty of Science, Chulalongkorn University.

Data Availability Statement: The data presented in this study are available on request from the corresponding author.

Acknowledgments: The authors would like to thank the Second Century Fund (C2F), Chulalongkorn University for providing postdoctoral fellowship to Saeid Jafari and Khursheed Ahmad Shiekh.

Conflicts of Interest: The authors declare that they have no known competing financial interests or personal relationships that could have appeared to influence the work reported in this paper.

References

1. Sovacool, B.K.; Bazilian, M.; Griffiths, S.; Kim, J.; Foley, A.; Rooney, D. Decarbonizing the food and beverages industry: A critical and systematic review of developments, sociotechnical systems and policy options. *Renew. Sustain. Energy Rev.* **2021**, *143*, 110856. [CrossRef]
2. Sirichan, T.; Kijpatanasilp, I.; Asadatorn, N.; Assatarakul, K. Optimization of ultrasound extraction of functional compound from makiang seed by response surface methodology and antimicrobial activity of optimized extract with its application in orange juice. *Ultrason. Sonochemistry* **2022**, *83*, 105916. [CrossRef] [PubMed]
3. Kijpatanasilp, I.; Narumonlittikrai, P.; Sheikh, K.A.; Jafari, S.; Worobo, R.W.; Assatarakul, K. Microbial inhibition and shelf-life extension of longan (*Dimocarpus longan*) juice by UV radiation. *Food Control* **2023**, *149*, 109694. [CrossRef]
4. Ibarz, A.; Garvín, A.; Falguera, V. Ultraviolet in food preservation and processing. In *Conventional and Advanced Food Processing Technologies*; Wiley Online Library: Hoboken, NJ, USA, 2014; pp. 411–436.
5. Liao, H.; Jiang, L.; Cheng, Y.; Liao, X.; Zhang, R. Application of nisin-assisted thermosonication processing for preservation and quality retention of fresh apple juice. *Ultrason. Sonochemistry* **2018**, *42*, 244–249. [CrossRef]
6. Verma, D.K.; Thakur, M.; Singh, S.; Tripathy, S.; Gupta, A.K.; Baranwal, D.; Patel, A.R.; Shah, N.; Utama, G.L.; Niamah, A.K.; et al. Bacteriocins as antimicrobial and preservative agents in food: Biosynthesis, separation and application. *Food Biosci.* **2022**, *46*, 101594. [CrossRef]
7. Lanclos, C.E. A Study of UV Radiation and Lactic Acid Bacteria Derived Bacteriocins on the Reduction of Bacterial Loads on Shrimp. Master's Thesis, Louisiana State University, Baton Rouge, LA, USA, 2021.
8. Ferreira, T.V.; Mizuta, A.G.; de Menezes, J.L.; Dutra, T.V.; Bonin, E.; Castro, J.C.; dos Anjos Szczerepa, M.M.; Pilau, E.J.; Nakamura, C.V.; Mikcha, J.M.G.; et al. Effect of ultraviolet treatment (UV–C) combined with nisin on industrialized orange juice in *Alicyclobacillus acidoterrestris* spores. *LWT* **2020**, *133*, 109911. [CrossRef]
9. Li, Y.; Wu, Y.; Quan, W.; Jia, X.; He, Z.; Wang, Z.; Adhikari, B.; Chen, J.; Zeng, M. Quantitation of furosine, furfurals, and advanced glycation end products in milk treated with pasteurization and sterilization methods applicable in China. *Food Res. Int.* **2021**, *140*, 110088. [CrossRef]
10. AOAC. *Official Method of Analysis of AOAC International*, 15th ed.; Association of Official Analytical Chemists: Washington, DC, USA, 1995.
11. Jafari, S.; Karami, Z.; Shiekh, K.A.; Kijpatanasilp, I.; Worobo, R.W.; Assatarakul, K. Ultrasound-Assisted Extraction of Bioactive Compounds from Cocoa Shell and Their Encapsulation in Gum Arabic and Maltodextrin: A Technology to Produce Functional Food Ingredients. *Foods* **2023**, *12*, 412. [CrossRef] [PubMed]
12. Jafari, S.; Rungroj, N.; Worobo, R.W.; Assatarakul, K. Kinetic study of selected microorganisms and quality attributes during cold storage of mango and passion fruit smoothie subjected to dimethyl dicarbonate. *Int. J. Food Microbiol.* **2021**, *358*, 109404. [CrossRef]
13. Shiekh, K.A.; Luanglaor, T.; Hanprerakriengkrai, N.; Jafari, S.; Kijpatanasilp, I.; Asadatorn, N.; Assatarakul, K. Antioxidants and Quality Changes of Thermally Processed Purple Corn (*Zea mays* L.) Milk Fortified with Low Sucrose Content during Cold Storage. *Foods* **2023**, *12*, 277. [CrossRef]
14. Gayán, E.; Condón, S.; Álvarez, I. Biological Aspects in Food Preservation by Ultraviolet Light: A Review. *Food Bioprocess Technol.* **2014**, *7*, 1–20. [CrossRef]
15. Singh, H.; Bhardwaj, S.K.; Khatri, M.; Kim, K.-H.; Bhardwaj, N. UVC radiation for food safety: An emerging technology for the microbial disinfection of food products. *Chem. Eng. J.* **2021**, *417*, 128084. [CrossRef]
16. Aaliya, B.; Sunooj, K.V.; Navaf, M.; Akhila, P.P.; Sudheesh, C.; Mir, S.A.; Sabu, S.; Sasidharan, A.; Hlaing, M.T.; George, J. Recent trends in bacterial decontamination of food products by hurdle technology: A synergistic approach using thermal and non-thermal processing techniques. *Food Res. Int.* **2021**, *147*, 110514. [CrossRef] [PubMed]
17. Colás-Medà, P.; Nicolau-Lapeña, I.; Viñas, I.; Neggazi, I.; Alegre, I. Bacterial Spore Inactivation in Orange Juice and Orange Peel by Ultraviolet-C Light. *Foods* **2021**, *10*, 855. [CrossRef]
18. Liu, G.; Nie, R.; Liu, Y.; Mehmood, A. Combined antimicrobial effect of bacteriocins with other hurdles of physicochemic and microbiome to prolong shelf life of food: A review. *Sci. Total Environ.* **2022**, *825*, 154058. [CrossRef]
19. Jensen, C.; Li, H.; Vestergaard, M.; Dalsgaard, A.; Frees, D.; Leisner, J.J. Nisin Damages the Septal Membrane and Triggers DNA Condensation in Methicillin-Resistant *Staphylococcus aureus*. *Front. Microbiol.* **2020**, *11*, 1007. [CrossRef]
20. Mok, J.H.; Pyatkovskyy, T.; Yousef, A.; Sastry, S.K. Effects of combination shear stress, moderate electric field (MEF), and nisin on kinetics and mechanisms of inactivation of *Escherichia coli* K12 and *Listeria innocua* in fresh apple-kale blend juice. *J. Food Eng.* **2021**, *292*, 110262. [CrossRef]
21. Jeon, M.J.; Ha, J.W. Inactivating foodborne pathogens in apple juice by combined treatment with fumaric acid and ultraviolet-A light, and mechanisms of their synergistic bactericidal action. *Food Microbiol.* **2020**, *87*, 103387. [CrossRef]
22. Ling, J.K.U.; Sam, J.H.; Jeevanandam, J.; Chan, Y.S.; Nandong, J. Thermal Degradation of Antioxidant Compounds: Effects of Parameters, Thermal Degradation Kinetics, and Formulation Strategies. *Food Bioprocess Technol.* **2022**, *15*, 1919–1935. [CrossRef]
23. de Oliveira Junior, A.A.; Couto, H.G.S.D.A.; Barbosa, A.A.T.; Carnelossi, M.A.G.; de Moura, T.R. Stability, antimicrobial activity, and effect of nisin on the physico-chemical properties of fruit juices. *Int. J. Food Microbiol.* **2015**, *211*, 38–43. [CrossRef]
24. Pravallika, K.; Chakraborty, S. Effect of nonthermal technologies on the shelf life of fruits and their products: A review on the recent trends. *Appl. Food Res.* **2022**, *2*, 100229. [CrossRef]

25. Visuthiwan, S.; Assatarakul, K. Kinetic modeling of microbial degradation and antioxidant reduction in lychee juice subjected to UV radiation and shelf life during cold storage. *Food Control* **2021**, *123*, 107770. [CrossRef]
26. Fundo, J.F.; Miller, F.A.; Mandro, G.F.; Tremarin, A.; Brandão, T.R.S.; Silva, C.L.M. UV-C light processing of Cantaloupe melon juice: Evaluation of the impact on microbiological, and some quality characteristics, during refrigerated storage. *LWT* **2019**, *103*, 247–252. [CrossRef]
27. Polydera, A.C.; Stoforos, N.G.; Taoukis, P.S. Comparative Shelf Life Study and Vitamin C Loss Kinetics in Pasteurised and High Pressure Processed Reconstituted Orange Juice. *J. Food Eng.* **2003**, *60*, 21–29. [CrossRef]
28. Chia, S.L.; Rosnah, S.; Noranizan, M.A.; Wan Ramli, W.D. The effect of storage on the quality attributes of ultraviolet-irradiated and thermally pasteurised pineapple juices. *Int. Food Res. J.* **2012**, *19*, 1001–1010.
29. Mandha, J.; Shumoy, H.; Matemu, A.O.; Raes, K. Characterization of fruit juices and effect of pasteurization and storage conditions on their microbial, physicochemical, and nutritional quality. *Food Biosci.* **2023**, *51*, 102335. [CrossRef]

foods

MDPI

Article

Effects of Different Bacteriostats on the Dynamic Germination of *Clostridium perfringens* Spores

Dong Liang [1,2,†], Shengnan Liu [1,2,†], Miaoyun Li [1,2,*], Yaodi Zhu [1,2], Lijun Zhao [1,2], Lingxia Sun [1,2], Yangyang Ma [1,2] and Gaiming Zhao [1,2]

[1] College of Food Science and Technology, Henan Agricultural University, Zhengzhou 450002, China; liangdong0221@126.com (D.L.); 18839004375@163.com (S.L.)
[2] International Joint Laboratory of Meat Processing and Safety in Henan Province, Henan Agricultural University, Zhengzhou 450002, China
* Correspondence: limiaoyun@henau.edu.cn; Tel.: +86-371-63558150
† These authors contributed equally to this work.

Abstract: Bacteriostats, as chemical substances that inhibit bacterial growth, are widely used in the sterilization process; however, their effects on spindle spores are unclear. In this study, the effects of bacteriostats, including nine commonly used food additives and four detergents, on the growth of *Clostridium perfringens* spores were investigated. The results showed that 0.07‰ ethylenediaminetetraacetate had a good inhibitory effect on *C. perfringens* spore growth, and the spore turbidity decreased by 4.8% after incubation for 60 min. Furthermore, 0.3‰ tea polyphenols, 0.8‰ D-isoascorbic acid, and 0.75‰ potassium sorbate promoted leakage of contents during spore germination. Among the four detergents, 5‰ glutaraldehyde solution presented the best inhibitory effect on the growth of *C. perfringens* spores, and the spore turbidity decreased by 5.6% after incubation for 60 min. Further analysis of the inactivation mechanism of spores by the bacteriostats was performed by comparing the leakage of UV-absorbing substances during germination. The results revealed that bacteriostats could not directly kill the spores, but could inactivate them by inhibiting germination or damaging the spore structure during germination, thus preventing the formation of bacterial vegetative bodies. These findings provide important information and reference for the mechanism underlying the effects of different bacteriostatic agents on spore growth.

Keywords: *Clostridium perfringens*; bacteriostat; spores; germination

1. Introduction

Clostridium perfringens (*C. perfringens*) is a common food-borne bacterium that can form spores in harsh growth environments. These bacterial spores are widely distributed in air, soil, sewage, and food, and are difficult to kill owing to their unique structure [1–3]. Under suitable conditions for bacterial growth, the spores germinate and become vegetative forms, causing food contamination and bag swelling, resulting in serious economic losses and threatening the health and safety of consumers [4–7]. In the current food production process, bacteriostatic agents are commonly added to raw food materials and auxiliary materials, and cleaning agents are sprayed in the production environment to eliminate and kill harmful bacteria, thereby preventing food spoilage, prolonging the shelf life of food, and ensuring food safety [8–11].

In recent years, the effects of a variety of chemical and physical components on the germination and expansion of spores have been well investigated. Some studies have shown that nisin could inhibit the germination and reproduction of heat-activated spores, and that ethylene oxide could inactivate proteins and nucleic acids by reacting with different chemical groups, essentially destroying spores [12]. However, it is difficult to identify basic pressure breaking as the primary cause of spore death [3], and the changes in the external environment pH, osmotic pressure, temperature, chemical treatment, etc., are insufficient to

completely kill the spores [13]. Nevertheless, once the spores germinate and become vegetative forms, the bacteriostatic agent can enter the thalli and cause acidification or extraction, possibly leading to metabolic disorders and cell death [11,14,15]. Many antibacterial agents have been shown to be effective against most of the Gram-positive and Gram-negative bacteria by destroying the cell wall or cell membrane, acting on intracellular nucleic acids or proteins, affecting their expression and synthesis, and inhibiting the activity of related enzymes in the cells [10,11,15,16]. For example, ε-polylysine hydrochloride, nitrite and other substances can destroy the integrity of the bacterial cell membrane and are thus selected as food preservatives [17]. Potassium sorbate inhibits the activity of microbial dehydrogenase and destroys multiple major enzyme systems to achieve preservative efficacy [11,16,18]. D- isoascorbic acid could reduce the oxygen concentration in the system and inhibit bacterial propagation [10]. "Tea polyphenols" is the general name for phenols in tea, including flavanols (catechins), flavonols and their predecessors, flavonoids (anthoxanthin), hydroxy-4-flavanols, anthocyanins, phenolic acids, phenolic acids, and other polyphenols [19]. Since tea polyphenols can change the normal morphology of bacteria and damage the cell wall structure, they have gradually become a natural antibacterial agent and are widely used [9]. Whey protein baking powder is a natural fresh-keeping food raw material. Unlike traditional bacteriostatic agents, it can be used in various foods to maximize the maintenance of food freshness and shelf life and block the spread of food-borne diseases. However, there is relatively little research on whey protein baking powder at present, and its antibacterial mechanism is still unclear. Glutaraldehyde is a high-efficiency disinfectant commonly used in industry [12]. Its bactericidal mechanism is mainly through the protein alkylation reaction of microorganisms, blocking the outer layer of cells of bacteria, and inactivating cell enzymes to kill bacteria. Trichloroisocyanuric acid and hydrogen peroxide Ag+ are industrial disinfectants with certain corrosivity [20]. Under certain conditions, they can be decomposed into small molecular substances and destroy the cell structure. Therefore, they are used as a new generation of high-efficiency disinfectants [12]. However, it is still unclear whether these agents can produce the same effects on spore growth. Studies have indicated that the resistance of spores varies with the chemicals [21]. Some oxidants have been found to damage the inner membrane of the spores, rupturing the inner membrane during germination [22], while other compounds, such as nitrous acid and formaldehyde, can kill spores through DNA damage [7,23]. Moreover, the mechanism by which some compounds kill spores is still unknown. While the majority of previous studies have focused on Bacillus spores, research on *Clostridium* spores, and particularly the wild-type spores from industry, is still limited. Moreover, the effect of a single antibacterial treatment on spore germination has only rarely been recorded [21,24,25].

The objective of this study was to test the inhibition and killing mechanisms of different bacteriostats on the representative strain of wild-type spores, *C. perfringens*. Spores were studied by comparing the effects of different microbial agents on spore germination and growth.

2. Materials and Methods

2.1. Materials and Reagents

Sodium dichloroisocyanurate, trichloroisocyanuric acid, 4-chloro-3,5-dimethylphenol, McLean Biochemical Technology Co., Ltd., Shanghai, China; terbium chloride($TbCl_3$), Nycodenz, tea polyphenols (catechin content accounted for 41.31%, epicatechin content accounted for 19.72%, quercetin content accounted for 3.71%, and gallic acid content accounted for 4.75%), Macklin Biochemical Technology Co., Ltd., Shanghai, China; nisin, nitrite, potassium sorbate, D-isoascorbic acid, sodium diacetate, ε-polylysine hydrochloride, Sigma-Aldrich Trading Co., Ltd., Shanghai, China; tryptose Sulfite cycloserine Agar Base (TSC), thioglycollate medium (FTG), Hi-tech Industrial Park Haibo Biotechnology Co., Ltd., Shandong, China; whey protein fermentation powder, yinong biology science and technology Co., Ltd., Shanghai, China; Other reagents such as glutaraldehyde, silver nitrate standard solution and hydrogen peroxide solution are analytically pure in China.

2.2. Instrumentation and Equipment

SpectraMax M2e multifunctional microplate reader, Finland, California USA; MIR-254 Low-temperature Incubator, SANYO Company, Osaka, Japan; SW-CJ-2F clean bench, Suzhou Aetna Air Technology Co., Ltd., Jiangsu, China; Vortex-2 Genee Vortex Oscillator, ScientificIndustries, CA, USA; ECLIPSE 80i Biological Microscope, NIKON, Osaka, Japan; FA 2004A Electronic Analytical Balance, Jingtian Electronic Instrument Co., Ltd., Shanghai, China; HVE-50 steam autoclave, HIRAYAMA Co., Ltd., Osaka, Japan; Fluorescence Spectrometry, Thermo Fisher Scientific Shile Technology (China) Co., Ltd., Shanghai, China; ALLEGRA-64A high-speed refrigerated centrifuge Beckman Coulter, USA; HH-501 digital display super constant temperature water bath, Jintan Jerry Electric Appliance Co., Ltd., Changzhou, China.

2.3. Preparation of C. perfringens Suspension and Spores

In this study, a wild-type *C. perfringens* was used, which was isolated directly from a vacuum-packaged cooked meat by the Microbiology Laboratory of the College of Food Science and Technology, Henan Agricultural University (China) and identified by Sangon Biotech Co., Ltd., (Shanghai, China).

To prepare *C. perfringens* suspension, typical black colonies of *C. perfringens* on TSC plates were selected and inoculated into fresh FTG medium for anaerobic cultivation at 37 °C for 18 h until growth stability stage, according to Ren's method [26]. For anaerobic cultivation at 37 °C for 48 h, the usual black colonies of *C. perfringens* chosen from TSC plates were inoculated into 10 mL of cornstarch medium. The *C. perfringens* spores were prepared as described previously [27], and the spore suspension was centrifuged at 5000× *g* and 4 °C for 10 min, washed with sterile water 5–7 times, suspended in sterile peptone water, and stored at 20 °C until further use.

2.4. Treatment of Spore Suspension with Different Bacteriostats

A known standard of spore suspension and a bacteriostat were added to a sterile polytetrafluoroethylene centrifuge tube. The concentrations of food additive bacteriostats, including tea polyphenols, nisin, nitrite, potassium sorbate, D-isoascorbic acid, sodium diacetate, ε-polylysine hydrochloride, whey protein fermentation powder, and ethylenediaminetetraacetate, were adjusted to 0.3‰, 0.5‰, 0.15‰, 0.75‰, 0.8‰, 3‰, 5%, 1.5‰, and 0.07‰ in water, according to the allowable maximum addition amount of the national standard for food safety, respectively, while the concentrations of detergent bacteriostats, including 4-chloro-3,5-dimethylphenol, hydrogen peroxide Ag+, sodium dichloroisocyanurate and trichloroisocyanuric acid mixed solution, and glutaraldehyde, were adjusted to 0.45‰, 0.5‰, 1.2‰, and 5‰, respectively, according to industrial production standards [28].

2.5. Determination of Antibacterial Activity

A total of 4–5 rings of *C. perfringens* were picked out by inoculation ring and inoculated into FTG medium at 37 °C for 12 h. Subsequently, *C. perfringens* suspension containing cells at a concentration of 10^8 CFU/mL (optical density (OD_{600}) 0.8–1.0) was prepared using sterilized normal saline, and 100 μL of the bacterial suspension was evenly inoculated onto a sterile plate with Oxford cup in the center of the plate. The Oxford cup contained 100 μL of the bacteriostat. The blank control comprised distilled water. All of the plates were incubated in a constant-temperature incubator at 37 °C for 12 h. After incubation, the Oxford cup was taken out for observation, and the size of the bacteriostatic ring was measured and recorded [29].

2.6. Determination of Spore Survival Rate

The spore samples were incubated with a bacteriostat at 37 °C for 12 h in a water bath, gradient-diluted, and then incubated in TSC medium at 37 °C for 24 h for enumeration, and the viable number of *C. perfringens* spores was determined by the plate counting method.

2.7. Determination of Spore Turbidity

A total of 200 μL of *C. perfringens* spore suspension was collected every 5 min for 1 h, and the spore turbidity (OD_{600}%) was determined at 600 nm (Equation (1)), as described previously [30].

$$OD_{600}\% = \frac{D_d}{D_i} \times 100, \quad (1)$$

where OD_{600}% is the rate of change of OD_{600}, D_d is the decreasing value of OD_{600}, and D_i is the initial OD_{600} value.

2.8. Determination of 2,6-Pyridinedicarboxylic Acid Release from Spores

To determine 2,6-pyridinedicarboxylic acid (DPA) release from the spores, the spore suspension was centrifuged at 5180× *g* and 4 °C for 4 min, and the supernatant was treated with 50 μmol $TBCl_3$ (pH = 5.6) at a ratio of 1:3. Subsequently, the fluorescence intensity of the sample was measured using a fluorescence spectrophotometer at an excitation wavelength of 270 nm and emission wavelength of 545 nm [31]. The untreated sample served as the negative control, and the sample that was heated at 121 °C for 20 min served as the positive control. The DPA release was calculated using Equation (2) as follows:

$$\text{DPA } (\%) = \frac{F_1 - F_0}{F_2 - F_0} \times 100 \quad (2)$$

where F_0, F_1, and F_2 are the fluorescence intensities of untreated samples, bacteriostat-treated samples, and positive control samples, respectively.

2.9. Determination of Leakage of UV-Absorbing Substances from Spores

After treatment with various bacteriostats, the spore suspension was centrifuged at 4500× *g* for 15 min at 4 °C, and the supernatant was incubated with a germination inducer at 37 °C for 1 h. Subsequently, the absorbance of the sample was measured at 260 nm (for nucleic acid) and 280 nm (for protein) [32]. The untreated bacterial suspension was used as the control group, and sterile water was utilized as the blank control.

2.10. Determination of Refractive Power

To ascertain the refractive power of the spores treated with different bacteriostats, a few drops of spore suspension were placed onto a slide, covered with a coverslip, and observed for 12 h under a phase contrast microscope.

2.11. Statistical Analysis

There were at least three independent replicates, with two samples per replicate, for each treatment. Average microbial reductions, expressed in logarithmic values, were used in the statistical analyses. Comparisons between several groups were performed by one-way analysis of variance (ANOVA) using SPSS (version 26.0, Norman H. Nie, CA, USA), and the statistically significant differences were determined by Tukey's post hoc analysis to analyze mean differences. Differences at $p < 0.05$ were considered significant. Graphs were constructed using Origin 2021 software.

3. Results

3.1. Bacteriostatic Activity of Different Bacteriostats

The commonly used food additives (including tea polyphenols, nisin, nitrite, potassium sorbate, D-isoascorbic acid, sodium diacetate, ε-polylysine hydrochloride, whey protein fermentation powder, and ethylenediaminetetraacetate) and detergents (such as 4-chloro-3,5-dimethylphenol, hydrogen peroxide Ag+, mixed solution of sodium dichloroisocyanurate and trichloroisocyanuric acid, and glutaraldehyde) were selected in this study to examine their antibacterial activity against *C. perfringens*. The diameter of the inhibition zone was used to assess the antibacterial activity of the bacteriostat. An

inhibition zone with a diameter of >9 mm indicated antibacterial activity of the bacteriostat, and the larger the diameter of the inhibition zone, the stronger was the antibacterial activity of the bacteriostat [23]. Subsequently, the inhibitory effects of various bacteriostats on *C. perfringens* were compared, and the outcomes are presented in Table 1. The inhibitory effects of several food additives on *C. perfringens* significantly varied. The diameter of the inhibition zone for ethylenediaminetetraacetate, which had the best inhibitory effect on *C. perfringens* growth, was 35.33 mm, followed by those for nitrite and D-erythorbic acid, which were 32.53 and 24.67 mm, respectively. In contrast, whey protein fermentation powder did not impede the growth of *C. perfringens* vegetative cells. All four detergents could effectively inhibit *C. perfringens* growth. The diameter of the inhibition zone for the mixed solution of sodium dichloroisocyanurate and trichloroisocyanuric acid reached 30.27 mm. The antibacterial effect of the four detergents presented the following trend: glutaraldehyde > sodium dichloroisocyanurate and trichloroisocyanuric acid > hydrogen peroxide Ag+ > 4-chloro-3,5-dimethylphenol.

Table 1. Inhibitory effects of different bacteriostats on *C. perfringens*.

Sort	Name of Inhibition Agent	Diameter of Inhibition Circle/mm
Food additives	Control	8.00 ± 0.11^{a}
	Tea Polyphenols	9.20 ± 0.18^{ab}
	Nisin	13.67 ± 0.21^{b}
	Nitrite	32.53 ± 0.98^{e}
	Potassium sorbate	17.60 ± 0.31^{bc}
	D-isoascorbic acid	24.67 ± 0.83^{cd}
	Sodium diacetate	20.20 ± 0.97^{c}
	ε-Polylysine hydrochloride	16.40 ± 0.37^{b}
	Whey protein baking powder	8.00 ± 0.13^{a}
	Ethylenediaminetetraacetate	35.33 ± 0.79^{d}
Cleaning agent	Hydrogen peroxide Ag+	25.57 ± 0.53^{d}
	Sodium dichloroisocyanurate + trichloroisocyanuric acid	30.00 ± 0.79^{e}
	4-Chloro-3,5-dimethylphenol	22.57 ± 0.51^{cd}
	Glutaraldehyde	37.77 ± 0.84^{f}

Note: Mean ± standard deviation; different superscript letters indicate significant differences ($p < 0.05$).

3.2. Effects of Different Bacteriostats on Spore Inactivation

Spore viability was characterized by the number of colonies formed on the plate after a 24-h culture of the spores (Figure 1). When compared with the untreated spores, treatment with tea polyphenols exhibited the highest spore inactivation rate, reducing the number of *C. perfringens* spores by 5.015 log. Furthermore, treatment with potassium sorbate and D-isoascorbic acid caused a 3.222 log and 3.327 log decrease in spore vitality, respectively. Treatment with the four detergents dramatically decreased the survival rate of *C. perfringens* spores, and the following trend was observed: glutaraldehyde > hydrogen peroxide Ag+ > sodium dichloroisocyanurate and trichloroisocyanuric acid mixture > 4-chloro-3,5-dimethylphenol. Several bacteriostats exhibited good spore inactivation effects, as indicated by the plate counting assay. Although antibacterial agents are known to destroy spores before or after germination, the underlying mechanism is still unclear. Hence, in the present study, to better investigate the mechanisms of spore inactivation by bacteriostats, the precise stage of spore inactivation was identified by monitoring the dynamics of spore germination.

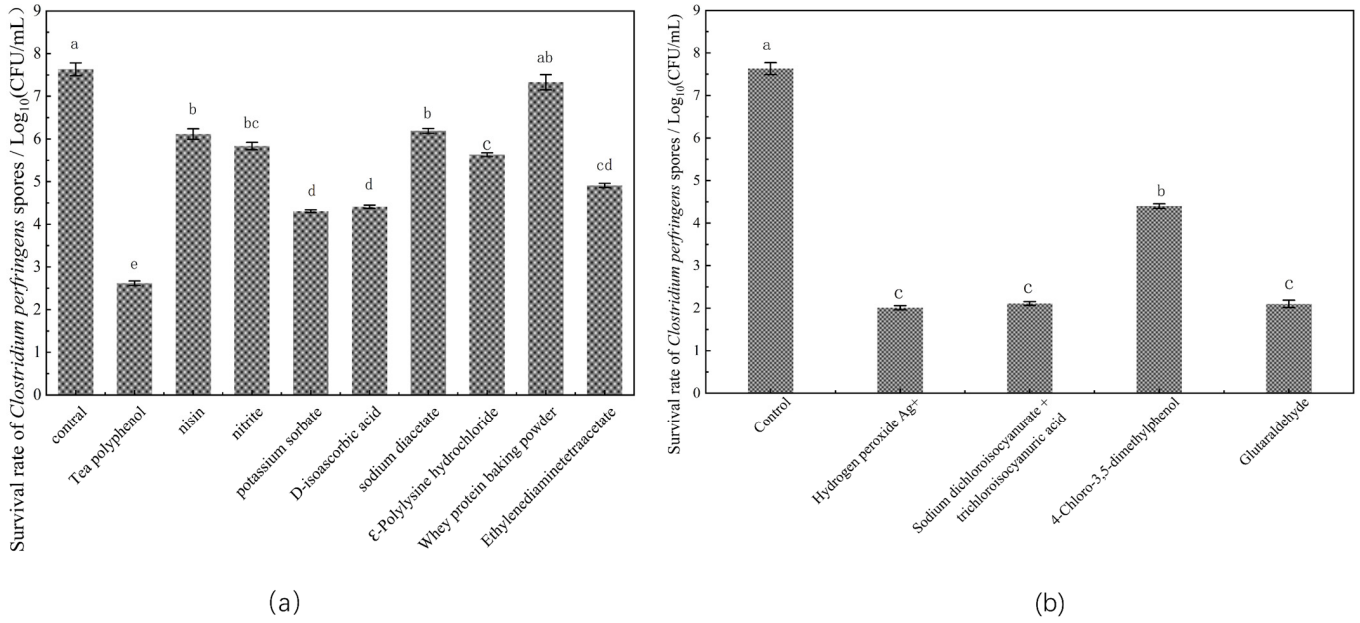

Figure 1. Inactivation of *C. perfringens* spores by different bacteriostats: (**a**) effects of food additives on spore inactivation; (**b**) effects of detergents on spore inactivation. Those with the same superscript letters indicated that the difference was not significant.

3.3. Effects of Different Bacteriostats on Spore Germination

3.3.1. Effects of Different Bacteriostats on the Turbidity of Spores

The *C. perfringens* spores treated with various bacteriostats were induced in FTG medium to study the effects of these bacteriostats on the dynamics of spore germination. During spore germination, the cores expand by absorbing water, thus altering the refractive index. The OD_{600} value of the spore suspension presented a downward trend, and the brightness of the spores gradually decreased under phase contrast microscope [18,33] (Figure 2). The turbidity of spores treated with various antimicrobial agents did not significantly change after incubating for 20 min. After incubation for 60 min, significant differences were found between the turbidity of spores treated with ethylenediaminetetraacetate, nisin, tea polyphenols, D-isoascorbic acid, and ε-polylysine hydrochloride and the untreated spores. While the $OD_{6\,00}$ value of the untreated spore suspension decreased by 13.3% after 60 min, that treated with ethylenediaminetetraacetate did not present a significant decrease, indicating that ethylenediaminetetraacetate could inhibit germination and growth of *C. perfringens* spores. The turbidity of the spore suspension treated with glutaraldehyde decreased by 5.53%, when compared with those of untreated spores and spores treated with other detergents, indicating that glutaraldehyde inhibited germination of spores and prevented the formation of vegetative bodies.

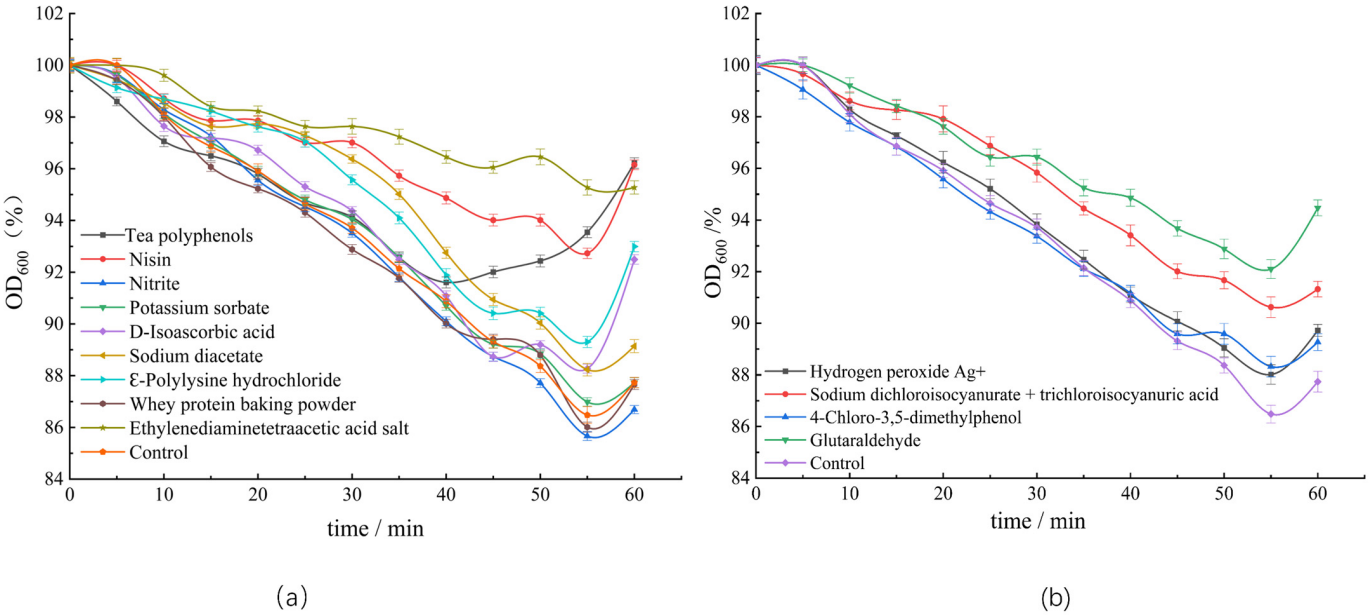

Figure 2. Effects of different bacteriostats on the turbidity of spores: (**a**) effects of food additives on the turbidity of spores; (**b**) effects of detergents on the turbidity of spores.

3.3.2. Effects of Different Bacteriostats on DPA Release Rate from Spores

Dormant spores contain a large amount of DPA, and germination of spores releases DPA, which is often used to characterize spore germination [31]. Therefore, in the present study, the effects of different bacteriostats on the germination dynamics of the spores were determined by investigating the release of DPA from the treated spores. As shown in Figure 3, the DPA release steadily increased with increasing incubation time, suggesting the commencement of spore germination. After incubation for 60 min, the released amount of DPA from untreated spores reached 43.52%, while the amounts from spores treated with ethylenediaminetetraacetate, nisin, and tea polyphenols were 20.18%, 22.77%, and 23.22%, respectively, which were significantly lower, indicating that these bacteriostats had good inhibitory effects on spore germination. Among them, *C. perfringens* spores treated with tea polyphenol could germinate, although the number of colonies formed was significantly low, as determined by the plate culture method, suggesting that food additives such as tea polyphenols may play a role in the pathogenesis of *C. perfringens*. The release of DPA after treatment with glutaraldehyde was 19.18% among the four detergents and was consistent with the results of spore turbidity change. In contrast, treatment with hydrogen peroxide Ag+ and 4-chloro-3,5-dimethylphenol did not significantly reduce the DPA release, when compared with that noted in the control group, indicating that these bacteriostats did not considerably inhibit spore germination. The results of the plate counting assay showed that the inhibitory effect of the bacteriostats on the spores was related to the antibacterial activity of these agents and degree of spore germination.

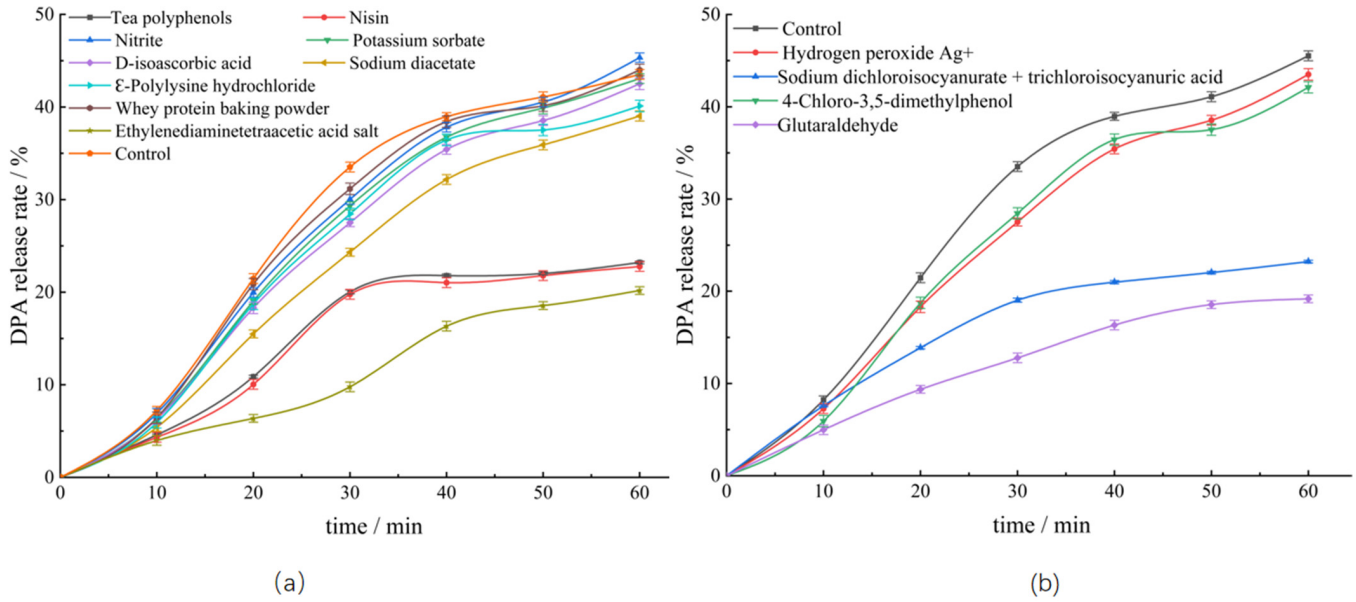

Figure 3. Effects of different bacteriostats on DPA release from spores. (**a**) Effects of food additives on DPA release from spores. (**b**) Effects of detergents on DPA release from spores.

3.4. Effects of Different Bacteriostats on Spore Structure during Germination

As the inner membrane of the spores is closely related to spore germination and activity, the effects of bacteriostats on the structure of spores during germination were examined by incubating the treated spores in FTG medium at 37 °C for 1 h and ascertaining the inner membrane damage by measuring the leakage of nucleic acids and proteins at 260 and 280 nm, respectively. As shown in Figure 4, the leakage of spore nucleic acids and proteins treated with tea polyphenol, potassium sorbate, and D-erythorbic acid was significantly higher than that in the untreated group within 1 h of incubation with the germination agent, implying that the membrane permeability might have been altered after bacteriostat treatment, leaking the contents out of the spores during the germination process. Infiltration of tea polyphenol, potassium sorbate, and D- isoascorbic acid into the spores could have promoted changes in membrane fluidity and permeability, causing leakage of more contents from the spores and inactivation of spores. In contrast, treatment with detergents, such as hydrogen peroxide Ag+ and 4-chloro-3,5-dimethylphenol, did not cause a significant increase in the leakage of nucleic acids or proteins from the spores, suggesting that these detergents do not penetrate into the interior of the spores at the initial stages of spore germination, do not affect the spore penetration barrier, and, therefore, do not cause substantial leakage of contents, consistent with the results of DPA release from the spores during germination. Interestingly, glutaraldehyde inhibited germination of spores and prevented leakage of spore contents owing to its sealing effect on the outer layer of the spores. After incubation for 12 h, most of the spores treated with ethylenediaminetetraacetate and glutaraldehyde were phase-bright under phase contrast microscope (Figure 5), indicating that the spores did not germinate completely, further confirming that these bacteriostats prevented the formation of nutrients by inhibiting spore germination [12]. Tea polyphenols, potassium sorbate, and D-isoascorbic acid inhibited germination of some spores by disrupting energy metabolism and acidification, respectively, and also caused further damage to the structure of the budding spores, resulting in the efflux of contents, thus significantly reducing spore survival [34]. Whey protein baking powder neither killed the spores directly nor killed them after germination or prevented the formation of vegetative cells. The other bacteriostats achieved inactivation of spores mainly during the vegetative body formation stage after spore germination and did not cause any significant damage to the spore structure.

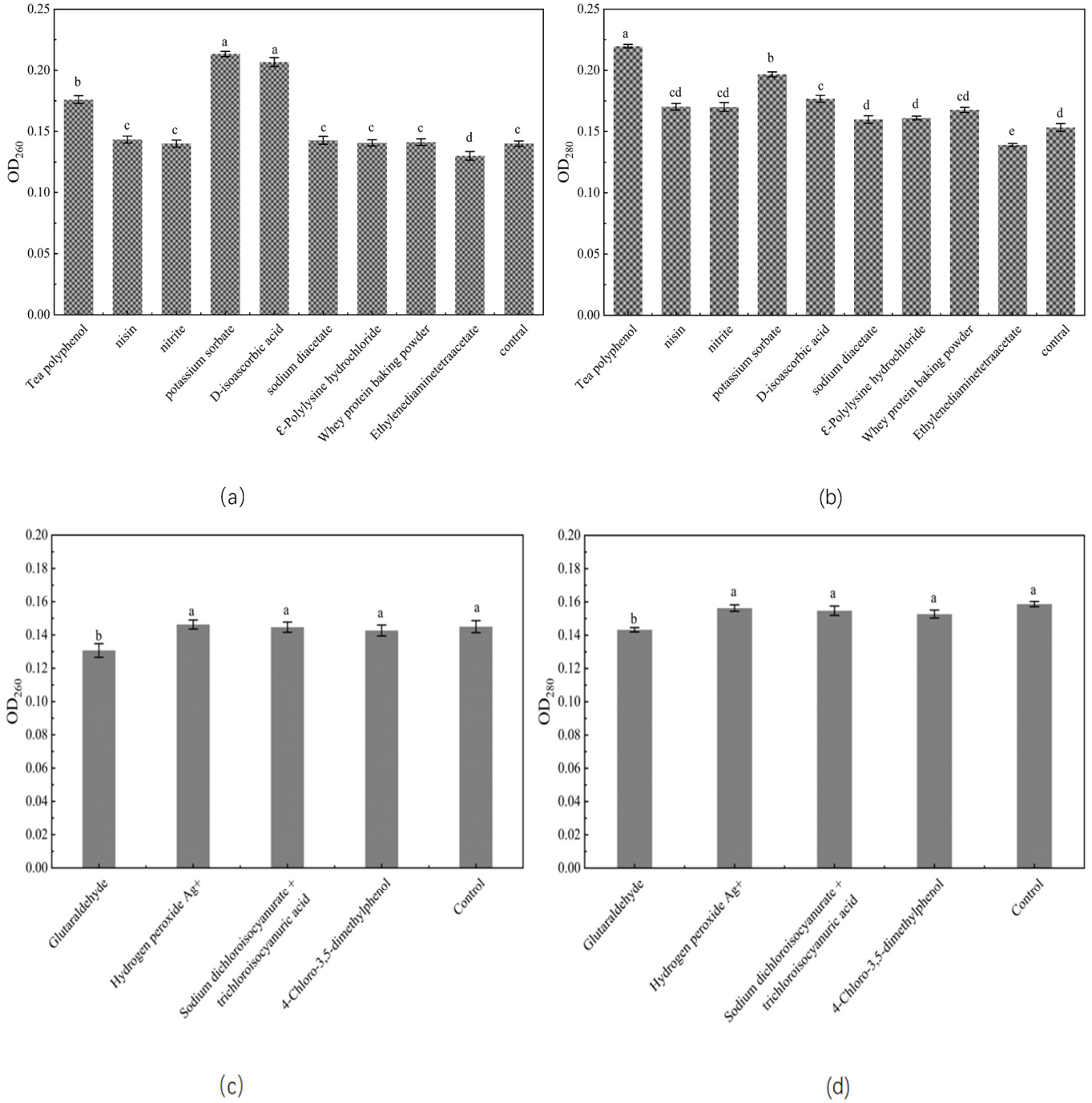

Figure 4. Effects of bacteriostats on the leakage of spore contents. (**a**) Effects of food additives on the leakage of spore nucleic acids. (**b**) Effects of food additives on the leakage of spore proteins. (**c**) Effects of detergents on the leakage of spore nucleic acids. (**d**) Effects of detergents on the leakage of spore proteins. Those with the same superscript letters indicated that the difference was not significant.

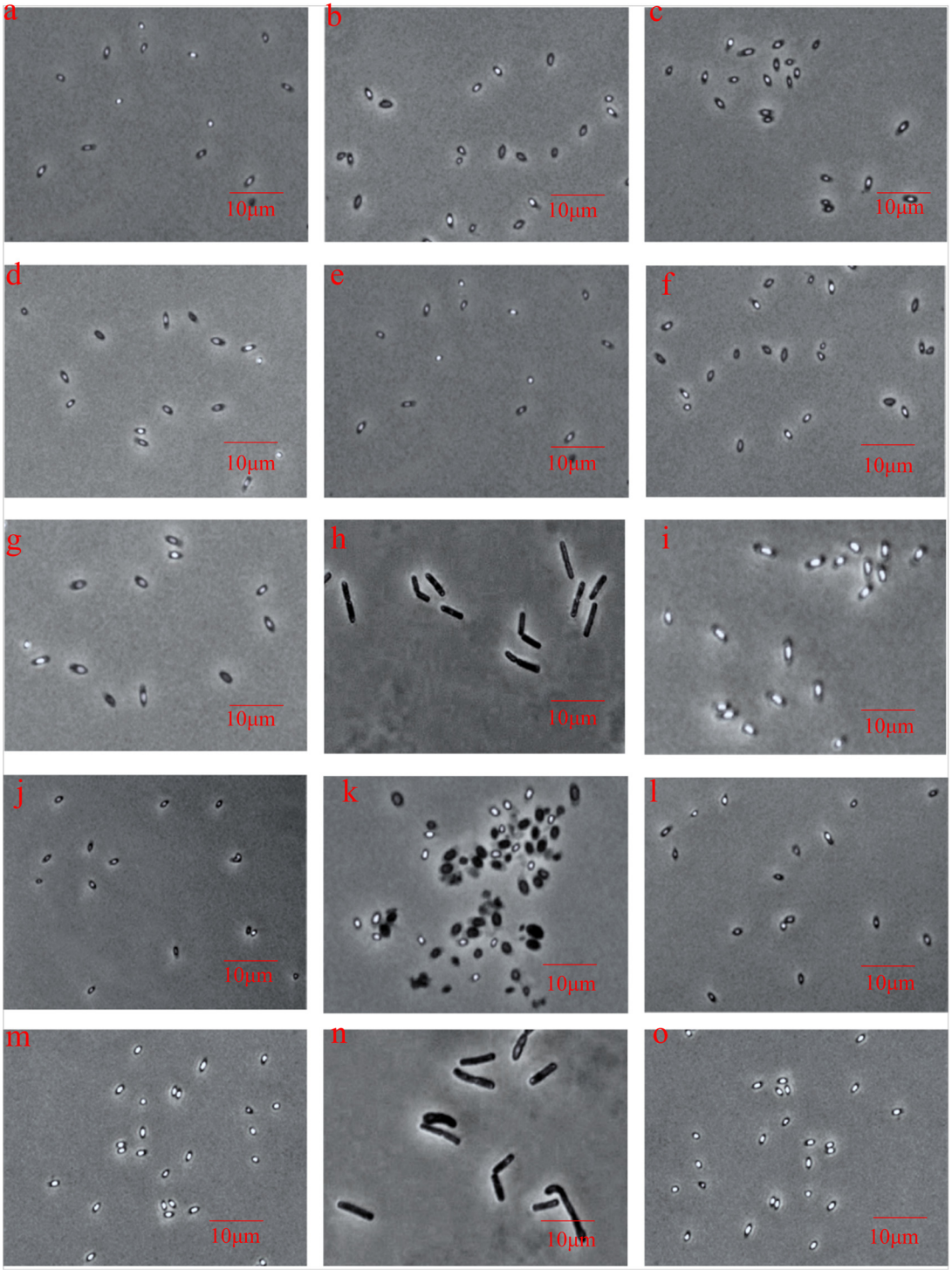

Figure 5. Effects of different bacteriostats on the growth of budding spores. (**a**) Tea polyphenol; (**b**) nisin; (**c**) nitrite; (**d**) potassium sorbate; (**e**) D-isoascorbic acid; (**f**) sodium diacetate; (**g**) ε-polylysine hydrochloride; (**h**) whey protein baking powder; (**i**) ethylenediaminetetraacetate; (**j**) hydrogen peroxide Ag+; (**k**) sodium dichloroisocyanurate + trichloroisocyanuric acid; (**l**) 4-chloro-3,5-dimethylphenol; (**m**) glutaraldehyde; (**n**) control; (**o**) non-germinating spores.

4. Discussion

Bacteriostats are essential ingredients in the food industry's production process because they effectively control foodborne germs and guarantee food safety. Few studies have looked at the impact on *C. perfringens* and its spores, despite several studies demon-

strating the effectiveness and mechanisms of bacteriostats against major food-borne infections. Accordingly, in the present study, the inhibitory effects and killing mechanisms of 13 different bacteriostats on *C. perfringens*, a representative strain of wild-type spores, were examined. The spores were studied by comparing the effects of different bacteriostats on spore germination and growth. Nitrite is one of the most widely used food additives in meat production and is an efficient broad-spectrum antibacterial agent. The results of antimicrobial activity (Table 1) indicated that nitrite effectively inhibited the growth of *C. perfringens*, which was consistent with the previous reports [10]. The tea polyphenols, a new natural antibacterial agent, could significantly inhibit the growth of *Escherichia coli*, *Klebsiella pneumoniae*, *Shewanella putrefaciens*, and other microbes [35]; however, they have little inhibitory effect on *C. perfringens*. It might be because *C. perfringens* itself differs from other bacteria in certain ways. The growth of *C. perfringens* was not significantly inhibited by Mauricio's addition of erythorbate to meat, but it was somewhat inhibited by D-isoascorbic acid [10]. This may be because D-isoascorbic acid caused *C. perfringens* to grow in an acidic environment, which inhibited the growth of bacteria [10,16]. Hydrogen peroxide Ag+ and sodium dichloroisocyanurate + trichloroisocyanuric acid are disinfectants with certain irritations. Studies have shown that the small molecular structures formed after decomposition could penetrate into bacteria and destroy the genetic material in the nucleus, so they are commonly used broad-spectrum disinfectants in industrial production [20]. In addition, the 4-chloro-3,5-dimethylphenol could inhibit the growth and reproduction of *C. perfringens*, and similar results were obtained in *Staphylococcus aureus* and *Escherichia coli*. These results indicated that most broad-spectrum antibacterial agents had certain antibacterial activity against *C. perfringens*. The modes of action of bacteriostats in killing *C. perfringens* spores varied, and the effects were strongly related to the antibacterial activity of these bacteriostats.

In recent years, more and more reports have begun to pay attention to the killing effect of antibacterial agents on spores. It was found that common antibacterial agents could also reduce the number of spores on the plate. Therefore, it was believed that antibacterial agents could also kill spores, as shown in our results (Figure 1). However, it was not clear whether the spores were really dead. Our results demonstrated that fewer spores were able to develop into vegetative forms on the plates after treatment with the antibacterial agents; however, spore turbidity increased and more Ca^{2+}-DPA was released with increasing the incubation time, indicating that the antibacterial agents did not directly kill the spores (Figures 2 and 3).

Tea polyphenols have been studied, and an intriguing discovery is that while they do not have great inhibitory effectiveness against *C. perfringens*, they do efficiently prevent the growth of their spores. The rate of the spore germination was not considerably impacted during the early stages, but later on, the spores seemed to stop developing. Spores released more protein throughout the entire germination process. The survival rate of *C. perfringens* spores was greatly decreased by tea polyphenols; it could be primarily attributed to the inactivation of enzymes and disruption of cell metabolism after these substances had penetrated into spores after germination [35]. At the same time, during the spore germination process, tea polyphenols might infiltrate into the spore and act on the spore genetic material, which also increases the possibility that the spore could not grow [36,37]. One theory is that the interior of the spores could become infected with bacteriostats, which could then inhibit respiration and interfere with energy homeostasis, preventing the spores from producing nutrients during later phases of spore germination [27]. While D-isoascorbic acid and potassium sorbate could not stop spore germination, they could decrease spore survival rates and increase protein and nucleic acid leakage during germination (Figure 4). This could be because these bacteriostats also compromised the cell membrane's integrity and increased cellular permeability, causing the contents of the cell to flow out [9,23,38,39]. The inhibitory effects of nitrite and ε-polylysine hydrochloride on *C. perfringens* spores could be attributed to the effect of these compounds on the cell membrane of propagules, enzyme activity, and energy metabolism, thus impairing bacterial metabolism [10,11,40].

Additionally, 4-chloro-3,5-dimethylphenol, a solution of sodium dichloroisocyanurate and trichloroisocyanuric acid, and hydrogen peroxide Ag+ treatments reduced the survival rate of spores. This could be explained by the inactivation of spores and the prevention of nutrient formation after the entry of these substances into the spores after germination [14]. In contrast, whey protein fermentation powder did not exhibit any antibacterial activity against *C. perfringens* spores and could not effectively inhibit spore germination or damage the spores even after their loss of resistance after germination. The antibacterial effect of sodium diacetate is mainly derived from acetic acid. Acetic acid could infiltrate into the spore wall and interfere with various enzymes activities, denaturing proteins. It is worth noting that a number of small compounds exhibited strong antibacterial activities against *C. perfringens*, which may be due to the fact that tiny molecules can more easily penetrate the bacterial cells, alter the formation of compounds associated with bacterial development, hinder the action of enzymes necessary for bacterial life, and destroy bacterial cell structures, instantaneously killing the bacteria [27]. However, spore coatings can prevent the infiltration of macromolecular substances, reduce the infiltration rate of small molecules, and protect the spore cortex [14]. This fully explains why sodium diacetate was able to grow spores of *C. perfringens*. Compounds such as ethylenediaminetetraacetate and glutaraldehyde could prevent spore germination by blocking the spore's outer layer and inhibiting spore growth by denaturing the protein coat of spores, consistent with other reports [28,41]. In addition, spore germination could alter the permeability of the inner membrane, which may weaken the spore's ability to withstand chemicals, resulting in the entry of bacteriostats into the spore's nucleus, leading to inactivation of the spore [14]. Nevertheless, although these findings demonstrated that the inhibition of spores is achieved by penetration of the bacteriostats into the cells after spore germination, the precise stage of penetration of these compounds into the spores, the inhibitory effect, and the specific location of the chemical activity are still unclear.

5. Conclusions

Although bacteriostats have been used extensively to eradicate microorganisms, it is unknown how they affect spores. In this study, the effects of various bacteriostats on *C. perfringens* and its spores' dynamic germination and growth were investigated. The results demonstrated that the bacteriostatic agents primarily prevented spore development in the following three ways: (1) Bacteriostats combine with certain distinct sites in the spore cortex and prevent cortex hydrolysis and inhibit spore germination, keeping the spore in a dormant state for a long time. (2) The germination agents induce hydrolysis of the spore cortex and trigger DPA release. At the same time, the resistance of the spores weakens, and the bacteriostats penetrate into the spores, resulting in decreases in the activity of proteins related to spore germination, changes in the structural components of the spores, and delays in spore germination or inactivation of spores. (3) After spore germination, the resistance of the spores to bacteriostats disappears. The bacterial barrier function is damaged after the entry of the bacteriostats, and the expression and synthesis of intracellular substances such as nucleic acids, proteins, etc., are disturbed, and the normal energy metabolism of cells is affected, leading to impairment of cell respiration and normal growth. Although most of the bacteriostats could not directly kill the spores, they could enter the spores after germination, owing to weakened resistance of the spores, and effectively inhibit nutrient formation and inactivate the spores. These results provide important information on the inhibition mechanism of different bacteriostats on the growth of spores and offer effective insights for the prevention and control of spores to ensure food safety.

Author Contributions: D.L.: Conceptualization, Designed the study, Formal analysis, Data curation, Writing—review and editing. S.L.: Finished the experiment, Writing—original draft. M.L.: Supervision, Writing—review and editing, Funding acquisition. Y.Z.: Supervision. L.Z.: Supervision. L.S.: Supervision. Y.M.: Supervision. G.Z.: Supervision. All authors have read and agreed to the published version of the manuscript.

Funding: This research was funded by the Major Science and Technology special sub-projects in Henan Province (221100110500), the Science Foundation for Outstanding Youth of Henan Province (212300410008), the Science and Technology Innovation Team of Henan Universities (22 IRTS THN021), and National modern agriculture (beef yak) industrial technology system construction special (CARS-37).

Data Availability Statement: Data is not available due to privacy and ethical restrictions.

Conflicts of Interest: The authors declare no conflict of interest.

References

1. Liang, D.; Chen, F.; H, X.S. Advance in spore germination. *J. China Food* **2018**, *18*, 221–228.
2. Ren, H.R.; Li, M.Y.; Zhu, Y.D.; Zhao, G.M.; Zhao, L.J.; Wu, H.L.; Xiao, K.; Cui, W.M. Advances in research on the hazards and control of Clostridium perfringens in food. *Food Sci.* **2021**, *42*, 352–359.
3. Jones, C.; Padula, N.; Setlow, P. Effect of mechanical abrasion on the viability, disruption and germination of spores of Bacillus subtilis. *J. Appl. Microbiol.* **2005**, *99*, 1484–1494. [CrossRef]
4. Zhang, Y.Y.; Li, M.Y.; Zhao, L.J.; Zhu, Y.D.; Zhao, G.M.; Liang, D.; Ma, Y.Y. Research progress on harm and control of spores in vacuum-packed food. *Packag. Eng.* **2021**, *42*, 29–35.
5. Young, S.; Setlow, P. Mechanisms of Bacillus subtilis spore resistance to and killing by aqueous ozone. *J. Appl. Microbiol.* **2004**, *96*, 1133–1142. [CrossRef]
6. Webb, J.E.; Regev, G.J.; Garfin, S.R.; Kim, C.W. Navigation-assisted fluoroscopy in minimally invasive direct lateral interbody fusion: A cadaveric study. *SAS J.* **2010**, *4*, 115–121. [CrossRef] [PubMed]
7. Lv, R.; Liu, D.; Zhou, J. Bacterial spore inactivation by non-thermal technologies: Resistance and inactivation mechanisms. *Curr. Opin. Food Sci.* **2021**, *42*, 31–36. [CrossRef]
8. Zhang, C.; Yang, G.; Shen, P.; Shi, Y.; Yang, Y.; Liu, Y.; Xia, X.; Wang, S. Inactivation mechanism of slightly acidic electrolyzed water on Bacillus cereus spores. *Food Microbiol.* **2022**, *103*, 103951. [CrossRef]
9. Mooyottu, S.; Flock, G.; Venkitanarayanan, K. Carvacrol reduces Clostridium difficile sporulation and spore outgrowth in vitro. *J. Med. Microbiol.* **2017**, *66*, 1229–1234. [CrossRef]
10. Redondo-Solano, M.; Valenzuela-Martinez, C.; Cassada, D.A.; Snow, D.D.; Juneja, V.K.; Burson, D.E.; Thippareddi, H. Effect of meat ingredients (sodium nitrite and erythorbate) and processing (vacuum storage and packaging atmosphere) on germination and outgrowth of Clostridium perfringens spores in ham during abusive cooling. *Food Microbiol.* **2013**, *35*, 108–115. [CrossRef]
11. Roberts, T.A.; Ingram, M. The effect of sodium chloride, potassium nitrate and sodium nitrite on the recovery of heated bacterial spores. *Int. J. Food Sci. Tech.* **2007**, *1*, 147–163. [CrossRef]
12. Cho, W.-I.; Chung, M.-S. Sporicidal activities and mechanism of surfactant components against Clostridium sporogenes spores. *J. Food Sci. Technol.* **2018**, *55*, 4675–4680. [CrossRef]
13. Boix, E.; Couvert, O.; André, S.; Coroller, L. The synergic interaction between environmental factors (pH and NaCl) and the physiological state (vegetative cells and spores) provides new possibilities for optimizing processes to manage risk of *C. sporogenes* spoilage. *Food Microbiol.* **2021**, *100*, 103832. [CrossRef] [PubMed]
14. Arnaouteli, S.; Bamford, N.C.; Stanley-Wall, N.R.; Kovács, T. Bacillus subtilis biofilm formation and social interactions. *Nat. Rev. Microbiol.* **2021**, *19*, 600–614. [CrossRef] [PubMed]
15. Wen, J.; Vischer, N.O.E.; de Vos, A.L.; Manders, E.M.M.; Setlow, P.; Brul, S. Organization and dynamics of the SpoVAEa protein and its surrounding inner membrane lipids, upon germination of Bacillus subtilis spores. *Sci. Rep.* **2022**, *12*, 4944. [CrossRef]
16. Szabo, J.G.; Adcock, N.J.; Rice, E.W. Rice, Disinfection of Bacillus spores with acidified nitrite. *Chemosphere* **2014**, *113*, 171–174. [CrossRef]
17. Bi, K.; Liu, Y.; Xin, W.; Yang, J.; Zhang, B.; Zhang, Z. Combined treatment of epsilon-polylysine and heat damages protective structures and spore inner membranes to inactivate Bacillus subtilis spores. *Food Microbiol.* **2023**, *109*, 104–137. [CrossRef]
18. Redondo-Solano, M.; Valenzuela-Martinez, C.; Juneja, V.K.; Burson, D.E.; Thippareddi, H. Control of Clostridium perfringens spore germination and outgrowth by potassium lactate and sodium diacetate in ham containing reduced sodium chloride. *LWT* **2021**, *137*, 110395. [CrossRef]
19. Yang, Y.; Zhang, T. Antimicrobial Activities of Tea Polyphenol on Phytopathogens: A Review. *Molecules* **2019**, *24*, 816. [CrossRef]
20. Sun, X.; Kong, X.; Li, C.; Wang, M.; Yi, J.; Deng, Z.; Niu, B.; Chen, Q. Sporicidal mechanism of the combination of ortho-phthalaldehyde and benzyldimethyldodecylammonium chloride as a disinfectant against the Bacillus subtilis spores. *Braz. J. Microbiol.* **2022**, *53*, 547–556. [CrossRef]
21. Leggett, M.; McDonnell, G.; Denyer, S.; Setlow, P.; Maillard, J.-Y. Bacterial spore structures and their protective role in biocide resistance. *J. Appl. Microbiol.* **2012**, *113*, 485–498. [CrossRef]
22. Gauvry, E.; Mathot, A.-G.; Couvert, O.; Leguérinel, I.; Coroller, L. Effects of temperature, pH and water activity on the growth and the sporulation abilities of Bacillus subtilis BSB1. *Int. J. Food Microbiol.* **2021**, *337*, 108–115. [CrossRef]
23. Ojha, S.C.; Phanchana, M.; Harnvoravongchai, P.; Chankhamhaengdecha, S.; Singhakaew, S.; Ounjai, P.; Janvilisri, T. Teicoplanin Suppresses Vegetative Clostridioides difficile and Spore Outgrowth. *Antibiotics* **2021**, *10*, 984. [CrossRef] [PubMed]
24. Doona, C.J.; Feeherry, F.E.; Setlow, B.; Wang, S.; Li, W.; Nichols, F.C.; Talukdar, P.K.; Sarker, M.R.; Li, Y.-Q.; Shen, A.; et al. Effects of High-Pressure Treatment on Spores of Clostridium Species. *Appl. Environ. Microbiol.* **2016**, *82*, 5287–5297. [CrossRef]

25. Rao, L.; Feeherry, F.E.; Ghosh, S.; Liao, X.; Lin, X.; Zhang, P.; Li, Y.; Doona, C.J.; Setlow, P. Effects of lowering water activity by various humectants on germination of spores of Bacillus species with different germinants. *Food Microbiol.* **2018**, *72*, 112–127. [CrossRef] [PubMed]
26. Ren, H.R.; Li, M.Y.; Zhu, Y.D.; Zhao, G.M.; Zhang, J.Y.; Zhao, L.J.; Zhang, Y.Y.; Wang, W.T. Induction of spore germination of Clostridium perfringens by peptidoglycan of different bacteria. *Mod. Food Sci.* **2020**, *36*, 178–184.
27. Baloh, M.; A Sorg, J. Clostridioides difficile spore germination: Initiation to DPA release. *Curr. Opin. Microbiol.* **2022**, *65*, 101–107. [CrossRef]
28. Setlow, B.; Cowan, A.; Setlow, P. Germination of spores of Bacillus subtilis with dodecylamine. *J. Appl. Microbiol.* **2003**, *95*, 637–648. [CrossRef]
29. Huang, Z.W.; Wu, X.H.; Zhou, Y.; Lan, X.H.; Zhang, B. Study on bacteriostasis of edible composite film of cinnamon essential oil. *China Condiment* **2022**, *47*, 22–25.
30. Sun, J.; Zhang, J.Y.; Hu, X.S.; Zhang, Y.; Du, W.B.; Zhang, Z. Ultra-high pressure causes sublethal damage to spores and further increases the thermal sensitivity of spores. *Food Sci.* **2017**, *42*, 313–317.
31. Rao, L. *Efficacy and Mechanisms of High Pressure Carbon Dioxide Combined with Temperature in Killing Bacillus Subtilis Spores*; China Agricultural University: Guangzhou, China, 2017.
32. Li, F.J. *Inactivation Efficiency and Mechanism of High Pressure CO2 on Bacillus Subtilis Spores*; Hefei University of Technology: Hefei, China, 2013.
33. Setlow, P.; Wang, S.; Li, Y.-Q. Germination of Spores of the Orders Bacillales and Clostridiales. *Annu. Rev. Microbiol.* **2017**, *71*, 459–477. [CrossRef] [PubMed]
34. Talukdar, P.K.; Udompijitkul, P.; Hossain, A.; Sarker, M.R. Inactivation Strategies for Clostridium perfringens Spores and Vegetative Cells. *Appl. Environ. Microbiol.* **2017**, *83*, e02731-16. [CrossRef]
35. Zhang, F.; Zhu, J.; Wang, H. Inhibitory Activity of Tea Polyphenols on Biofilm Development of Shewanella putrefaciens. *J. Food Process. Preserv.* **2016**, *40*, 910–917. [CrossRef]
36. Rao, L.; Liao, X.; Setlow, P. Bacillus spore wet heat resistance and evidence for the role of an expanded osmoregulatory spore cortex. *Lett. Appl. Microbiol.* **2016**, *63*, 247–253. [CrossRef]
37. Rao, L.; Zhou, B.; Serruya, R.; Moussaieff, A.; Sinai, L.; Ben-Yehuda, S. Glutamate catabolism during sporulation determines the success of the future spore germination. *iScience* **2022**, *25*, 1042–1052. [CrossRef] [PubMed]
38. Setlow, P.; Christie, G. Bacterial Spore mRNA—What's Up With That? *Front. Microbiol.* **2020**, *11*, 592–596. [CrossRef] [PubMed]
39. Yasugi, M.; Motooka, D.; Nakamura, S.; Miyake, M. Phosphorothioation of foreign DNA influences the transformation efficiency in Clostridium perfringens NCTC 8239. *Anaerobe* **2020**, *61*, 102–185. [CrossRef]
40. Roberts, T.A.J.L. Smart Inhib. Spores *Clostridium* spp. by Sodium Nitrite. *J. Appl. Bacteriol.* **1974**, *37*, 261–264. [CrossRef]
41. Janganan, T.K.; Mullin, N.; Dafis-Sagarmendi, A.; Brunt, J.; Tzokov, S.B.; Stringer, S.; Moir, A.; Chaudhuri, R.R.; Fagan, R.; Hobbs, J.K.; et al. Architecture and Self-Assembly of Clostridium sporogenes and Clostridium botulinum Spore Surfaces Illustrate a General Protective Strategy across Spore Formers. *mSphere* **2020**, *5*, e00424-20. [CrossRef]

foods

MDPI

Article

Investigating the Effect of Rosemary Essential Oil, Supercritical CO_2 Processing and Their Synergism on the Quality and Microbial Inactivation of Chicken Breast Meat

Fabio Santi [1], Riccardo Zulli [1], Elisa Lincetti [1], Alessandro Zambon [2] and Sara Spilimbergo [1,*]

[1] Industrial Engineering Department, University of Padova, Via Marzolo 9, 35131 Padova, Italy
[2] Department of Civil, Chemical, Environmental, and Materials Engineering (DICAM), University of Bologna, Via Terracini 28, 40131 Bologna, Italy
* Correspondence: sara.spilimbergo@unipd.it

Abstract: Fresh chicken meat is a very perishable good, even at refrigerated storage conditions, due to psychrophilic microbial growth and physicochemical changes. The present study focuses on the use of rosemary (*Rosmarinus officinalis* L.) essential oil (REO), supercritical CO_2 processing and their synergism to increase the microbial inactivation in chicken breast meat. *E. coli* and *L. innocua* were inoculated on the chicken breast surface, and the inactivation effects of two different processes, namely SC-CO_2 and SC-MAPCO_2, were compared with or without the addition of REO. Moreover, the impact of the treatments on the superficial color of the meat was considered. The study demonstrated a synergic effect with 1% REO and supercritical CO_2 for the inactivation of *E. coli* on chicken meat, while for *L. innocua*, there was no synergism. Regarding SC-CO_2 treatment, the *E. coli* reduction was 1.29 and 3.31 log CFU/g, while for *L. innocua*, it was 1.42 and 1.11 log CFU/g, respectively, without and with the addition of 1.0% of REO. The same amount of REO allowed us to obtain a reduction of 1.3 log CFU/g of *E. coli* when coupled with SC-MAPCO_2. For *L. innocua*, no reduction was obtained, either with SC-MAPCO_2 or together with REO. The synergism of SC-MAPCO_2 with 1% REO was confirmed for the total psychrophilic bacteria, demonstrating a strong dependence on the microorganism. The color modification induced by the SC-MAPCO_2 process was lower than the SC-CO_2 treatment. Overall, this study demonstrated a possible synergism of the technologies which can support the development of innovative methods to improve the safety and shelf-life of chicken breast meat.

Keywords: supercritical CO_2; MAP; essential oils; *Escherichia coli*; *Listeria innocua*; mesophilic and psychrophilic microorganisms

1. Introduction

Chicken breast meat is a product consumed worldwide. The world production of chicken meat is growing and growing, and it is expected to reach 139.19 million tons per year in 2025 [1]. Chicken breast meat is highly consumed thanks to its low cost, versatility and quick preparation, and for the absence of religious restrictions related to its consumption [2,3]. Chicken meat has better nutritional characteristics compared to other types of meat. In particular, if compared with red meat, it has a lower fat content (especially saturated fats), a higher content of proteins, and a lower caloric content [4]. For these reasons, it is recommended for people who want to reduce their fat intake or those who suffer from coronary heart diseases [4].

Fresh chicken meat is very perishable, despite refrigerated storage, due to psychotropic microbial growth and physicochemical changes [5]. The presence and availability of several nutrients such as proteins, free amino acids, vitamins, fats, mineral salts, and moisture allow for the survival and growth of different microorganisms throughout the whole production and distribution chain. The main step that enhances the possibility

of microbial contamination and colonization of the muscle tissues is the slaughtering process, during which the microorganisms normally present in the gastrointestinal tract, skin, lungs and feathers might contaminate the meat [3]. Outbreaks associated with the incorrect handling and the presence of pathogenic microorganisms in chicken meat, such as *Escherichia coli* O157:H7, *Salmonella* spp., *Campylobacter* spp. and *Listeria monocytogenes*, are very common [3,6]. A recent multi-country outbreak of *Salmonella* Mbandaka ST413 linked with the consumption of chicken was reported by the EFSA (European Food Safety Authority). From September 2021 to November 2022, this epidemic led to 196 cases in different European countries (Czechia, Estonia, Finland, France, Germany, Ireland, Netherlands, United Kingdom and Israel), among which were 19 hospitalizations, five cases of septicemia and one death [7]. Current technologies to increase the safety of raw chicken meat are still limited. Indeed, the use of heat, which is the most effective technique to kill microorganisms, cannot be used for the raw/chilled food segment. For this reason, research on low-temperature technologies has been focused on developing innovative processes to improve the safety and shelf-life of raw chicken meat without using high temperatures. Some innovative techniques such as ultrasounds (US) [8], UV-C irradiations [6] and gamma-irradiations [9] have been studied on chicken meat. However, these techniques have some disadvantages. US usually leads to the formation of free radicals, and its industrialization has some limitations due to the high investment costs and lack of regulative agreements [8]. UV-C, instead, might have negative effects such as off-flavor, browning, texture breakdown, damage and cell malfunction on meat [10]. Gamma-irradiations, instead, are effective for meat treatment and are already authorized by the FDA (Food and Drug Administration); however, this technique still has strict regulations in Europe and cannot yet be used for the majority of food products. Another obstacle to the industrialization of this method is that consumers frequently show aversion towards food irradiation [10]. Moreover, the implementation of this technique needs both high investment costs and measures for the operators' safety [11]. Another technique that might be used to improve the shelf-life of chicken meat is high hydrostatic processing (HHP), which uses high pressures (>300 MPa) to inactivate microorganisms and has been demonstrated to be effective on chicken breast meat, especially against *L. monocytogenes*, *E. coli* and *S. typhimurium* [12]. However, this technology has strong impacts on structural, physiochemical, morphological and textural characteristics of the meat. In particular, an increase in the product hardness, cohesiveness, gumminess and chewiness has been observed, together with a strong lipid oxidation induced by pressures higher than 450 MPa [12].

Supercritical carbon dioxide (SC-CO_2) treatment has been studied as an alternative low-temperature method to inactivate microorganisms on different food matrices [3,13–15] at relatively low pressure, compared to HHP. Recently, a new method for supercritical food inactivation using modified atmosphere packaging (MAP) with a high concentration of CO_2 (SC-MAPCO_2) has been developed by Spilimbergo et al. [16]. SC-MAPCO_2 consists of pressurizing products already packaged in a CO_2-rich atmosphere, avoiding any product handling after the process, thus reducing the risk of post-process contamination. In this way, the gas inside the packaging reaches the supercritical condition, exerting its antimicrobial power during the treatment.

This new method has been demonstrated to be effective at lab scale on fresh-cut carrots and coconut and coriander, obtaining inactivation results very close to the SC-CO_2 method, but with milder effects on the product aspect [17,18]. This new method has never been studied on animal-origin products, but SC-CO_2 has been demonstrated to be effective in the inactivation of microorganisms on meat products. Therefore, there is interest in understanding the potential of this new decontamination technology and its comparison with SC-CO_2 in terms of quality retention and microbial inactivation. Bae et al. [19], for instance, obtained 1.69 log CFU/cm^2 of inactivation for mesophilic bacteria by treating fresh pork meat at 12 MPa and 40 °C for 30 min. Chicken breast meat has been treated with SC-CO_2, thereby obtaining 3.96 log CFU/g of inactivation of inoculated *E. coli* after a 45 min treatment at 14 MPa and 45 °C [3]. The method has also been coupled with antimicrobial

substances, especially essential oils, such as rosemary and coriander, in a proof-of-concept study obtaining promising results in terms of inactivation [3]. However, little is known about the synergistic effect of SC-CO_2 and antimicrobial agents including essential oils, but it can hypothesized that an increment of the inactivation can be achieved by choosing a correct amount of oil.

In this context, several studies have shown the potential to improve the preservation of different food products by coupling innovative inactivation techniques [20] with antimicrobial substances such as essential oils [3], spice extracts [21] and bacteriocins [22]. In a recent paper, Chen et al. [23] applied HHP on chicken meat pretreated with papaya extract to inactivate inoculated *Salmonella*, obtaining an inactivation of 6 log CFU/g. Stratakos et al. [24], instead, explored the possible synergism between HHP and a packaging activated with 10% of a coriander essential oil solution in ethanol to inactivate *Listeria monocytogenes* in ready-to-eat chicken meat.

Among these substances, the antimicrobial and antifungal activity of rosemary essential oil (REO, *Rosmarinus officinalis* L.) has been extensively demonstrated against different microorganisms, such as different strains of *E. coli* [25], and in different matrices such as soft cheese [26] and broccoli florets [27]. Moreover, its synergic effect with SC-CO_2 has been studied and demonstrated effective on raw almonds [13].

The present study aims to investigate the effect of REO, CO_2-based processing (SC-CO_2 and SC-MAPCO_2) and their synergism in the treatment of raw chicken meat. Results were focused on the microbial inactivation capacity against inoculated *E. coli* and *L. innocua* at different REO concentrations, following a 3 × 4 design of experiment. Additionally, the effect of the treatments on the qualitative aspects in terms of color, pH and water activity was evaluated.

2. Materials and Methods

2.1. Culture and Cell Suspension

Escherichia coli NCTC 9001 and *Listeria innocua* NCTC 11288 strains were used for the inoculation of the samples. The cultures' preparation methods are described, respectively in [3] and in [28], with some modifications. Briefly, the *E. coli* and *L. innocua* cultures were incubated overnight in Luria–Bertani (LB) medium broth (Lennox, Sacco System, Como, Italy) and in BHI Broth (Microbiol diagnostici, Cagliari, Italy) at 37 °C, respectively. The microbial suspensions were centrifuged (Rotina 380 R, Hettich, Tuttlingen, Germany) at 6000 rpm for 8 min, the supernatant was removed, and the pellet was resuspended in Ringer's solution (Merck, Darmstadt, Germany) in order to reach a final concentration of 10^8 CFU/mL.

2.2. Sample Preparation and Microbial Inoculation

The chicken breasts used in this study were purchased from a local market in Padova (Italy) and processed on the same day to ensure freshness. Similar squared chicken breast pieces weighing 5 ± 0.05 g were prepared under a laminar flow cabinet to minimize contamination. Samples were used without further manipulation for the detection of natural microflora and for physicochemical analyses on untreated samples. For the inactivation experiments with *E. coli* and *L. innocua*, 100 µL of the microbial suspension was added to the chicken pieces cubes and left for 15 min at room temperature under the laminar flow cabinet. For the treatment with rosemary (*Rosmarinus officinalis* L.) essential oil (REO) (Erbamea, Perusa, Italy), the chicken cubes were sprinkled with different percentages (0.1, 0.5, and 1.0% volume/weight) of REO and left for 15 min at room temperature under the laminar flow cabinet. The samples were either analyzed directly as controls or processed before analysis.

2.3. High-Pressure Processes

Two high-pressure processes were investigated and compared. The first one (SC-CO_2), previously described by González-Alonso et al. [3], treats the samples by direct contact

with supercritical CO_2. Briefly, a sample was inserted in a stainless steel vessel, which was then closed, filled and pressurized with CO_2 (Nippon gasses, carbon dioxide 4.0, Milan, Italy). After the desired pressure was reached, it was maintained for a specific holding time. The second process (SC-MAPCO_2), previously described by Barberi et al. [17], is instead performed on samples inserted in a high-gas barrier, multilayer (PA/EVOH/PA/PE) film (Euralpack, Schoten, Belgium) filled with CO_2 and pressurized in a water-driven plant. The packaging material was selected thanks to its low CO_2 permeability (<6.5 $cm^3/m^2/d/bar$) and its resistance to high pressure. The volume of the plastic bags was fixed at 100 ± 10 mL. To study the possible synergic effects between the two methods with and without REO, process conditions were chosen to guarantee a significant but not complete inactivation of *E. coli* and *L. innocua* when REO was not used; in particular, 14 MPa and 40 °C for 15 min were selected. Moreover, in applications with REO, temperature should not exceed 40 °C to avoid thermal degradation of the oil [29]. In both treatments, the desired pressure was reached in approximately 2 min, while the depressurization was almost instantaneous.

2.4. Microbial Enumeration

Each sample was placed in a sterile 50 mL falcon tube, to which 45 mL of sterile Ringer's solution was added. The tube was vortexed (ZX3 Advanced Vortex Mixer, Velp Scientifica, Usmate Velate, Italy) at 2200 rpm for 90 sec. Successively, this solution was serially diluted (1:10) in Ringer's solution. For the enumeration of *E. coli* [30] and *L. innocua* [28], 100 µL of the selected dilutions were spread-plated on MacConkey agar with crystal violet (Microbiol diagnostici, Cagliari, Italy) and BHI agar (Microbiol diagnostici, Cagliari, Italy), respectively. Plates were incubated for 24 h at 37 °C in an incubator (Memmert, Schwaback, Germany) and then enumerated. For mesophilic and psychrophilic natural microflora, non-inoculated samples were similarly analyzed by pour-plating in plate count agar (PCA, Microbiol diagnostici, Cagliari, Italy), in 1 mL of solution. The plates were then incubated at 30 °C for 72 h and at 10 °C for 120 h, for mesophilic and psychrophilic bacteria, respectively. Results are expressed as log CFU/g.

2.5. Physicochemical Analysis: Color, pH and a_w

The surface color of the samples was measured using a Tristimulus colorimeter (NR100, 3nh, Guangzhou, China) in the CIE 1976 (L*, a*, b*) color space. The color modification caused by treatments was expressed as total color change (ΔE) according to Equation (1) [31]:

$$\Delta E = \sqrt{(\Delta a^*)^2 + (\Delta b^*)^2 + (\Delta L^*)^2} \quad (1)$$

where L* is the lightness index (100 for white to 0 for black), a* is the redness index (red when positive to green when negative), and b* is the yellowness index (yellow when positive to blue when negative).

The pH was determined with a pH meter (pH1100, VWR, Leuven, Belgium) with an electrode for solid samples (spear 220, VWR, Leuven, Belgium), while a_w was measured with an a_w meter (HygroPalm HP23-AW-A, Bassersdorf, Switzerland).

Each measurement was performed at least in triplicate.

2.6. Design of Experiment and Statistical Analysis

The possible synergism between the treatments and the REO concentration was evaluated by a randomized 3 × 4 design of experiment to analyze the effect on three different response variables: color modification and *E. coli* and *L. innocua* inactivation. Specifically, the processing method consists of three levels: control, SC-CO_2 and SC-MAPCO_2, while REO concentration has four levels: 0, 0.1, 0.5 and 1.0%.

Statistical analyses were performed in Minitab®. Mean values were used to compare differences between treatments. The existence of significant differences (α = 0.05) between different treatments was studied with an ANOVA and pair comparison within a group with its post hoc analysis (Tukey HSD).

3. Results

3.1. Comparison between SC-CO_2 and SC-MAPCO_2 without REO

Chicken breast samples were treated with SC-CO_2 and SC-MAPCO_2 at the following process conditions: 14.0 MPa, 40 °C and 15 min. Pressure and temperature were chosen in accordance with Gonzáles-Alonso et al. [3], while 15 min was chosen as the processing time, because a longer time (≥30 min) led to complete inactivation of *E. coli* when the samples were treated with SC-CO_2 alone. Figure 1 shows the pictures of the raw untreated samples in comparison with the treated ones. The CIELAB color parameters (L*, a* and b*) and the total color difference between the treated and untreated samples (ΔE) are reported in Figure 2.

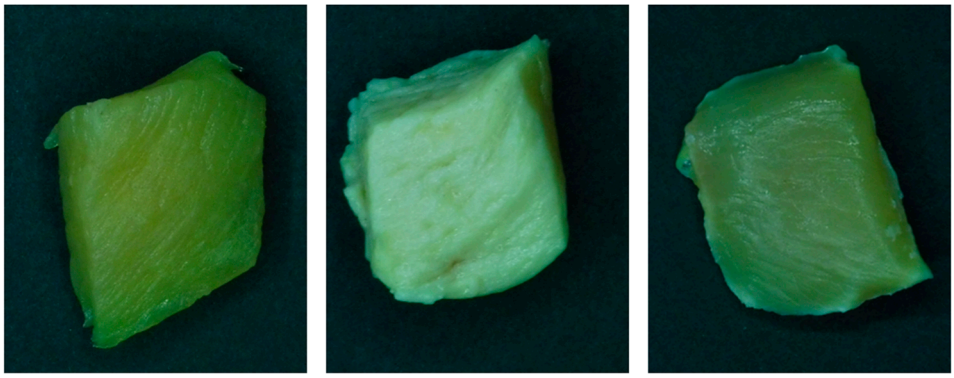

(**a**) (**b**) (**c**)

Figure 1. Pictures of raw (**a**), treated with SC-CO_2 (**b**) and treated with SC-MAPCO_2 (**c**) chicken breast samples. Treatment conditions: 14 MPa, 40 °C, 15 min.

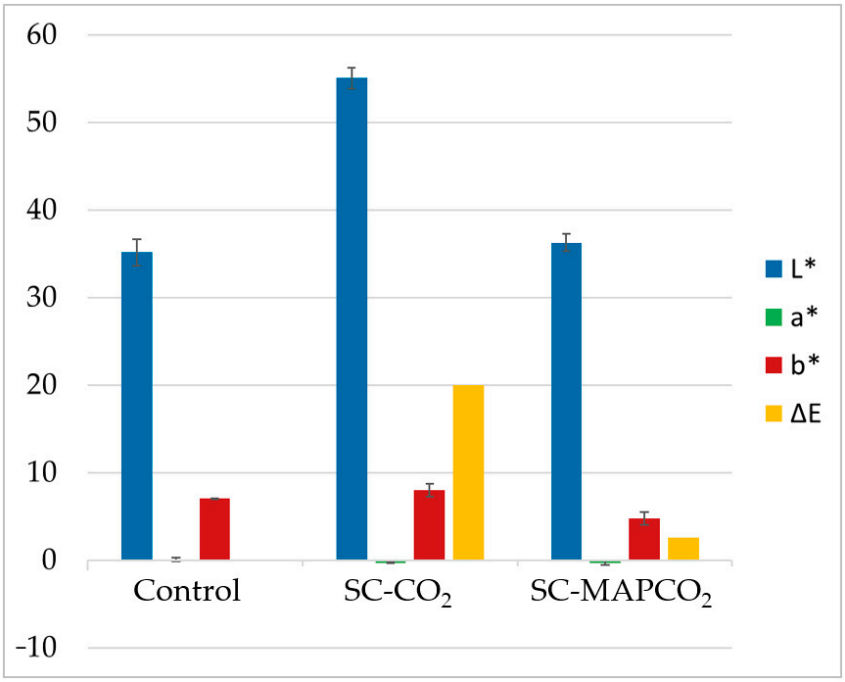

Figure 2. CIELAB color parameters (L*, a* and b*) and total color difference (ΔE) with respect to the raw chicken, for raw (Control), treated with SC-CO_2, and treated with SC-MAPCO_2 samples.

The SC-CO_2 treatment led to significant modifications in the visual aspect of the chicken meat. The lightness parameter L* increased from 35.15 ± 2.98 to 55.07 ± 2.36, resulting in a total color difference equal to 19.94 and a cooked-like visual appearance. Similar results were also obtained by González-Alonso et al. [3], in whose study the

chicken samples treated with SC-CO_2 (40 °C, 45 min, 8 and 14 MPa) showed a significant increase in superficial lightness L*. Indeed, other studies on protein matrices, in particular shrimps [32], pork [19] and ground beef [33], showed important color modifications caused by the treatment.

These modifications may be caused, in accordance with [19,34], by the effect of high-pressure CO_2 on the molecular interaction and conformation of proteins, which can lead to their denaturation. In particular, the process may cause the denaturation of myoglobin and the consequent release of heme groups and coagulation of myofibrillar proteins [35]. Moreover, Monhemi et al. [36] simulated the effect of SC-CO_2 on the molecular response of two different proteins: myoglobin and lysozyme, concluding that the protein denaturation could be caused by the weakening of the hydrophobic interactions and therefore the integrity of the tertiary structure.

Regarding the SC-MAPCO_2, the color change was less if compared with the SC-CO_2 treatment, resulting in a ΔE lower than 3, meaning that the visual modification with respect to the non-treated product is not substantial [31].

In Table 1, pH and water activity (a_w) values for non-treated (control), treated with SC-CO_2 and treated with SC-MAPCO_2 are reported. The treatments did not significantly change the pH of the chicken breast meat. The a_w of the treated samples is slightly lower than the control samples. This little change may be due to the loss of water by applying high pressures, which is confirmed by the weight reduction of the samples after the treatment, which was about 8% for SC-CO_2 and 5.5% for SC-MAPCO_2.

Table 1. pH and water activity of samples non-treated (control), treated with SC-CO_2 and treated with SC-MAPCO_2. Means with different superscript letters are significantly different ($p < 0.05$).

Sample	pH	a_w
Control	5.85 ± 0.05^{a}	0.971 ± 0.002^{a}
SC-CO_2	5.90 ± 0.09^{a}	0.951 ± 0.003^{b}
SC-MAPCO_2	5.72 ± 0.07^{a}	0.954 ± 0.007^{b}

In order to compare the microbial inactivation efficiency of the two methods, two fecal contamination indicators, *Escherichia coli* and *Listeria innocua*, were used as test microorganisms for the challenge test. In this work, the strains *E. coli* NCTC 9001 and *L. innocua* NCTC 11288, were used as surrogates of the pathogenic strains *E. coli* O157:H7 and *L. monocytogenes* [37]. Table 2 reports the inactivation data.

Table 2. *E. coli* and *L. innocua* load, expressed in log CFU/g, on the inoculated samples non-treated (control), treated with SC-CO_2 and treated with SC-MAPCO_2. Means with different superscript letters are significantly different ($p < 0.05$).

Sample	*E. coli* (log CFU/g)	*L. innocua* (log CFU/g)
Control	7.03 ± 0.06^{a}	7.41 ± 0.14^{a}
SC-CO_2	5.74 ± 0.62^{b}	5.99 ± 0.11^{b}
SC-MAPCO_2	6.40 ± 0.21^{ab}	7.25 ± 0.06^{a}

Approximately 1.29 log CFU/g of *E. coli* and 1.42 log CFU/g of *L. innocua* were reduced by SC-CO_2. The inactivation achieved for *E.coli* confirmed the data obtained by González-Alonso et al. [3] at the same process conditions on chicken breast meat. In another study, Morbiato et al. [38] obtained a similar inactivation, 1.76 ± 0.16 log CFU/g, for the *Salmonella enterica* on chicken breast meat at 40 °C and 10 MPa. In their case, the product was processed for supercritical drying, and the vessel was pressurized from 6 MPa up to 10 MPa at a rate of 0.4 MPa/min and then depressurized at a rate of 1 MPa/min.

Similar results have been achieved on other meat products. Bae et al. [19] obtained an inactivation of 2.00 log CFU/cm^2 of *Salmonella typhimurium* and 1.99 log CFU/cm^2 of *E. coli* O157:H7 by treating fresh pork meat at 12 MPa and 40 °C for 30 min.

The inactivation achieved for *L. innocua* is slightly higher than that achieved by Wei et al. [39]. Specifically, they reduced 85% of *L. monocytogenes* after 2 h at 13.7 MPa and 35 °C. The higher inactivation achieved for *L. innocua* might be caused by the higher temperature used, and also by the different resistance to the process due to the different strain used compared with Wei et al.

In the case of SC-MAPCO$_2$, the treatment was able to slightly reduce the initial load; however, the difference in microbial content was not significant if compared with the untreated control sample. This result suggests a strong dependence on the treatment with the food matrix. Indeed, in the case of other food matrices such as carrot and coriander [17,18], the inactivation of inoculated *E. coli* on the sample surface was also found to be higher after the treatment with the SC-CO$_2$ method compared to the SC-MAPCO$_2$ method. However, the inactivation with SC-MAPCO$_2$ was significant, suggesting a better inactivation capacity of the treatment for vegetables than meat. In the case of meat, the presence of fats and proteins could play a significant role in protecting microorganisms from high-pressure CO$_2$ bactericidal action [40]. However, a deeper investigation of the inactivation mechanisms should be addressed to confirm any hypothesis, also including the effect on more food matrices.

The difference in microbial reduction within the two CO$_2$ treatments could be attributed to the lower amount of CO$_2$ used in the SC-MAPCO$_2$ compared to the one in the SC-CO$_2$. Indeed, considering the selected conditions (14 MPa and 40 °C), the CO$_2$ density is about 628.65 kg/m^3 [41]; thus, the CO$_2$ contained in the reactor used in the SC-CO$_2$ method (15 mL) is about 6.92 g, and in the case of SC-MAPCO$_2$ is about 0.17 g (considering a volume of the pouch of 100 mL at ambient pressure). This difference in CO$_2$ quantity between the two methods could also support the color modification results.

3.2. Effect of REO Alone and with CO$_2$ Treatments

After comparing the two treatments alone, the effect of REO and the evaluation of a possible synergic effect together with the supercritical CO$_2$ treatments was investigated. The effect of the oil was studied in terms of both color change and the inactivation capacity against *E. coli* and *L. innocua* for both methods, following a randomized 3 × 4 design of experiment.

Three REO concentrations were selected: 0.1, 0.5 and 1.0% according to previous works by González-Alonso et al. and Hamedo et al. [3,26].

The CIELAB color parameters and the total color difference for the untreated and treated samples with different REO concentrations are reported in Table 3.

The application of REO in the unprocessed samples (control) did not significantly change the superficial color of chicken breast; in fact, the values L*, a* and b* were not significantly different, and the ΔE values were lower than 1.5 for the entire range of REO concentrations used. Additionally, the results demonstrated that different percentages of REO did not further increase the color change in the case of SC-CO$_2$ treated samples. On the contrary, REO caused an increment of the parameter L* and the ΔE after the SC-MAPCO$_2$ process, but these values were still significantly lower than the ones achieved after the application of SC-CO$_2$ treatment. Moreover, the color difference was not influenced by the concentration of the oil. Overall, these data confirm that the SC-MAPCO$_2$ had a lower effect on the change of product color, even when REO was added.

The results regarding the Inactivation of the inoculated samples with *E. coli* and *L. innocua* are reported in Table 4.

Table 3. CIELAB color parameters (L*, a* and b*) and total color difference (ΔE) with respect to the raw chicken, for raw (control), treated with SC-CO_2, and treated with SC-MAPCO_2, sprinkled with different percentages of REO. Means with different superscript letters in the same column are significantly different ($p < 0.05$).

	REO (%)	L*	a*	b*	ΔE
Control	0.0	35.15 ± 2.98^{c}	0.06 ± 0.33^{a}	7.03 ± 0.06^{a}	/
	0.1	33.93 ± 0.53^{c}	-0.02 ± 0.48^{a}	6.50 ± 0.26^{abc}	1.33
	0.5	33.93 ± 1.06^{c}	0.14 ± 0.26^{a}	6.97 ± 0.14^{ab}	1.22
	1.0	33.72 ± 1.49^{c}	0.29 ± 0.50^{a}	6.93 ± 0.01^{ab}	1.45
SC-CO_2	0.0	55.07 ± 2.36^{a}	-0.31 ± 0.16^{a}	7.96 ± 1.49^{a}	19.95
	0.1	52.29 ± 1.02^{a}	-0.08 ± 0.78^{a}	6.26 ± 2.53^{ab}	17.16
	0.5	53.43 ± 2.15^{a}	0.29 ± 0.51^{a}	7.02 ± 0.20^{ab}	18.28
	1.0	53.11 ± 0.81^{a}	-0.30 ± 0.17^{a}	5.79 ± 1.28^{abc}	18.01
SC-MAPCO_2	0.0	36.27 ± 2.06^{c}	-0.33 ± 0.50^{a}	4.74 ± 1.42^{abc}	2.58
	0.1	42.84 ± 2.97^{b}	-0.59 ± 0.70^{a}	2.53 ± 0.77^{c}	8.83
	0.5	42.56 ± 0.26^{b}	-0.99 ± 0.35^{a}	3.94 ± 1.05^{bc}	8.10
	1.0	43.26 ± 2.13^{b}	-0.99 ± 0.31^{a}	3.66 ± 0.74^{bc}	8.84

Table 4. *E. coli* and *L. innocua* concentration, expressed in log CFU/g, for raw (control), treated with SC-CO_2, and treated with SC-MAPCO_2, sprinkled with different percentages of REO. Means with different superscript letters are significantly different ($p < 0.05$).

	REO (%)	*E. coli* (log CFU/g)	*L. innocua* (log CFU/g)
Control	-	7.03 ± 0.06^{a}	7.41 ± 0.14^{a}
	0.1	6.50 ± 0.26^{abc}	7.50 ± 0.11^{a}
	0.5	6.97 ± 0.14^{ab}	7.30 ± 0.06^{a}
	1.0	6.93 ± 0.01^{ab}	7.48 ± 0.25^{a}
SC-CO_2	-	5.74 ± 0.62^{cde}	5.99 ± 0.11^{c}
	0.1	5.02 ± 0.08^{de}	6.44 ± 0.13^{bc}
	0.5	4.58 ± 0.25^{ef}	6.31 ± 0.01^{c}
	1.0	3.62 ± 0.26^{f}	6.30 ± 0.62^{c}
SC-MAPCO_2	-	$6.40 \pm 0{,}21^{abc}$	7.25 ± 0.06^{a}
	0.1	6.56 ± 0.36^{abc}	6.96 ± 0.06^{ab}
	0.5	5.98 ± 0.10^{bc}	7.02 ± 0.05^{ab}
	1.0	5.73 ± 0.74^{cd}	7.19 ± 0.22^{a}

The data obtained showed that the addition of REO in raw chicken meat (untreated samples) was not able to reduce *E. coli* and *L. innocua*, even at the highest concentration applied. A possible explanation may be the matrix composition, since proteins and fats are able to bind the volatile compounds of essential oils [42], becoming less effective than in non-protein matrices. Indeed, the antimicrobial effect of REO is mainly caused by volatile components such as 1,8-cineole, α-pinene, camphor, camphene, borneol, myrcene, bornyl acetate, terpineol, linalool, limonene and caryophyllene [27,43]. Our result is in accordance with the work by Hamedo et al. [26] on soft cheese, to which REO was similarly added. Different studies reported instead a significant inactivation of various microorganisms on fruits and vegetables after the application of essential oils. Zhang et al. showed the

application of thyme essential oil on organic cantaloupes, obtaining a reduction of 2.26, 3.06 and 1.49 log CFU/cm^2 for *E. coli* O157:H7, *S. enterica* and *L. monocytogenes*, respectively [44].

In the case of *E. coli*, a synergic effect on the inactivation was observed when 1% REO was used in combination with high-pressure processing. In the case of SC-CO_2, 1% REO caused an additional 2.12 log CFU/g reduction compared to the SC-CO_2 alone. On the contrary, when a lower concentration of oil (0.1 and 0.5%) was used, no significant effect was achieved. A similar synergic effect was also observed for SC-MAPCO_2. The inactivation became significantly different in comparison with the untreated control only for 1% REO, reaching a reduction of 1.3 log CFU/g. The effect of the oil and its synergism with the treatments was also confirmed by the Pareto chart reported in Figure 3, which shows that the process is the most influential parameter for inactivation, followed by the oil concentration, followed by the combination of the process and REO.

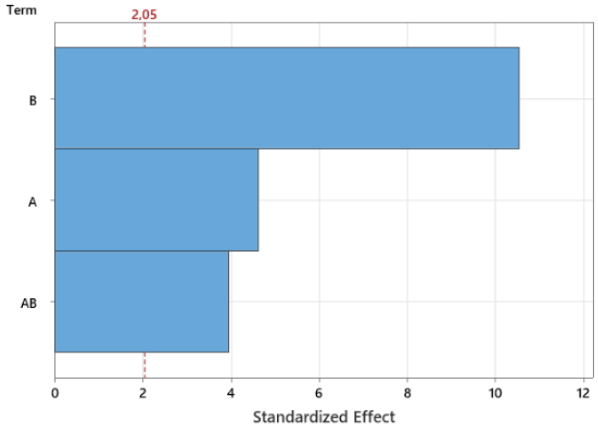

Figure 3. Pareto chart regarding the effect of the REO concentration (A), the processing method (B), and the combination of the two (AB) with respect to *E. coli* inactivation. The red dotted line indicated the minimum *t*-value at a confidence level of 95.0%.

The synergism between SC-CO_2 and REO for chicken breast meat was also investigated by González-Alonso et al. [3], who treated the inoculated samples at 14 MPa and 45 °C for 45 min. In that case, the only application of SC-CO_2 led to an inactivation of 4.74 ± 1.05 log CFU/g of *E. coli* (ATCC 25922), and the addition of REO (1%) did not improve the process performance significantly. These results are in contrast with the ones obtained in this study. A possible explanation might be due to different strains of *E. coli* that are more sensitive to the process being used. Indeed, in this study, a complete inactivation was achieved after 30 min, while González-Alonso et al. were still able to count cells after 45 min of treatment.

The precise mechanism of the synergism between REO and high-pressure CO_2 should be further investigated, including in the study the effect of different types of essential oils and different microorganisms. However, a possible explanation of the synergism might be already explained by the high solvating power and lipophilicity of supercritical CO_2. Specifically, the good solubility of the oil volatile components in SC-CO_2 can enhance their penetration through the bacterial membrane. A higher percentage of essential oil (more than 1%) might also have a stronger effect, but this may negatively influence the consumer acceptance of the process.

In this study, a strong dependence on the bacterial strain was also observed for the synergism. Specifically, in the case of *L. innocua*, REO was not able to increase the inactivation capacity of the two methods, even with the highest concentrations used. This difference with *E. coli* could be caused by the lower antimicrobial power of the oil against this strain, and not only by the membrane composition. Texeira et al. [45] observed a higher MIC (minimum inhibitory concentration) of REO on *L. innocua* compared with that of *E. coli*, and consequently a greater amount of REO may have been needed to obtain an antimicrobial effect. As a further demonstration of the dependence on the type of microorganism, some inactivation experiments for the natural present total mesophilic and

total psychrophilic bacteria were performed using SC-MAPCO$_2$ coupled with 1% of REO. The results are reported in Table 5.

Table 5. Mesophilic and psychrophilic microbial population, expressed as log CFU/g, of fresh chicken breast (control) and that treated with SC-MAPCO$_2$, with and without REO (1%). Means with different superscript letters are significantly different ($p < 0.05$).

Sample	Mesophilic Bacteria	Psychrophilic Bacteria
Control	5.38 ± 0.04^{a}	5.24 ± 0.30^{a}
Control + 1% REO	5.12 ± 0.17^{ab}	5.52 ± 0.47^{a}
SC-MAPCO$_2$	4.10 ± 0.66^{bc}	4.56 ± 0.15^{a}
SC-MAPCO$_2$ + 1% REO	3.27 ± 0.62^{c}	3.19 ± 0.70^{b}

Fresh chicken meat presented an initial microbial load equal to 5.38 and 5.24 log CFU/g of mesophilic and psychrophilic bacteria, respectively. Additionally, in this case, the only addition of 1% of REO did not significantly reduce the natural present bacteria load. SC-MAPCO$_2$ alone was able to significantly reduce the total mesophilic bacteria of 1.28 log CFU/g, while the psychrophilic load was not different from the control. Adding 1% REO caused a reduction of both mesophilic and psychrophilic bacteria. The synergism was significant only for the psychrophilic bacteria.

This is an interesting result, since in the work of Gonzales-Alonso et al. [3], a mesophilic microbial reduction of 2.64 ± 0.32 log CFU/g was obtained with SC-CO$_2$ coupled with fresh rosemary at the same pressure and temperature conditions, but after 45 min of treatment. These findings are promising for the obtainment of a prolonged shelf-life of the product; however, further data are needed to confirm this hypothesis.

4. Conclusions

This work studied the effect of REO and two CO$_2$-based processes on the microbial inactivation and retention of qualitative aspects of raw chicken breast meat. The inactivation capacity was evaluated for inoculated *E. coli* and *L. innocua*. The SC-MAPCO$_2$ method was able to better maintain the visual aspect of the product compared with SC-CO$_2$. On the contrary, the inactivation capacity was significant only for the SC-CO$_2$ treatment for both microorganisms. The REO alone was not able to induce any significant reduction of inoculated *E. coli* and *L. innocua*. When REO was used in a synergistic manner with SC-CO$_2$ at 1%, the inactivation was higher compared with SC-CO$_2$ alone, but only for *E. coli*. Similarly, a significant inactivation capacity compared to the control samples is possible with SC-MAPCO$_2$, but only in synergism with 1% REO. In this case, the inactivation is significant only for *E. coli* and the total psychrophilic bacteria, but not significant for *L. innocua* and the total mesophiles.

Regarding the color change, SC-CO$_2$ has a strong impact on L*, a* and b* while SC-MAPCO$_2$ has a mild effect. However, when REO was added to the SC-MAPCO$_2$ process, the color change became significantly different for L*, compared to the untreated samples with a higher value of the ΔE. In any case, the overall color change was still lower compared to SC-CO$_2$.

Overall, the results demonstrated the possible synergism between the SC-CO$_2$/SC-MAPCO$_2$ at a specific percentage of REO, but also a strong dependence on the type of microorganism investigated. Future studies should focus on the possible synergisms with different types of EO and microbial strains. Moreover, the effect of the process and REO on the sensorial and quality attributes of the product should be studied for further application at industrial level, as well as for their effect on the possible extension of storage time.

Author Contributions: Conceptualization, F.S., R.Z., A.Z. and S.S.; methodology, F.S., R.Z., A.Z. and S.S.; validation, F.S., R.Z., A.Z. and S.S.; formal analysis, F.S. and R.Z.; investigation, F.S., E.L. and R.Z.; resources, A.Z. and S.S.; data curation, F.S., R.Z., E.L., A.Z. and S.S.; writing—original draft preparation, F.S., R.Z., E.L., A.Z. and S.S.; writing—review and editing, F.S., R.Z., E.L., A.Z. and S.S.; visualization, F.S., R.Z., E.L., A.Z. and S.S.; supervision, A.Z. and S.S.; project administration, A.Z. and S.S.; funding acquisition, S.S. All authors have read and agreed to the published version of the manuscript.

Funding: This research received no external funding.

Institutional Review Board Statement: Not applicable.

Informed Consent Statement: Not applicable.

Data Availability Statement: The data are available from the corresponding author.

Conflicts of Interest: A.Z. and S.S. are co-inventors of the patent describing the new method for food pasteurization: Italian patent n. 10201700009804, European patent application n. 17787252.0, Chinese Patent application n. 201780094448.6 and US Patent application n. 16/642401.

References

1. Uzundumlu, A.S.; Dilli, M. Estimating Chicken Meat Productions of Leader Countries for 2019–2025 Years. *Cienc. Rural* **2023**, *53*, 2. [CrossRef]
2. Tong, H.; Cao, C.; Du, Y.; Liu, Y.; Huang, W. Ultrasonic-Assisted Phosphate Curing: A Novel Approach to Improve Curing Rate and Chicken Meat Quality. *Int. J. Food Sci. Technol.* **2022**, *57*, 2906–2917. [CrossRef]
3. González-Alonso, V.; Cappelletti, M.; Bertolini, F.M.; Lomolino, G.; Zambon, A.; Spilimbergo, S. Research Note: Microbial Inactivation of Raw Chicken Meat by Supercritical Carbon Dioxide Treatment Alone and in Combination with Fresh Culinary Herbs. *Poult. Sci.* **2020**, *99*, 536–545. [CrossRef] [PubMed]
4. Yucel, B.; Taskin, T. *Animal Husbandry and Nutrition*; BoD—Books on Demand: Burlington, ON, Canada, 2018.
5. Katiyo, W.; de Kock, H.L.; Coorey, R.; Buys, E.M. Sensory Implications of Chicken Meat Spoilage in Relation to Microbial and Physicochemical Characteristics during Refrigerated Storage. *LWT* **2020**, *128*, 109468. [CrossRef]
6. Chun, H.H.; Kim, J.Y.; Lee, B.D.; Yu, D.J.; Song, K.B. Effect of UV-C Irradiation on the Inactivation of Inoculated Pathogens and Quality of Chicken Breasts during Storage. *Food Control* **2010**, *21*, 276–280. [CrossRef]
7. European Centre for Disease Prevention and Control, European Food Safety Authority. Multi-Country Outbreak of Salmonella Mbandaka ST413, Possibly Linked to Consumption of Chicken Meat in the EU/EEA, Israel and the UK. *EFSA Support. Publ.* **2022**, *19*, 7707E.
8. Piñon, M.; Alarcon-Rojo, A.; Paniwnyk, L.; Mason, T.; Luna, L.; Renteria, A. Ultrasound for Improving the Preservation of Chicken Meat. *Food Sci. Technol.* **2018**, *39*, 129–135. [CrossRef]
9. Chouliara, E.; Badeka, A.; Savvaidis, I.; Kontominas, M.G. Combined Effect of Irradiation and Modified Atmosphere Packaging on Shelf-Life Extension of Chicken Breast Meat: Microbiological, Chemical and Sensory Changes. *Eur. Food Res. Technol.* **2008**, *226*, 877–888. [CrossRef]
10. D'Souza, C.; Apaolaza, V.; Hartmann, P.; Brouwer, A.R.; Nguyen, N. Consumer Acceptance of Irradiated Food and Information Disclosure—A Retail Imperative. *J. Retail. Consum. Serv.* **2021**, *63*, 102699. [CrossRef]
11. Režek Jambrak, A. *Nonthermal Processing in Agri-Food-Bio Sciences: Sustainability and Future Goals*; Springer Nature: Berlin, Germany, 2022.
12. Kruk, Z.A.; Yun, H.; Rutley, D.L.; Lee, E.J.; Kim, Y.J.; Jo, C. The Effect of High Pressure on Microbial Population, Meat Quality and Sensory Characteristics of Chicken Breast Fillet. *Food Control* **2011**, *22*, 6–12. [CrossRef]
13. Chen, H.; Guan, Y.; Wang, A.; Zhong, Q. Inactivation of Escherichia Coli K12 on Raw Almonds Using Supercritical Carbon Dioxide and Thyme Oil. *Food Microbiol.* **2022**, *103*, 103955. [CrossRef]
14. Ferrentino, G.; Belscak-Cvitanovic, A.; Komes, D.; Spilimbergo, S. Quality Attributes of Fresh-Cut Coconut after Supercritical Carbon Dioxide Pasteurization. *J. Chem.* **2013**, *2013*, 703057. [CrossRef]
15. Spilimbergo, S.; Komes, D.; Vojvodic, A.; Levaj, B.; Ferrentino, G. High Pressure Carbon Dioxide Pasteurization of Fresh-Cut Carrot. *J. Supercrit. Fluids* **2013**, *79*, 92–100. [CrossRef]
16. Spilimbergo, S.; Zambon, A.; Michelino, F.; Polato, S. Method for Food Pasteurization. Patent no. WO2019043442A1, 25 June 2020.
17. Barberi, G.; González-Alonso, V.; Spilimbergo, S.; Barolo, M.; Zambon, A.; Facco, P. Optimization of the Appearance Quality in CO_2 Processed Ready-to-Eat Carrots through Image Analysis. *Foods* **2021**, *10*, 2999. [CrossRef]
18. Zambon, A.; González-Alonso, V.; Lomolino, G.; Zulli, R.; Rajkovic, A.; Spilimbergo, S. Increasing the Safety and Storage of Pre-Packed Fresh-Cut Fruits and Vegetables by Supercritical CO_2 Process. *Foods* **2022**, *12*, 21. [CrossRef]
19. Bae, Y.Y.; Choi, Y.M.; Kim, M.J.; Kim, K.H.; Kim, B.C.; Rhee, M.S. Application of Supercritical Carbon Dioxide for Microorganism Reductions in Fresh Pork. *J. Food Saf.* **2011**, *31*, 511–517. [CrossRef]
20. De Souza Pedrosa, G.T.; Pimentel, T.C.; Gavahian, M.; de Medeiros, L.L.; Pagán, R.; Magnani, M. The Combined Effect of Essential Oils and Emerging Technologies on Food Safety and Quality. *LWT* **2021**, *147*, 111593. [CrossRef]

21. Sivarajan, M.; Lalithapriya, U.; Mariajenita, P.; Vajiha, B.A.; Harini, K.; Madhushalini, D.; Sukumar, M. Synergistic Effect of Spice Extracts and Modified Atmospheric Packaging towards Non-Thermal Preservation of Chicken Meat under Refrigerated Storage. *Poult. Sci.* **2017**, *96*, 2839–2844. [CrossRef]
22. Bhattacharya, D.; Nanda, P.K.; Pateiro, M.; Lorenzo, J.M.; Dhar, P.; Das, A.K. Lactic Acid Bacteria and Bacteriocins: Novel Biotechnological Approach for Biopreservation of Meat and Meat Products. *Microorganisms* **2022**, *10*, 2058. [CrossRef]
23. Chen, F.; Zhang, M.; Yang, C. Application of Ultrasound Technology in Processing of Ready-to-Eat Fresh Food: A Review. *Ultras. Sonochem.* **2020**, *63*, 104953. [CrossRef]
24. Stratakos, A.C.; Delgado-Pando, G.; Linton, M.; Patterson, M.F.; Koidis, A. Synergism between High-Pressure Processing and Active Packaging against Listeria Monocytogenes in Ready-to-Eat Chicken Breast. *Innov. Food Sci. Emerg. Technol.* **2015**, *27*, 41–47. [CrossRef]
25. Bozin, B.; Mimica-Dukic, N.; Samojlik, I.; Jovin, E. Antimicrobial and Antioxidant Properties of Rosemary and Sage (*Rosmarinus Officinalis* L. and *Salvia Officinalis* L., *Lamiaceae*) Essential Oils. *J. Agric. Food Chem.* **2007**, *55*, 7879–7885. [CrossRef] [PubMed]
26. Hamedo, H.A.; Abdelmigid, H.M. Use of Antimicrobial and Genotoxicity Potentiality for Evaluation of Essential Oils as Food Preservatives. *Open Biotechnol. J.* **2009**, *3*, 50–56. [CrossRef]
27. Alvarez, M.V.; Ortega-Ramirez, L.A.; Silva-Espinoza, B.A.; Gonzalez-Aguilar, G.A.; Ayala-Zavala, J.F. Antimicrobial, Antioxidant, and Sensorial Impacts of Oregano and Rosemary Essential Oils over Broccoli Florets. *J. Food Process. Preserv.* **2019**, *43*, e13889. [CrossRef]
28. Vrinda Menon, K.; Garg, S.R. Inhibitory Effect of Clove Oil on Listeria Monocytogenes in Meat and Cheese. *Food Microbiol.* **2001**, *18*, 647–650. [CrossRef]
29. Garcia-Sotelo, D.; Silva-Espinoza, B.; Perez-Tello, M.; Olivas, I.; Alvarez-Parrilla, E.; González-Aguilar, G.A.; Ayala-Zavala, J.F. Antimicrobial Activity and Thermal Stability of Rosemary Essential Oil:B−cyclodextrin Capsules Applied in Tomato Juice. *LWT* **2019**, *111*, 837–845. [CrossRef]
30. Yang, H.-J.; Lee, J.-H.; Lee, K.-Y.; Song, K.B. Antimicrobial Effect of an Undaria Pinnatifida Composite Film Containing Vanillin against Escherichia Coli and Its Application in the Packaging of Smoked Chicken Breast. *Int. J. Food Sci. Technol.* **2017**, *52*, 398–403. [CrossRef]
31. Pathare, P.B.; Opara, U.L.; Al-Said, F.A.-J. Colour Measurement and Analysis in Fresh and Processed Foods: A Review. *Food Bioprocess Technol.* **2013**, *6*, 36–60. [CrossRef]
32. Chen, M.; Sui, X.; Ma, X.; Feng, X.; Han, Y. Application of Response Surface Methodology to Optimise Microbial Inactivation of Shrimp and Conch by Supercritical Carbon Dioxide. *J. Sci. Food Agric.* **2015**, *95*, 1016–1023. [CrossRef]
33. Sirisee, U.; Hsieh, F.; Huff, H.E. Microbial Safety of Supercritical Carbon Dioxide Processes1. *J. Food Proc. Preserv.* **1998**, *22*, 387–403. [CrossRef]
34. Zhou, L.; Wang, Y.; Hu, X.; Wu, J.; Liao, X. Effect of High Pressure Carbon Dioxide on the Quality of Carrot Juice. *Inn. Food Sci. Emerg. Technol.* **2009**, *10*, 321–327. [CrossRef]
35. Bak, K.H.; Bolumar, T.; Karlsson, A.H.; Lindahl, G.; Orlien, V. Effect of High Pressure Treatment on the Color of Fresh and Processed Meats: A Review. *Crit. Rev. Food Sci. Nutr.* **2019**, *59*, 228–252. [CrossRef]
36. Monhemi, H.; Housaindokht, M.R. The Molecular Mechanism of Protein Denaturation in Supercritical CO_2: The Role of Exposed Lysine Residues Is Explored. *J. Supercrit. Fluids* **2019**, *147*, 222–230. [CrossRef]
37. Hu, M.; Gurtler, J.B. Selection of Surrogate Bacteria for Use in Food Safety Challenge Studies: A Review. *J Food Prot.* **2017**, *80*, 1506–1536. [CrossRef]
38. Morbiato, G.; Zambon, A.; Toffoletto, M.; Poloniato, G.; Dall'Acqua, S.; de Bernard, M.; Spilimbergo, S. Supercritical Carbon Dioxide Combined with High Power Ultrasound as Innovate Drying Process for Chicken Breast. *J. Supercrti. Fluids* **2019**, *147*, 24–32. [CrossRef]
39. Wei, C.I.; Balaban, M.O.; Fernando, S.Y.; Peplow, A.J. Bacterial Effect of High Pressure CO_2 Treatment on Foods Spiked with Listeria or Salmonella. *J. Food Prot.* **1991**, *54*, 189–193. [CrossRef]
40. Garcia-Gonzalez, L.; Geeraerd, A.H.; Spilimbergo, S.; Elst, K.; Van Ginneken, L.; Debevere, J.; Van Impe, J.F.; Devlieghere, F. High Pressure Carbon Dioxide Inactivation of Microorganisms in Foods: The Past, the Present and the Future. *Int. J. Food Microbiol.* **2007**, *117*, 1–28. [CrossRef]
41. Sievers, U. *Die Thermodynamischen Eigenschaften von Kohlendioxid*; Springer Nature: Berlin, Germany, 1984; Volume 50.
42. Ji, J.; Shankar, S.; Royon, F.; Salmieri, S.; Lacroix, M. Essential Oils as Natural Antimicrobials Applied in Meat and Meat Products-a Review. *Crit. Rev. Food Sci. Nutr.* **2021**, *63*, 993–1009. [CrossRef]
43. Sarïcaoglu, F.T.; Turhan, S. Antimicrobial Activity and Antioxidant Capacity of Thyme, Rosemary and Clove Essential Oils and Their Mixtures. *J. Inn. Sci. Eng.* **2018**, *2*, 25–33.
44. Zhang, Y.; Ma, Q.; Critzer, F.; Davidson, P.M.; Zhong, Q. Organic Thyme Oil Emulsion as an Alternative Washing Solution to Enhance the Microbial Safety of Organic Cantaloupes. *Food Control* **2016**, *67*, 31–38. [CrossRef]
45. Teixeira, A.A. Thermal Food Preservation Techniques (Pasteurization, Sterilization, Canning and Blanching). In *Conventional and Advanced Food Processing Technologies*; John Wiley & Sons, Ltd.: Hoboken, NJ, USA, 2014; pp. 115–128.

foods

MDPI

Article

Non-Thermal Plasma Decontamination Using a Multi-Hollow Surface Dielectric Barrier Discharge: Impact of Food Matrix Composition on Bactericidal Efficacy

Klaas De Baerdemaeker [1], Amber Van Reepingen [1], Anton Nikiforov [2], Bruno De Meulenaer [3], Nathalie De Geyter [2] and Frank Devlieghere [1,*]

[1] Research Unit Food Microbiology and Food Preservation (FMFP), Department of Food Technology, Safety and Health, Ghent University, Coupure Links 653, 9000 Ghent, Belgium
[2] Research Unit Plasma Technology (RUPT), Department of Applied Physics, Ghent University, Sint-Pietersnieuwstraat 41, 9000 Ghent, Belgium
[3] NutriFOODchem Research Group, Department of Food Technology, Safety and Health, Ghent University, Coupure Links 653, 9000 Ghent, Belgium
* Correspondence: frank.devlieghere@ugent.be; Tel.: +32-9-264-61-77

Abstract: The non-thermal plasma (NTP) treatment of food products as an alternative for thermal processing has been investigated over the last few years. This quasi-neutral gas contains a wide variety of reactive oxygen and nitrogen species (RONS), which could be lethal for bacterial cells present in the product. However, apart from only targeting bacteria, the RONS will also interact with components present in the food matrix. Therefore, these food components will protect the microorganisms, and the NTP treatment efficiency will decrease. This effect was investigated by supplementing a plain agar medium with various representative food matrix components. After inoculation with *Escherichia coli* O157:H7 (STEC) MB3885, the plates were treated for 30 s by a multi-hollow surface dielectric barrier discharge (MSDBD) generated in either dry air or air at 75% humidity, at constant power (25.7 $\pm$ 1.7 W). Subsequently, the survival of the cells was quantified. It has been found that the addition of casein hydrolysate (7.1 $\pm$ 0.2 m%), starch (2.0 m%), or soybean oil (4.6 m%) decreased the inactivation effect significantly. Food products containing these biomolecules might therefore need a more severe NTP treatment. Additionally, with increasing humidity of the plasma input gas, ozone levels decreased, and the bactericidal effect was generally less pronounced.

Keywords: multi-hollow SDBD; cold plasma; non-thermal technologies; food matrix; bacterial inactivation; lipid oxidation

1. Introduction

Thermal treatment of food products for preservation purposes has been used for around 6000 years, initially by drying and smoking of the foods. Later, with the industrial revolution, thermal pasteurization and sterilization technologies were developed, increasing the preservation power even more [1]. However, in recent times, the consumer has shown an increased interest in minimally processed foods that have the characteristics of freshness but without compromising on safety [2]. As conventional thermal treatment processes result in the loss of heat-sensitive nutritional components and changes in texture and organoleptic qualities, non-thermal techniques have been developed to respond to consumer demand [3,4]. Technologies such as high-pressure processing, pulsed electric field, and irradiation are non-thermal and established concepts in the food industry, but in the last years, a growing interest is also shown in non-thermal plasma (NTP) for bacterial inactivation [5]. PlAgri (2022) reported that the annual production of scientific documents in the field of plasma technology in the food industry increased from one to 255 in the period from 2003 to 2020 [6]. Surowsky et al., (2015) even mentioned around 800 publications dealing with non-thermal plasma-based microbial inactivation in foods in 2013 [7].

The concept of plasma was first described by Langmuir (1928) to define the gas region containing balanced charges of ions and electrons [8]. Plasma reactivity is the result of the presence of free electrons and radicals, ions, excited atoms and molecules, reactive oxygen and nitrogen species (RONS), and electromagnetic radiation (UV photons and visible light) [9–12]. Although the electrons in a non-thermal plasma are at a temperature of 10^4–10^5 °C, the heavy particles are close to ambient temperature. Apart from avoiding heat degradation, the advantages of NTP for food treatment are its energy efficiency [13], the possibility to operate at atmospheric pressure (so avoiding the need for vacuum equipment) [14], and the fact that it could be created from gasses that are conventionally used for modified atmosphere packaging (MAP) [15]. Additionally, for the treatment of solid foods, NTP acts only on the surface of the product, retaining the nutritional qualities on the inside [16].

The bactericidal effect of NTP treatment is the result of various modes of action. NTP irradiation is said to cause the denaturation of membrane proteins, being detrimental to the survival and duplication of the cell [17]. Reactive oxygen species will oxidize and/or damage essential biomolecules such as DNA, proteins, enzymes, lipids, and fatty acids (e.g., in the cell membrane). The cell membrane and cell wall will be disintegrated by chemical alterations and the breaking of important bonds, including C-O, C-N, and C-C. This will cause cell leakage and loss of cell functionality [18]. On the other hand, there is no scientific consensus on the contribution of UV photons in NTP to bacterial decontamination as they show bactericidal potential in various ways but are easily absorbed by the gas atoms and molecules at atmospheric pressure [19,20].

Earlier research by De Baerdemaeker et al., (2022) and Huang et al., (2020) showed that the bactericidal effect of NTP decreased when bacteria were inoculated and treated on real food products compared to agar plates. This could be explained by, among other things, the roughness of the food surface, protecting the bacterial cells [21,22]. Han et al., (2020) showed that this negative correlation between surface roughness and bacterial inactivation was linear [23]. Furthermore, Ziuzina et al., (2015) reported the entrance of bacterial cells into the pores of plant leaves, reducing the antimicrobial efficacy of NTP [24]. However, as food constituents such as lipids and proteins are prone to oxidation by ROS [25,26], it would be expected that those components also affect NTP's efficacy. Nevertheless, there are only limited studies on the effect of the food matrix. In the current study, the aim is to explore this matrix effect by investigating the impact of various food components on bacterial inactivation using non-thermal plasmas generated from the air at both low and high relative humidity (RH) based on the humidity of gasses recommended for food packaging [27] and the composition of the plasma.

2. Materials and Methods

First, agar media supplemented with various food components at different levels representative of their potential presence in food products were prepared. The plates were inoculated with a standardized amount of *Escherichia coli* cells, and the NTP was treated at constant power (25.7 $\pm$ 1.7 W) and using air at 0% or 75% relative humidity (high levels and near absence of ozone, respectively, see Section 3.1), after which the bacterial cells were recovered, and surviving cells were quantified. A comparison of the recovery between the different components, their concentrations, and the humidity of the input gas allowed for understanding the effect of those components and relative humidity on bactericidal efficacy. Additionally, the plasma was characterized under the same conditions, and NTP inactivation on different supplemented media was evaluated with respect to the plasma composition.

2.1. Supplemented Agar Media Preparation

Agar plates were prepared, containing plain (pure) bacteriological agar (15 g/L, LP0011B, Oxoid), which was supplemented with one of the three concentrations of a certain major food matrix component (Table 1), each agar containing only one type of

biomolecule. For all those components, changes in inactivation levels with increasing concentration were compared against a reference sample with no addition of the particular component but containing all chemicals facilitating its dissolution and undergoing the same preparation methods. For low-humidity plasma, all concentrations (reference, low, middle, and high) were analyzed, while the reference sample was only compared with the highest concentration when applying high-humidity plasma. Seven different components from five classes were added to the agars: proteins (casein hydrolysate (22090, Sigma-Aldrich, St. Louis, MO, USA)), carbohydrates (glucose (CL00.0710, Chem-Lab, Zedelgem, Belgium) and soluble starch (S9765, Sigma-Aldrich)), lipids (refined soybean oil and stripped soybean oil (AH slaolie, Albert Heijn, Zaandam, The Netherlands)), salt (NaCl (CL00.1429, Chem-Lab)), and anti-oxidants (β-carotene (C9750, Sigma-Aldrich)). Casein is a protein with very little secondary and tertiary structure [28], meaning all the amino acids are available, and none are structurally protected from interaction with the RONS. With the hydrolyzed protein, also referred to as peptone from casein, this is even more the case. Soybean oil consists of a good mixture of saturated fatty acids (SFA, 15%), mono-unsaturated fatty acids (MUFA, 23%), and poly-unsaturated fatty acids (PUFA, 62%) [29,30]. The refined oil was prepared by removing only oxidation products already present in commercial soybean oil by means of column chromatography on silica gel (1.15101, Millipore, Burlington, MA, USA). The stripped oil was, in addition, stripped of naturally occurring anti-oxidants (column chromatography with aluminum oxide (11503, Thermo Fisher Scientific, Waltham, MA, USA) following the silica gel column chromatography). Column chromatography was carried out using the method described by Wang et al., (2018) [31].

Table 1. Concentrations of the food matrix components in the supplemented agar media applied in this study based on their presence in real-life food products. Seven different components from five classes (indicated in bold) were added to the agars.

	Low Conc. [1]	**Middle Conc.** [1]	**High Conc.** [1]	**Additional Chemicals** [2]
Protein				
Casein hydrolysate	2.6	5.1	7.1 ± 0.2	HCl and NaOH
Carbohydrates				
Glucose	2.0	10.0	18.0	-
Starch	2.0	10.0	18.0	-
Lipids [3]				
Stripped soybean oil	4.5	21.0	37.5	Tween 20 (2.0 m%)
Refined soybean oil	4.6	21.7	38.7	Tween 20 (2.0 m%)
Salt				
NaCl	0.1	1.6	3.0	-
Anti-oxidants				
β-carotene	0.1	3.6	7.0	DMSO (5.8 v/m%) and Tween 20 (1.2 v/m%)

[1] Concentrations are expressed as g/100 g agar medium for all components, except β-carotene (mg/100 g medium). [2] Present in low, medium, and high concentration agar media and in reference medium (agar medium without food component), always in same concentrations. [3] Concentration of triglycerides in the agar medium is identical for both types of oils, which explains the differences in addition of both types of soybean oil.

For the glucose and NaCl, the procedure for medium preparation was identical. Plain agar medium and a solution of the food constituent, both at double concentration, were autoclaved and filter sterilized (0.45 µm pore size, 296–4545, Thermo Fisher Scientific, Waltham, MA, USA), respectively, and subsequently aseptically mixed at a 1:1 ratio. A casein medium was prepared by making a casein hydrolysate solution at a double concentration in distilled water and adapting the pH to 10.5 by the addition of a 0.1 M and 10 M NaOH (71690, Sigma-Aldrich) solution. This casein solution was sonicated for 30 min at 50 °C and filter sterilized (0.2 µm pore size, 596–4520, Thermo Fisher Scientific, Waltham, MA, USA), and the loss of precipitate was quantified by analyzing the weight of the filter after drying. The sterile solution was mixed with plain double-strength agar medium (1:1),

and the pH was reduced to 8.5 in a sterile manner with a 1 M and 6 M HCl (30721, Sigma-Aldrich) solution. For the starch agar medium, plain agar medium and a concentrated starch solution were mixed and sterilized (autoclaved). Soybean oil, whether stripped or unstripped of anti-oxidants, was mixed with Tween 20 (233362500, Acros Organics, Morris Plains, NJ, USA) while heating and kept at 48 °C before the addition of a sterile agar medium of higher strength to form a homogeneous mixture. The anti-oxidant β-carotene was first suspended in a mixture of dimethyl sulfoxide (DMSO, CL00.0422, Sigma-Aldrich) and Tween 20 and subsequently added to a sterile agar medium. To ensure an equal concentration of DMSO (5.8 mL/100 g medium) and Tween 20 (1.2 mL/100 g medium) over all supplemented agar media, an extra amount of the mixture of those components (without β-carotene) was required for some agar media and the reference.

Since the distance between the sample and electrodes has been shown to affect NTP bactericidal potential (data not shown), the height and, therefore, the volume of (supplemented) agar medium in all plates was standardized to ensure equal treatment. For all different samples, small Petri dishes (Ø 5.5 cm) were filled with 10 mL of the respective supplemented agar medium. Plates with soybean oil or β-carotene were stored for a maximum of 1 week in an anaerobic environment (AnaeroGen, AN0025A, Thermo Fisher Scientific, Waltham, MA, USA) to prevent oxidation of the biomolecules. All plates were kept at 4 °C until further use.

2.2. Plasma Treatment

Plasma was generated using the multi-hollow surface dielectric barrier discharge (MSDBD) setup shown in Figure 1. The MSDBD consists of two gold mesh electrodes placed at a distance of 0.20 mm with the interelectrode space filled with a dielectric barrier (Al_2O_3). An airflow (synthetic air, 14746, Air Products), whether or not humidified to 75% RH (near absence of ozone, see Section 3.1) by bubbling through a water column of ca. 89 cm, of 5 standard L/min (slm) went perpendicular through 260 holes (Ø 1.00 mm), arranged symmetrically in a hexagonal configuration in the electrode system. This gas flow was controlled by mass flow controllers (Bronkhorst). The discharge was generated by a high voltage pulse generator (Redline Technologies) at alternating current (frequency of 64.01 kHz) and supplied energy to the system at constant power (25.7 ± 1.7 W). Samples were NTP treated for 30 s at a distance of 18 mm from the electrodes, after which the active atmosphere was removed by flushing the reactor for 2 more minutes before opening.

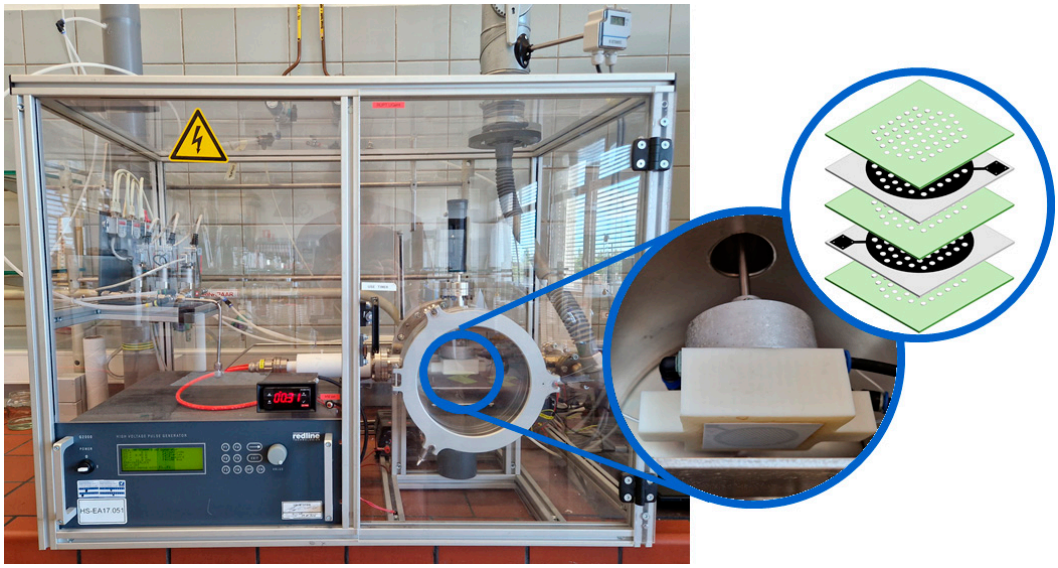

Figure 1. Multi-hollow surface dielectric barrier discharge setup used in the current study. On the right, a detailed image and schematic overview of the electrode system are presented (green = dielectric; black = electrode).

Under those conditions, the temperature increase of the plasma exhaust, measured with an iButton data logger (Maxim Integrated), was limited to ca. 8.5 °C, which proved the non-thermal properties of the applied NTP. The plasma-treated gas was analyzed by Fourier-transformed infrared spectroscopy (FTIR) using a Matrix-MG2 Bruker FTIR spectrometer, enabling the quantitative analysis of the concentrations of NO, NO_2, N_2O_5, N_2O, and ozone. The detection was performed by a collection of the effluent gas and stable products at a 3 m distance from the plasma reactor. The optical multi-pass gas cell of 5.0 m length was used to measure the absorption, and the absolute calibrations were performed by Bruker. Spectra were obtained with an average of 50 scans with a resolution of 0.5 cm^{-1}. The system was flushed thoroughly with air for at least 15 min in between measurements.

2.3. Strain Preparation

Escherichia coli O157:H7 (STEC) MB3885 was obtained from the FMFP (Ghent University) culture collection as cryobeads in a 15% glycerol (CL00.0736, Chem-Lab) in brain heart infusion (BHI, CM1135, Oxoid) broth at −75 °C. Two beads were transferred to fresh BHI and incubated for 2 days at 37 °C. A pure culture, obtained by the four-quadrant streak method (37 °C, 1 day) on tryptone soy agar (TSA, CM0131, Oxoid), was transferred to TSA slants (37 °C, 1 day) and kept as such for no more than 6 weeks (4 °C).

The day before every experiment, a loopful of the subculture was transferred to fresh BHI broth and incubated at 37 °C for ca. 1 day. One mL of the homogenized cell suspension was brought in an Eppendorf tube and centrifuged (8000 rpm, 5 min), after which the supernatant was replaced by fresh peptone physiological solution (PPS). This centrifugation and washing step was repeated twice more, resulting in an inoculum at a high concentration. Finally, the cell suspension was diluted to obtain an inoculum at a concentration of ca. 7 log CFU/mL. Actual concentrations and purity were determined by the standard pour-plating technique with both TSA and RAPID'E.coli 2 Medium (3564024, Bio-Rad Laboratories Inc., Hercules, CA, USA).

2.4. Sample Handling

The (supplemented) media plates were inoculated with 0.1 mL (ca. 6 log CFU/sample) of the diluted inoculum and dried for 15 min by air. Consequently, the plates were NTP treated (see Section 2.2). Cells were recovered from the (supplemented) agar medium by making a tenfold dilution with PPS and extraction in a Stomacher device. Survival of STEC was quantified by the standard pour-plating technique with TSA.

2.5. Statistical Analysis

All tests regarding inactivation levels on agar media supplemented with different concentrations of the food components were performed in triplicates. Inactivation was determined as the difference in survival of treated and their respective untreated plates. Homoscedasticity was determined by Levene's test (based on the median) with $\alpha = 0.01$. For plasma generated from dry air (comparison of four concentration levels from the same component), ANOVA (post-hoc Tukey or Games-Howell in case of homo- or heteroscedasticity, respectively) was used for analyzing the significance ($\alpha = 0.05$) of the differences in inactivation levels. For humid air plasma (comparison of two concentration levels from the same component), the same comparison was made by means of the independent sample *t*-test. For both levels of RH, the inactivation on agars supplemented with monomeric glucose was compared with the inactivation on starchy (polymeric glucose) agars at the same concentration by using the independent sample *t*-test ($\alpha = 0.05$). The same statistical tests were performed to compare both types of oily agars. Finally, for every component at a certain concentration, the effect of relative humidity of the plasma input gas was analyzed by the independent sample *t*-test ($\alpha = 0.05$).

3. Results

Plain agar plates were supplemented with various food matrix components in different concentrations, inoculated with STEC, and treated with non-thermal plasma in a multi-hollow surface dielectric barrier discharge. Plasma was generated from either dry air (0% RH) or humid air (75% RH).

3.1. Plasma Characterization

The concentrations of various long-living RONS (N_2O, N_2O_5, NO, NO_2 and O_3) generated during the first 50 s of treatment were measured for input air with increasing RH using Fourier-transform infrared spectroscopy. These characterization results are shown in Figure 2. With increasing %RH, the ozone concentration in the plasma drops remarkably, from 796 ± 1 ppm at 0% RH to 9 ± 1 ppm at 100% RH. On the other hand, the concentrations of NO and even more so NO_2 increase with increasing %RH. N_2O levels remain quasi-constant, while N_2O_5 decreases with increasing RH and is already absent at 75% RH. These decreasing ozone and N_2O_5 concentrations and increasing levels of NO_2 and NO at increasing RH will have an impact on the antibacterial efficiency of the MSDBD treatment. This motivates the choice to compare the bactericidal potential of plasma at 0% and 75% RH with an ozone-rich atmosphere and the near absence of ozone in dry and humid air plasma, respectively. Next to this, an RH of 75% is representative of the relative humidity of the headspace of packaged microbiologically unstable food products.

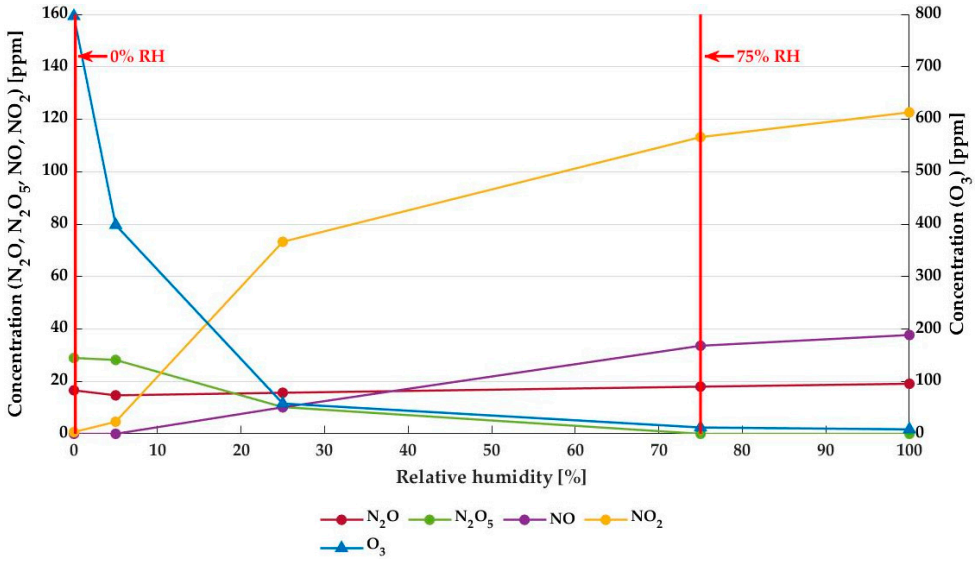

Figure 2. Characterization of NTP by FTIR in the first 50 s of plasma generation as a function of relative humidity of the input air. The left axis shows the concentration of N_2O, N_2O_5, NO, and NO_2 (circles); on the right axis, the concentration of ozone (O_3) in the plasma is projected (triangles).

3.2. NTP Inactivation with Dry and Humid Air Plasma

Inactivation levels of STEC when using dry air for plasma generation are shown in Figure 3. Without the addition of food components, inactivation reached levels of around 3.8 log CFU/sample, except for β-carotene (2.7 log CFU/sample, possibly due to the reaction between DMSO used for making a stable agar media and OH radicals in the plasma [32]). However, all those reference media reached the limit of detection (LOD) for at least one of three repeats (with the same exception), so inactivation could, in reality, be even higher. Agar medium supplemented with casein did show a reduced bactericidal effect with increasing protein concentration, although this was only significant ($p \leq 0.05$) for the highest level of casein addition (7.1 ± 0.2 m%). For starch agar, the decrease in inactivation potential was even more explicit, and even at the lowest concentration (2.0 m%) evaluated, the effect of starch on the inactivation of STEC was statistically significant ($p \leq 0.05$). Middle and high-starch concentrations did not differ significantly from each other. In contrast to

the starch polysaccharide, its monomeric building blocks (glucose) did not significantly alter the NTP inactivation of STEC ($p > 0.05$), even at concentrations as high as 18.0 m%. This resulted in a significant difference ($p \leq 0.05$) between inactivation on high-starch and high-glucose agar media. Additionally, STEC inactivation in the presence of lipids differed significantly from the reference sample, and this was for all investigated concentrations (low, middle, and high). However, for all tested concentrations (except the middle one), there was no significant difference between stripped and refined oil. Finally, in analogy to media supplemented with glucose, the addition of β-carotene or NaCl did not result in any significant changes in bactericidal effect ($p > 0.05$), although for the latter component, a slight but not statistically relevant decrease in inactivation was noticed.

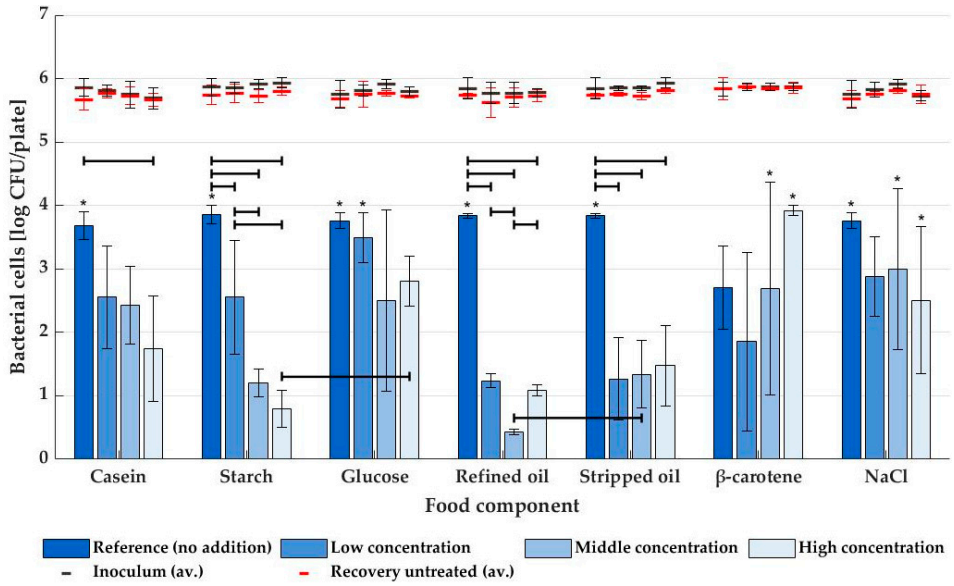

Figure 3. Average NTP inactivation levels (and standard deviations) of STEC on agar media supplemented with various food matrix components ($n = 3$), with plasma generated from dry air. An asterisk (*) indicates that inactivation reached LOD for at least one repeat. All components were tested at low, middle, and high concentrations (see Table 1) and compared against a reference sample without addition. The average inoculum and number of cells recovered from untreated samples are given as black and red lines, respectively. Significant differences between inactivation levels are indicated with black horizontal lines.

Levels of inactivation for plasma generated from humid air at 75% RH are shown as red bars in Figure 4. A significant effect ($p \leq 0.05$) of casein addition was observed, even resulting in a complete drop of bactericidal potential to approximately 0 log CFU/sample. Just as for dry air plasma, it was statistically shown that the polysaccharide starch chain negatively affected the decontamination efficiency ($p \leq 0.05$), while this was not the case for the monomeric glucose units ($p > 0.05$). Furthermore, the effect of refined oil and stripped oil was quasi-identical: a decrease from >3.0 log CFU to ca. 1.0 log CFU inactivation after the addition of the lipid component. Finally, neither β-carotene nor NaCl impacted the humid air plasma inactivation.

For non-thermal plasma treatment on unsupplemented (reference) media, STEC inactivation was always lower when humidified air was used for plasma generation (see Figure 4). However, this was only significant ($p \leq 0.05$) for the casein-, glucose- and NaCl-reference media. Although these food matrix components themselves were not present in the reference media, the additional chemicals used during media preparation (see Table 1) and the sometimes rather high standard deviation might have played a role. When the food constituents were added in high concentrations, only for the casein- and β-carotene-supplemented media did the NTP inactivation differ significantly at 75% RH compared to 0% RH.

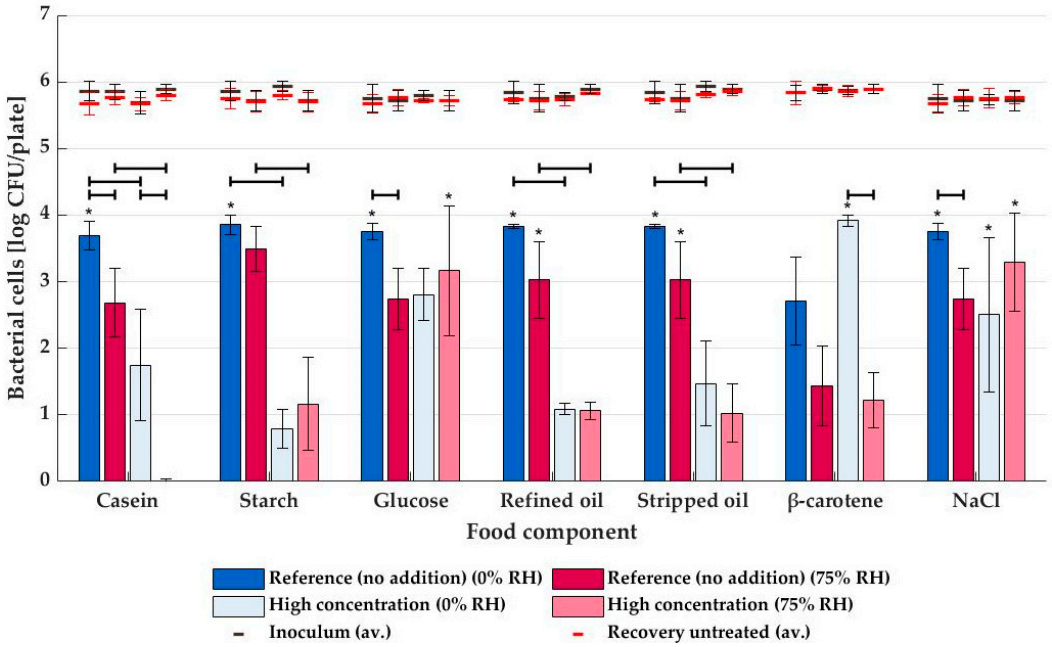

Figure 4. Average NTP inactivation levels (and standard deviations) of STEC on agar media supplemented with various food matrix components (n = 3), with plasma generated from dry air (0% RH, blue bars) and humid air (75% RH, red bars). An asterisk (*) indicates that inactivation reached LOD for at least one repeat. All components were tested at high concentrations (see Table 1) and compared against a reference sample without addition. The average inoculum and number of cells recovered from untreated samples are given as black and red lines, respectively. Significant differences between inactivation levels are indicated with black horizontal lines.

4. Discussion

The main long-living RONS were characterized using FTIR spectroscopy. As shown in Figure 2, the most abundant long-living RONS in the dry air MSDBD exhaust was ozone. Its production in non-thermal air plasma happens by various pathways, although the mechanism is rather complex due to the presence of nitrogen [13,33]. The main reaction for ozone formation involves O_2, atomic oxygen (O), and molecular oxygen or nitrogen (M). O was formed due to electron impact dissociation of molecular O_2. This simple mechanism, given by Equations (1) and (2), does not include reactions with excited species or other molecules (e.g., NO and NO_2), nor does it take into account ozone self-destruction reactions [33].

$$e + O_2 \rightarrow O + O + e, \quad (1)$$

$$O + O_2 + M \rightarrow O_3 + M, \quad (2)$$

The ozone concentration drops drastically with the increasing humidity of the carrier gas. According to Patil et al., (2014), this could be attributed to the quenching/attachment of electrons to H_2O, leading to water dissociation and a direct ozone reaction with the water molecules. It has been shown by optical absorption spectroscopy (OAS) that increasing %RH results in a lower ozone concentration due to the formation of N_2O_5, peroxides (mainly H_2O_2), HNO_4, OH and to a lesser extent also N_2O_4 and HONO [34]. Nevertheless, in the current study, the concentration of N_2O_5 decreased (Figure 2), while the other RONS mentioned were not measured due to the limitation of the IR detection of the short-living RONS. It is said that the electronic dissociation of water in a non-thermal plasma leads to the formation of an OH radical, which rapidly reacts with ozone to form the peroxy-radical HO_2. The latter component itself also reacts with ozone molecules, again forming OH and O_2 [13]. Correspondingly, it is expected that the chemistry initiated by NTP in conditions of dry air and humid air should be substantially different. In the case of dry air, the main

mechanism will be ozone driven, whereas active nitrogen species and peroxide radicals are defining the chemistry at high RH.

The bactericidal potential of non-thermal plasma technology for the treatment of (contaminated) solid (food) surfaces has been proven before [21,35–37]. Nevertheless, research has also shown that this microbial inactivation is lower when treating real food products compared to agar plates [38,39]. The reason for this observation can most probably not be attributed to one factor but is rather a combination of several elements. Han et al., (2020) have shown that surface roughness is negatively correlated with the NTP bacterial inactivation rate [23], and Ziuzina et al., (2015) found how bacteria could enter stomata on the produce surface, which protects them from inactivation by NTP [24]. However, it has been shown by De Baerdemaeker et al., (2022), although to a limited extent, that the composition of the food matrix also has a major influence on the bactericidal effect of non-thermal plasma [21].

The effect of proteins and their amino acids was investigated in the current study by supplementing casein hydrolysate (peptone from casein) to plain agar medium. As seen in Figures 3 and 4, concentrations as high as 7.1 $\pm$ 0.2 m% had a significantly negative impact on the MSDBD plasma efficacy. Cataldo (2003) observed the interaction of ozone with some individual amino acids, mainly tryptophan, but also methionine, cystine, tyrosine, and phenylalanine [40]. According to Liu et al., (2019), these amino acids make up ca. 16.1 m% of the casein molecule [41]. These interactions between amino acids and the RONS might render the reactive plasma components unavailable for interaction with microorganisms, which explains the decrease in NTP inactivation efficacy on protein-rich media. In NTP generated from the air with high humidity, the ozone concentration drops close to zero, and NO_2 seems to be most abundantly present (98.23 ppm). This nitrogen species, proven to be bactericidal [42], interacts strongly with tryptophan and, to a lesser extent, tyrosine [43], which might cause the bactericidal effect to disappear completely at 75% RH.

The presence of glucose did not seem to have an immediate impact on the bactericidal effect of NTP treatment, neither at low nor high concentrations. Interestingly, in contrast to its monomeric units, the polymeric starch chain does impact the bactericidal efficacy of NTP treatment negatively, even at concentrations of only 2.0 m%. This shows the interaction between the polymer and the reactive plasma species, which could be the result of various pathways. The depolymerization process results in the formation of several fragments [44–46], and although it has been reported that NTP treatment can also induce cross-linking of the chain and/or increase its molecular weight (MW) [46–48], the degree of polymerization and MW of the starch molecules generally decrease during plasma treatment, depending on the type of starch and treatment dose [46–49]. Additionally, oxidation of the starch by the RONS will also induce changes to the starch molecules, as well as the introduction of functional groups by the RONS [45,46,50]. Again, the more interaction between the RONS and starch, the lower the bactericidal effect of NTP treatment will be, illustrated by a decrease in bacterial inactivation at higher starch concentrations in Figures 3 and 4. Both ozone and NO_2, the major components in dry and humid air plasma, respectively (see Figure 2), are known to interact with the polysaccharide [51,52], expressed by a similar reduction of NTP inactivation potential on starchy surfaces for dry and humid air plasmas. Additionally, peroxynitrite ($ONOO^-$) and hydrogen peroxide (H_2O_2), two bactericidal agents [53–55] that are known to be present in humid air plasma or the gas-liquid interface [34,56], might increase the decontamination efficiency of the humid air NTP treatment. As H_2O_2 reaction with starch is very slow or requires high temperatures [57], this oxygen species can still react with bacteria, even on starchy surfaces. However, analysis of peroxynitrite and hydrogen peroxide was not possible by means of FTIR, so no results on their concentrations in the plasma are available. A remark needs to be made on the surface properties of high-starch media plates, as these media had a more gel-like and rough surface that could protect the bacterial cells from reactive plasma species.

Lipids are known to be prone to oxidation, even when exposed only to air [58]. Characterization of NTP used in the current study indicated the presence of ozone, NO_2,

and/or NO, all of which have been shown to impact the lipid oxidation process [26,58–61]. Due to this interaction between lipids and the RONS, the efficacy of the MSDBD treatment decreased both for low and high RH plasmas. It has been proven by Rød et al., (2012) that NTP treatment as short as five seconds could result in the formation of oxidation products [62]. Furthermore, there were generally no differences between inactivation levels when using soybean oil with or without its naturally occurring anti-oxidants, although it would be expected that those anti-oxidants would protect bacterial cells even more by capturing the RONS in the plasma. However, it would be too soon to conclude that these components intrinsically do not impact plasma inactivation, as their naturally occurring concentrations might be too low to have a considerable effect. It has been found that higher concentrations of α-tocopherol, an anti-oxidant present in soybean oil [63], do show a protective effect on bacteria during NTP treatment by scavenging ROS [64].

Analogously, no significant effect of β-carotene, another anti-oxidant, supplementation to the agar medium was observed. Since this vitamin A precursor is known to scavenge, e.g., ozone [65], a decrease in bacterial decontamination was expected. Possibly, the presence of DMSO in the agar impacts the effect of the β-carotene as the former has been shown to react with alkenes, abundantly present with β-carotene, with the formation of methyl sulfones. This reaction needs hydroxyl radicals, which could be supplied by the plasma discharge [66].

The addition of NaCl to the agar could impact NTP inactivation in different ways. Earlier research has shown that ozone and NaCl could form the bactericidal component hypochlorous acid [67,68]. On the other hand, the salt ions (presumably Cl^-) may protect the microorganisms by increasing the solution density, resulting in a decreased movement of reactive plasma species and lower accessibility to bacterial cells [69]. Nevertheless, no significant effect on NTP efficacy was found by supplementing NaCl to the agars when using dry or humid air.

5. Conclusions

This study shows that various food matrix components do have an important effect on NTP inactivation efficacy against STEC. Treatment of (food) products with a significant lipid or starch content (>4.5 and 2.0 m%, respectively) will result in an important reduction of bacterial decontamination during treatment, although this also depends on saturation degree and amino acid composition, respectively. The concentration of anti-oxidants naturally present in the oil is too low to impact the NTP inactivation potential. On the other hand, protein content needs to be rather high (7.1 ± 0.2 m%) in order to have a clear effect, although the effect is more pronounced when humid air is used for plasma generation (no bacterial reduction at high casein concentration and 75% RH). For these reasons, protein-rich and sugary food products seem to be better suited to be NTP treated compared to greasy foods. This could be fruits and vegetables, although their surfaces will also be of major importance. Furthermore, NTP might be advantageous compared to other (conventional or novel) technologies for the microbial decontamination of lean meats. For fish and meat products with higher fat content, the treatment dose needs to be increased. Nevertheless, it needs to be taken into account that a higher treatment dose might also induce a more intense nutrient loss (e.g., protein degradation), although, for solid foods, this will be limited to the surface of the product. Therefore, these changes to the nutritional value due to the current MSDBD plasma treatment should be investigated as such. Additionally, the relative humidity of the headspace at the moment of plasma treatment of packaged products is a critical factor for the efficiency of the NTP treatment, especially when both NTP and packaging technologies are integrated into one system. These considerations are of utmost importance when an (MSDBD) non-thermal plasma treatment is implemented in the production chain and show the need for an appropriate design.

Author Contributions: Conceptualization, K.D.B., A.N., B.D.M., N.D.G. and F.D.; methodology, K.D.B., A.V.R. and F.D.; validation, K.D.B., A.V.R. and F.D.; formal analysis, K.D.B. and A.V.R.; investigation, A.V.R. and A.N.; resources, A.N., B.D.M., N.D.G. and F.D.; data curation, K.D.B., A.V.R. and F.D.; writing—original draft preparation, K.D.B.; writing—review and editing, K.D.B., A.V.R., A.N., B.D.M., N.D.G. and F.D.; visualization, K.D.B. and A.V.R.; supervision, N.D.G. and F.D.; project administration, N.D.G. and F.D.; funding acquisition, B.D.M., N.D.G. and F.D. All authors have read and agreed to the published version of the manuscript.

Funding: This research was funded by The Special Research Fund of Ghent University, grant number 01G00120.

Data Availability Statement: The data presented in this study are openly available in Zenodo at https://doi.org/10.5281/zenodo.7385615.

Acknowledgments: The authors would like to thank Danyang Liu (NutriFOODchem, Ghent University) for his help with oil and lipid handling.

Conflicts of Interest: The authors declare no conflict of interest.

References

1. Knorr, D.; Watzke, H. Food Processing at a Crossroad. *Front. Nutr.* **2019**, *6*, 85. [CrossRef] [PubMed]
2. Alzamora, S.M.; López-Malo, A.; Tapia, M.S.; Welti-Chanes, J. Minimally Processed Foods. In *Encyclopedia of Food and Health*; Academic Press: Kidlington, Oxford, UK, 2016; Volume 3, pp. 767–771. ISBN 9780123849533.
3. Barba, F.J.; Orlien, V.; Mota, M.J.; Lopes, R.P.; Pereira, S.A.; Saraiva, J.A. Implementation of Emerging Technologies. In *Innovation Strategies in the Food Industry*; Academic Press: Kidlington, Oxford, UK, 2022; pp. 121–143.
4. Jadhav, H.B.; Annapure, U.S.; Deshmukh, R.R. Non-Thermal Technologies for Food Processing. *Front. Nutr.* **2021**, *8*, 248. [CrossRef] [PubMed]
5. Khouryieh, H.A. Novel and Emerging Technologies Used by the U.S. Food Processing Industry. *Innov. Food Sci. Emerg. Technol.* **2021**, *67*, 102559. [CrossRef]
6. COST Action CA19110 (PlAgri). WG5 Technical Roadmap—Key Food Applications and Standardized Procedures. 2022. Available online: https://plagri.eu/wg5-applications-of-plasma-processes-and-technologies-in-food-industry/ (accessed on 2 December 2022).
7. Surowsky, B.; Schlüter, O.; Knorr, D. Interactions of Non-Thermal Atmospheric Pressure Plasma with Solid and Liquid Food Systems: A Review. *Food Eng. Rev.* **2015**, *7*, 82–108. [CrossRef]
8. Langmuir, I. Oscillations in Ionized Gases. *Proc. Natl. Acad. Sci. USA* **1928**, *14*, 627–637. [CrossRef]
9. Bourke, P.; Ziuzina, D.; Boehm, D.; Cullen, P.J.; Keener, K. The Potential of Cold Plasma for Safe and Sustainable Food Production. *Trends Biotechnol.* **2018**, *36*, 615–626. [CrossRef]
10. Whitehead, J.C. Plasma-Catalysis: The Known Knowns, the Known Unknowns and the Unknown Unknowns. *J. Phys. D Appl. Phys.* **2016**, *49*, 243001. [CrossRef]
11. Fridman, A. Introduction to Theoretical and Applied Plasma Chemistry. In *Plasma Chemistry*; Cambridge University Press: Cambridge, UK, 2008; pp. 1–11.
12. Misra, N.N.; Ziuzina, D.; Cullen, P.J.; Keener, K.M. *Characterization of a Novel Cold Atmospheric Air Plasma System for Treatment of Packaged Liquid Food Products*; American Society of Agricultural and Biological Engineers: St. Joseph, MI, USA, 2012; Volume 3.
13. Whitehead, J.C. The Chemistry of Cold Plasma. In *Cold Plasma in Food and Agriculture: Fundamentals and Applications*; Misra, N.N., Schlüter, O., Cullen, P.J., Eds.; Academic Press, 2016; pp. 53–81. ISBN 9780128013656.
14. von Woedtke, T.; Reuter, S.; Masur, K.; Weltmann, K.D. Plasmas for Medicine. *Phys Rep* **2013**, *530*, 291–320. [CrossRef]
15. Wang, J.; Zhuang, H.; Hinton, A.; Zhang, J. Influence of In-Package Cold Plasma Treatment on Microbiological Shelf Life and Appearance of Fresh Chicken Breast Fillets. *Food Microbiol* **2016**, *60*, 142–146. [CrossRef]
16. Surowsky, B.; Bußler, S.; Schlüter, O.K. Cold Plasma Interactions With Food Constituents in Liquid and Solid Food Matrices. In *Cold Plasma in Food and Agriculture: Fundamentals and Applications*; Misra, N.N., Schlüter, O., Cullen, P.J., Eds.; Academic Press: Kidlington, Oxford, UK, 2016; pp. 179–203, ISBN 9780128013656.
17. Kim, Y.-M.; Yun, H.-S.; Eom, S.-H.; Sung, B.-J.; Lee, S.-H.; Jeon, S.-M.; Chin, S.-W.; Lee, M.-S. Bactericidal Action Mechanism of Nonthermal Plasma: Denaturation of Membrane Proteins. *IEEE Trans. Radiat. Plasma Med. Sci.* **2018**, *2*, 77–83. [CrossRef]
18. Misra, N.N.; Jo, C. Applications of Cold Plasma Technology for Microbiological Safety in Meat Industry. *Trends Food Sci. Technol.* **2017**, *64*, 74–86. [CrossRef]
19. Vleugels, M.; Shama, G.; Deng, X.T.; Greenacre, E.; Brocklehurst, T.; Kong, M.G. Atmospheric Plasma Inactivation of Biofilm-Forming Bacteria for Food Safety Control. *IEEE Trans. Plasma Sci.* **2005**, *33*, 824–828. [CrossRef]
20. Roth, S.; Feichtinger, J.; Hertel, C. Characterization of Bacillus Subtilis Spore Inactivation in Low-Pressure, Low-Temperature Gas Plasma Sterilization Processes. *J. Appl. Microbiol.* **2010**, *108*, 521–531. [CrossRef]

21. de Baerdemaeker, K.; van der Linden, I.; Nikiforov, A.; Zuber, S.; de Geyter, N.; Devlieghere, F. Non-Thermal Plasma Inactivation of Salmonella Typhimurium on Different Matrices and the Effect of Selected Food Components on Its Bactericidal Efficacy. *Food Res. Int.* **2022**, *151*, 110866. [CrossRef] [PubMed]
22. Huang, Y.M.; Chen, C.K.; Hsu, C.L. Non-Thermal Atmospheric Gas Plasma for Decontamination of Sliced Cheese and Changes in Quality. *Food Sci. Technol. Int.* **2020**, *26*, 715–726. [CrossRef] [PubMed]
23. Han, J.-Y.; Song, W.-J.; Eom, S.; Kim, S.B.; Kang, D.-H. Antimicrobial Efficacy of Cold Plasma Treatment against Food-Borne Pathogens on Various Foods. *J. Phys. D Appl. Phys.* **2020**, *53*, 204003. [CrossRef]
24. Ziuzina, D.; Han, L.; Cullen, P.J.; Bourke, P. Cold Plasma Inactivation of Internalised Bacteria and Biofilms for Salmonella Enterica Serovar Typhimurium, Listeria Monocytogenes and Escherichia Coli. *Int. J. Food Microbiol.* **2015**, *210*, 53–61. [CrossRef]
25. Hayashi, N.; Yagyu, Y. Treatment of Protein Using Oxygen Plasma Produced by RF Discharge. *Trans. Mater. Res. Soc. Jpn.* **2008**, *33*, 791–794. [CrossRef]
26. Sarangapani, C.; Ryan Keogh, D.; Dunne, J.; Bourke, P.; Cullen, P.J. Characterisation of Cold Plasma Treated Beef and Dairy Lipids Using Spectroscopic and Chromatographic Methods. *Food Chem.* **2017**, *235*, 324–333. [CrossRef]
27. Gross, K.C.; Wang, Y.; Saltveit, M. *The Commercial Storage of Fruits, Vegetables, and Florist and Nursery Stocks*; United States Department of Agriculture: Washington, DC, USA, 2016; Volume 66.
28. Bhat, M.Y.; Dar, T.A.; Rajendrakumar Singh, L. Casein Proteins: Structural and Functional Aspects. In *Milk Proteins—From Structure to Biological Properties and Health Aspects*; InTech: Rijeka, Croatia, 2016. [CrossRef]
29. Gunstone, F.D.; Harwood, J.L.; Dijkstra, A.J. *The Lipid Handbook with CD-ROM*, 3rd ed.; CRC Press: Boca Raton, FL, USA, 2007.
30. Carrera, C.S.; Dardanelli, J.L. Water Deficit Modulates the Relationship between Temperature and Unsaturated Fatty Acid Profile in Soybean Seed Oil. *Crop Sci.* **2017**, *57*, 3179–3189. [CrossRef]
31. Obando, M.; Soto, E.; de Meulenaer, B. Influence of Oxidized Oils on Digestibility of Caseins in O/W Emulsions. *Eur. J. Lipid Sci. Technol.* **2018**, *120*, 1700331. [CrossRef]
32. Lee, Y.; Lee, C.; Yoon, J. Kinetics and Mechanisms of DMSO (Dimethylsulfoxide) Degradation by UV/H2O2 Process. *Water Res.* **2004**, *38*, 2579–2588. [CrossRef]
33. Pekárek, S. Non-Thermal Plasma Ozone Generation. *Acta Polytech.* **2003**, *43*, 47–51. [CrossRef] [PubMed]
34. Patil, S.; Moiseev, T.; Misra, N.N.; Cullen, P.J.; Mosnier, J.P.; Keener, K.M.; Bourke, P. Influence of High Voltage Atmospheric Cold Plasma Process Parameters and Role of Relative Humidity on Inactivation of Bacillus Atrophaeus Spores inside a Sealed Package. *J. Hosp. Infect.* **2014**, *88*, 162–169. [CrossRef] [PubMed]
35. Pasquali, F.; Stratakos, A.C.; Koidis, A.; Berardinelli, A.; Cevoli, C.; Ragni, L.; Mancusi, R.; Manfreda, G.; Trevisani, M. Atmospheric Cold Plasma Process for Vegetable Leaf Decontamination: A Feasibility Study on Radicchio (Red Chicory, *Cichorium Intybus* L.). *Food Control* **2016**, *60*, 552–559. [CrossRef]
36. Timmons, C.; Pai, K.; Jacob, J.; Zhang, G.; Ma, L.M. Inactivation of Salmonella Enterica, Shiga Toxin-Producing Escherichia Coli, and Listeria Monocytogenes by a Novel Surface Discharge Cold Plasma Design. *Food Control* **2018**, *84*, 455–462. [CrossRef]
37. Ziuzina, D.; Misra, N.N.; Han, L.; Cullen, P.J.; Moiseev, T.; Mosnier, J.P.; Keener, K.; Gaston, E.; Vilaró, I.; Bourke, P. Investigation of a Large Gap Cold Plasma Reactor for Continuous In-Package Decontamination of Fresh Strawberries and Spinach. *Innov. Food Sci. Emerg. Technol.* **2020**, *59*, 102229. [CrossRef]
38. Yong, H.I.; Kim, H.J.; Park, S.; Alahakoon, A.U.; Kim, K.; Choe, W.; Jo, C. Evaluation of Pathogen Inactivation on Sliced Cheese Induced by Encapsulated Atmospheric Pressure Dielectric Barrier Discharge Plasma. *Food Microbiol.* **2015**, *46*, 46–50. [CrossRef]
39. Critzer, F.J.; Kelly-Wintenberg, K.; South, S.L.; Golden, D.A. Atmospheric Plasma Inactivation of Foodborne Pathogens on Fresh Produce Surfaces. *J. Food Prot.* **2007**, *70*, 2290–2296. [CrossRef]
40. Cataldo, F. On the Action of Ozone on Proteins. *Polym. Degrad. Stab.* **2003**, *82*, 105–114. [CrossRef]
41. Liu, J.; Klebach, M.; Visser, M.; Hofman, Z. Amino Acid Availability of a Dairy and Vegetable Protein Blend Compared to Single Casein, Whey, Soy, and Pea Proteins: A Double-Blind, Cross-over Trial. *Nutrients* **2019**, *11*, 2613. [CrossRef] [PubMed]
42. Fang, F.C. Mechanisms of Nitric Oxide-Related Antimicrobial Activity. *J. Clin. Investig.* **1997**, *99*, 2818–2825. [CrossRef] [PubMed]
43. Kikugawa, K.; Kato, T.; Okamoto, Y. Damage of Amino Acids and Proteins Induced by Nitrogen Dioxide, a Free Radical Toxin, in Air. *Free Radic. Biol. Med.* **1994**, *16*, 373–382. [CrossRef]
44. Klein, B.; Vanier, N.L.; Moomand, K.; Pinto, V.Z.; Colussi, R.; da Rosa Zavareze, E.; Dias, A.R.G. Ozone Oxidation of Cassava Starch in Aqueous Solution at Different PH. *Food Chem.* **2014**, *155*, 167–173. [CrossRef] [PubMed]
45. Lii, C.; Liao, C.-D.; Stobinski, L.; Tomasik, P. Effect of Corona Discharges on Granular Starches. *J. Food Agric. Environ.* **2003**, *1*, 143–149.
46. Thirumdas, R.; Kadam, D.; Annapure, U.S. Cold Plasma: An Alternative Technology for the Starch Modification. *Food Biophys.* **2017**, *12*, 129–139. [CrossRef]
47. Bie, P.; Pu, H.; Zhang, B.; Su, J.; Chen, L.; Li, X. Structural Characteristics and Rheological Properties of Plasma-Treated Starch. *Innov. Food Sci. Emerg. Technol.* **2016**, *34*, 196–204. [CrossRef]
48. Wongsagonsup, R.; Deeyai, P.; Chaiwat, W.; Horrungsiwat, S.; Leejariensuk, K.; Suphantharika, M.; Fuongfuchat, A.; Dangtip, S. Modification of Tapioca Starch by Non-Chemical Route Using Jet Atmospheric Argon Plasma. *Carbohydr. Polym.* **2014**, *102*, 790–798. [CrossRef]
49. Zhang, B.; Xiong, S.; Li, X.; Li, L.; Xie, F.; Chen, L. Effect of Oxygen Glow Plasma on Supramolecular and Molecular Structures of Starch and Related Mechanism. *Food Hydrocoll.* **2014**, *37*, 69–76. [CrossRef]

50. Morent, R.; de Geyter, N.; Gengembre, L.; Leys, C.; Payen, E.; van Vlierberghe, S.; Schacht, E. Surface Treatment of a Polypropylene Film with a Nitrogen DBD at Medium Pressure. *Eur. Phys. J. Appl. Phys* **2008**, *43*, 289–294. [CrossRef]
51. Kerr, R.W. The Action of Nitrogen Dioxide on Corn Starch and Its Fractions. *J. Am. Chem. Soc.* **1950**, *72*, 816–820. [CrossRef]
52. Castanha, N.; Miano, A.C.; Jones, O.G.; Reuhs, B.L.; Campanella, O.H.; Augusto, P.E.D. Starch Modification by Ozone: Correlating Molecular Structure and Gel Properties in Different Starch Sources. *Food Hydrocoll.* **2020**, *108*, 106027. [CrossRef]
53. Zhu, L.; Gunn, C.; Beckman, J.S. Bactericidal Activity of Peroxynitrite. *Arch Biochem. Biophys.* **1992**, *298*, 452–457. [CrossRef]
54. Hernandez, P.; Sager, B.; Fa, A.; Liang, T.; Lozano, C.; Khazzam, M. Bactericidal Efficacy of Hydrogen Peroxide on Cutibacterium Acne. *Bone Jt. Res.* **2019**, *8*, 3–10. [CrossRef]
55. Zhou, R.; Zhou, R.; Prasad, K.; Fang, Z.; Speight, R.; Bazaka, K.; Ostrikov, K. Cold Atmospheric Plasma Activated Water as a Prospective Disinfectant: The Crucial Role of Peroxynitrite. *Green Chem.* **2018**, *20*, 5276–5284. [CrossRef]
56. Bruno, G.; Wenske, S.; Lackmann, J.W.; Lalk, M.; von Woedtke, T.; Wende, K. On the Liquid Chemistry of the Reactive Nitrogen Species Peroxynitrite and Nitrogen Dioxide Generated by Physical Plasmas. *Biomolecules* **2020**, *10*, 1687. [CrossRef] [PubMed]
57. Dias, A.R.G.; Zavareze, E.D.R.; Helbig, E.; de Moura, F.A.; Vargas, C.G.; Ciacco, C.F. Oxidation of Fermented Cassava Starch Using Hydrogen Peroxide. *Carbohydr. Polym.* **2011**, *86*, 185–191. [CrossRef]
58. Zhou, Y.; Park, H.; Kim, P.; Jiang, Y.; Costello, C.E. Surface Oxidation under Ambient Air-Not Only a Fast and Economical Method to Identify Double Bond Positions in Unsaturated Lipids but Also a Reminder of Proper Lipid Processing. *Anal. Chem.* **2014**, *86*, 5697–5705. [CrossRef]
59. Kim, T.J.; Silva, J.L.; Chamul, R.S.; Chen, T.C. Influence of Ozone, Hydrogen Peroxide, or Salt on Microbial Profile, TBARs and Color of Channel Catfish Fillets. *J. Food Sci.* **2000**, *65*, 1210–1213. [CrossRef]
60. Pryor, W.A.; Lightsey, J.W. Mechanisms of Nitrogen Dioxide Reactions: Initiation of Lipid Peroxidation and the Production of Nitrous Acid. *Science* **1981**, *214*, 435–437. [CrossRef]
61. Hogg, N.; Kalyanaraman, B. Nitric Oxide and Lipid Peroxidation. *Biochim. Biophys. Acta* **1999**, *1411*, 378–384. [CrossRef] [PubMed]
62. Rød, S.K.; Hansen, F.; Leipold, F.; Knøchel, S. Cold Atmospheric Pressure Plasma Treatment of Ready-to-Eat Meat: Inactivation of Listeria Innocua and Changes in Product Quality. *Food Microbiol.* **2012**, *30*, 233–238. [CrossRef] [PubMed]
63. Niki, E.; Abe, K. CHAPTER 1. Vitamin E: Structure, Properties and Functions. In *Food Chemistry, Function and Analysis No. 11*; Royal Society of Chemistry: Croydon, UK, 2019; pp. 1–11. ISBN 978-1-78801-240-9.
64. Joshi, S.G.; Cooper, M.; Yost, A.; Paff, M.; Ercan, U.K.; Fridman, G.; Friedman, G.; Fridman, A.; Brooks, A.D. Nonthermal Dielectric-Barrier Discharge Plasma-Induced Inactivation Involves Oxidative DNA Damage and Membrane Lipid Peroxidation in Escherichia Coli. *Antimicrob. Agents Chemother.* **2011**, *55*, 1053–1062. [CrossRef] [PubMed]
65. Benevides, C.M.D.J.; Veloso, M.C.D.C.; de Paula Pereira, P.A.; de Andrade, J.B. A Chemical Study of β-Carotene Oxidation by Ozone in an Organic Model System and the Identification of the Resulting Products. *Food Chem.* **2011**, *126*, 927–934. [CrossRef]
66. Jiang, Y.; Loh, T.-P. Catalytic and Direct Methyl Sulfonylation of Alkenes and Alkynes Using a Methyl Sul-fonyl Radical Generated from a DMSO, Dioxygen and Copper System. *Chem. Sci.* **2014**, *5*, 4939–4943. [CrossRef]
67. Bocci, V.; Zanardi, I.; Travagli, V. Answer on Letter to Professor E. I. Nazarov (from Velio Bocci). Available online: http://ozonetherapy.org/answer-bocci-nazarov/ (accessed on 2 December 2022).
68. Bocci, V.; Zanardi, I.; Travagli, V. Oxygen/Ozone as a Medical Gas Mixture. A Critical Evaluation of the Various Methods Clarifies Positive and Negative Aspects. *Med. Gas Res.* **2011**, *1*, 6. [CrossRef]
69. Kang, M.H.; Hong, Y.J.; Attri, P.; Sim, G.B.; Lee, G.J.; Panngom, K.; Kwon, G.C.; Choi, E.H.; Uhm, H.S.; Park, G. Analysis of the Antimicrobial Effects of Nonthermal Plasma on Fungal Spores in Ionic Solutions. *Free Radic. Biol. Med.* **2014**, *72*, 191–199. [CrossRef]

foods

MDPI

Article

Effects of Atmospheric Plasma Corona Discharge on *Saccharomyces cerevisiae:* Viability, Permeability, and Morphology

Irina Amar Dubrovin, Efrat Emanuel, Yulia Lazra and Rivka Cahan *

Department of Chemical Engineering, Ariel University, Ariel 40700, Israel
* Correspondence: rivkac@ariel.ac.il; Tel.: +972-54-7740293

Abstract: Food spoilage is a routine challenge in food production. *Saccharomyces cerevisiae* is a major contaminating microorganism associated with fruit pulps and juices. Our study demonstrated the effect of a plasma corona discharge on *S. cerevisiae* viability, membrane permeability, and morphology when the cells were prepared in both dry and wet modes. The *S. cerevisiae* viability was examined as a function of the duration of plasma exposure, the sample's distance from the treating head, initial cell concentration, and yeast suspension volume. The results showed a linear correlation between the exposure duration and the CFU/mL in both dry and wet modes. When the initial yeast concentration was 10^6 CFU/mL, complete eradication in the dry and wet modes occurred after 45 and 240 s, respectively. Exposure of different initial concentrations of *S. cerevisiae* to plasma in dry (20 s) or wet (90 s) mode led to 2 to 3 orders of magnitude reduction. In both modes, there was total eradication when the initial cell concentration was about 10^3 CFU/mL. The cell-membrane permeability was examined using a flow cytometer and the fluorescent dye propidium iodide (PI). Plasma treatment in the dry mode for 30 and 45 s led to 51% and 76% PI-positive cells. Similar results were obtained in the wet mode but with a longer exposure for 120 and 240 s, respectively. Atmospheric plasma may provide disinfection technology for the food industry in a short process without heating.

Keywords: atmospheric plasma corona discharge; yeasts; *Saccharomyces cerevisiae*; viability

1. Introduction

Food spoilage is a common problem in the food industry. Factors that influence food spoilage are water availability and quality, storage temperature, pH, and initial microbial loads of fungi and bacteria [1]. Yeasts play an important role in the production of alcoholic and non-alcoholic beverages, the baking industry, and the production of volatile aroma compounds [2]. However, yeasts are commonly found in spoiling foods where bacterial growth is inhibited due to low pH and high sugar content [3]. *Saccharomyces cerevisiae* is a major contaminating microorganism associated with fruit pulps and packed fruit juices [4]. The inactivation of microorganisms in the food industry is commonly performed with thermal treatments [5]. For example, in the beverage industry, *S. cerevisiae* needs to be controlled at the end of the production process, and thermal treatment is mainly applied to prevent yeast proliferation. However, thermal treatment can affect nutritional and organoleptic properties [6]. Nonthermal disinfection methods include the addition of preservative compounds, such as the antimicrobial peptides Leg1 (RIKTVTSFDLPALR-FLKL) and Leg2 (RIKTVTSFDLPALRWLKL) [7] or natural substances, such as phenolic compounds [8,9]. In several types of wine, such as sparkling wine, there is a final production step where the yeasts are removed by agitating and inclining the bottle, letting the yeasts settle into the bottleneck. However, this method takes two months [10,11]. Recently, physical nonthermal methods such as pulsed electric fields [12,13] and cold plasma have been used for microorganism eradication [14,15].

Atmospheric plasma corona discharge holds promise as an alternate technology, providing the advantage of a short process without heating. Plasma is an ionized gas containing an equal number of positively and negatively charged particles. It can be categorized as "hot" or "cold". In hot plasma, the particles are in thermal equilibrium. Cold plasma is classified by its temperature corresponding to different particles, where the temperature of heavy particles is lower than the temperature of electrons (with an energy of 1–10 eV). The electrons' energy is sufficient for the generation of energetic and chemically reactive species (excited atoms, free radicals, molecules, ions, and ultraviolet photons), which are the driving force for the plasma's chemical reactions. Cold plasma can be generated under different gas pressures; low-pressure plasma discharges are created under a vacuum of 0.1–0.5 Torr. In contrast, atmospheric-pressure plasmas are generated under atmospheric pressure [16,17]. Cold-plasma technology is currently used in various fields, including surface modification [18], bioremediation of toxic pollutants using biofilm on plasma-pretreated wood waste [19], microbial electrolysis cells based on a pretreated plasma anode [20], advanced treatment of agricultural seeds [21], and water and soil remediation [17].

The plasma's antimicrobial mechanism is believed to be based mainly on its reactive oxygen species (ROS) and reactive nitrogen species (RNS) [22]. They include hydroxyl hydrogen peroxide (H_2O_2), atomic oxygen (O), radicals ($^{\bullet}OH$), singlet oxygen ($^1O_2$), ozone (O_3), [23,24], nitrates (NO_3^-), nitric oxide (NO), peroxinitrites ($ONOO^-$), and nitrites (NO^{2-}) [25]. These reactive molecules were found to alter the phospholipid bilayer of a cell, gene expressions and the structure of nucleic acids and cellular proteins [26,27].

Exposing *Listeria monocytogenes* grown on agar plates to an atmospheric-pressure plasma jet with He, He + O_2, N_2, or N_2 + O_2, for 2 min, led to cell reduction by 0.87, 4.19, 4.26, and 7.59 log units, respectively. When the *L. monocytogenes* were inoculated on sliced ham and chicken breast, the plasma treatment decreased the bacterial number by 1.94 to 6.52, and by 1.37 to 4.73 log, respectively. These results showed that the input gas used with the N_2 + O_2 mixture was the most efficient [28]. Braised chicken was air-packed and stored at 4 $\pm$ 1 °C for 15 days. During this period, the yeasts and molds increased sharply from 1.98 log (CFU/g) to 5.80 log (CFU/g). When the braised chicken was treated with dielectric barrier discharge cold plasma, molds and yeasts proliferation was significantly restrained [29]. Inactivation of *Zygosaccharomyces rouxii* LB and 1130 (initial concentration of about 1×10^7 CFU/mL) in apple juice was studied using a gas-phase surface discharge plasma system at different peak discharge voltages. Plasma treatment for 30 min at a voltage of 11.3 kV, led to a reduction of *Z. rouxii* LB and 1130 by 2.39 and 2.60 log10. At a higher voltage of 21.3 kV, the reduction was 6.58 log10 and 6.82 log10, respectively. These results indicated that raising discharge voltage levels could decrease the plasma treatment time for microbial inactivation [30]. Recently, the effect of atmospheric plasma corona discharges on soil bacteria viability was examined. Exposure to the soil for 5 min led to a reduction of 2.5 orders of magnitude. The plasma-resistant bacteria were of the phylum Firmicutes (98.5%) and were comprised of the taxonomic orders *Bacillales* (95%) and *Clostridiales* (2%) [15]. Studying the effect of plasma corona on *Agrobacterium tumefaciens*, a soil-borne pathogenic bacterium, showed that, in a liquid environment, in an initial concentration of 2.02×10^6 CFU/mL after 90 s of plasma exposure, there was a reduction of 5 orders of magnitude [14].

In our study, the effect of a plasma corona discharge on *S. cerevisiae* viability, membrane permeability, and morphology was examined, where the cells were prepared in both dry and wet modes. The *S. cerevisiae* viability was examined as a function of plasma exposure time, distance between the treating head and the sample, initial cell concentration, and the yeast suspension volume.

2. Materials and Methods

2.1. Plasma Corona Discharge System

The plasma corona discharge device (3DT, MULTIDYNE 1000, Germantown, WI, USA) (Figure 1) used in this study was comprised of a treating head containing two electrodes. To generate the plasma, the device was operated under a high voltage of 2 × 12 kV and a frequency of 50 Hz under atmospheric pressure conditions, using ambient air as a carrier gas. A rotating table (Figure 1) covered with a layer of PVC was positioned beneath the treating head. The upper part of the table was rotated at controlled rounds per min (rpm) using a power supply (PowerPac^{tm} Basic, Bio-Rad, Hercules, CA, USA). A plastic Petri dish containing the *S. cerevisiae* sample was placed in the center of the rotating table.

Figure 1. Plasma corona discharge device and the rotating table.

2.2. Preparation of S. cerevisiae for Exposure to Plasma Corona Discharge, Experimental Conditions

S. cerevisiae (70468) was purchased from DSMZ (Braunschweig, Germany). It was grown in yeast mold broth (YMB) (Neogen, MI, USA) for 24–48 h at 30 °C and diluted to an appropriate OD (660 nm). The suspension was divided into 1 mL portions in Eppendorf tubes and washed in PBS as follows: centrifuged at 10,000 rpm for 10 min, decanted the supernatant, and suspended the *S. cerevisiae* sediment in 1 mL PBS. This final suspension of 10^3–10^8 CFU/mL was again centrifuged at 10,000 rpm for 10 min. When the experiment was conducted in dry mode, the *S. cerevisiae* sediment was suspended in 0.05 mL PBS and spread in the middle of a Petri dish (about 1 × 1 cm). For wet mode, the sediment was suspended in 10–30 mL PBS. The samples were exposed to plasma for 10–240 s, at a distance of 2–6 cm from the treating head, and rotated at 40 rpm as indicated for each experiment. The control samples were treated with the same procedure, excluding exposure to plasma.

2.3. Viable Count Assay

The live *S. cerevisiae* concentration was measured as a function of plasma treatment by a visible count assay. The plasma-treated dry-mode *S. cerevisiae* were harvested from the Petri dish with PBS (1 mL) into a sterile tube. A suspension (100 µL) was serially diluted, and the appropriate dilutions were pour-plated onto YM agar (Neogen, MI, USA), followed by incubation for 24–48 h at 30 °C. Viable *S. cerevisiae* cells were identified by CFU counting and multiplying it by the corresponding dilutions. The same procedure was carried out with the wet-mode *S. cerevisiae* cells, except that the 100 µL suspension was collected directly from the 10–30 mL in the Petri dish.

2.4. Examination of the S. cerevisiae Membrane Cell Size and Permeability by Flow Cytometry (FCM) Analysis

A volume of 1 mL of plasma-treated *S. cerevisiae* (10^6 CFU/mL) and a nontreated sample were transferred to an Eppendorf tube, followed by the addition of fluorescent propidium iodide (PI) dye at a final concentration of 1.5 µM. The samples were incubated at 37 °C for 5 min. Afterward, 200 µL were transferred to an ELISA plate, and the *S. cerevisiae* sample (about 50,000 cells) was examined for membrane permeability using FCM (Beckman Coulter, Atlanta, GA, USA). Data were analyzed using FlowJo software (Tree Star, San Carlos, CA, USA).

2.5. Scanning Electron Microscope (SEM) Analysis

Plasma-treated *S. cerevisiae* and nontreated samples were washed gently (×3) with PBS. The *S. cerevisiae* (0.2 µL) were fixed by incubation in Karnovsky's fixative solution (4% formaldehyde and 5% glutaraldehyde in 0.064 M phosphate buffer, pH 7.2), and were then incubated for 1 h in tannic acid (1%) and OsO4 (4%). After each process, the samples were washed three times with PBS (pH 7.2). Then the samples were dehydrated using ethanol (30–100%) and acetone (50–100%) for 10 min at each concentration. The samples were air-dried and sputtered with gold (using Quorum Q15OT ES, Quorum Technologies Ltd., Laughton, UK). The morphology of the *S. cerevisiae* cells was examined using a MAIA3 SEM (TESCAN, Kohoutovice, Czech Republic) at ultra-high resolution.

2.6. Statistics

Data were expressed as means ± STDEV (standard deviation) from 3 to 5 replicates.

3. Results and Discussion

3.1. S. cerevisiae Viability as a Function of Plasma Corona Discharge Exposure Duration

A suspension of *S. cerevisiae* was washed with PBS, divided into volumes of 1 mL, and centrifuged. The washed *S. cerevisiae* sediment was exposed to a plasma corona discharge in dry mode (0.05 mL of the sediment dispersed on a Petri dish), and in wet mode (0.05 mL of the sediment diluted in 10 mL PBS and placed in a Petri dish). In both experiments, the Petri dish with the sample was placed under the plasma corona discharge treating head at a distance of 2 cm. The samples were exposed to plasma corona for 10–240 s in dry and wet mode. Following this process, the dry-mode samples were collected into an Eppendorf tube using 1 mL PBS. For wet mode, 1 mL of the 10 mL was collected for a viable count assay. The control samples received the same treatment but, without exposure to plasma corona. The concentration of viable *S. cerevisiae* as a function of plasma corona exposure duration is shown in Figure 2. In both modes, the first duration that is shown was a decrease in CFU/mL of about two orders of magnitude, and the last one is when total eradication was observed.

As shown in Figure 2A, when the *S. cerevisiae* cells were exposed to plasma corona, there was a linear correlation between the exposure duration and the CFU/mL in both dry mode and wet mode. When the experiment was performed in dry mode, the nontreated *S. cerevisiae* concentration was 2.14×10^6 CFU/mL. After 30 s, the CFU/mL was reduced to 2.40×10^2, and exposure for 45 s led to complete eradication. However, when the

S. cerevisiae cells were exposed to plasma corona in wet mode, the nontreated *S. cerevisiae* concentration was 8.90×10^6, and exposure for 120 s led to a reduction by five orders of magnitude; after prolonged exposure for 240 s, no CFU/mL was observed.

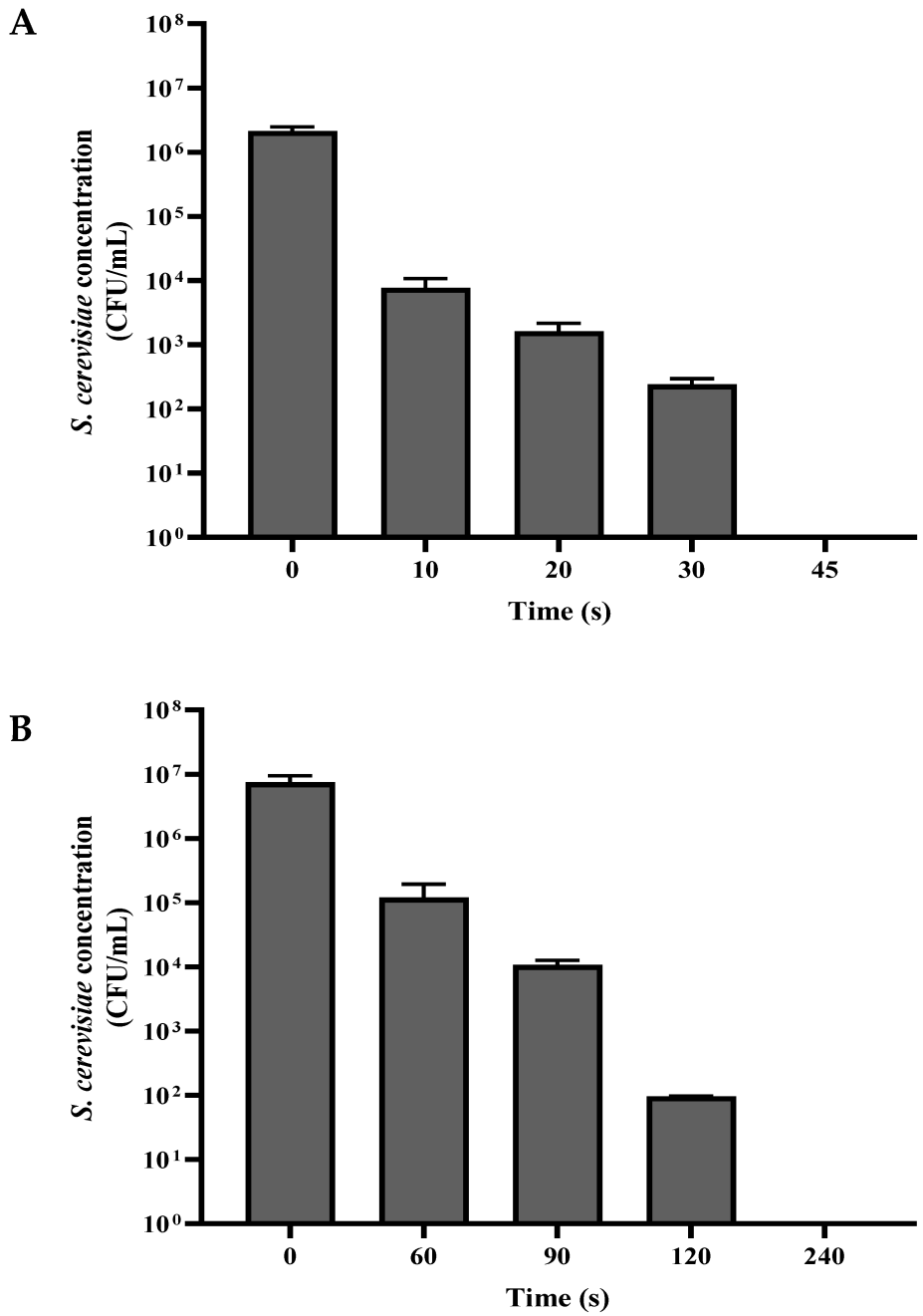

Figure 2. The concentration of the viable *S. cerevisiae* (CFU/mL) as a function of plasma corona exposure duration in dry mode (**A**) and wet mode (**B**).

3.2. S. cerevisiae Viability as a Function of the Distance from the Sample to the Plasma Corona Discharge Treating Head

The *S. cerevisiae* sample in the Petri dish was placed at a distance of 2, 4, and 6 cm from the plasma treating head (Figure 3A,B). The dry-mode *S. cerevisiae* sample was exposed to plasma for 30 s, while the wet-mode sample was exposed for 120 s. The *S. cerevisiae* samples that served as controls were treated the same but without exposure to plasma treatment.

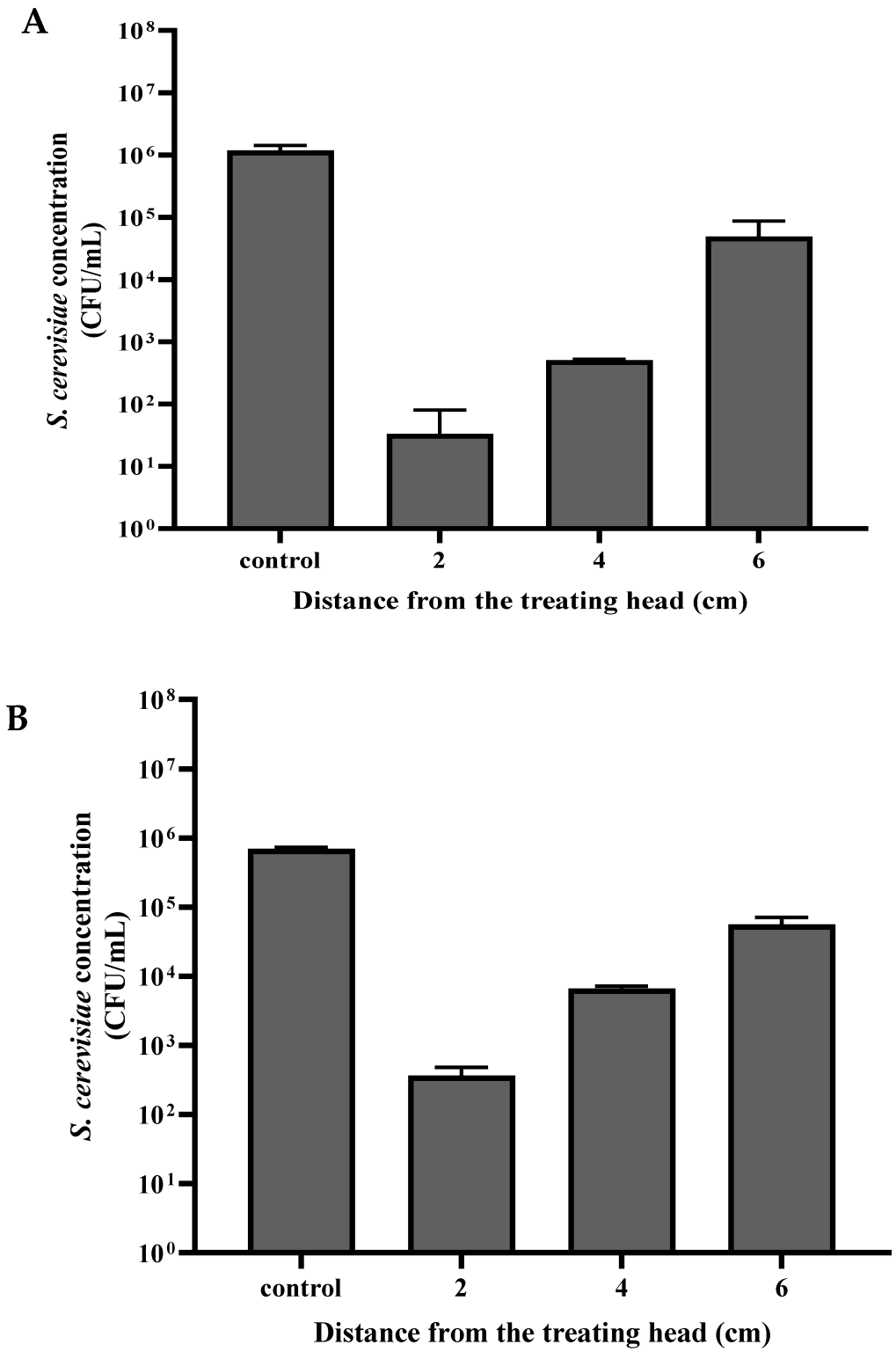

Figure 3. *S. cerevisiae* viability (CFU/mL) as a function of the distance between the sample and the plasma corona discharge treating head in dry mode, exposure for 30 s (**A**) and wet mode, exposure for 120 s (**B**), control column- without plasma exposure.

As can be seen in Figure 3, the distance of the sample from the treating head influenced the *S. cerevisiae* viability. In the control samples, the *S. cerevisiae* concentrations in dry mode and wet mode were 1.17×10^6 and 6.93×10^5 CFU/mL, respectively. The viability of cells that were exposed in dry mode at a distance of 6, 4, and 2 cm was 3.30×10^1, 5.10×10^2,

and 4.92×10^4 CFU/ mL, respectively. The viable cell concentration in wet mode decreased to 3.68×10^2, 6.63×10^3, and 5.60×10^4 CFU/ mL, respectively.

3.3. S. cerevisiae Viability as a Function of the Initial Cell Concentration

A suspension of *S. cerevisiae* was grown overnight, washed, and diluted in PBS to ~10^7, ~10^5, and ~10^3 CFU/mL. Each of the three suspensions was divided into volumes of 1 mL and centrifuged. For the dry-mode experiment, sediment (0.05 mL) from each concentration was dispersed in a Petri dish and exposed to plasma corona for 20 s. For the wet-mode examination, each concentration sample (0.05 mL) was diluted in 10 mL of PBS, placed in a Petri dish, and received 90 s exposure. The control samples were treated the same, except for the exposure to plasma.

As shown in Figure 4A,B, exposure of the *S. cerevisiae* to plasma in dry (20 s) or wet (90 s) mode, with the different initial concentrations, resulted in a population reduction by 2 to 3 orders of magnitude. In both modes, there was total eradication when the initial cell concentration was about 10^3 CFU/mL.

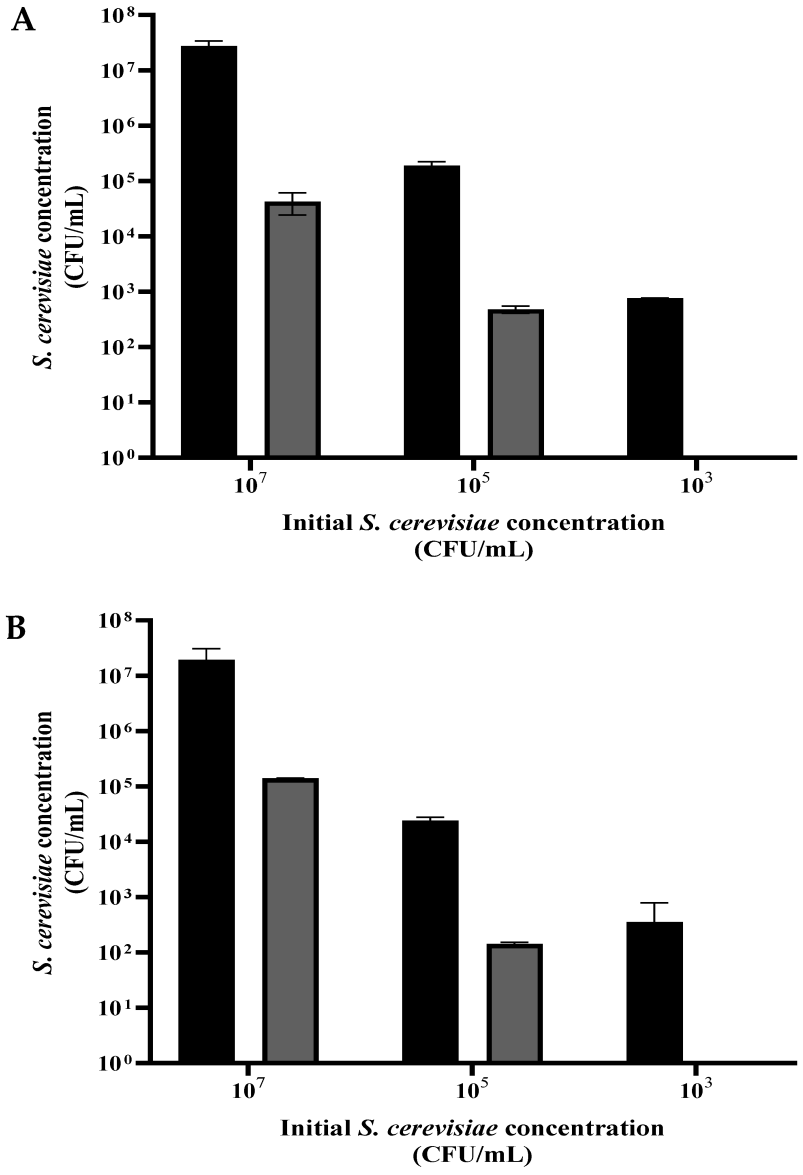

Figure 4. The concentration of *S. cerevisiae* (CFU/mL) as a function of the initial concentration, in dry mode, exposure for 20 s (**A**) and wet mode, exposure for 90 s (**B**). Grey and black column: with and without plasma treatment.

3.4. S. cerevisiae Viability as a Function of the Yeast Suspension Volume

A suspension of *S. cerevisiae* was grown overnight, then washed and diluted in PBS to 1.0 OD (~10^7 CFU/mL). The suspension was divided into portions of 1 mL, centrifuged, and washed in PBS. The sediment was then diluted in 10, 20, and 30 mL. Each suspension was placed in a Petri dish. The liquid surface height in the Petri dish was 1, 2, and 3 mm, respectively. The samples were placed under the plasma treating head at a distance of 2 cm for 90 s. The control samples were treated the same, except for no exposure to plasma corona. This step was followed by a viable count assay was performed.

As shown in Figure 5, in all three initial volumes where the *S. cerevisiae* concentration was about the same (~10^7 CFU/mL), the reduction in the yeast concentration was 2–3 orders of magnitude. The initial concentration of the control samples with 10, 20, and 30 mL were 7.32×10^6, 8.83×10^6, and 2.32×10^7 CFU/mL, respectively. After the plasma treatment, the CFU/mL were 1.89×10^4, 1.54×10^4, and 3.51×10^4, respectively. It may be important to note that the fan which connects the plasma corona facility with the rotating table led to high turbulence of the exposed liquid.

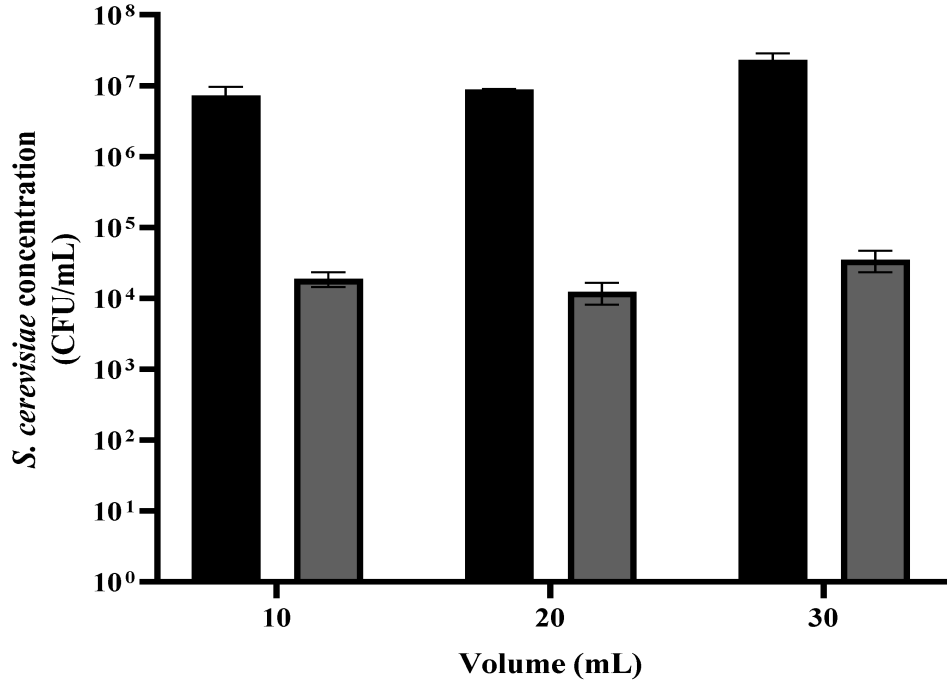

Figure 5. *S. cerevisiae* viability as a function of the yeast suspension volume. The samples were placed under the plasma treating head at a distance of 2 cm for 90 s. Grey and black column: with and without plasma treatment.

Pankaj et al. (2017) reported that treatment with nonthermal high-voltage (80 kV) atmospheric cold plasma for 4 min caused a 7.4 log CFU/ mL reduction in *S. cerevisiae* suspended in white grape juice, with no significant change in pH or electrical conductivity [31]. Gan et al. (2021) investigated cold plasma inactivation of *E. coli and S. cerevisiae* suspended in chokeberry juice (1–5 mL) after exposure for 1 to 5 min. When the treatment time was 4 min, the inactivation of *E. coli* and *S. cerevisiae* decreased as the sample volume increased. When a sample of 2 mL was treated for 4 min, the total number of *S. cerevisiae* and *E. coli* colonies declined by 1.31 and 2.83 log, respectively. Increasing the treatment time from 1 min to 5 min led to a higher eradication effect. When *E. coli* and *S. cerevisiae* were suspended in 2 mL with 4 min of plasma exposure, the colonies reduced by 2.27 and 1.23 log, respectively [32]. Stulič et al. (2019) examined the reduction of *S. cerevisiae* suspended in 190 mL 0.01 M $NaNO_3$ sterile solution with a conductivity of 100 μS/cm. The samples were treated for 5 and 10 min. It was shown that treatment for 10 min led to a higher effect approaching total eradication (5.61 log10 CFU/mL) [33]. Wang et al. (2018)

used plasma technology at different discharge voltages for inactivating yeasts (*Zygosaccharomyces rouxii* LB and 1130) in apple juice. When the initial populations of *Z. rouxii* LB and 1130 in apple juice were approximately 1×10^7 CFU mL^{-1}, plasma exposure at a peak discharge voltage of 11.3 kV for 30 min reduced their populations by 2.39 and 2.60 log, respectively. By increasing the discharge voltages to 21.3 kV for the same treatment time, the number of *Z. rouxii* LB cells was reduced by 6.58 log, and that of *Z. rouxii* 1130 cells by 6.82 log [30]. Our results along with the cited results indicate a negative correlation between the sample volume and the corona plasma bactericidal effect. However, there is a linear correlation between treatment time and eradication effect.

3.5. Examination of S. cerevisiae Cell-Membrane Permeability

The *S. cerevisiae* cell membrane permeability was examined using flow cytometry analysis and the fluorescent dye propidium iodide (PI). When the cell membrane is damaged, PI enters the cell and binds to nucleic acid, displaying red under fluorescent light.

In these experiments, the cells were prepared for exposure to plasma in dry and wet modes, as described in Section 2.4, with an initial concentration of 10^6 CFU/mL. The samples were placed at a distance of 2 cm from the treating head. When the cells were exposed to plasma in dry mode, the plasma corona exposure duration was for 30 and 45 s. After the treatment, the samples were collected from the plates into Eppendorf tubes using 1 mL PBS. When the cells were exposed in wet mode, the duration was for 120 and 240 s. Then, 1 mL of the 10 mL suspended cells in the Petri dish was collected. The PI dye was added to each sample and then incubated at 37 °C for 5 min. The samples were subjected to a flow cytometer, and the membrane permeability was examined. The same regime was performed for the control samples but without plasma exposure. A PI-positive control was prepared by incubating 10^6 CFU/mL with isopropanol (100%) for 0.5 h. As shown in Figure 6A, the control sample, which was treated with isopropanol, exhibited 83% PI-positive cells. In contrast, the control of the nontreated samples exhibited only 13% and 15% in dry and wet modes, respectively. When the cells were plasma-treated in the dry mode for 30 s, the PI-positive cells were 51%. Longer exposure for 45 s increased the PI-positive cells to 76%. A similar result was observed when the *S. cerevisiae* cells were treated with plasma in the wet mode, Figure 6B. The histograms of the PI-positive cells in the dry mode (a–d) are shown in Figure 6C.

Xu et al. (2021) examined the cell viability of yeast using the dyes PI (staining dead cells or cells with damaged membranes) and SYTO 9 (staining cells with intact membranes). The survival rate significantly reduced in a time-dependent manner, observed as 81.3%, 34.6%, and 19.0% after 2.5, 5, and 10 min plasma treatments, respectively [34]. Gan et al. (2021) showed flow cytometry results from plasma-treated *S. cerevisiae* and *E. coli*, where the percentage of green-colored cells gradually increased when the cells were plasma-treated (suspended in 2 mL, treatment time of 1–5 min). The percentage of green-colored *E.coli* cells rose from 4.2% to 19.0%, which was correlated with longer treatment time. Similar observation was reported for *S. cerevisiae*, where the green-colored cells percentage was increased from 4.8% to 10.7% with a treatment time of 1–5 min [32].

3.6. Examination S. cerevisiae Morphology

The *S. cerevisiae* cells were prepared for plasma treatment in dry mode. Sediment (10^6 CFU/mL) was spread on a Petri dish, placed under the treating head at a distance of 2 cm, and exposed to plasma corona for 30 and 60 s. Samples that were prepared the same way but without exposure were used as controls. The samples were collected from the plate and fixed for SEM analysis. The images of the plasma-treated and control samples at a magnification of 5 kx and 15 kx are shown in Figure 7.

In Figure 7A,B, it can be seen that the nontreated *S. cerevisiae* samples mainly included intact cells, some of which were in the budding process. The plasma-treated images Figure 7C–F, show deformed cells. Treatment for 60 s led to about 84% of defective cells (E,F), compared to 30 s of treatment, which led to 71% (C,D). The nontreated sample, in

contrast, exhibited only 13% of defective cells, probably due to the fixation procedure for SEM analysis (A,B).

Gan et al. (2021) studied the effects of a cold plasma jet with a dielectric barrier configuration on *E. coli* and *S. cerevisiae* suspended in chokeberry juice. SEM images showed that the nontreated *E. coli* and *S. cerevisiae* cells were oval in shape, with smooth and intact surfaces. However, plasma-treated *E. coli* cells exhibited noticeable damage, including breakages, folds, and dents; and plasma-treated *S. cerevisiae* cells were typically stretched and slightly broken with some surface dents [32]. Stulič et al. (2019) analyzed *S. cerevisiae* morphology using transmission electron microscopy (TEM). Their images showed nontreated yeast cells exhibiting well-defined cellular organelles (nucleus, mitochondria, and endoplasmic reticulum). After plasma treatment, disintegrated cells were observed, with some completely vacuolated, so their organelles and cell membranes were indistinguishable. In addition, there was partial leakage of cellular contents into the surrounding medium [33]. Wang et al. (2018) reported that plasma-treated yeasts showed severe damage, with rough, ridged surfaces containing discrete holes [30]. Xu et al. (2021) analyzed ROS generation ($^{\cdot}OH$, $^{1}O_2$, $^{\cdot}O_2^{-}$, and H_2O_2) in a plasma-liquid interaction system. They suggested that plasma can effectively inactivate yeast cells mainly by destroying their membranes, attributed to $^{\cdot}OH$ and H_2O_2. In contrast, cell metabolism disruption was attributed primarily to $^{1}O_2$. SEM images revealed that plasma treatments wrinkled and disrupted yeast cells, producing cell debris. It was reported that the degree of damage increased together with plasma treatment time [34].

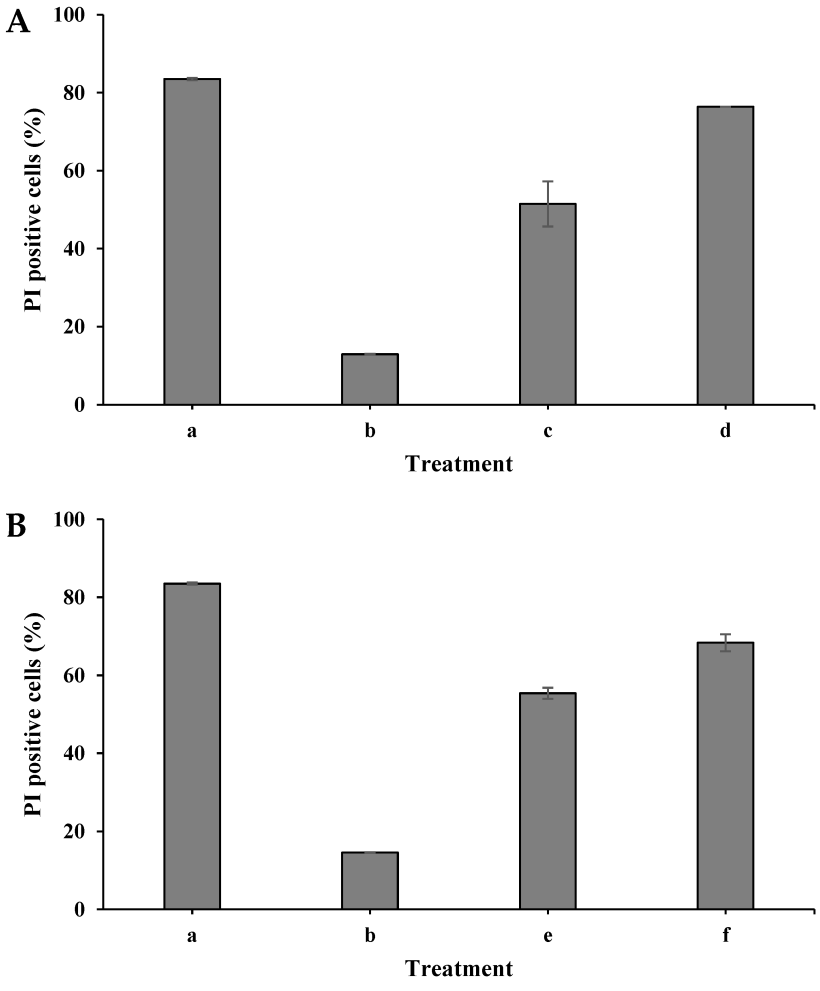

Figure 6. *Cont.*

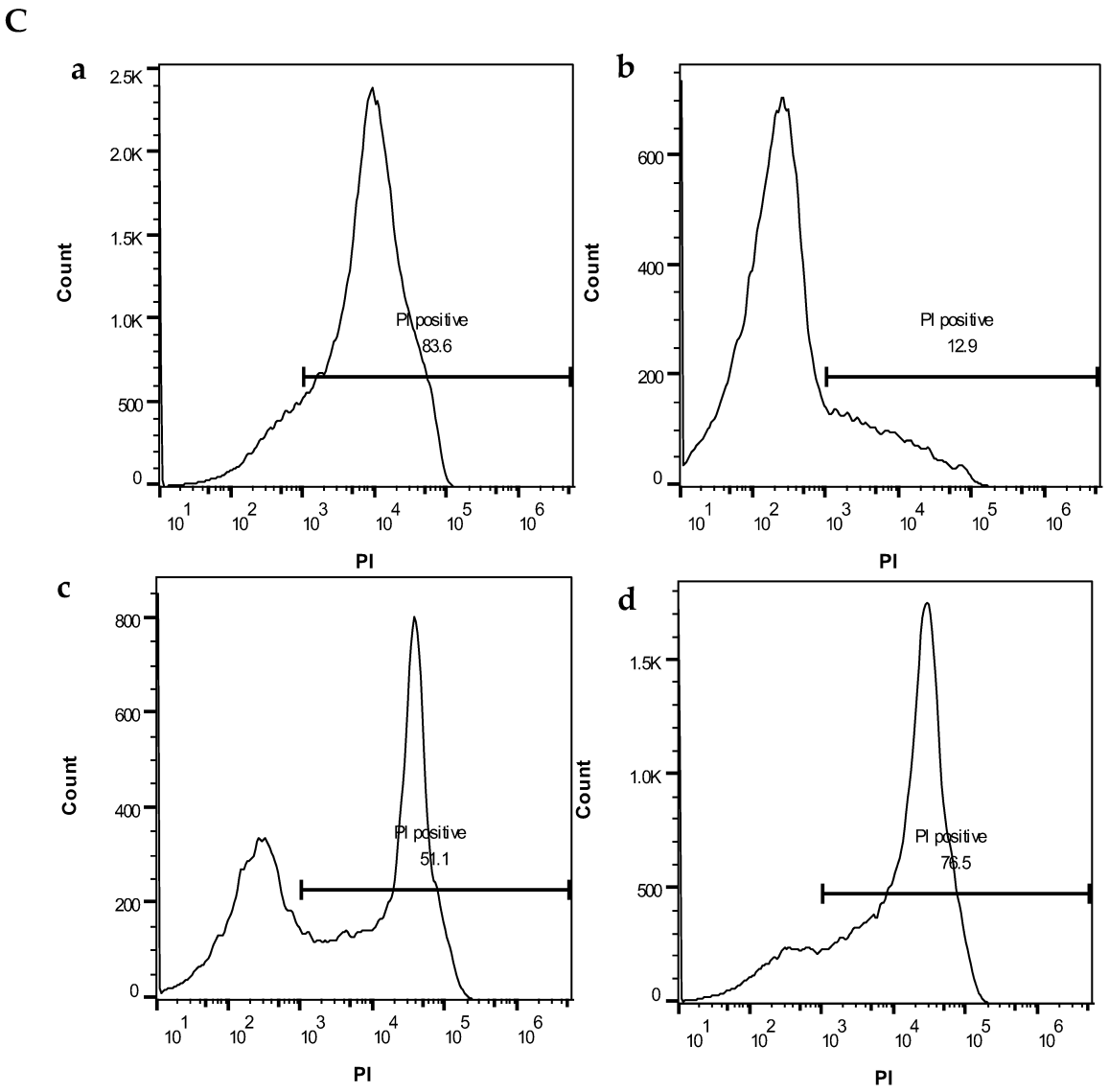

Figure 6. PI-positive *S. cerevisiae* as a function of plasma corona treatment in dry mode (**A**) and wet mode (**B**). *S. cerevisiae* cells that were treated with isopropanol (**a**); nontreated cells (**b**); *S. cerevisiae* cells that were exposed to plasma corona for 30 s (**c**); 45 s (**d**); 120 s (**e**); and 240 s (**f**). The histograms of the PI-positive cells in the dry mode (**a**–**d**) are shown in (**C**).

The results of our study showed a linear correlation between the exposure duration and the reduction of the CFU/mL in both dry and wet modes. The eradication effect of the plasma treatment was higher when the sample was treated in the dry mode. The distance between the sample and the treating head was an essential factor, with shorter distance increasing the efficiency of eradication. Another critical factor was the *S. cerevisiae* initial concentration. In both modes, there was total eradication when the initial cell concentration was about 10^3 CFU/mL. When different volumes with the same *S. cerevisiae* concentration were exposed to plasma while mixing the suspensions, the same decrease, about 3 orders of magnitude, was observed. From these results, we assume that this technology may be applied on a large scale. However, the plasma exposure must be performed continuously, including the time when the liquid is agitated while passing through a narrow pipe.

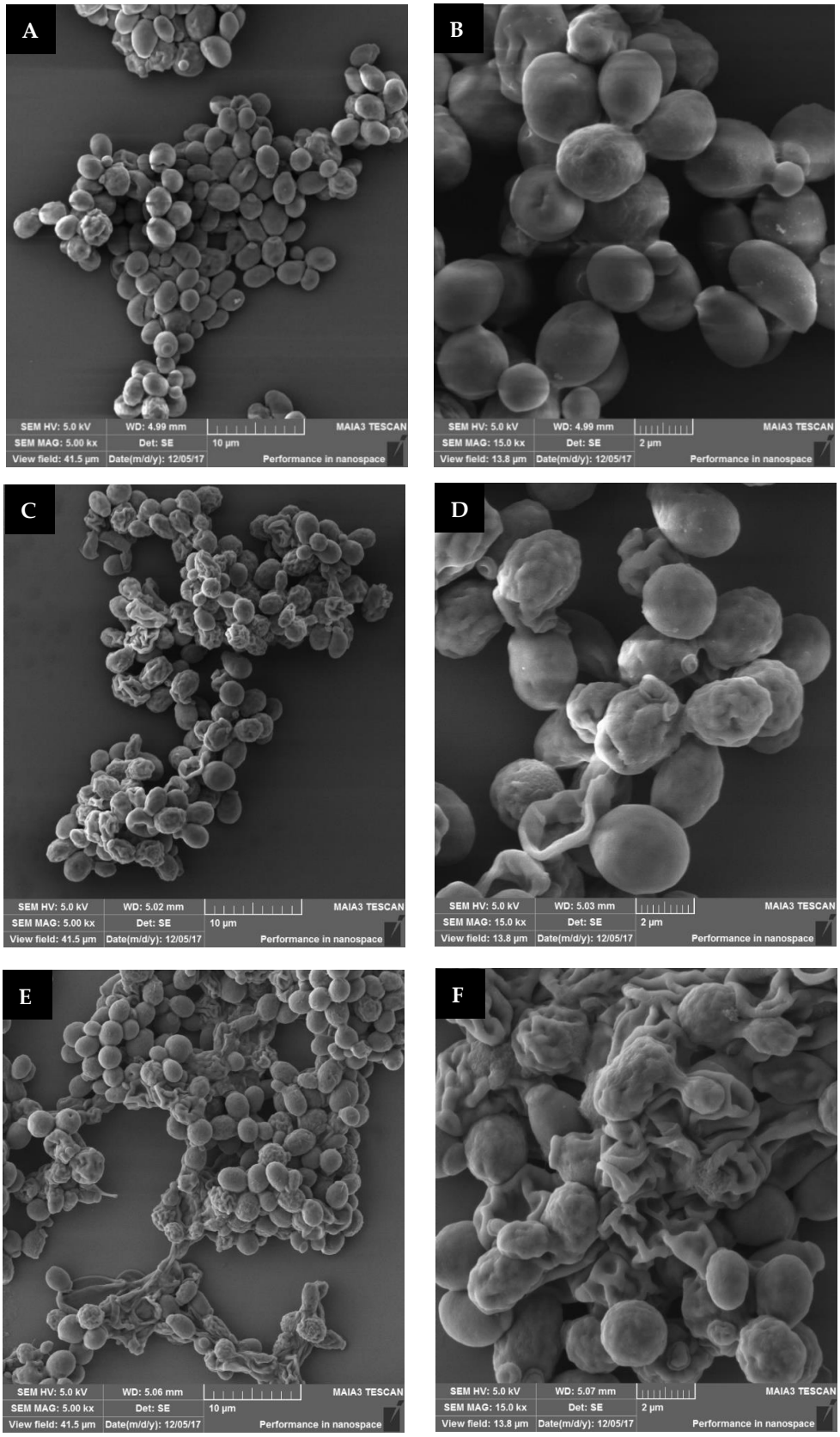

Figure 7. SEM images of nontreated *S. cerevisiae* cells (control) (**A**,**B**); plasma-treated cells for 30 s (**C**,**D**); and 60 s (**E**,**F**). Magnification of 5 kx (5000 fold) (**A**,**C**,**E**) and 15 kx (15,000 fold) (**B**,**D**,**F**).

Examination of the cell-membrane permeability using a flow cytometer showed that plasma treatment led to penetration of the PI fluorescent dye into the cells. SEM analysis confirmed that plasma treatment led to cell deformation. We assume that, since plasma treatment caused physical damage, such as holes in the cell membrane and cell deformation, this technology may be useful for the eradication of different microorganisms.

4. Conclusions

S. cerevisiae is a major contaminating microorganism associated with fruit juices. The inactivation of microorganisms in the food industry is commonly performed with thermal treatments. However, this treatment can affect the nutritional properties. Several studies including our study emphasized microorganism eradication using cold plasma technology.

In this study, the effect of cold plasma exposure on *S. cerevisiae* viability was examined when the cells were prepared in two modes: suspended in PBS (wet mode) and concentrated in a minimum volume of PBS (50 μL) (dry mode). The results showed a linear correlation between the exposure duration and the eradication effect. When the initial concentration was about 10^6 CFL/mL, complete eradication was observed after exposure for 45 and 240 s in the dry and wet modes, respectively. The distance between the sample and the plasma treating head (6, 4, and 2 cm) influenced the *S. cerevisiae* viability. When the plasma treating head was adjusted at 2 cm from the sample, the highest eradication (two orders of magnitude) was observed after treating times of 30 s for the dry mode and 90 s for the wet mode. When different initial cell concentrations were examined, a total *S. cerevisiae* eradication was observed when the initial cell concentration was about 10^3 CFU/mL. Plasma treatment (90 s) of different volumes while mixing the suspended *S. cerevisiae* showed a reduction of two orders of magnitude. In addition, plasma exposure led to PI permeability, and SEM analysis showed cell deformation.

We assume that, since plasma treatment caused physical damage, such as holes in the cell membrane and cell deformation, this technology may be useful for eradicating different microorganisms. Applying this technology on a large scale should be done when the liquid is agitated continuously. The main advantage of cold plasma technology for microorganism eradication in the fruit juice industry is that disinfection is achieved in a short process without heating.

Author Contributions: Experiment, conceptualization, and methodology: I.A.D. and R.C.; contributions to the experiment: I.A.D.; experimental data analysis: I.A.D.; investigation: I.A.D., Y.L. and E.E.; research administration and supervision: R.C.; writing, original draft preparation: I.A.D., E.E. and R.C.; writing—review and editing: R.C. and I.A.D. All authors have read and agreed to the published version of the manuscript.

Funding: This research received no external funding.

Data Availability Statement: Data are available in this publication.

Acknowledgments: We acknowledge the Research Authority of Ariel University, Israel, for supporting this research.

Conflicts of Interest: No conflict of interest is disclosed for the work reported in this study.

References

1. Odeyemi, O.A.; Alegbeleye, O.O.; Strateva, M.; Stratev, D. Understanding spoilage microbial community and spoilage mechanisms in foods of animal origin. *Compr. Rev. Food Sci. Food Saf.* **2020**, *19*, 311–331. [CrossRef] [PubMed]
2. Maicas, S. The role of yeasts in fermentation processes. *Microorganisms* **2020**, *8*, 1142. [CrossRef] [PubMed]
3. Deak, T. *Handbook of Food Spoilage Yeasts*, 2nd ed.; CRC Press: Boca Raton, FL, USA, 2007; ISBN 9781420044935.
4. Azeredo, D.R.P.; Alvarenga, V.; Sant'Ana, A.S.; Sabaa Srur, A.U.O. An overview of microorganisms and factors contributing for the microbial stability of carbonated soft drinks. *Food Res. Int.* **2016**, *82*, 136–144. [CrossRef]
5. Schottroff, F.; Fröhling, A.; Zunabovic-Pichler, M.; Krottenthaler, A.; Schlüter, O.; Jäger, H. Sublethal injury and Viable but Non-culturable (VBNC) state in microorganisms during preservation of food and biological materials by nonthermal processes. *Front. Microbiol.* **2018**, *9*. [CrossRef] [PubMed]

6. Tabanelli, G.; Montanari, C.; Arioli, S.; Magnani, M.; Patrignani, F.; Lanciotti, R.; Mora, D.; Gardini, F. Physiological response of Saccharomyces cerevisiae to citral combined with thermal treatment. *LWT* **2019**, *101*, 827–834. [CrossRef]
7. Heymich, M.L.; Nißl, L.; Hahn, D.; Noll, M.; Pischetsrieder, M. Antioxidative, antifungal and additive activity of the antimicrobial peptides leg1 and leg2 from chickpea. *Foods* **2021**, *10*, 585. [CrossRef]
8. Kimani, B.G.; Kerekes, E.B.; Szebenyi, C.; Krisch, J.; Vágvölgyi, C.; Papp, T.; Takó, M. In vitro activity of selected phenolic compounds against planktonic and biofilm cells of food-contaminating yeasts. *Foods* **2021**, *10*, 1652. [CrossRef]
9. Sabel, A.; Bredefeld, S.; Schlander, M.; Claus, H. Wine phenolic compounds: Antimicrobial properties against yeasts, lactic acid and acetic acid bacteria. *Beverages* **2017**, *3*, 29. [CrossRef]
10. Ribereau-Gayon, P.; Dubourdieu, D.; Doneche, B.; Lonvaud, A. Red winemaking. In *Handbook of Enology: The Microbiology of Wine and Vinifications*, 2nd ed.; John Wiley & Sons: New York, NY, USA, 2006; ISBN 9780470010365.
11. Berovic, M.; Berlot, M.; Kralj, S.; Makovec, D. A new method for the rapid separation of magnetized yeast in sparkling wine. *Biochem. Eng. J.* **2014**, *88*, 77–84. [CrossRef]
12. Emanuel, E.; Dubrovin, I.; Hanya, E.; Pinhasi, G.A.; Pogreb, R.; Cahan, R. Eradication of Saccharomyces cerevisiae by Pulsed Electric Field Treatments. *Microorganisms* **2020**, *8*, 1684. [CrossRef]
13. Emanuel, E.; Dubrovin, I.; Pogreb, R.; Pinhasi, G.A.; Cahan, R. Resuscitation of pulsed electric field-treated Staphylococcus aureus and Pseudomonas putida in a rich nutrient medium. *Foods* **2021**, *10*, 660. [CrossRef] [PubMed]
14. Lazra, Y.; Gandu, B.; Amar Dubrovin, I.; Emanuel, E.; Cahan, R. Effects of atmospheric plasma corona discharge on agrobacterium tumefaciens survival. *Microorganisms* **2022**, *10*, 32. [CrossRef] [PubMed]
15. Lazra, Y.; Dubrovin, I.; Multanen, V.; Bormashenko, E.; Bormashenko, Y.; Cahan, R. Effects of atmospheric plasma corona discharges on soil bacteria viability. *Microorganisms* **2020**, *8*, 704. [CrossRef] [PubMed]
16. Lieberman, M.A.; Michael, A.; Lichtenberg, A.J. *Principles of Plasma Discharges and Materials Processing*; Wiley-Interscience: Hoboken, NJ, USA, 2005; ISBN 9780471720010.
17. Aggelopoulos, C.A. Recent advances of cold plasma technology for water and soil remediation: A critical review. *Chem. Eng. J.* **2022**, *428*, 131657. [CrossRef]
18. Thomas, M.; Mittal, K.L. *Atmospheric Pressure Plasma Treatment of Polymers: Relevance to Adhesion*; Thomas, M., Mittal, K., Eds.; Scrivener Publishing LLC: Salem, MA, USA, 2013; ISBN 9781118596210.
19. Farber, R.; Dabush-Busheri, I.; Chaniel, G.; Rozenfeld, S.; Bormashenko, E.; Multanen, V.; Cahan, R. Biofilm grown on wood waste pretreated with cold low-pressure nitrogen plasma: Utilization for toluene remediation. *Int. Biodeterior. Biodegrad.* **2019**, *139*, 62–69. [CrossRef]
20. Rozenfeld, S.; Ouaknin Hirsch, L.; Gandu, B.; Farber, R.; Schechter, A.; Cahan, R. Improvement of Microbial Electrolysis Cell Activity by Using Anode Based on Combined Plasma-Pretreated Carbon Cloth and Stainless Steel. *Energies* **2019**, *12*, 1968. [CrossRef]
21. Bormashenko, E.; Shapira, Y.; Grynyov, R.; Whyman, G.; Bormashenko, Y.; Drori, E. Interaction of cold radiofrequency plasma with seeds of beans (Phaseolus vulgaris). *J. Exp. Bot.* **2015**, *66*, 4013–4021. [CrossRef]
22. Iuchi, K.; Morisada, Y.; Yoshino, Y.; Himuro, T.; Saito, Y.; Murakami, T.; Hisatomi, H. Cold atmospheric-pressure nitrogen plasma induces the production of reactive nitrogen species and cell death by increasing intracellular calcium in HEK293T cells. *Arch. Biochem. Biophys.* **2018**, *654*, 136–145. [CrossRef]
23. Machala, Z.; Tarabova, B.; Hensel, K.; Spetlikova, E.; Sikurova, L.; Lukes, P. Formation of ROS and RNS in water electro-sprayed through transient spark discharge in air and their bactericidal effects. *Plasma Process. Polym.* **2013**, *10*, 649–659. [CrossRef]
24. Lukes, P.; Dolezalova, E.; Sisrova, I.; Clupek, M. Aqueous-phase chemistry and bactericidal effects from an air discharge plasma in contact with water: Evidence for the formation of peroxynitrite through a pseudo-second-order post-discharge reaction of H_2O_2 and HNO_2. *Plasma Sources Sci. Technol.* **2014**, *23*, 015019. [CrossRef]
25. Xu, Z.; Cheng, C.; Shen, J.; Lan, Y.; Hu, S.; Han, W.; Chu, P.K. In vitro antimicrobial effects and mechanisms of direct current air-liquid discharge plasma on planktonic Staphylococcus aureus and Escherichia coli in liquids. *Bioelectrochemistry* **2018**, *121*, 125–134. [CrossRef]
26. Stoffels, E.; Sakiyama, Y.; Graves, D.B. Cold atmospheric plasma: Charged species and their interactions with cells and tissues. *IEEE Trans. Plasma Sci.* **2008**, *36*, 1441–1457. [CrossRef]
27. Xu, Z.; Wei, J.; Shen, J.; Liu, Y.; Ma, R.; Zhang, Z.; Qian, S.; Ma, J.; Lan, Y.; Zhang, H.; et al. Genetic effects of an air discharge plasma on Staphylococcus aureus at the gene transcription level. *Appl. Phys. Lett.* **2015**, *106*, 213701. [CrossRef]
28. Lee, Y.; Nirmalakhandan, N. Electricity production in membrane-less microbial fuel cell fed with livestock organic solid waste. *Bioresour. Technol.* **2011**, *102*, 5831–5835. [CrossRef] [PubMed]
29. Zhang, Y.; Lei, Y.; Huang, S.; Dong, X.; Huang, J.; Huang, M. In-package cold plasma treatment of braised chicken: Voltage effect. *Food Sci. Hum. Wellness* **2022**, *11*, 845–853. [CrossRef]
30. Wang, Y.; Wang, T.; Yuan, Y.; Fan, Y.; Guo, K.; Yue, T. Inactivation of yeast in apple juice using gas-phase surface discharge plasma treatment with a spray reactor. *LWT* **2018**, *97*, 530–536. [CrossRef]
31. Pankaj, S.K.; Wan, Z.; Colonna, W.; Keener, K.M. Effect of high voltage atmospheric cold plasma on white grape juice quality. *J. Sci. Food Agric.* **2017**, *97*, 4016–4021. [CrossRef] [PubMed]
32. Gan, Z.; Feng, X.; Hou, Y.; Sun, A.; Wang, R. Cold plasma jet with dielectric barrier configuration: Investigating its effect on the cell membrane of E. coli and S. cerevisiae and its impact on the quality of chokeberry juice. *LWT* **2021**, *136*, 110223. [CrossRef]

33. Stulić, V.; Vukušić, T.; Butorac, A.; Popović, D.; Herceg, Z. Proteomic analysis of Saccharomyces cerevisiae response to plasma treatment. *Int. J. Food Microbiol.* **2019**, *292*, 171–183. [CrossRef]
34. Xu, H.; Zhu, Y.; Du, M.; Wang, Y.; Ju, S.; Ma, R.; Jiao, Z. Subcellular mechanism of microbial inactivation during water disinfection by cold atmospheric-pressure plasma. *Water Res.* **2021**, *188*, 116513. [CrossRef]

foods

MDPI

Article

Increasing the Safety and Storage of Pre-Packed Fresh-Cut Fruits and Vegetables by Supercritical CO_2 Process

Alessandro Zambon [1,*], Víctor González-Alonso [1], Giovanna Lomolino [2], Riccardo Zulli [1], Andreja Rajkovic [3,4] and Sara Spilimbergo [1]

[1] Department of Industrial Engineering, University of Padova, 35131 Padova, Italy
[2] Department of Agronomy, Food, Natural Resources, Animals and Environment (DAFNAE), University of Padova, 35020 Legnaro, Italy
[3] Department of Food Safety and Quality Management, University of Belgrade—Faculty of Agriculture, 11080 Belgrade, Serbia
[4] Department of Food Technology, Safety and Health, Faculty of Bioscience Engineering, Ghent University, 9000 Ghent, Belgium
* Correspondence: alessandro.zambon@unipd.it

Abstract: This work presents a feasibility lab-scale study for a new preservation method to inactivate microorganisms and increase the shelf life of pre-packed fresh-cut products. Experiments were conducted on coriander leaves and fresh-cut carrots and coconut. The technology used the combination of hydrostatic pressure (<15 MPa), low temperature ($\leq$45 °C), and CO_2 modified atmosphere packaging (MAP). The inactivation was achieved for the naturally present microorganisms (total mesophilic bacteria, yeasts and molds, total coliforms) and inoculated *E. coli*. Yeasts and molds and coliform were under the detection limit in all the treated samples, while mesophiles were strongly reduced, but below the detection limit only in carrots. Inoculated *E. coli* strains were completely inactivated (>6.0 log CFU/g) on coconut, while a reduction >4.0 log CFU/g was achieved for carrots and coriander. For all the treated products, the texture was similar to the fresh ones, while a small alteration of color was detected. Microbiological stability was achieved for up to 14 days for both fresh-cut carrots and coconut. Overall, the results are promising for the development of a new mild and innovative food preservation technique for fresh food.

Keywords: modified atmosphere packaging; carbon dioxide; ready-to-eat; high pressure; shelf life

1. Introduction

The consumption of fresh fruits and vegetables as ready-to-eat (RTE) products has revolutionized the food industry, and it is expected to grow owing to the changing lifestyle of consumers [1]. However, when fresh-cut products are used as RTE, they usually have a limited shelf life (2–5 days), since they are affected by quick spoilage, mainly caused by oxidative enzymatic deterioration and microorganisms. Moreover, food safety in RTE food is still a challenge because a high risk of cross-contamination by pathogens can occur during the whole food chain. Good handling practices and an improvement in storage conditions and processing technologies are of primary importance to reduce the risk of outbreaks. Current technologies to increase the safety and shelf life of fresh-like products should be improved [2]. Modified atmosphere packaging (MAP) is the most widespread technology used to increase the shelf life of fresh RTE products [3]. By tuning the gas mixtures (usually N_2, O_2, and CO_2) and the specific gas barrier characteristics of the packaging materials, MAP is able to slow down the spoilage process and the microbial growth rate, thus increasing product shelf life [4]. However, MAP technology has almost no impact on the microbial inactivation [5,6]. Preservatives [7] and additional pre-treatments [8] are often used to increase the quality and safety of the products in MAP. Moreover, the possibility of combining MAP with non-thermal technologies has been investigated. For example, MAP

was used in combination with gamma irradiation [9,10] and high hydrostatic pressure (HHP) [11,12] to increase the microbial inactivation and the product shelf life. However, irradiation may raise safety concerns and can be negatively perceived by consumers [13], while the very high pressure needed for HHP (<4000 bars) might induce the irreversible transformation of the texture in the fresh products [14].

High-pressure carbon dioxide ($HPCO_2$) was extensively investigated as an alternative low-temperature pasteurization process [15], showing microbial and enzymatic inactivation in both liquid and solid products [16]. In solids, the process has been successfully applied to several food categories, such as vegetables [17,18], fruits [19,20], poultry [21], meat [22], seeds [23], and mushrooms [24]. The process is effective at supercritical conditions, meaning that it can be carried out at mild temperatures because the critical temperature of CO_2 is relatively low (31.1 °C), thus enhancing the maintenance of heat-sensitive components [25]. In the $HPCO_2$ process, liquid CO_2 is pumped inside a high-pressure chamber where the food is placed until reaching the desired process pressure. Following this, the pressure is maintained until achieving the desired microbial inactivation. At the end of the process, the CO_2 is released, and the treated food can be further packaged. Currently, the process itself needs post-processing packaging, which might increase the risk of cross-contamination; thus, it might represent a barrier to industrialization.

Here, we present a preliminary study at the lab scale of a new patented method [26] for the microbial inactivation of fresh and cut RTE solid food. This new process combines the inactivation capacity of high-pressure CO_2 within modified atmosphere packaging (HPMAP-CO_2). The food is firstly packaged with CO_2 as the modified atmosphere, and then the packaged sample is pressurized (pressure <15 MPa) until reaching supercritical CO_2 ($ScCO_2$) conditions using a pre-heated hydrostatic pressure vessel. The presented process is able to increase the current inactivation capacity of MAP technologies. Moreover, it avoids post-processing contamination, which might be possible after the $HPCO_2$ process, because the inactivation is achieved after packaging.

The inactivation was evaluated for the naturally present microorganisms (total mesophilic bacteria, total coliforms, and yeasts and molds) and a typical contaminant and food hygiene and safety model organism (*Escherichia coli*) inoculated on the surface of the product before the treatment. The process was compared with conventional $HPCO_2$ pasteurization for microbial inactivation performance on three products: coriander, carrots, and coconut. Texture and color analyses were used to assess the quality of the treated products.

2. Material and Methods

2.1. Sample Preparation

Fresh carrots, coconut, and coriander were purchased from a local market in Padua, Italy, and prepared according to the literature [27–30]. All foods were kept refrigerated at 4 °C and used within a few days. Carrots were washed and cut into round pieces of 2.0 ± 0.1 g, with a thickness of 3.0–5.0 mm; coconut was washed and cut into cubes of 2.0 ± 0.1 g; and coriander leaves of similar dimensions were selected and weighed to amount to 2.0 ± 0.1 g. After that, some products were directly treated with the $HPCO_2$ process, while others were packaged as explained in Section 2.2.

2.2. Plastic Pouches Preparation

In total, 10 cm squared pouches were crafted manually using a high gas barrier plastic film (CO_2 permeability $\leq$6.5 $cm^3/m^2/d/bar$; PA/EVOH/PA/PE, EuralPack, Shoten, Belgium). Each bag was loaded with 2.0 ± 0.1 g of food products, filled with either air or CO_2 (Rivoira, Milan, Italy), and manually closed with a thermal sealer (Impulse sealer PFS-300, Zhejiang, China). The pouch volume was 100 ± 10 mL. Gas composition inside the bags was measured with a gas analyzer (Oxybaby M+I O_2/CO_2, WITT, Witten, Germany).

2.3. High-Pressure Processes

The $HPCO_2$ processes were carried out within a multi-batch high-pressure apparatus, as explained previously [31,32]. Each product was inserted in a small high-pressure vessel. After the treatment, each reactor was opened under a laminar flow hood. The processed samples were collected in sterile containers and cooled down immediately to 4 °C until further analysis. The HPMAP-CO_2 process was carried out using the equipment previously described by Barberi et al. [33]; the packaged products were pressurized by pre-heated water. The products were packaged with 100% CO_2 or air (HPMAP-air); HPMAP-air was used as the additional control. At the end of the process, the pouches were removed, dried gently with paper towel, and stored at 4 °C until further analysis.

Process conditions were the same for both processes: 120 bar/40 °C/20 min for carrots, 120 bar/45 °C/30 min for coconut, and 100 bar/40 °C/1 min for coriander. The process conditions were selected from the literature in order to maximize the microbial inactivation [27–30,34].

2.4. Microbial Count for the Natural Flora

A standard plate count technique was used to analyze the microbial load. Samples were placed in 50 mL falcon tubes in sterility conditions, diluted 1:10 in phosphate-buffered saline solution (PBS; 0.01 M, pH 7.4; Oxoid, Hampshire, UK), and homogenized at 24.0 Hz for 1 min (Stomacher 400, International P.B.I., Milan, Italy). The solution was serially diluted (1:10) in PBS. Next, 100 µL of the appropriate dilutions was spread-plated onto the chosen media: chromogenic agar (Biolife Italiana s.r.l, Monza, Italy) for total coliforms and *E. coli*, and rose bengal (RB) (Sacco, Cadorago, Italy) for yeasts and molds; 1.0 mL was instead pour-plated into plate count agar (PCA) (Sacco, Cadorago, Italy) for the determination of the total mesophilic count. The incubation conditions were 37 °C and 24 h for *E. coli*, 30 °C and 48 h for total coliforms, 22 °C and 96 h for yeasts and molds, and 30 °C and 72 h for total mesophiles. At least three independent experiments were carried out for each single treatment condition, and the results were expressed as mean and standard deviation.

2.5. Culture and Inoculation of Escherichia coli

A clinically isolated *Escherichia coli* (Migula) Castellani and Chalmers (ATCC 25922) strain was used. From a frozen culture at −80 °C, the strain was resuscitated by successive overnight incubation of 100.0 µL culture in 10.0 mL of Luria-Bertani (LB) medium broth (Lennox, L3022, Sigma-Aldrich, St. Louis, MO, USA) at 37 °C. Bacterial culture was incubated at 37 °C with constant shaking (200 rpm), and the growth was carefully monitored spectrophotometrically until the stationary phase. The microbial suspension was centrifuged at 6000 rpm for 8 min; the supernatant was removed, and the pellet re-suspended in PBS reaching a final concentration of 1.0×10^{10} CFU/mL. Inoculated samples were spiked with 20 µL of *E. coli* suspension to reach a final inoculation level of 1.0×10^{8} CFU/g. Spiked samples were dried under laminar flow for 30 min before further processing.

2.6. Texture Measurement

A TA.XTplus Texture analyzer (Stable Micro System, Godalming, UK) was used to measure the firmness of the carrot and coconut samples. A 500.0 N load cell, equipped with a 35.0 mm diameter compression probe, was applied; the compression rate was 2.0 mm/s, 25.0% of the initial height of the sample. For the measurement, carrots were cut into cylinders of 5.0 mm height and 10.0 mm diameter; coconut was cut into pieces and the measurement determined on the height of 10.0 mm. Results were expressed as mean value obtained from 10 different samples. The cutting test was also performed on the samples using a stainless-steel blade of 1.0 mm thickness (Lloyd Instruments LS5, Ametek, Berwyn, PA, USA) with a deformation rate of 2.0 mm/s and 75.0% strain. The cutting test was expressed as the maximum force (Newton) required to cut the sample from the beginning of the test. The parameter was acquired and processed with the Software Texture Exponent (Stable Micro Systems, Godalming, UK).

2.7. pH Measurement

The pH values were measured with an electronic pH meter equipped with a Sension + 5053T penetration pH electrode (Cri-son Instruments Sa, Barcelona, Spain) for food applications, which allowed automatic temperature compensation. At least 10 determinations were executed. The pH was measured 24 h after the process.

2.8. Color Measurement

The color measurement was carried out with a Chroma Meter Minolta CM-600d Sensing colorimeter (Minolta Sensing Inc., Osaka, Japan), on treated and untreated samples (carrot and coconut). The device was set with a CIE (Commission Internationale de l'Éclairage), 8° standard angle observer, and D65 illuminant. The parameters lightness (L*), redness (a*), and yellowness (b*) were recorded and calculated with the CIELAB system (1978) with 400–700 nm reflectance spectrum range. The Hue angle (H*) was calculated as:

$$H^* = \tan^{-1}(b^*/a^*), \quad (1)$$

while Chroma (C*) as:

$$C^* = \sqrt{(a^*)^2 + (b^*)^2} \quad (2)$$

respectively. For each condition, 10 measurements were carried out.

2.9. Microbiological Storage Test

Samples of carrot and coconut were prepared, packaged, and treated as described in the previous sections, and then stored for 14 days at 4 °C, with monitoring of the microbial growth of the natural flora and the evolution of the gas composition of the pouches. Untreated products packaged in air (MAP-air) and CO_2 (MAP-CO_2) were used as the controls. Analyses were performed after the treatment (day 0) and after 3, 7, and 14 days of storage.

2.10. Statistical Analysis

Statistical testing was performed in RStudio. Mean values were used to compare differences between treatments. The existence of significant differences (α = 95%) between different treatments was further considered using ANOVA and its subsequent post-hoc analysis (Tukey HSD); the Kruskal–Wallis rank-sum test and Wilcoxon rank-sum tests were used when the assumptions for an ANOVA were not fulfilled.

3. Results and Discussion

3.1. Microbial Inactivation

Figure 1 shows the comparison between the microbial inactivation achieved with the two processes (HPCO$_2$ and HPMAP-CO$_2$) for three food products: coriander (Figure 1a), carrot (Figure 1b), and coconut (Figure 1c).

The inactivation was demonstrated over a range of microbial groups in terms of naturally present microorganisms: total mesophiles, yeasts and molds, and total coliforms. A specific fecal indicator (*E. coli*) was also investigated by inoculation on the surface at a high concentration (1.0×10^8 CFU/g). The inactivation achieved with HPMAP-CO$_2$ was comparable to the one achieved with the HPCO$_2$ for total mesophilic bacteria, yeasts and molds, and coliforms in all the products. Instead, a slightly higher *E. coli* inactivation was achieved for coriander and carrots with the HPCO$_2$ process. For coriander, a total inactivation of the mesophiles was not possible for either treatment, while a complete inactivation was achieved for yeasts and molds with the HPCO$_2$, and total coliforms using both processes. These results agree with our previous results achieved with coriander. Indeed, mesophilic bacteria were more resistant to the supercritical CO_2 treatment compared with yeasts and molds [27]. Spiked *E. coli* on coriander was under the detection limit after the HPCO$_2$ process, while almost a 3.0 log CFU/g reduction was achieved with the HPMAP-CO$_2$.

Bordeaux et al. showed that a complete inactivation of spiked *E. coli* was possible after the $HPCO_2$ process [28].

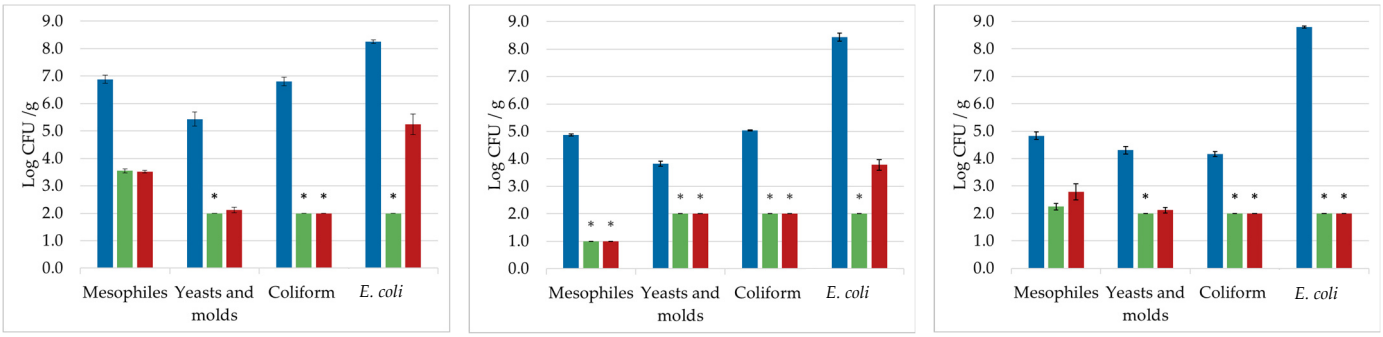

Figure 1. Microbial counts of total mesophiles, yeasts and molds, total coliforms, and spiked *E. coli*, measured on coriander (**a**), carrot (**b**), and coconut (**c**), in the untreated samples (■), the ones treated directly with high-pressure carbon dioxide ($HPCO_2$, ■) and the ones treated inside the packaging (HPMAP-CO_2, ■). Treatment conditions were: 120 bar/40 °C/20 min for carrots, 100 bar/40 °C/1 min for coriander, and 120 bar/45 °C/30 min for coconut. * ND—Not detected. No colonies were found at the lowest dilution possible (<2.0 log CFU/g for yeasts and molds, coliforms, and *E. coli*, <1.0 log CFU/g for mesophiles).

For carrots, a similar inactivation for all naturally present microorganisms was achieved with the two processes. Regarding the inoculated *E. coli*, a total inactivation was achieved only after the $HPCO_2$ treatment, while 4.66 log CFU/g were reduced with HPMAP-CO_2. Tamburini et al. [35] also showed a complete inactivation when spiked carrots were treated with $HPCO_2$ at 120 bar—35 °C—10 min, while Ferrentino et al. [36] showed a complete inactivation also at a lower pressure (100 bar).

For coconut, a total inactivation of total coliforms and *E. coli* with both processes was observed, but not for the total mesophilic bacteria. Yeasts and molds were under the detection limit only after the $HPCO_2$ process. In the case of mesophilic bacteria, $HPCO_2$ resulted in a slightly higher inactivation compared to HPMAP-CO_2, which nevertheless was not found to be significant. Previous studies, with $HPCO_2$ at similar process conditions [30,36], showed a similar inactivation degree; however, a direct comparison might be misleading because the initial load was slightly different. Previous studies with $HPCO_2$ treatment with *E. coli* on coconut showed a reduction at 60 bar/25 min/35 °C up to 5.0 log CFU/g [34]. These data indicate that *E. coli* in coconut is easily inactivated by CO_2 even at milder conditions.

Overall results demonstrated that at a small scale the inactivation with HPMAP-CO_2 and $HPCO_2$ was comparable for the naturally present microorganisms, while the inactivation of inoculated *E. coli* was different between the two processes in carrots and coriander. The lower inactivation achieved with HPMAP-CO_2 for *E. coli* in carrots and coriander should be further investigated with a wider number of strains and process conditions. The lower inactivation in the case of HPMAP-CO_2 might also be explained by the presence of the packaging, which is known to influence the inactivation in the thermal pasteurization [37,38]. It might be possible that the packaging reduces the heat mass transfer, thus reducing the effective process time in which the CO_2 is at a supercritical state. However, further studies are needed to confirm any hypothesis.

Two different controls with the HPMAP-CO_2 process were carried out (Figure 2) to demonstrate that the microbial inactivation was due to the effect of CO_2 at a supercritical state. In the first one, the products were packaged with air instead of CO_2, and then processed with HPMAP (HPMAP-air). In the second one, the products were packaged in CO_2 and then maintained at the processing temperature for the whole processing time (TMAP-CO_2). Microbial inactivation was not achieved when air was used instead of CO_2 in the HPMAP process, demonstrating that the pressure itself was not responsible for any

microbial reduction. The need for a simultaneous application of pressure, temperature, time, and CO_2 was also confirmed by TMAP-CO_2. In addition, in this case, the inactivation was negligible for all microorganisms in all the products.

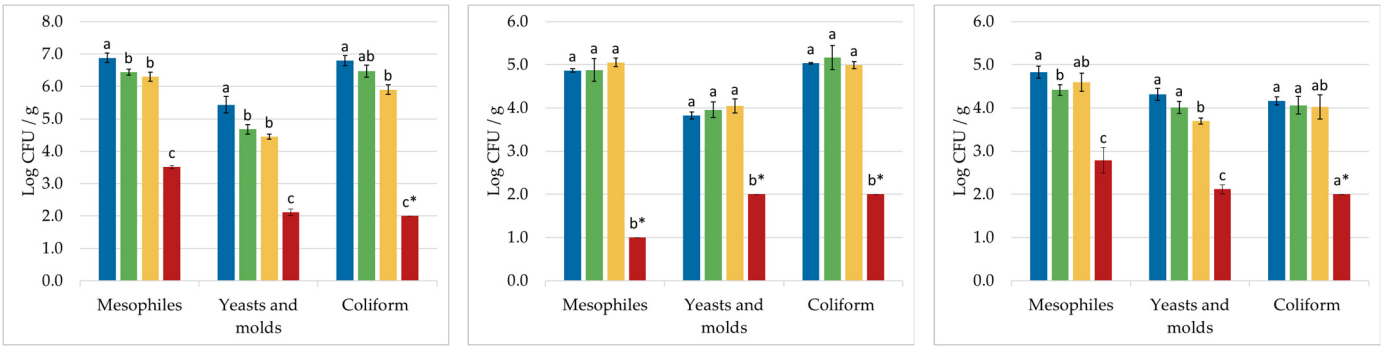

Figure 2. Microbial counts of total mesophiles, yeasts and molds, and total coliforms, on coriander (**a**), carrot (**b**), and coconut (**c**), in the untreated samples (■), the ones treated inside the packaging with air (HPMAP-air, ■), the ones packaged in CO_2 and maintained at the processing temperature and time (TMAP-CO_2, ■), and the ones treated inside the packaging in CO_2 (HPMAP-CO_2, ■). Treatment conditions were: 120 bar/40 °C/20 min for carrot, 100 bar/40 °C/1 min for coriander, and 120 bar/45 °C/30 min for coconut. Means with different small superscript letters in the same group of microorganisms are significantly different ($p < 0.05$). * ND—Not detected. No colonies were found at the lowest dilution possible (<2.0 log CFU/g for yeasts and molds, coliforms, and *E. coli*, <1.0 log CFU/g for mesophiles).

Statistical testing confirmed the significant difference (p-value < 0.05) for all microbial groups (mesophiles, yeasts and molds, and coliforms), in all food products tested, between the samples treated with high-pressure CO_2 (HPCO$_2$ and HPMAP-CO_2) and the others (untreated control sample, HPMAP-air, and TMAP-CO_2).

The gas composition and the volume of the packages were also measured. These values were not significantly different between the treated and untreated samples.

3.2. Texture, pH, and Color Analysis

Traditional HPCO$_2$ and HPMAP-CO_2 processes were compared for texture, pH, and color change. As regards the texture, previous works suggested that fruits and vegetables treated with HPCO$_2$ could lose their consistency, and thus becoming useless as an RTE product. Specifically, Valverde et al. [39] reported that pears treated with pressurized CO_2 lost their consistency, and this loss was higher as the pressure was increased. Haas et al. [40] reported similar findings for strawberries and melons treated with HPCO$_2$.

The HPMAP-CO_2 process induced a consistent change of color and integrity on coriander leaves, similarly to what we reported previously with HPCO$_2$ [41]. A discoloration and a reduction in the firmness were also previously observed on spinach leaves after the HPCO$_2$ [18] and HPP processes [42], suggesting that in general, leaves are not good candidates for high-pressure processes. On the contrary, the visual appearance of coconut and carrots was very similar to the fresh product, demonstrating that firm products could be good food products for both HPCO$_2$ and HPMAP-CO_2 processes. For this reason, only carrots and coconuts were further investigated in this study for qualitative analysis.

The cutting force applied with a blade on a food matrix could provide indications of the fracture resistance (using the maximum force during the cutting cycle), and the rubbery behavior of the tissue, as indicated by the increase in both displacement and cutting force. A low cutting force might indicate a food matrix with a fragile structure. The results reported in Table 1 show that the untreated carrots (packaged in air (MAP-air) or CO_2 (MAP-CO_2)) and the ones treated with HPMAP-CO_2 did not show significant differences for the cutting force, indicating that the process did not change the original

texture and firmness of the carrots. On the contrary, samples treated with the traditional $HPCO_2$ process presented a lower cutting force value, which was statistically different from the other samples. The low value after the $HPCO_2$ process could be due to the de-structuring effect of the high pressures on the carrots' tissue that could modify the cellular microstructure with consequent texture alteration [43]. In fact, as reported by Sun et al. [44], the high pressures can cause cell corruption and cell collapse up to destructive damage, cell disruption, cell wall dissolution, and overall texture degradation. These findings suggest that the HPMAP-CO_2 process could reduce the de-structuring effect caused by the $HPCO_2$ process, making the treatment more suitable for the development of minimally processed RTE products.

Table 1. Texture analysis: effect of the different treatments on the cutting test (N) and textural firmness (J), carried out on carrots and coconut. Treatment conditions were the same as detailed in Section 3.1. Values in brackets are SD. Means with different small superscript letters in the same column are significantly different ($p < 0.05$).

Treatment	Carrot (N)	Coconut (N)	Carrot (J)	Coconut (J)
MAP-air	77.56 (12.29) ^{a}	31.34 (3.93) ^{a}	0.17 (0.02) ^{a}	0.14 (0.02) ^{a}
MAP-CO_2	76.27 (11.48) ^{a}	31.21 (3.11) ^{a}	0.16 (0.01) ^{a}	0.14 (0.02) ^{a}
HPMAP-CO_2	79.17 (12.39) ^{a}	30.81 (4.62) ^{a}	0.16 (0.03) ^{a}	0.15 (0.03) ^{a}
$HPCO_2$	61.69 (11.72) ^{b}	32.23 (6.15) ^{a}	0.14 (0.02) ^{a}	0.14 (0.03) ^{a}

Coconut, on the other hand, did not show significant differences in the cutting force parameter, which was similar in all the samples (treated and untreated). This evidence may be due to the chemical composition and the particular structure of the coconut tissue which were minimally affected by the treatments applied. This finding was already demonstrated by Ferrentino et al. [19], who showed that coconut treated with $HPCO_2$ maintained the same consistency compared to the fresh, untreated one.

Finally, the textural firmness did not show significant differences for all the samples. The stress–strain curves did not present statistically significant differences in the tracings and repetitions for all the trials.

The pH for the untreated products was 6.10 and 6.17 for the carrot and coconut, respectively. These pH values are similar to the literature [19,29,45]. Neither the MAP-CO_2 itself nor the high-pressure treatments significantly changed the pH, in contrast to what was reported in the literature for the $HPCO_2$ treatment [19,29], where a slight reduction in the pH was observed after the treatment. In our case, the measurements were performed 24 h after the treatment, allowing the establishment of an equilibrium of the solubilized CO_2 with the environment and a subsequent return to the original pH. This observation is important for the development of RTE products and consumers' acceptance, since small changes in the pH could influence the sensorial perception.

The color measurements are reported in Table 2 for carrots and coconut. The carrots treated with the HPMAP-CO_2 and $HPCO_2$ processes had the highest and significantly different b* values compared to the not-treated products (MAP-air and MAP-CO_2). Significant differences were observed for the parameter a* (red/green). The highest a* values were present in the untreated products, while the processes induced lower a* values, according to what was reported by Trejo Araya et al. [46]. Based on the colorimetric data, the control samples had a more intense orange color than the treated ones. The non-treated samples did not show significant differences for the L* (lightness) parameter. On the contrary, the treated samples showed significantly lower L* values. The spatial distribution of the color was given by the hue angle (H*) and chroma (C*). The hue angle parameter showed significant differences among the carrot samples. In particular, the treated samples showed the greatest hue angle, i.e., an inclination towards yellow. Additionally, the chroma parameter had higher values for the treated samples rather than for the control.

Table 2. Effect of the different treatments on the color of carrots and coconut, measured by CIELAB system, hue angle (H*), and chroma (C*). Treatment conditions were the same as detailed in Section 3.1. Values in brackets are SD. Means with different small superscript letters in the same column are significantly different ($p < 0.05$).

	L*	a*	b*	Chroma	Hue
Carrot					
MAP-air	62.46 (1.33) ^{a}	31.70 (0.86) ^{a}	42.65 (1.37) ^{a}	53.15 (1.37) ^{a}	53.37 (0.94) ^{a}
MAP-CO_2	60.24 (1.67) ^{a}	33.59 (0.95) ^{a}	45.74 (3.75) ^{ab}	56.77 (3.42) ^{ab}	53.62 (1.88) ^{a}
HPMAP-CO_2	60.44 (3.58) ^{a}	28.31 (2.10) ^{b}	49.42 (2.78) ^{b}	56.98 (2.97) ^{b}	60.19 (1.87) ^{b}
HPCO_2	57.99 (1.23) ^{b}	26.90 (1.18) ^{b}	50.33 (5.91) ^{b}	57.12 (5.48) ^{b}	61.68 (2.52) ^{b}
Coconut					
MAP-air	83.26 (2.48) ^{a}	−0.65 (0.16) ^{a}	3.66 (0.60) ^{a}	3.72 (0.59) ^{a}	100.47 (3.54) ^{a}
MAP-CO_2	82.86 (2.34) ^{a}	−0.78 (0.09) ^{ac}	3.63 (0.63) ^{a}	3.72 (0.61) ^{a}	102.40 (2.53) ^{ab}
HPMAP-CO_2	81.70 (1.62) ^{ab}	−0.87 (0.18) ^{bc}	3.43 (0.89) ^{a}	3.55 (0.86) ^{a}	105.08 (4.07) ^{b}
HPCO_2	79.82 (2.54) ^{b}	−0.98 (0.17) ^{b}	4.38 (1.24) ^{a}	4.49 (1.23) ^{a}	103.25 (3.06) ^{ab}

Furthermore, the coconut showed some significant differences for the parameters a* and L*, which were lower in the treated sample, indicating a variation in the coloring toward green. The parameters b* and C* were not affected by the treatment. On the contrary, the hue angle had significantly higher values in the coconut samples that were subjected to the treatments.

These findings indicate that the process induced a visual change of the original color of the fresh products. For this reason, it has become more and more important to develop and improve methodologies to optimize the process minimizing the change of color, as previously reported by Barberi et al. [33]. A sensorial analysis should also be performed to confirm the perception of the consumers caused by the treatment.

3.3. Microbiological Stability

A storage test at 4 °C for up to 14 days was performed for fresh-cut carrots and coconut as a proof-of-concept for the potentiality of the new HPMAP-CO_2 technology at improving the product's shelf life.

Figure 3 reports the microbial load on fresh-cut carrot for the treated HPMAP-CO_2 and two controls (MAP-air and MAP-CO_2). The initial microbial load was 4.2, 2.6, and 3.5 log CFU/g for mesophiles (Figure 3a), yeasts and molds (Figure 3b), and coliforms (Figure 3c), respectively. The average gas composition in terms of % CO_2 and % O_2 was also recorded (Figure 2d).

The results showed that the HPMAP-CO_2 treatment was able to reduce the microbial load to undetectable levels of mesophiles, yeasts and molds, and total coliforms, and that microbial counts remained stable over a 14-day storage period. Untreated products showed microbial growth in both CO_2 and MAP-air, eventually reaching spoilage levels.

The gas composition of the pouches filled with 100% CO_2 (both treated and not treated) remained stable between 95.0 and 98.0% over the storage period, while the packages filled with air underwent a decrease in O_2 down to 16.0% by day 14, and a slight increase in CO_2 concentration probably caused by the growth of microorganisms and the respiration of the plant tissues.

The bacteriostatic effect of MAP-CO_2 in the untreated product was revealed for yeasts and molds and coliforms compared with the MAP-air. Yeasts and molds have been previously reported to be sensitive to high CO_2 concentrations during MAP [6]. On the contrary, for total mesophilic bacteria, the load of samples in MAP-CO_2 started to be slightly higher than the MAP-air on day 7, reaching a 1.5 log higher load on day 14 compared with the MAP-air sample. This could indicate an overgrowth of lactic acid bacteria in the 100% CO_2 samples due to the absence of oxygen [4,6].

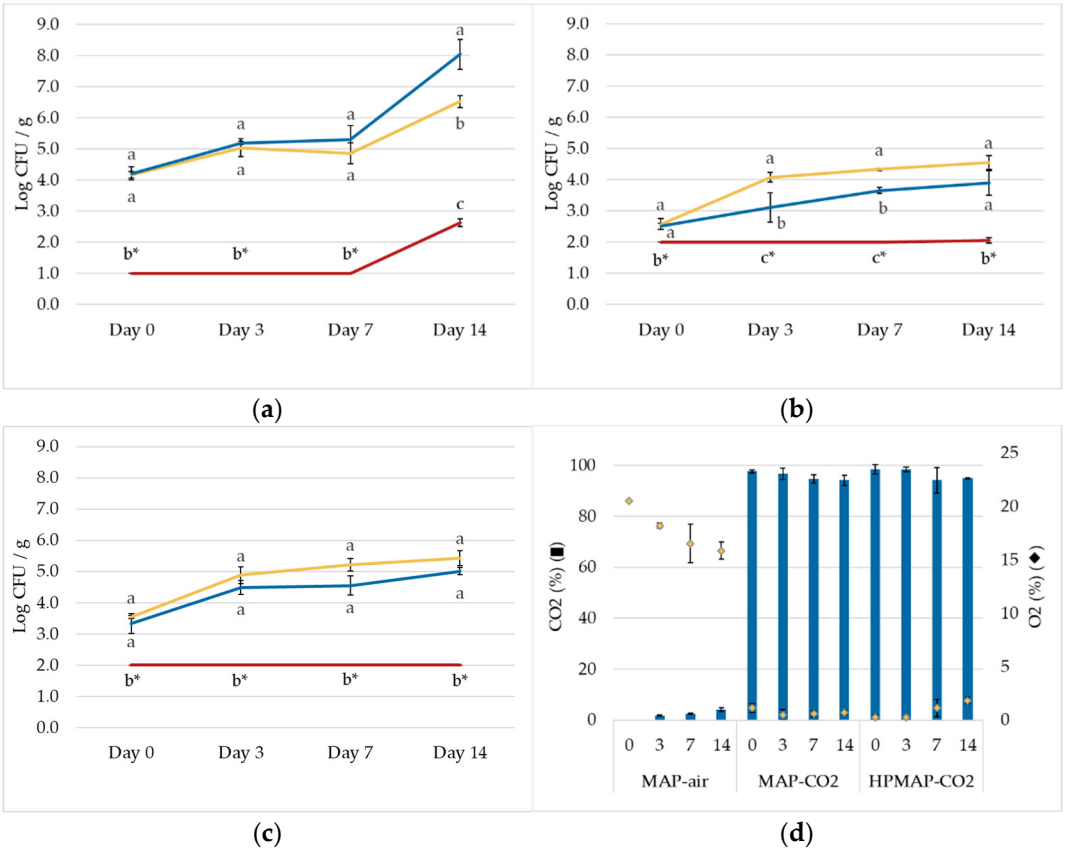

Figure 3. Fresh-cut carrot microbial levels of total mesophiles (**a**), yeasts and molds (**b**), and total coliforms (**c**), and gas composition (**d**), in the control packaged in air (MAP-air) (—), control packaged in CO_2 (MAP-CO_2) (—), and the treated packaged in CO_2 (HPMAP-CO_2) (—), during a shelf-life trial at 4 °C. Treatment conditions were 120 bar—40 °C—20 min. Points with different small letters at the same time point represent significantly different values ($p < 0.05$). * ND—Not detected. No colonies were found at the lowest dilution possible (< 1.0 log CFU/g).

Compared to traditional MAP technology, HPMAP-CO_2 could extend the shelf life of fresh-cut carrots up to 14 days (or more). Recently, the use of pectin-coating showed the ability to increase the shelf life of fresh-cut carrots up to 12 days [47]. The technology could be potentially coupled with HPMAP-CO_2 to obtain a synergistic effect. Microbial inactivation could be increased by tuning pressure, temperature, and treatment time, inducing a higher inactivation. Sensorial studies should be also performed to validate the consumers' acceptance of the technology.

Figure 4 shows the microbial counts found on fresh-cut coconut for mesophiles (Figure 4a), yeasts and molds (Figure 4b), and coliforms (Figure 4c), as well as the gas composition of the plastic pouches (Figure 4d) during a storage trial of 14 days. The initial microbial load was 6.5, 4.5, and 6.3 log CFU/g for mesophiles, yeasts and molds, and coliforms, respectively. The results showed higher variability compared to the shelf-life trial performed on carrots. On day 0, reductions of 2.2, 2.4, and 3.3 log CFU/g were achieved for mesophiles, yeasts and molds, and coliforms, respectively, compared to the untreated products, which were statistically significant ($p < 0.05$). In all three microbial groups, the counts of MAP-air at day 14 were higher than 7.0 log CFU/g for mesophiles and coliforms. However, the count up to day 7 did not show a significant increment compared to day 0, which could indicate a higher variability on the initial count due to a random contamination with the shell. However, data on day 14 demonstrated that untreated samples in MAP-CO_2 had a lower growth compared to MAP-air, which is consistent with a bacteriostatic effect of high CO_2 concentration MAP. The treated bags did not reach spoilage levels during the 14-day storage trial.

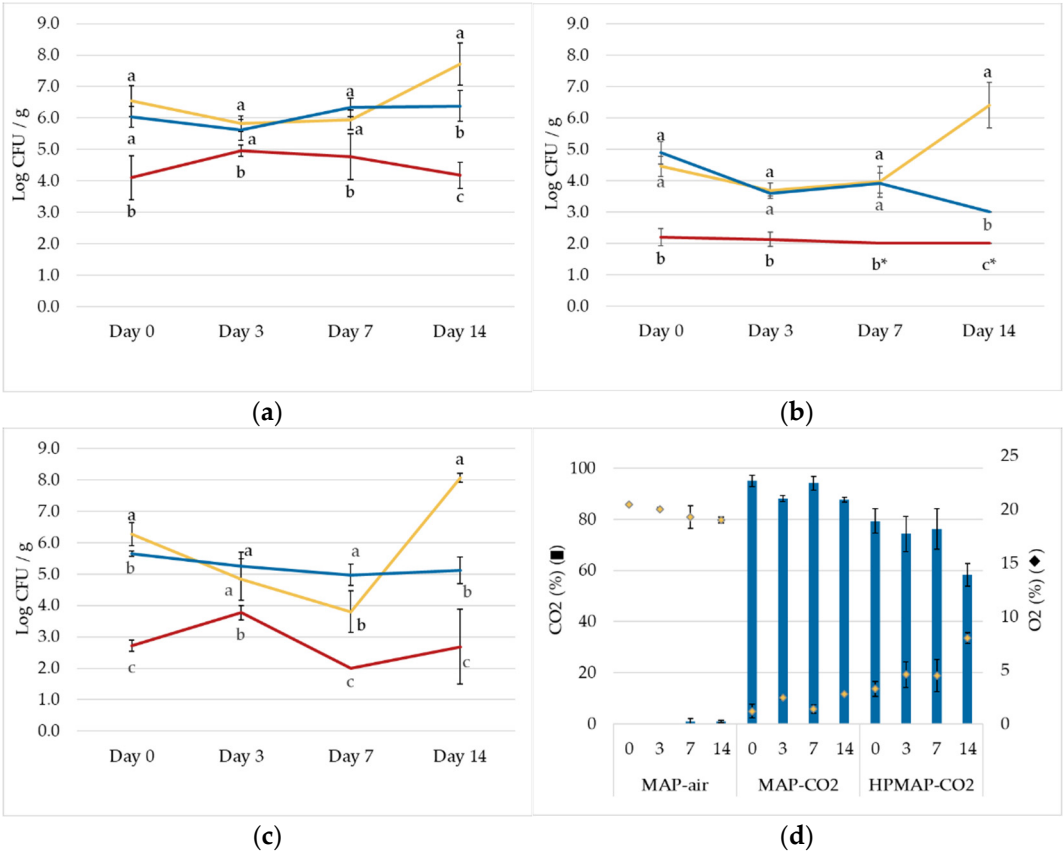

Figure 4. Fresh-cut coconut microbial levels of total mesophiles (**a**), yeasts and molds (**b**), and total coliforms (**c**), and gas composition (**d**), in the control packaged in air (MAP-air) (—), control packaged in CO_2 (MAP-CO_2) (—), and the treated packaged in CO_2 (HPMAP-CO_2) (—), during a shelf-life trial at 4 °C. Treatment conditions were 120 bar—45 °C—30 min. Points with different small letters at the same time point represent significantly different values ($p < 0.05$). * ND – Not detected. No colonies were found at the lowest dilution possible (<1.0 log CFU/g) in at least one repetition.

The HPMAP-CO_2 coconut shelf life at 4 °C could be extended up to 14 days (or longer) in terms of microbial spoilage in comparison to samples stored in air at the same temperature. Our finding is promising for the obtainment of an extension of the shelf life of fresh-cut coconut, which in a previous study by Sinigalli et al. [48] was only 7 days.

The gas composition (Figure 4d) of the pouches loaded with fresh-cut coconut showed a different behavior compared with carrots. The concentration of O_2 in MAP-air was reduced from 20.4% on day 0 to 19.0% on day 14. The different O_2 consumption can be explained by the different respiration rates of coconut and carrot [49]. The CO_2 in the MAP-CO_2 was reduced from 95.0% CO_2 on day 0, to 87.7% on day 14, while for the HPMAP-CO_2, the composition was 79.0% after the treatment, and 58.0% on day 14. It is not very clear how the change in gas permeability observed compared with carrots, and additional experiments with different kinds of products and packaging materials should be performed.

4. Conclusions

This work compared a new HPMAP-CO_2 process with the traditional HPCO_2 inactivation treatment. Despite its benefit, HPCO_2 has never been used industrially to produce RTE foodstuff. Within this work, we proved the potential of HPMAP-CO_2 to be used as an alternative technology to increase the safety and the shelf life of fresh RTE food. The comparison between the two technologies was performed at the lab scale on three food categories: fresh-cut carrots, fresh-cut coconut, and coriander leaves. The inactivation de-

gree was similar between the processes, even if a slightly higher inactivation was achieved for mesophilic bacteria and inoculated *E. coli* in carrots with the $HPCO_2$. The microorganisms in coconut were easily inactivated with both the processes. The microbiological shelf life was achieved up to 14 days with the HPMAP-CO_2. HPMAP-CO_2 was able to preserve the original texture of the fresh carrots better than $HPCO_2$, while for the coconut, no differences were found after both treatments. The treatments induced a slight change in color compared to the untreated products. A further analysis should be performed to demonstrate the inactivation capacity over a wider group of spiked pathogens and the process scalability by processing bigger amounts of products. Moreover, the enzymatic activity and the retention of the nutritional properties on the treated and untreated products during the storage should be also considered in further studies. Overall, the technology results are promising for the development of a new low-temperature inactivation treatment that could be applied to strong, firm, fresh products.

Author Contributions: Conceptualization, A.Z. and S.S.; methodology, A.Z., V.G.-A., G.L. and S.S.; formal analysis, V.G.-A., G.L.; investigation, V.G.-A.; resources, G.L. and S.S.; data curation, A.Z., V.G.-A. and R.Z.; writing—original draft preparation, A.Z., V.G.-A., G.L., R.Z., A.R. and S.S.; writing—review and editing, A.Z., V.G.-A., G.L., R.Z., A.R. and S.S.; supervision, A.Z., A.R. and S.S.; project administration, A.Z. and S.S.; funding acquisition, A.Z. and S.S. All authors have read and agreed to the published version of the manuscript.

Funding: This research was funded by "Fondazione Cassa di Risparmio di Padova e Rovigo" through the grant "CARIPARO Visiting Programme 2018", Innovation Voucher funded by the Interreg ADRION—ADRIATIC-IONIAN Programme "OISAIR" Proof of Concept Call-AREA Science Park; the Department of Industrial Engineering (University of Padova) "Progetto Strategico di Dipartimento" (CoSID) SPIL_SID18_01; the H2020 ERA-NETs SUSFOOD2 and CORE Organic Cofunds, under the Joint SUSFOOD2/CORE Organic Call 2019, project "HO-FOOD, Innovative High pressure process to increase the preservation of ready-to-eat Organic FOOD" CUP C95F20000930001.

Institutional Review Board Statement: Not applicable.

Informed Consent Statement: Not applicable.

Data Availability Statement: The data are available from the corresponding author.

Acknowledgments: All the authors thank Massimo Vetralla for the support in the experimental activity. G.L. thanks Luciano Magro of the LaCHI Laboratory of the DAFNAE Department (University of Padua), and Fabio Santi for the support for the analytical activity.

Conflicts of Interest: A.Z. and S.S. are co-inventors of the patent describing the new method for food pasteurization: Italian patent n. 10201700009804, European patent application n. 17787252.0, Chinese patent application n. 201780094448.6, and US patent application n. 16/642,401.

References

1. Sgroi, F.; Piraino, F.; Donia, E. Determinants of Ready-to-Eat Products Purchase Intentions: An Empirical Study among the Italian Consumers. *HortScience* **2018**, *53*, 656–660. [CrossRef]
2. De Corato, U. Improving the Shelf-Life and Quality of Fresh and Minimally-Processed Fruits and Vegetables for a Modern Food Industry: A Comprehensive Critical Review from the Traditional Technologies into the Most Promising Advancements. *Crit. Rev. Food Sci. Nutr.* **2020**, *60*, 940–975. [CrossRef] [PubMed]
3. Wilson, M.D.; Stanley, R.A.; Eyles, A.; Ross, T. Innovative Processes and Technologies for Modified Atmosphere Packaging of Fresh and Fresh-Cut Fruits and Vegetables. *Crit. Rev. Food Sci. Nutr.* **2019**, *59*, 411–422. [CrossRef] [PubMed]
4. Ghidelli, C.; Pérez-Gago, M.B. Recent Advances in Modified Atmosphere Packaging and Edible Coatings to Maintain Quality of Fresh-Cut Fruits and Vegetables. *Crit. Rev. Food Sci. Nutr.* **2018**, *58*, 662–679. [CrossRef] [PubMed]
5. Brown, S.R.B.; Forauer, E.C.; D'Amico, D.J. Effect of Modified Atmosphere Packaging on the Growth of Spoilage Microorganisms and Listeria monocytogenes on Fresh Cheese. *J. Dairy Sci.* **2018**, *101*, 7768–7779. [CrossRef]
6. Caleb, O.J.; Mahajan, P.V.; Al-Said, F.A.-J.; Opara, U.L. Modified Atmosphere Packaging Technology of Fresh and Fresh-Cut Produce and the Microbial Consequences—A Review. *Food Bioprocess Technol.* **2013**, *6*, 303–329. [CrossRef]
7. Stoops, J.; Ruyters, S.; Busschaert, P.; Spaepen, R.; Verreth, C.; Claes, J.; Lievens, B.; Van Campenhout, L. Bacterial Community Dynamics during Cold Storage of Minced Meat Packaged under Modified Atmosphere and Supplemented with Different Preservatives. *Food Microbiol.* **2015**, *48*, 192–199. [CrossRef]

8. Choi, D.S.; Park, S.H.; Choi, S.R.; Kim, J.S.; Chun, H.H. The Combined Effects of Ultraviolet-C Irradiation and Modified Atmosphere Packaging for Inactivating Salmonella Enterica Serovar Typhimurium and Extending the Shelf Life of Cherry Tomatoes during Cold Storage. *Food Packag. Shelf Life* **2015**, *3*, 19–30. [CrossRef]
9. Ravindran, R.; Jaiswal, A.K. Wholesomeness and Safety Aspects of Irradiated Foods. *Food Chem.* **2019**, *285*, 363–368. [CrossRef]
10. Reale, A.; Sorrentino, E.; Iaffaldano, N.; Rosato, M.P.; Ragni, P.; Coppola, R.; Capitani, D.; Sobolev, A.P.; Tremonte, P.; Succi, M.; et al. Effects of Ionizing Radiation and Modified Atmosphere Packaging on the Shelf Life of Aqua-Cultured Sea Bass (Dicentrarchus Labrax). *World J. Microbiol. Biotechnol.* **2008**, *24*, 2757–2765. [CrossRef]
11. Al-Nehlawi, A.; Guri, S.; Guamis, B.; Saldo, J. Synergistic Effect of Carbon Dioxide Atmospheres and High Hydrostatic Pressure to Reduce Spoilage Bacteria on Poultry Sausages. *LWT Food Sci. Technol.* **2014**, *58*, 404–411. [CrossRef]
12. Sterr, J.; Fleckenstein, B.S.; Langowski, H.-C. The Effect of High-Pressure Processing on Tray Packages with Modified Atmosphere. *Food Eng. Rev.* **2015**, *7*, 209–221. [CrossRef]
13. Galati, A.; Tulone, A.; Moavero, P.; Crescimanno, M. Consumer Interest in Information Regarding Novel Food Technologies in Italy: The Case of Irradiated Foods. *Food Res. Int.* **2019**, *119*, 291–296. [CrossRef]
14. Hu, X.; Ma, T.; Ao, L.; Kang, H.; Hu, X.; Song, Y.; Liao, X. Effect of High Hydrostatic Pressure Processing on Textural Properties and Microstructural Characterization of Fresh-Cut Pumpkin (*Cucurbita Pepo*). *J. Food Process Eng.* **2020**, *43*, e13379. [CrossRef]
15. Silva, E.K.; Meireles, M.A.A.; Saldaña, M.D.A. Supercritical Carbon Dioxide Technology: A Promising Technique for the Non-Thermal Processing of Freshly Fruit and Vegetable Juices. *Trends Food Sci. Technol.* **2020**, *97*, 381–390. [CrossRef]
16. Ferrentino, G.; Spilimbergo, S. High Pressure Carbon Dioxide Pasteurization of Solid Foods: Current Knowledge and Future Outlooks. *Trends Food Sci. Technol.* **2011**, *22*, 427–441. [CrossRef]
17. Ferrentino, G.; Spilimbergo, S. High Pressure Carbon Dioxide Combined with High Power Ultrasound Pasteurization of Fresh Cut Carrot. *J. Supercrit. Fluids* **2015**, *105*, 170–178. [CrossRef]
18. Zhong, Q.; Black, D.G.; Davidson, P.M.; Golden, D.A. Nonthermal Inactivation of Escherichia Coli K-12 on Spinach Leaves, Using Dense Phase Carbon Dioxide. *J. Food Prot.* **2008**, *71*, 1015–1017. [CrossRef]
19. Ferrentino, G.; Belscak-Cvitanovic, A.; Komes, D.; Spilimbergo, S. Quality Attributes of Fresh-Cut Coconut after Supercritical Carbon Dioxide Pasteurization. *J. Chem.* **2013**, *2013*, 703057. [CrossRef]
20. Marszałek, K.; Woźniak, Ł.; Barba, F.J.; Skąpska, S.; Lorenzo, J.M.; Zambon, A.; Spilimbergo, S. Enzymatic, Physicochemical, Nutritional and Phytochemical Profile Changes of Apple (*Golden Delicious* L.) Juice under Supercritical Carbon Dioxide and Long-Term Cold Storage. *Food Chem.* **2018**, *268*, 279–286. [CrossRef]
21. González-Alonso, V.; Cappelletti, M.; Bertolini, F.M.; Lomolino, G.; Zambon, A.; Spilimbergo, S. Research Note: Microbial Inactivation of Raw Chicken Meat by Supercritical Carbon Dioxide Treatment Alone and in Combination with Fresh Culinary Herbs. *Poult. Sci.* **2020**, *99*, 536–545. [CrossRef] [PubMed]
22. Huang, S.; Liu, B.; Ge, D.; Dai, J. Effect of Combined Treatment with Supercritical CO_2 and Rosemary on Microbiological and Physicochemical Properties of Ground Pork Stored at 4 °C. *Meat Sci.* **2017**, *125*, 114–120. [CrossRef]
23. Bourdoux, S.; Zambon, A.; Van der Linden, I.; Spilimbergo, S.; Devlieghere, F.; Rajkovic, A. Inactivation of Foodborne Pathogens on Leek and Alfalfa Seeds with Supercritical Carbon Dioxide. *J. Supercrit. Fluids* **2022**, *180*, 105433. [CrossRef]
24. Manzocco, L.; Ignat, A.; Valoppi, F.; Burrafato, K.R.; Lippe, G.; Spilimbergo, S.; Nicoli, M.C. Inactivation of Mushroom Polyphenoloxidase in Model Systems Exposed to High-Pressure Carbon Dioxide. *J. Supercrit. Fluids* **2016**, *107*, 669–675. [CrossRef]
25. Tomic, N.; Djekic, I.; Zambon, A.; Spilimbergo, S.; Bourdoux, S.; Holtze, E.; Hofland, G.; Sut, S.; Dall'Acqua, S.; Smigic, N.; et al. Challenging Chemical and Quality Changes of Supercritical Co2 Dried Apple during Long-Term Storage. *LWT* **2019**, *110*, 132–141. [CrossRef]
26. Spilimbergo, S.; Zambon, A.; Michelino, F.; Polato, S. Method for Food Pasteurization. PCT/IB2017/055465, 11 September 2017.
27. Zambon, A.; Michelino, F.; Bourdoux, S.; Devlieghere, F.; Sut, S.; Dall'Acqua, S.; Rajkovic, A.; Spilimbergo, S. Microbial Inactivation Efficiency of Supercritical CO_2 Drying Process. *Dry. Technol.* **2018**, *36*, 2016–2021. [CrossRef]
28. Bourdoux, S.; Rajkovic, A.; De Sutter, S.; Vermeulen, A.; Spilimbergo, S.; Zambon, A.; Hofland, G.; Uyttendaele, M.; Devlieghere, F. Inactivation of Salmonella, Listeria Monocytogenes and Escherichia Coli O157:H7 Inoculated on Coriander by Freeze-Drying and Supercritical CO_2 Drying. *Innov. Food Sci. Emerg. Technol.* **2018**, *47*, 180–186. [CrossRef]
29. Spilimbergo, S.; Komes, D.; Vojvodic, A.; Levaj, B.; Ferrentino, G. High Pressure Carbon Dioxide Pasteurization of Fresh-Cut Carrot. *J. Supercrit. Fluids* **2013**, *79*, 92–100. [CrossRef]
30. Ferrentino, G.; Balzan, S.; Dorigato, A.; Pegoretti, A.; Spilimbergo, S. Effect of Supercritical Carbon Dioxide Pasteurization on Natural Microbiota, Texture, and Microstructure of Fresh-Cut Coconut. *J. Food Sci.* **2012**, *77*, E137–E142. [CrossRef]
31. Ferrentino, G.; Balzan, S.; Spilimbergo, S. Supercritical Carbon Dioxide Processing of Dry Cured Ham Spiked with Listeria Monocytogenes: Inactivation Kinetics, Color, and Sensory Evaluations. *Food Bioprocess Technol.* **2013**, *6*, 1164–1174. [CrossRef]
32. Spilimbergo, S.; Mantoan, D. Kinetic Analysis of Microorganisms Inactivation in Apple Juice by High Pressure Carbon Dioxide. *Int. J. Food Eng.* **2006**, *2*, 1065. [CrossRef]
33. Barberi, G.; González-Alonso, V.; Spilimbergo, S.; Barolo, M.; Zambon, A.; Facco, P. Optimization of the Appearance Quality in CO_2 Processed Ready-to-Eat Carrots through Image Analysis. *Foods* **2021**, *10*, 2999. [CrossRef] [PubMed]
34. Galvanin, F.; De Luca, R.; Ferrentino, G.; Barolo, M.; Spilimbergo, S.; Bezzo, F. Bacterial Inactivation on Solid Food Matrices through Supercritical CO_2: A Correlative Study. *J. Food Eng.* **2014**, *120*, 146–157. [CrossRef]

35. Tamburini, S.; Foladori, P.; Ferrentino, G.; Spilimbergo, S.; Jousson, O. Accurate Flow Cytometric Monitoring of *Escherichia Coli* Subpopulations on Solid Food Treated with High Pressure Carbon Dioxide. *J. Appl. Microbiol.* **2014**, *117*, 440–450. [CrossRef]
36. Ferrentino, G.; Komes, D.; Spilimbergo, S. High-Power Ultrasound Assisted High-Pressure Carbon Dioxide Pasteurization of Fresh-Cut Coconut: A Microbial and Physicochemical Study. *Food Bioprocess Technol.* **2015**, *8*, 2368–2382. [CrossRef]
37. Mangalassary, S.; Dawson, P.L.; Rieck, J.; Han, I.Y. Thickness and Compositional Effects on Surface Heating Rate of Bologna during In-Package Pasteurization. *Poult. Sci.* **2004**, *83*, 1456–1461. [CrossRef]
38. Murphy, R.Y.; Duncan, L.K.; Marcy, J.A.; Berrang, M.E.; Driscoll, K.H. Effect of Packaging-Film Thicknesses on Thermal Inactivation of Salmonella and Listeria Innocua in Fully Cooked Chicken Breast Meat. *J. Food Sci.* **2002**, *67*, 3435–3440. [CrossRef]
39. Valverde, M.T.; Marín-Iniesta, F.; Calvo, L. Inactivation of Saccharomyces Cerevisiae in Conference Pear with High Pressure Carbon Dioxide and Effects on Pear Quality. *J. Food Eng.* **2010**, *98*, 421–428. [CrossRef]
40. Haas, G.J.; Prescott, H.E.; Dudley, E.; Dik, R.; Hintlian, C.; Keane, L. Inactivation of Microorganisms by Carbon Dioxide under Pressure. *J. Food Saf.* **1989**, *9*, 253–265. [CrossRef]
41. Michelino, F.; Zambon, A.; Vizzotto, M.T.; Cozzi, S.; Spilimbergo, S. High Power Ultrasound Combined with Supercritical Carbon Dioxide for the Drying and Microbial Inactivation of Coriander. *J. CO2 Util.* **2018**, *24*, 516–521. [CrossRef]
42. Préstamo, G.; Arroyo, G. High Hydrostatic Pressure Effects on Vegetable Structure. *J. Food Sci.* **1998**, *63*, 878–881. [CrossRef]
43. Denoya, G.I.; Polenta, G.A.; Apóstolo, N.M.; Budde, C.O.; Sancho, A.M.; Vaudagna, S.R. Optimization of High Hydrostatic Pressure Processing for the Preservation of Minimally Processed Peach Pieces. *Innov. Food Sci. Emerg. Technol.* **2016**, *33*, 84–93. [CrossRef]
44. Sun, Y.; Kang, X.; Chen, F.; Liao, X.; Hu, X. Mechanisms of Carrot Texture Alteration Induced by Pure Effect of High Pressure Processing. *Innov. Food Sci. Emerg. Technol.* **2019**, *54*, 260–269. [CrossRef]
45. Barry-ryan, C.; Beirne, D.O. Engineering/Processing MS 5857 Quality and Shelf-Life of Fresh Cut Carrot Slices as Affected by Slicing Method. *J. Food Sci.* **1998**, *63*, 851–856. [CrossRef]
46. Trejo Araya, X.I.; Smale, N.; Zabaras, D.; Winley, E.; Forde, C.; Stewart, C.M.; Mawson, A.J. Sensory Perception and Quality Attributes of High Pressure Processed Carrots in Comparison to Raw, Sous-Vide and Cooked Carrots. *Innov. Food Sci. Emerg. Technol.* **2009**, *10*, 420–433. [CrossRef]
47. Ranjitha, K.; Sudhakar Rao, D.V.; Shivashankara, K.S.; Oberoi, H.S.; Roy, T.K.; Bharathamma, H. Shelf-Life Extension and Quality Retention in Fresh-Cut Carrots Coated with Pectin. *Innov. Food Sci. Emerg. Technol.* **2017**, *42*, 91–100. [CrossRef]
48. Sinigaglia, M.; Corbo, M.R.; Amato, D.D.; Campaniello, D.; Altieri, C. Shelf-Life Modelling of Ready-to-Eat Coconut. *J. Food Sci. Technol.* **2003**, *38*, 547–552. [CrossRef]
49. Iqbal, T.; Rodrigues, F.A.S.; Mahajan, P.V.; Kerry, J.P. Mathematical Modeling of the Influence of Temperature and Gas Composition on the Respiration Rate of Shredded Carrots. *J. Food Eng.* **2009**, *91*, 325–332. [CrossRef]

foods

MDPI

Article

Bactericidal Effect and Associated Properties of Non-Electrolytic Hypochlorite Water on Foodborne Pathogenic Bacteria

Xiangyu Gao, Xueqiang Liu *, Jialin He, Hanbing Huang, Xiaoya Qi and Jianxiong Hao

College of Food Science and Biology, Hebei University of Science and Technology, No.26 Yuxiang Street, Shijiazhuang 050018, China
* Correspondence: caulxq@163.com

Abstract: This study investigated the broad-spectrum bactericidal activity of non-electrolytic hypochlorite water (NEHW) and detected its hydroxyl radical content compared with that of slightly acidic electrolytic water (SAEW). Based on the results of UV scanning and storage stability, higher hypochlorite content and stronger oxidation were found to be responsible for the stronger bactericidal effect of NEHW. NEHW can achieve 99% bacterial disinfection effect by treating with 10 mg/L available chlorine concentration for more than 5 minutes. At the same time, the storage stability of NEHW was higher than that of SAEW. After 20 days of storage under sealed and dark conditions, the pH value only increased by 7.9%, and the effective chlorine concentration remained nearly 80%. The results showed that NEHW had higher germicidal efficacy and storage stability than SAEW.

Keywords: non-electrolytic hypochlorite water; slightly acidic electrolytic water; disinfection; UV scanning; hydroxyl radicals; storage stability

1. Introduction

A part of biological pollution caused by foodborne bacteria pathogens has attracted increasing attention of consumers and scientists, and has become an important issue endangering food safety [1]. Particularly in the process of food storage and transportation, contamination of bacteria pathogens, such as *Listeria monocytogenes* will form a biofilm on the pipeline [2]. Most of these bacteria are highly tolerant to environmental stress factors, and some even form biofilms [3]. They attach to the food surface and enter the human body through ingestion, causing diseases such as meningitis [3], food poisoning, and bacteremia [4].

To reduce the threat of foodborne pathogens, various methods are used in food storage and processing, including high hydrostatic pressure processing, ultrasounds, non-thermal atmospheric plasma, pulsed electric fields, electrolyzed water, and plasma-activated water [5–10]. However, the increased focus of people on food safety, the relatively low sterilization rate, and the impact of treatment on food quality have limited the application of these methods. Slightly acidic electrolytic water (SAEW) is less corrosive than other chemical disinfectants. It can effectively eliminate pathogens from fresh vegetables, fruits, seafood [9], and poultry [11]. However, SAEW development is limited because of its high dependence on production equipment. Non-electrolytic hypochlorite water (NEHW) is an aqueous solution containing hypochlorous acid as the main bactericidal component. NEHW is characterized by a rapid preparation time, broad-spectrum and efficient sterilization, high safety, harmlessness to humans, and green environmental protection [12]. NEHW has an evident sterilization effect and is reduced to an aqueous solution after the complete reaction. It does not produce highly toxic disinfection by-products and can maintain its safety characteristics during sterilization [13]. Its main substance is the same as hypochlorite produced in human body. The cells use mitochondrial binding enzymes to

convert O_2 into H_2O_2, and then, myeloperoxidase from neutrophils catalyzes the reaction between H_2O_2 and Cl^- to produce HClO, which plays a bactericidal role in humans [14]. Yu and others reported that NEHW cleared the acute oral toxicity, micronucleus, and acute inhalation tests according to the technical specifications for disinfection issued by the Ministry of Health of China [15]. The test results showed that pH was 6.5, and the acute oral LD_{50} of 50 ppm hypochlorous acid water in male and female mice at 25 °C was greater than 5000 mg/kg. The micronucleus test of polychromatic erythrocytes in the bone marrow of mice in hypochlorite water group was negative. The acute inhalation toxicity LC_{50} (2 h) of hypochlorite water to male and female mice was greater than 10,000 mg/m^3, which indicates that NEHW is non-toxic [15].

NaClO is dissolved in water to produce sodium hypochlorite solution, which contains HClO. HClO oxidation is the main factor responsible for bacterial inactivation [16]. Studies have shown that the HClO concentration in NaClO solution changes with a change in pH [17]. When the pH of the solution ranged from 2–3, the existing form of effective chlorine was mostly Cl_2, and when the pH was close to alkaline, the existing form was ClO^-. When the pH ranged from 5.5–6.5, the existing form was HClO [18]. The bactericidal activity of Cl_2 and ClO^- is weaker than that of HClO. Therefore, NEHW with a high bactericidal activity can be obtained by adjusting the pH value of the sodium hypochlorite solution. Compared with acid electrolytic water (AEW, pH 2.3–2.8, available chlorine concentration 60–200 mg/L) and SAEW (pH 5.5–6.5, available chlorine concentration 10–30 mg/L), NEHW showed strong corrosivity, high chlorine residue content, great dependence on equipment, and a complex preparation method [19–21]. However, most current studies have only proven that NEHW has a certain bactericidal activity and has a low production cost [22]. NEHW has not been compared with the germicidal efficacy of other existing disinfectants, and relevant studies on the germicidal mechanism, pertinent physical and chemical indicators, and storage stability of NEHW are lacking.

In this experiment, the bactericidal activity of NEHW and SAEW under the same pH available chlorine and bactericidal time treatment was compared. The factors causing the difference of bactericidal activity between NEHW and SAEW were studied by ultraviolet scanning of hypochlorite content of the two biocides under the same pH and available chlorine conditions and detection of hydroxyl radical. Finally, the research on storage stability further shows the advantages of NEHW in the production process.

2. Materials and Methods

2.1. Bacterial Strain

Listeria monocytogenes ATCC19114 was purchased from Beijing Solarbio Biotechnology Co., Ltd. (Beijing, China) *Escherichia coli* O78, used in the experiments, was obtained from Institute of Microbiology, Chinese Academy of Sciences (Beijing, China). The standard strain of *Staphylococcus aureus* ATCC6538 was provided by Guangdong Microbial Strain Collection Center (Guangzhou, China). The *Candida albicans* strain AY93025 was purchased from the China Culture Preservation Center (Beijing, China). *Bacillus subtilis* CS27 was isolated and preserved by the Institute of Soil and Fertilizer, Fujian Academy of Agricultural Sciences (Fuzhou, China), and identified by the Institute of Microbiology, Chinese Academy of Sciences (Beijing, China).

In brief, all operations were performed according to the Technical Standard for Disinfection.

L. monocytogenes was cultured in 200 mL TSB-YE at 37 °C for 24 h with agitation (160 rpm). *E. coli* was cultured in 200 mL nutrient broth at 37 °C for 24 h with agitation (170 rpm). *S. aureus* was cultured in 200 mL Sabouraud glucose liquid medium at 37 °C for 24 h with agitation (155 rpm). *C. albicans* was cultured in 200 mL nutrient broth at 37 °C for 24 h with agitation (160 rpm), and *B. subtilis* was cultured in 200 mL Sabouraud glucose liquid medium at 28 °C for 24 h with agitation (155 rpm). After cultivation, 1 mL of each culture was harvested by centrifugation for 10 min at 8000× *g* (Model TGL-16G, Shanghai ANTING Scientific Instrument Factory, Shanghai, China). The pellets were washed twice with 1 mL normal saline and resuspended in normal saline to obtain the final

cell concentration of approximately 10^9 cfu/mL. The dilution coating plate method was used to estimate the bacterial solution concentration.

2.2. Preparation of Treatment Solutions

SAEW was prepared using a flow type electrolysis apparatus (non-membrane electrolytic cell, model AQUACIDO NDX-250KMS, OSG Company Ltd., Shinshiro, Japan), and NEHW was made from sodium hypochlorite solution by adjusting pH and diluting it with water. After preparation, the two types of water were stored in polypropylene containers, and immediately used for measurement. The pH values of these two water types were measured using a pH meter (Multifunctional laboratory pH meter, model ST2100, OHAUS Instrument Co., Ltd., Shanghai, China), and their available chlorine concentration (ACC) values were measured using the iodometric method. ACC was calculated using the following equation (the numbers 35.45 and 10 are according to the manufacturer):

$$\text{ACC (mg/L)} = (V \times M \times 35.45) \times 10 \quad (1)$$

V is the consumption of sodium thiosulfate (mL),
M is the concentration of sodium thiosulfate (mol/L).

To evaluate the germicidal efficacy of NEHW and SAEW with different ACC values, these two water types having different dilution times were used in this experiment. The tap water was used as a control. The pH and ACC of all the treatment solutions are shown in Table 1.

Table 1. [a,b] Chemical parameters of different solutions.

Solutions	pH	ACC (mg/L)
SAEW1	5.67 ± 0.04	10.63 ± 0.54
SAEW2	5.69 ± 0.10	30.13 ± 0.21
NEHW1	5.66 ± 0.06	10.98 ± 0.35
NEHW2	5.70 ± 0.12	30.84 ± 0.20
Tap water (TW)	7.79 ± 0.04	ND

[a] SAEW was the abbreviation of slightly acidic electrolyzed water and NEHW was the abbreviation of non electrolytic hypochlorite water. ACC was the abbreviation of available chlorine concentration. Tap water as control was the drinking water that came from Hebei University of Science and Technology. [b] Data are expressed by mean ± standard deviation (SD) and values were obtained by three replicated measurements.

2.3. NEHW and SAEW Treatments

According to the method of [23], 9 mL of NEHW and SAEW were transferred to separate test tubes containing 1 mL of 10^9 cfu/mL strain inoculum. After treatment with 10 and 30 effective chlorine concentration for 0.5 min, 1 min, 5 min, and 10 min, respectively, the reaction was stopped by adding 9 mL neutralizer (mixed with 7.14 g/L disodium hydrogen phosphate, 1.36 g/L potassium dihydrogen phosphate, and 1.56 g/L sodium thiosulfate) to 1 mL test suspension to eliminate the residual activities of NEHW and SAEW [24]. The results of sterilization will be described later in this paper.

2.4. Bacterial Enumeration

The spread plate method was used for bacterial enumeration. A total of 0.1 mL bacterial solution was first placed on the corresponding solid culture medium, and then applied evenly with the triangular plating rod [25,26]. *L. monocytogenes* was spread-plated onto TSB-YE solid medium. *E. coli* was spread-plated onto nutrient agar. *S. aureus* was spread-plated onto Sabouraud glucose agar medium. *C. albicans* was spread-plated onto nutrient agar. *B. subtilis* was spread-plated onto Sabouraud glucose agar medium. The plates were incubated at 37 °C for 24–48 h, colonies were counted, and the number of viable bacteria was expressed in lg cfu/mL.

2.5. UV Scanning of NEHW and SAEW

To explore the reasons for the different bactericidal effects of NEHW and SAEW, UV scanning was conducted using a spectrophotometer (Model UV-5200, YUANXI Instrument Co., Ltd., Shanghai, China) in the range of 220–380 nm [27]. A scan within the ultraviolet absorption wavelength of the existing form of the common effective chlorine present in the known disinfectant was used to detect the existing form and the difference in the effective chlorine content of the two disinfectants.

2.6. Hydroxyl Radical Content Detection

Hydroxyl radical content of the biocide was measured through UV spectrophotometry [28]. The detection reaction was designed based on the Fenton reaction. The change in the absorbance value, that is, the hydroxyl radical content, before and after the reaction was detected by dyeing with a dye, and compared. The number of free radicals in the system was determined through spectrophotometry after being dyed with salicylic acid [29], methylene blue [30], and crystal violet [31] and standing for 20 min. The absorbance of salicylic acid was measured at 660 nm, and that of methylene blue and crystal violet was measured at 530 nm. Scanning was performed using a spectrophotometer (Model UV-5200, Shanghai YUANXI Instrument Co., Ltd., Shanghai, China).

2.7. Storage Stability

We referred to previous studies for the methodology to be used for studying storage stability [32,33]. NEHW and SAEW adjusted to pH 5.7 and having an effective chlorine concentration of 36 were used for the storage experiment. The experiment was carried out for 20 days under the conditions of sealed and avoiding light, for which a brown bottle with a sealing cap and a transparent open glass conical bottle were used, respectively. The changes in pH and ACC of the two types of water were measured during the experiment. pH was measured using the pH meter, and the effective chlorine concentration was measured through iodometry. To ensure the comparability of results, each test was conducted in the same laboratory, and the sealed samples were no longer used after being opened. The pH values and effective chlorine concentrations of all samples were measured three times a day, and the average value was considered. Each measurement was completed within 30 min.

2.8. Statistical Analysis

Each treatment was repeated three times. For each treatment, data from independent replicate trials were pooled and the means and standard deviations were calculated. All data were analyzed using Duncan's multiple range test (SPSS16.0 for Windows, SPSS Inc., Chicago, IL, USA). Significant differences between treatments were established at a significance level of $p < 0.05$.

3. Results and Discussion

3.1. Broad Spectrum Bactericidal Activity of NEHW and SAEW

The physical and chemical parameters of NEHW and SAEW used in this study are shown in Table 1. Deionized water was used to dilute NEHW and SAEW into two effective chlorine concentrations, and four sterilization times were used to sterilize five bacteria and compare the sterilization effects of the two biocides (Figure 1).

The populations of *L. monocytogenes*, *E. coli*, *S. aureus*, *C. albicans*, and *B. subtilis* control groups treated with tap water were 9.25, 8.93, 9.05, 9.00, and 8.75 cfu/mL.

At 0.5 and 1 min of treatment, the biocides with two effective chlorine concentrations significantly reduced the number of five bacteria, but did not reach the 99% bactericidal rate. After 5 min of treatment, under 10 ACC, NEHW made *L. monocytogenes*, *E. coli*, *S. aureus*, *C. albicans,* and *B. subtilis* reduced by 1.99, 1.91, 2.21, 2.23, and 2.56 lg cfu/mL, respectively (Figure 1, $p < 0.05$). SAEW reduced *L. monocytogenes*, *E. coli*, *S. aureus*, *C. albicans,* and *B. subtilis* by 1.43, 1.71, 1.97, 2.01, and 2.26 lg cfu/mL, respectively (Figure 1, $p < 0.05$). Under

30 ACC, NEHW made *L. monocytogenes*, *E. coli*, *S. aureus*, *C. albicans*, and *B. subtilis* reduced by 2.09, 1.95, 2.33, 2.36, and 2.76 lg cfu/mL, respectively (Figure 1, $p < 0.05$). SAEW made *L. monocytogenes*, *E. coli*, *S. aureus*, *C. albicans*, and *B. subtilis* reduced by 1.48, 2.03, 2.20, 2.04, and 2.50 lg cfu/mL, respectively (Figure 1, $p < 0.05$). After 10 min of treatment, under 10 ACC, NEHW made *L. monocytogenes*, *E. coli*, *S. aureus*, *C. albicans*, and *B. subtilis* reduced by 2.15, 2.29, 2.35, 2.41, and 2.71 lg cfu/mL, respectively (Figure 1, $p < 0.05$). SAEW reduced *L. monocytogenes*, *E. coli*, *S. aureus*, *C. albicans*, and *B. subtilis* by 1.49, 1.91, 2.10, 2.30, and 2.63 lg cfu/mL, respectively (Figure 1, $p < 0.05$). Under 30 ACC, NEHW made *L. monocytogenes*, *E. coli*, *S. aureus*, *C. albicans*, and *B. subtilis* reduced by 2.24, 2.43, 2.56, 2.59, and 2.98 lg cfu/mL, respectively (Figure 1, $p < 0.05$). SAEW reduced *L. monocytogenes*, *E. coli*, *S. aureus*, *C. albicans*, and *B. subtilis* by 1.54, 2.18, 2.32, 2.36, and 2.76 lg cfu/mL, respectively (Figure 1, $p < 0.05$).

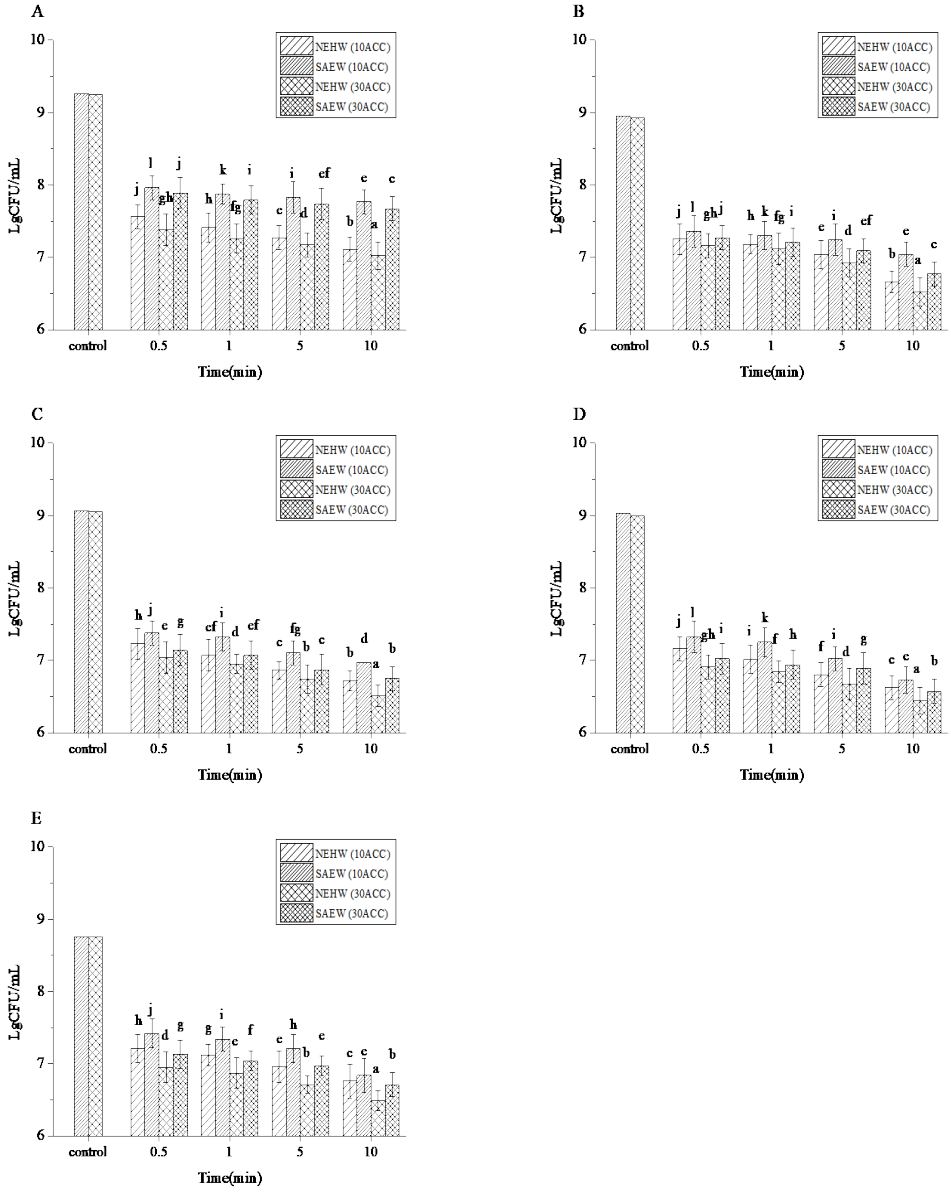

Figure 1. The number of remaining colonies of five bacteria after treatment with different concentrations of biocide and sterilization time, expressed by logarithm. (**A**) *Listeria monocytogenes*; (**B**) *Escherichia coli*; (**C**) *Staphylococcus aureus*; (**D**) *Candida albicans*; (**E**) *Bacillus subtilis*. All treatments and determinations were performed in triplicate. The different letters indicate significant differences ($p < 0.05$). Values are the means of three replicated measurements ± standard deviation (SD).

For *L. monocytogenes*, NEHW could achieve a 99.28% bactericidal rate after 10 min of treatment at 10 ACC, while the bactericidal rate of SAEW reached 97.37% after 10 min of treatment under 30 ACC. For *E. coli*, NEHW could achieve a 99.46% bactericidal rate after 10 min of treatment at 10 ACC, while the bactericidal rate of SAEW reached 99.31% after 10 min of treatment under 30 ACC. For *S. aureus*, NEHW could achieve a 99.36% bactericidal rate after 5 min of treatment at 10 ACC, while the bactericidal rate of SAEW reached 99.34% after 10 min of treatment under 30 ACC. For *C. albicans*, NEHW could achieve a 99.37% bactericidal rate after 5 min of treatment at 10 ACC, while the bactericidal rate of SAEW reached 99.46% after 10 min of treatment under 10 ACC. For *B. subtilis*, NEHW could achieve a 99.10% bactericidal rate after 5 mins of treatment at 30 ACC, while the bactericidal rate of SAEW reached 99.07% after 10 min of treatment under 30 ACC.

Under the conditions, both disinfectants could reduce the strain concentration by at least 1.5 lg cfu/mL. NEHW achieved the 99% killing rate after 15 min of sterilization at 10 ACC, while SAEW achieved the same effect after 5 min of sterilization at 30 ACC or 10 min of sterilization at 10 ACC. For the same strain, the difference in the bactericidal effect of NEHW at 30 and 10 ACC was greater than that of SAEW. The sterilization effect of NEHW was significantly higher than that of SAEW, which was not above the limitation < 3. Studies have focused on the bactericidal activity of SAEW against various bacteria, including *B. cereus*, *Vibrio vulnificus,* and *V. parahaemolyticus*, *Salmonella enteritidis,* and *Aspergillus flavus* [17,32,34,35]. Our results are in agreement with those of the previous report. For the previous similar studies, NEHW and plasma-activated water both showed good germicidal efficacy. At the same time, plasma-activated water has also proven that it can be used to inactivate biofilm-forming pathogens from stainless steel surfaces [10].

Although the pH did not change significantly after different dilution degrees of NEHW and SAEW, significant differences were observed in the germicidal efficacy of the two biocides at the same ACC. Previous studies considered ACC as the main disinfection factor [36,37]. However, in this study, almost the same ACC showed significantly different bactericidal effects of NEHW and SAEW. For example, NEHW at 30 ACC reduced *L. monocytogenes* by 2.24 lg cfu/mL (over the limitation < 3), but SAEW at the same ACC only decreased the bacteria by 1.59 lg cfu/mL. This may indicate that effective chlorine of similar concentrations may also comprise of different forms of effective chlorine, resulting in different bactericidal capacities.

3.2. Scanning Results of Effective Chlorine Substances

Scanning was conducted in the wavelength range of 220–380 nm, including HClO with the maximum absorption peak at 234 nm with molar absorptivity of 100 cm^{-1} M^{-1} and ClO^- with the maximum absorption peak at 292 nm with molar absorptivity 350 cm^{-1} M^{-1}. This allows us to detect and analyze the difference in the existing form and content of effective chlorine of two biocides with the same effective chlorine and pH. Scanning results showed that both NEHW and SAEW had maximum absorption at 234 nm, as shown in Figure 2. The results are consistent with those of the previously reported theoretical methods [27,38]. The two biocides were scanned at 10 and 30 ACC, respectively. The absorption peak at 234 nm for NEHW was significantly higher than that for SAEW ($p < 0.05$). Hypochloric acid concentration can be calculated by Beer's law equation, where A is absorbance, K is molar absorptivity (M^{-1} cm^{-1}), b is thickness of absorption layer (cm), and c (mol/L) is concentration of HClO. According to the formula, the K value and b value of NEHW and SAEW are the same, so the absorption value A can directly reflect the hypochlorite concentration c level of NEHW and SAEW. Therefore, it can be determined that the HClO concentration of NEHW is higher than that of SAEW.

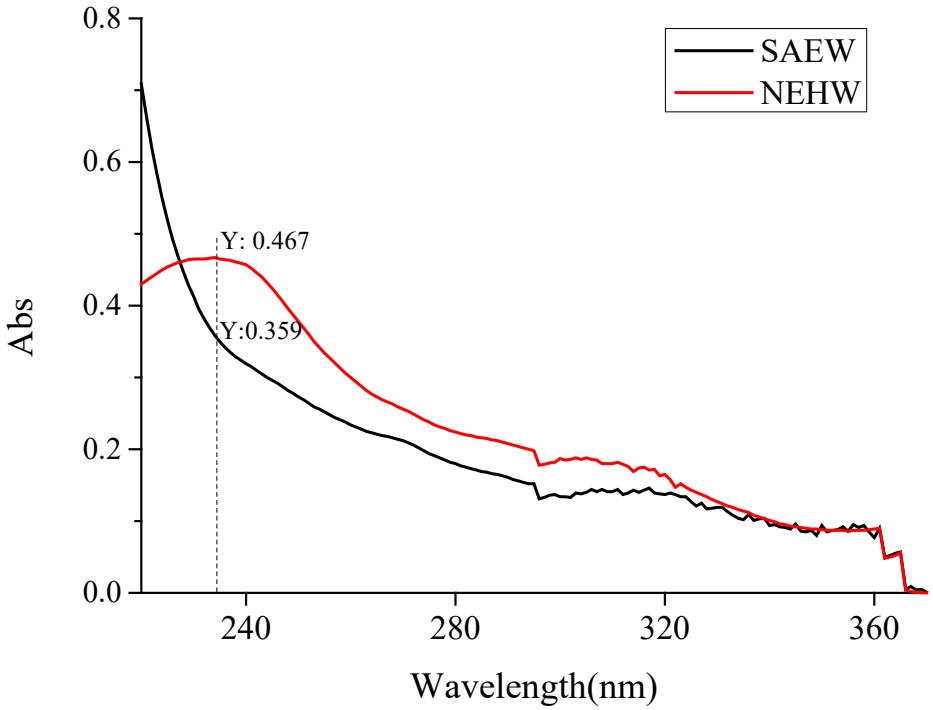

Figure 2. The results of NEHW and SAEW scanning at the wavelength of 220 nm—370 nm on the UV-Vis spectrophotometer. The physical and chemical parameters of NEHW and SAEW are both pH: 5.7; ACC: 30.

Previous studies have found that pH plays crucial role in determining the form of available chlorine in electrolyzed water biocides, including hypochlorite (HClO), hypochlorite ion (ClO^-), and chlorine (Cl_2). When the pH value ranged from 5.5–6.5, the main form of effective chlorine in the biocide was HClO. At the same concentration, the sterilization effect of hypochlorous acid on bacteria was dozens of times of that of the hypochlorite ion (ClO^-) [39,40]. Under alkaline conditions, the main existing effective chlorine form in the sodium hypochlorite disinfectant was ClO^-, and that in the acidic electrolytic water with pH of 2.0–2.5, was dissolved chlorine Cl_2. Because of the loss caused by its easy volatilization [33], the bactericidal activity of ClO^- was not as good as that of HClO, which also makes NEHW stronger than SAEW, NaClO, and AEW.

3.3. Hydroxyl Radical Detection of NEHW and SAEW

The ability of NEHW and SAEW to produce hydroxyl radicals was tested through the Fenton reaction [41,42]. The physical and chemical indices of NEHW and SAEW used are presented in Table 1. In this experiment, we evaluated the hydroxyl radical content of different types of NEHW and SAEW. After color development with three reagents, the results were obtained through UV scanning, which detected the loss of salicylic acid, crystal violet, and methylene blue [28,43]. The results are shown in Figure 3. At 10 and 30 ACC, the hydroxyl radical absorption of NEHW was 0.329 and 0.377, respectively, higher than that of SAEW at 0.304 and 0.342, respectively. During the detection of salicylic acid, the hydroxyl radical absorption of NEHW at 10 and 30 ACC was 0.148 and 0.195, which is higher than that of SAEW at 0.132 and 0.157, respectively. Under the detection of methylene blue, the hydroxyl radical absorption of NEHW at 10 ACC and 30 ACC reached 0.317 and 0.353, higher than that of SAEW at 0.312 and 0.342, respectively. At the same effective chlorine concentration and pH, the hydroxyl radical content of NEHW was always significantly higher than that of SAEW.

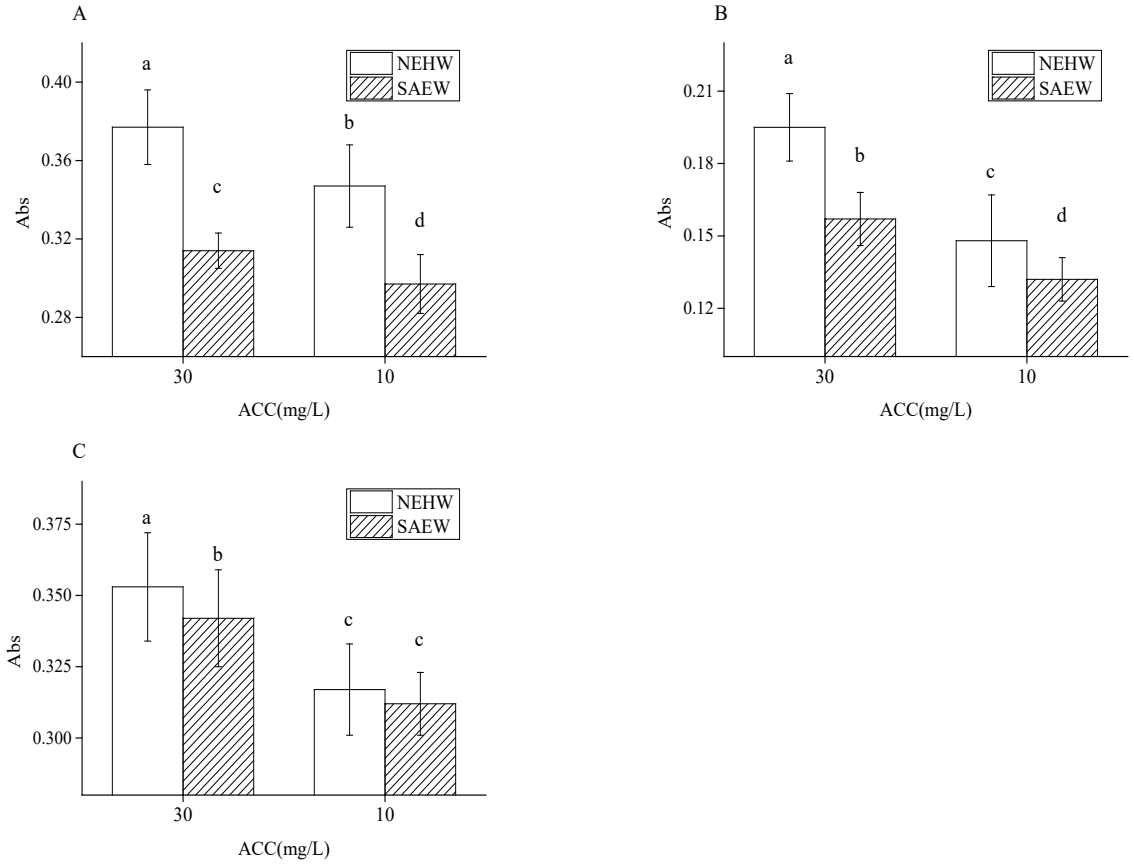

Figure 3. The detection of hydroxyl radical content by NEHW and SAEW under 30 and 10 ACC. (**A**) is the crystal violet detection method, (**B**) is the salicylic acid detection method, (**C**) is the methylene blue detection method. The different letters indicate significant differences ($p < 0.05$).

Hydroxyl free radicals have a strong oxidation ability [44]. They can react with proteins, lipids, and nucleic acids. Moreover, hydroxyl free radicals can locate mitochondria and cause mitochondrial dysfunction [45]. They are more detrimental to bacteria, and lead to cell destruction and death [39,40]. Compared to AEW, SAEW was recognized as a highly effective biocide in the food industry because of its lower ACC concentration and lower chlorine residue (Cl_2) after sterilization [46]. NEHW exhibited a higher bactericidal effect than SAEW at the same physical and chemical indicies. Because of its higher content of HClO and hydroxyl radicals at the same ACC compared with other chlorinated compounds, NEHW could easily penetrate the cell wall, irreversibly oxidize key cell components, and quickly eliminate pathogens [47]. According to the previous UV wavelength scanning experiment, at the same effective chlorine, NEHW exhibited a higher bactericidal effect than SAEW because it had a higher content of HClO and hydroxyl radicals. Simultaneously, UV scanning also revealed that the effective chlorine concentration was not the only key factor affecting the disinfection effect. At the same effective chlorine concentration, the contents of HClO and hydroxyl radicals in NEHW were significantly higher than those in SAEW. Thus, NEHW could achieve a higher disinfection effect at a lower effective chlorine concentration and shorter sterilization time.

3.4. Storage Stability Results of NEHW and SAEW

The pH of NEHW on configuration day was 5.7, and the effective chlorine concentration was 35.5. The pH of SAEW on configuration day was 5.7, and the effective chlorine concentration was 36. The changes in pH and effective chlorine concentration of the two types of water stored under different storage conditions for 20 days are presented in Figure 4. Over different storage times, the pH of the two biocides increased and the

effective chlorine concentration decreased with time. Different storage conditions have a significant impact on the change trends [46].

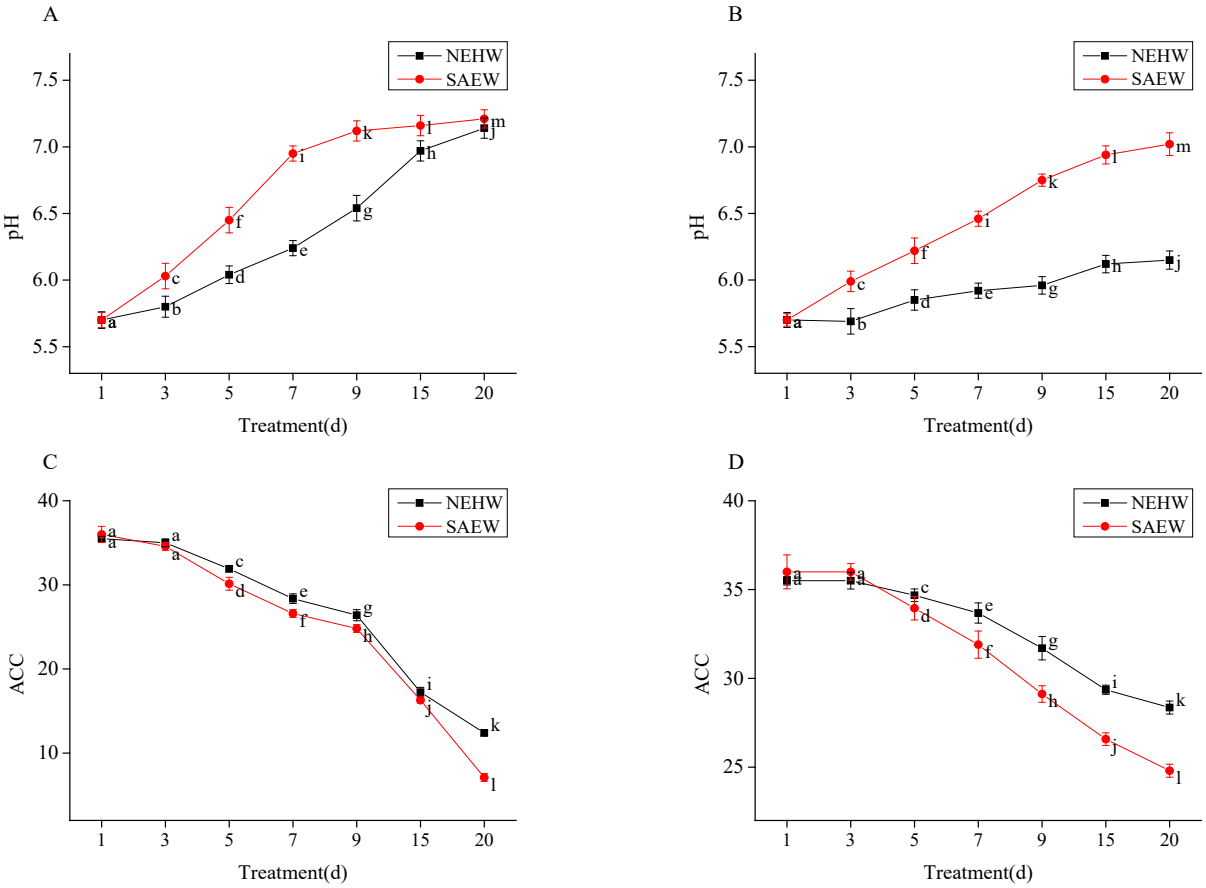

Figure 4. The changes of pH and ACC of NEHW and SAEW during 20 days of storage in open containers without avoiding light and sealed while avoiding light. (**A**,**C**) are the changes of pH and ACC in open containers without avoiding light, respectively; (**B**,**D**) are the changes of pH and ACC under the condition of sealed and avoiding light, respectively. The NEHW initial pH is 5.7 and ACC is 35.5; the SAEW initial pH is 5.7 and ACC is 36. ACC is the abbreviation for available chlorine concentration. All treatments and determinations were performed in triplicate. The different letters indicate significant differences ($p < 0.05$). Values are the means of three replicated measurements ± standard deviation (SD).

Under the condition of open without avoiding light, on the 7th day, the pH value of SAEW increased to 7 (Figure 4, $p < 0.05$). On the 15th day, the pH of NEHW increased to 7.14 (Figure 4, $p < 0.05$). The form of available chlorine changed from HClO to ClO^-, and the bactericidal activity decreased significantly.

Under the condition of sealed and avoiding light, on the 7th day of treatment, the pH of SAEW increased from 5.7 to 6.46 (12.3% changed), and ACC decreased from 36 to 31.9 (11.3% changed) (Figure 4, $p < 0.05$), while the pH of NEHW increased from 5.7 to 5.92 (3.8% changed), and ACC decreased from 35.5 to 33.68 (5.1% changed) (Figure 4, $p < 0.05$). On the 20th day of treatment, the pH value of SAEW increased from 5.7 to 7.02 (23.1% changed), and ACC decreased from 36 to 24.80 (31.1% changed) (Figure 4, $p < 0.05$), while the pH value of NEHW increased from 5.7 to 6.15 (7.9% changed), and ACC decreased from 35.5 to 28.36 (20.1% changed) (Figure 4, $p < 0.05$).

Unlike AEW, the effective chlorine of NEHW and SAEW was not Cl_2, which was strongly volatile. However, when hypochlorous acid was exposed to light and air, light accelerated the decomposition of hypochlorous acid into hydrochloric acid and oxygen, and exposure to air further volatilized these substances. This led to a rise of in the pH of the

biocide, a decrease in its effective chlorine concentration, and finally the loss of bactericidal activity. At almost the same pH and effective chlorine concentration, NEHW displayed a higher storage stability than SAEW, volatilized more slowly under the open without avoiding light condition, and could maintain approximately stable physical and chemical indices within 20 days under the sealed and avoiding light condition.

4. Conclusions

In this study, NEHW and SAEW were compared for their sterilization effect, effective chlorine content, hydroxyl radical content, and storage stability. The results showed that NEHW has a broad-spectrum bactericidal activity, and under the bactericidal conditions used in this study, NEHW achieved a 99% bactericidal rate after treatment for at least 5 min when the ACC was 10. However, bacteria in the VBNC state were not considered in this experiment. At the same pH, the contents of hypochlorite, HClO, and hydroxyl radicals in the available chlorine were significantly higher in NEHW than in SAEW. Regarding storage stability, NEHW could maintain relatively stable physical and chemical indices after 10 days in open storage and 20 days in closed storage. At present, the main indicators of electrolytic water are pH, available chlorine, and ORP. AEW is volatile and highly corrosive because of its low pH, which leads to the existence of chlorine as effective chlorine. Under the same conditions as SAEW, NEHW exhibited the characteristics of higher hydroxyl radical and HClO contents, and the NEHW is less expensive than the SAEW. For food manufacturers, NEHW does not need electrolysis equipment for preparation, but only needs pH adjustment and water dilution of sodium hypochlorite solution, which saves the cost of production equipment and power.

The stability of NEHW in production, packaging, storage, transportation, and use is affected by various factors. However, the stability research results under the experimental conditions have limited guiding significance for practical application. This experiment only proved that NEHW is more stable than SAEW, and the influence of exposure and light on the stability of these biocides requires to be explored further. At the same time, combined with other research results, our finding related to storage stability proves the advantages of NEHW. Some data show that the stability of biocides is also affected by the conditions of loading, temperature, and vibration. Hypochlorous acid decomposes at room temperature, and the higher the temperature, the faster the decomposition. Excessive vibration of the biocide not sealed in a full bottle will makes the biocide to more closely come in contact with the air, resulting in decomposition. With the extension of observation time, the experimental results may change. To ensure the quality of NEHW, we recommend filling NEHW in containers up to the brim during production and choosing colored containers to minimize vibration during transportation.

Author Contributions: Conceptualization, X.G. and J.H. (Jialin He); methodology, X.G.; software, X.G.; validation, X.G., X.L. and J.H. (Jianxiong Hao); formal analysis, X.G., J.H. (Jialin He), H.H. and X.Q.; investigation, X.G., J.H. (Jialin He) and H.H.; resources, J.H. (Jianxiong Hao) and X.L.; data curation, X.G.; writing—original draft preparation, X.G.; writing—review and editing, X.G., X.L. and J.H. (Jianxiong Hao); visualization, X.G.; supervision, X.G., X.L. and J.H. (Jianxiong Hao); project administration, X.G.; funding acquisition, X.L. and J.H. (Jianxiong Hao). All authors have read and agreed to the published version of the manuscript.

Funding: This work was financially supported by the Funded by Science and Technology Project of Hebei Education Department (No. QN2022162), National Natural Science Foundation of China (No. 31972170) and the Hebei Natural Science Foundation of China (No. C2022208010).

Institutional Review Board Statement: Not applicable.

Informed Consent Statement: Not applicable.

Data Availability Statement: Data is contained within the article.

Conflicts of Interest: The authors declare no conflict to interest.

References

1. Toushik, S.H.; Kim, K.; Ashrafudoulla, M.; Mizan, M.F.R.; Roy, P.K.; Nahar, S.; Kim, Y.; Ha, S.D. Korean kimchi-derived lactic acid bacteria inhibit foodborne pathogenic biofilm growth on seafood and food processing surface materials. *Food Control* **2021**, *129*, 108276. [CrossRef]
2. Mansell, P.D. Infectious Diseases: Listeriosis. In *Encyclopedia of Dairy Sciences*, 3rd ed.; McSweeney, P.L.H., McNamara, J.P., Eds.; Oxford Academic Press: Oxford, UK, 2022; pp. 343–351. [CrossRef]
3. Gómez-Camarasa, C. Listeria and Erysipelothrix. In *Encyclopedia of Infection and Immunity*; Rezaei, N., Ed.; Elsevier: Oxford, UK, 2022; pp. 573–579. [CrossRef]
4. Dunham-Snary, K.J.; Surewaard, B.G.J.; Mewburn, J.D.; Bentley, R.E.T.; Martin, A.Y.; Jones, O.; Al-Qazazi, R.; Lima, P.A.D.; Kubes, P.; Archer, S.L. Mitochondria in human neutrophils mediate killing of *Staphylococcus aureus*. *Redox Biol.* **2022**, *49*, 102225. [CrossRef] [PubMed]
5. Lone, S.A.; Raghunathan, S.; Davoodbasha, M.; Srinivasan, H.; Lee, S.Y. An investigation on the sterilization of berry fruit using ozone: An option to preservation and long-term storage. *Biocatal. Agric. Biotechnol.* **2019**, *20*, 101212. [CrossRef]
6. Pianpian, Y.; Ramachandran, C.; Hee, J.K.; Vijayalakshmi, S.; Xiuqin, C.; Yeong, J.H.; Hwan, O.D. Stability and Antibiofilm Efficiency of Slightly Acidic Electrolyzed Water Against Mixed-Species *of Listeria monocytogenes* and *Staphylococcus aureus*. *Front. Microbiol.* **2022**, *13*, 865918.
7. Fujimura, S.; Nagasawa, T.; Kawamura, M.; Sato, T.; Sato, T. The sterilization effect against *Staphylococcus aureus* and *Pseudomonas aeruginosa* on the contact lens using the Ultraviolet C irradiation. *J. Infect. Public Health* **2020**, *13*, 350. [CrossRef]
8. Byun, K.H.; Han, S.H.; Yoon, J.W.; Park, S.H.; Ha, S.D. Efficacy of chlorine-based disinfectants (sodium hypochlorite and chlorine dioxide) on *Salmonella* Enteritidis planktonic cells, biofilms on food contact surfaces and chicken skin. *Food Control* **2021**, *123*, 107838. [CrossRef]
9. Ekonomou, S.I.; Boziaris, I.S. Non-thermal methods for ensuring the microbiological quality and safety of seafood. *Appl. Sci.* **2021**, *11*, 833. [CrossRef]
10. Asimakopoulou, E.; Ekonomou, S.I.; Papakonstantinou, P.; Doran, O.; Stratakos, A.C. Inhibition of corrosion causing *Pseudomonas aeruginosa* using plasma activated water. *J. Appl. Microbiol.* **2021**, *132*, 2781–2794. [CrossRef] [PubMed]
11. Yoon, S.R.; Lee, J.Y.; Yang, J.S.; Ha, J.H. Bactericidal effects of diluted slightly acidic electrolyzed water in quantitative suspension and cabbage tests. *LWT* **2021**, *152*, 112291. [CrossRef]
12. Soli, K.W.; Yoshizumi, A.; Motomatsu, A.; Yamakawa, M.; Yamasaki, M.; Mishima, T.; Miyaji, N.; Honjoh, K.I.; Miyamoto, T. Decontamination of fresh produce by the use of slightly acidic hypochlorous water following pretreatment with sucrose fatty acid ester under microbubble generation. *Food Control* **2010**, *21*, 1240–1244. [CrossRef]
13. Morales, K.; Olesen, M.N.; Poulsen, E.T.; Larsen, U.G.; Enghild, J.J.; Petersen, S.V. The effects of hypochlorous acid and neutrophil proteases on the structure and function of extracellular superoxide dismutase. *Free Radic. Biol. Med.* **2015**, *81*, 38–46. [CrossRef] [PubMed]
14. Folkes, L.K.; Candeias, L.P.; Wardman, P. Kinetics and Mechanisms of Hypochlorous Acid Reactions. *Arch. Biochem. Biophys.* **1995**, *323*, 120–126. [CrossRef] [PubMed]
15. Yu, Y. Study on the Preservation Effects of Fresh-Cut Asparagus Lettuce using Non-electrolytic Slightly Acdic Hypochlorous Acid Water. *Food Process. Secur.* **2020**, *2020*, 1–15. [CrossRef]
16. Ampiaw, R.E.; Yaqub, M.; Lee, W. Electrolyzed water as a disinfectant: A systematic review of factors affecting the production and efficiency of hypochlorous acid. *J. Water Process Eng.* **2021**, *43*, 102228. [CrossRef]
17. Cao, W.; Zhu, Z.W.; Shi, Z.X.; Wang, C.Y.; Li, B.M. Efficiency of slightly acidic electrolyzed water for inactivation of *Salmonella enteritidis* and its contaminated shell eggs. *Int. J. Food Microbiol.* **2009**, *130*, 88–93. [CrossRef]
18. Zhang, C.; Xia, X.; Li, B.; Hung, Y.C. Disinfection efficacy of electrolyzed oxidizing water on brown rice soaking and germination. *Food Control* **2018**, *89*, 38–45. [CrossRef]
19. Al Zain, S. Effect of chemical, microwave irradiation, steam autoclave, ultraviolet light radiation, ozone and electrolyzed oxidizing water disinfection on properties of impression materials: A systematic review and meta-analysis study. *Saudi Dent. J.* **2020**, *32*, 161–170. [CrossRef]
20. Tania, V.B.; Alma, V.D.; Abraham, M.A. Effectiveness of electrolyzed oxidizing water on fungi and mycotoxins in food. *Food Control* **2022**, *131*, 108454. [CrossRef]
21. Lulu, L.; Hua, M.T.; Miao, Z. Contribution of ultrasound and slightly acid electrolytic water combination on inactivating *Rhizopus stolonifer* in sweet potato. *Ultrason. Sonochemistry* **2021**, *73*, 105528. [CrossRef]
22. Eryılmaz, M.; Palabıyık İsmail, M. Hypochlorous Acid—Analytical Methods and Antimicrobial Activity. *Trop. J. Pharm. Res.* **2013**, *12*, 123–126. [CrossRef]
23. Jiang, Y.; Ai, C.; Liao, X.; Liu, D.; Ding, T. Effect of slightly acidic electrolyzed water (SAEW) and ultraviolet light illumination pretreatment on microflora inactivation of coriander. *LWT* **2020**, *132*, 109898. [CrossRef]
24. Rahman, S.M.E.; Ding, T.; Oh, D.H. Effectiveness of low concentration electrolyzed water to inactivate foodborne pathogens under different environmental conditions. *Int. J. Food Microbiol.* **2010**, *139*, 147–153. [CrossRef]
25. Ogunniyi, A.D.; Dandie, C.E.; Brunetti, G.; Drigo, B.; Aleer, S.; Hall, B.; Ferro, S.; Deo, P.; Venter, H.; Myers, B.; et al. Neutral electrolyzed oxidizing water is effective for pre-harvest decontamination of fresh produce. *Food Microbiol.* **2021**, *93*, 103610. [CrossRef]

26. Blodgett, R.J. Mathematical treatment of plates with colony counts outside the acceptable range. *Food Microbiol.* **2008**, *25*, 92–98. [CrossRef]
27. Hao, J.; Qiu, S.; Li, H.; Chen, T.; Liu, H.; Li, L. Roles of hydroxyl radicals in electrolyzed oxidizing water (EOW) for the inactivation of *Escherichia coli*. *Int. J. Food Microbiol.* **2012**, *155*, 99–104. [CrossRef] [PubMed]
28. Lankone, R.S.; Deline, A.R.; Barclay, M.; Fairbrother, D.H. UV–Vis quantification of hydroxyl radical concentration and dose using principal component analysis. *Talanta* **2020**, *218*, 121148. [CrossRef] [PubMed]
29. Jen, J.F.; Leu, M.F.; Yang, T.C. Determination of hydroxyl radicals in an advanced oxidation process with salicylic acid trapping and liquid chromatography. *J. Chromatogr. A* **1998**, *796*, 283–288. [CrossRef]
30. Wang, H.; Hasani, M.; Wu, F.; Prosser, R.; MacHado, G.B.; Warriner, K. Hydroxyl-radical activated water for inactivation of *Escherichia coli* O157:H7, *Salmonella* and *Listeria monocytogenes* on germinating mung beans. *Int. J. Food Microbiol.* **2022**, *367*, 109587. [CrossRef]
31. Xie, J.; Zhang, C.; Waite, T.D. Hydroxyl radicals in anodic oxidation systems: Generation, identification and quantification. *Water Res.* **2022**, *217*, 118425. [CrossRef] [PubMed]
32. Quan, Y.; Choi, K.D.; Chung, D.; Shin, I.S. Evaluation of bactericidal activity of weakly acidic electrolyzed water (WAEW) against *Vibrio vulnificus* and *Vibrio parahaemolyticus*. *Int. J. Food Microbiol.* **2010**, *136*, 255–260. [CrossRef]
33. Cui, X.; Shang, Y.; Shi, Z.; Xin, H.; Cao, W. Physicochemical properties and bactericidal efficiency of neutral and acidic electrolyzed water under different storage conditions. *J. Food Eng.* **2009**, *91*, 582–586. [CrossRef]
34. Zhang, C.; Yang, G.; Shen, P.; Shi, Y.; Yang, Y.; Liu, Y.; Xia, X.; Wang, S. Inactivation mechanism of slightly acidic electrolyzed water on *Bacillus cereus* spores. *Food Microbiol.* **2022**, *103*, 103951. [CrossRef] [PubMed]
35. Xiong, K.; Liu, H.J.; Liu, R.; Li, L.T. Differences in fungicidal efficiency against *Aspergillus flavus* for neutralized and acidic electrolyzed oxidizing waters. *Int. J. Food Microbiol.* **2010**, *137*, 67–75. [CrossRef] [PubMed]
36. Zhao, L.; Li, S.; Yang, H. Recent advances on research of electrolyzed water and its applications. *Curr. Opin. Food Sci.* **2021**, *41*, 180–188. [CrossRef]
37. Yongji, Z.; Jie, Q.; Xianfang, X.; Lingling, Z. Disinfection Kinetics of Free Chlorine, Monochloramines and Chlorine Dioxide on Ammonia-Oxidizing Bacterium Inactivation in Drinking Water. *Water* **2021**, *13*, 3026.
38. Liao, X.; Xuan, X.; Li, J.; Suo, Y.; Liu, D.; Ye, X.; Chen, S.; Ding, T. Bactericidal action of slightly acidic electrolyzed water against *Escherichia coli* and *Staphylococcus aureus* via multiple cell targets. *Food Control* **2017**, *79*, 380–385. [CrossRef]
39. Ding, T.; Xuan, X.T.; Li, J.; Chen, S.G.; Liu, D.H.; Ye, X.Q.; Shi, J.; Xue, S.J. Disinfection efficacy and mechanism of slightly acidic electrolyzed water on *Staphylococcus aureus* in pure culture. *Food Control* **2016**, *60*, 505–510. [CrossRef]
40. Yuan, X.; Li, Y.; Qingnan, M.; Zhang, B.; Shu, D.; Sun, L.; Yang, H.; Xie, X.; Liu, Y.; Zang, Y. A combined approach using slightly acidic electrolyzed water spraying and chitosan and pectin coating on the quality of the egg cuticle, prevention of bacterial invasion, and extension of shelf life of eggs during storage. *Food Chem.* **2022**, *389*, 133129. [CrossRef]
41. Raheb, I.; Manlla, M.S. Kinetic and thermodynamic studies of the degradation of methylene blue by photo-Fenton reaction. *Heliyon* **2021**, *7*, e07427. [CrossRef] [PubMed]
42. Xiang, D.; Lu, S.; Ma, Y.; Zhao, L. Synergistic photocatalysis-fenton reaction of flower-shaped CeO_2/Fe_3O_4 magnetic catalyst for decolorization of high concentration congo red dye. *Colloids Surf. A Physicochem. Eng. Asp.* **2022**, *647*, 129021. [CrossRef]
43. Deng, T.; Hu, S.; Huang, X.A.; Song, J.; Xu, Q.; Wang, Y.; Liu, F. A novel strategy for colorimetric detection of hydroxyl radicals based on a modified Griess test. *Talanta* **2019**, *195*, 152–157. [CrossRef] [PubMed]
44. Schönherr, J.; Buchheim, J.; Scholz, P.; Stelter, M. Oxidation of carbon nanotubes with Ozone and hydroxyl radicals. *Carbon* **2017**, *111*, 631–640. [CrossRef]
45. Sakai, T.; Imai, J.; Ito, T.; Takagaki, H.; Ui, M.; Hatta, S. The novel antioxidant TA293 reveals the role of cytoplasmic hydroxyl radicals in oxidative stress-induced senescence and inflammation. *Biochem. Biophys. Res. Commun.* **2017**, *482*, 1183–1189. [CrossRef] [PubMed]
46. Issa-Zacharia, A.; Kamitani, Y.; Morita, K.; Iwasaki, K. Sanitization potency of slightly acidic electrolyzed water against pure cultures of *Escherichia coli* and *Staphylococcus aureus*, in comparison with that of other food sanitizers. *Food Control* **2010**, *21*, 740–745. [CrossRef]
47. Salazar-Mercado, S.A.; Torres-León, C.A.; Rojas-Suárez, J.P. Cytotoxic evaluation of sodium hypochlorite, using *Pisum sativum* L as effective bioindicator. *Ecotoxicol. Ecotoxicol. Environ. Saf.* **2019**, *173*, 71–76. [CrossRef] [PubMed]

foods

MDPI

Article

Efficacy of 405 nm Light-Emitting Diode Illumination and Citral Used Alone and in Combination for Inactivation of *Vibrio parahaemolyticus* on Shrimp

Yingying Zhang [1], Shuo Wang [1], Du Guo [1], Zhiyuan Liu [1], Jianxue Gao [1], Xiangjun Zhan [1], Yutang Wang [1], Chao Shi [1] and Xiaodong Xia [1,2,*]

[1] College of Food Science and Engineering, Northwest A&F University, Xianyang 712100, China; zhang_yingying@nwafu.edu.cn (Y.Z.); wangshuoddu@126.com (S.W.); duguo2911@163.com (D.G.); lzy022169@126.com (Z.L.); gaojianxue@xjtu.edu.cn (J.G.); zxj666@nwafu.edu.cn (X.Z.); wyt991023@nwsuaf.edu.cn (Y.W.); meilixinong@nwsuaf.edu.cn (C.S.)

[2] School of Food Science and Technology, National Engineering Research Center of Seafood, Dalian Polytechnic University, Dalian 116034, China

* Correspondence: foodscixiaodong@yahoo.com; Tel.: +86-29-8709-2486; Fax: +86-29-8709-1391

Abstract: *Vibrio parahaemolyticus* is a widely distributed pathogen, which is frequently the lead cause of infections related to seafood consumption. The objective of the present study was to investigate the antimicrobial effect of the combination of 405 nm light-emitting diode (LED) and citral on *V. parahaemolyticus*. The antimicrobial effect of LED illumination and citral was evaluated on *V. parahaemolyticus* not only in phosphate-buffered saline (PBS) but also on shrimp. Quality changes of shrimp were determined by sensory evaluation. Changes in bacteria cell membrane morphology, cell membrane permeability, cell lipid oxidation level, and DNA degradation were examined to provide insights into the antimicrobial mechanism. The combination of LED treatments and citral had better antimicrobial effects than either treatment alone. LED combined with 0.1 mg/mL of citral effectively reduced *V. parahaemolyticus* from 6.5 log CFU/mL to below the detection limit in PBS. Combined treatment caused a 3.5 log reduction of the pathogen on shrimp within 20 min and a 6 log reduction within 2 h without significant changes in the sensory score. Furthermore, combined LED and citral treatment affected *V. parahaemolyticus* cellular morphology and outer membrane integrity. The profile of the comet assay and DNA fragmentation analysis revealed that combination treatment did not cause a breakdown of bacterial genomic DNA. In conclusion, LED may act synergistically with citral. They have the potential to be developed as novel microbial intervention strategies.

Keywords: 405 nm LED; *Vibrio parahaemolyticus*; citral; shrimp; cell membrane

1. Introduction

The Gram-negative bacterium *Vibrio parahaemolyticus* is a natural constituent of fresh water, estuarine, and marine environments [1]. It is the primary cause of bacterial food poisoning in coastal areas, mostly related to contaminated seafood consumption [2]. As a widely consumed seafood, shrimps are often contaminated with *V. parahaemolyticus*. Previous studies have isolated and characterized various *V. parahaemolyticus* strains from commonly consumed fresh shrimps in domestic markets in China [3,4]. These studies provided data in support of the high risk of *V. parahaemolyticus* contamination in shrimp. After eating uncooked seafood contaminated by *V. parahaemolyticus*, people could develop acute gastroenteritis within 24 h. In addition, *V. parahaemolyticus* also causes nausea, vomiting, diarrhea, fever, and other symptoms [2].

Various methods have been used for microbial control of shrimp, such as the use of chlorine, modified atmosphere packaging, and irradiation [5]. As a very common strategy to control pathogens in seafood, the effect of chlorine to inactivate *Vibrio* cells on shrimp

has been reported [6]. However, a long contact time and high concentration of chlorine are required to destroy pathogens completely, which may cause health problems in workers, such as severe respiratory tract damage and permanently reduced lung function [7]. Furthermore, the seafoods treated with chlorine often have an undesirable smell with low consumer acceptance. Therefore, an environmentally friendly and safe method should be developed as an alternative to chlorine in the seafood industry.

Recently, many research studies have been focused on the antibacterial effect of artificial light treatments with different wavelengths in agriculture and the food industry. As an alternative energy-saving light source, light-emitting diodes (LED) have attracted attraction in the microbiological safety field [8]. As a conventional approach, UV light (wavelength < 400 nm) emitted by mercury vapor lamps is becoming a worldwide recognized strategy to against potential pathogens such as bacteria, yeasts, viruses, and fungi [9]. However, UV light has shortcomings, such as its decolorization effects on food products, and its potential health risk for the operator [10,11]. Compared to traditional visible light sources, LEDs with wavelengths in the range of 400–420 nm (blue light) have several advantages, such as low cost, high durability, low energy consumption, and a significant antibacterial effect [9]. Recent studies have proven the efficacy of 405 nm LED against various foodborne pathogens, such as *Escherichia coli* O157:H7, *Salmonella* Typhimurium, *L. monocytogenes*, *S. aureus,* and *V. parahaemolyticus* [12–14]. In addition, 405 nm LED has exhibited promising antimicrobial effectiveness in food such as fresh-cut papaya, fresh-cut mango, and ready-to-eat fresh salmon [15–17]. These results have been correlated with the photodynamic inactivation of bacteria (PDI) [18]. Some intracellular molecules known as photosensitizers will absorb oxygen and produce reactive oxygen species (ROS) under 400–420 nm LED irradiation [18,19]. These in turn react with cell membranes' lipids, enzymes, proteins, or DNA, leading to bacterial death [20].

Although the antimicrobial activity of 405 nm LED illumination has been widely studied, the limitations on the application of LED systems have also been found. In food production environments, 405 nm LED takes a long time to completely sterilize food matrices, causing food sensory and nutritional quality loss. Recently, Josewin et al. [21] demonstrated that the synergistic effects of an LED and riboflavin (100 μM) produced a 1.2 log reduction of *L. monocytogenes* on smoked salmon at 4 °C, which was more effective than either treatment alone. Thus, an additional hurdle combined with 405 nm LED illumination should be developed for the improvement of sterilization efficiency with less impact on food quality. Plant-derived compounds have been extensively used as flavoring agents and many exhibit a wide spectrum of antimicrobial activity [22]. The challenge for the practical application of plant origin antimicrobial agents is to exploit optimized low-dose combined processes to minimize toxicological effects and sensory changes [23]. Citral ($C_{10}H_{16}O$) is one of the essential oil compounds originating from herbal plants such as lemon myrtle, lemongrass, orange, lime, and bergamot [24]. It has been recognized as a safe food additive according to the National Food Safety Standard for Uses of Food Additives (GB 2760-2011) [25] and approved by the Food and Drug Administration of the United States (FDA) as a safe ingredient [26]. It has been reported to exert antimicrobial effects on *Campylobacter jejuni*, *E. coli* O157, *L. monocytogenes*, *Bacillus cereus*, *S. aureus,* and *Cronobacter sakazakii* in food matrices [27–30]. Additionally, there is increasing evidence that citral has potential anti-inflammatory and anti-corrosive effects [31,32].

These findings indicate that the use of LEDs or citral is a promising alternative to traditional preservation technologies for reducing the potential risk of food safety. However, little is known about the inactivating effect of the combination of LEDs and citral. The objective of this study was to examine the antimicrobial efficiency of the combination of 405 nm LED irradiation and citral against *V. parahaemolyticus* on fresh shrimp, as a novel application for seafood preservation. Moreover, it's possible antimicrobial mechanism was also elucidated by investigating the cell morphology, cell membrane permeability, as well as DNA degradation.

2. Materials and Methods

2.1. Reagents

Citral (CAS 5392-40-5) was obtained from LGC Labor GmbH (Germany) at a HPLC purity of at least 99%. Citral was dissolved in dimethyl sulfoxide (DMSO; Tianjin Kemiou Chemical Reagent Co., Ltd., Tianjin, China) before being used. The final concentration of DMSO in all treated and control sample solutions was 0.5% (*v*/*v*). Fresh shrimp (*Litopenaeus vannamei*) was purchased from a local retail market in Yangling, China.

2.2. Bacterial Strains and Culture Conditions

V. parahaemolyticus ATCC 17802 was purchased from the American Type Culture Collection (ATCC, Manassas, VA, USA). *V. parahaemolyticus* 240 and *V. parahaemolyticus* 245 were seafood isolates obtained from the Food Safety and Technology Research Centre in The Hong Kong Polytechnic University. Frozen cultures were recovered from the cryovial by surface spreading on plates of Tryptone soya agar (TSA; Beijing Land Bridge Technology Co., Ltd., Beijing, China), supplemented with 3% (*w*/*v*) NaCl, and were incubated for 24 h at 37 °C. To ensure strain purity, a single colony on TSA was cultured into Tryptone Soya Broth (TSB; Beijing Land Bridge Technology Co., Ltd., China) supplemented with 3% NaCl, incubated with shaking at 130 rpm overnight at 37 °C.

2.3. Light-Emitting Diode (LED) Illumination System

A slightly modified version of the illumination system comprising 405 nm LED was confirmed with the method of Zheng et al. [33], with slight modifications. Initially, the top of a heat sink with a cooling fan attached with 405 nm LED was used for minimizing the thermal production of the LED chip and preventing its thermal damage. To avoid the entry of extraneous light, an ABS (acrylonitrile butadiene styrene) housing was utilized to accommodate the system assembly. During LED illumination, the bacterial suspension below the system was subjected to temperature surveillance once every 3 min with a thermocouple thermometer (Everett, WA, USA).

The light dosage was calculated based on Equation (1) [14]. Derivation of the equation was based on the fact that an inverse-square law is obeyed by the intensity of point source-irradiated light or other linear waves:

$$P = 2\pi I_0 h^2 (1 - \frac{1}{\sqrt{1 + \left(\frac{r}{h}\right)^2}}), \quad (1)$$

where P (mW) refers to the quantity of energy falling on the plate every second, I_0 denotes the intensity reading at the plate center from a mobile LED radiometer (Linshang, Shenzhen, China), r (cm) represents the radius of the plate, and h (cm) refers to the LED (point source) height from the plate center. In this study, I_0 = 3.23 mW/cm^2, r = h = 4.5 cm, and P = 18.94 ± 0.05 mW/cm^2

The computational formula for dose, D (energy density) (J/cm^2), is shown below:

$$D = \frac{P}{A}t, \quad (2)$$

where A represents the overall area of the plate (cm^2), and t refers to the time (seconds).

2.4. Temperature Control

The temperature of the PBS bacterial suspension treated with LED increased due to the thermal effect of LED irradiation [14]. To monitor the temperature conditions, activated *V. parahaemolyticus* ATCC 17802, and isolates 240 and 245 were mixed equally. The ten milliliters of mixed bacterial liquid were placed in a sterile dish (d = 90 mm) and measured with a thermoelectric thermometer. The temperature changes of the fresh shrimp surface were also monitored with the thermometer (Hebei Shuangqiao Instrument

Factory, Hengshui, China). The LED assembly was placed in a refrigerator at 4 °C and the temperature of bacterial suspension and fresh shrimp was recorded every 3 min for 120 min. The 405 nm LED elevated the temperature rapidly from the set temperature of , to 9.4 and 8.9 °C of the bacterial suspension and fresh shrimp, respectively. For this reason, non-illuminated control experiments of PBS and shrimp were carried out at 9 °C to eliminate the effect of temperature rise during the irradiation.

2.5. Antimicrobial Activity of LED Combined with Citral against V. parahaemolyticus in PBS

The three working cultures of *V. parahaemolyticus* (ATCC 17802, isolate 240, isolate 245) were centrifuged (Eppendorf, Hamburg, Germany) at 8000× *g* for 5 min following washing twice with PBS (pH 7.2). The resultant pellets were re-suspended in PBS to make up an initial population of approximately 10^6 CFU/mL. Three working cultures were mixed to obtain the final bacterial suspension.

In the LED and the LED plus 0.1 mg/mL citral groups, 10 mL of the bacterial suspension was placed in a glass petri dish (d = 60 mm) and then illuminated for 1 h at 4 °C. Experiments of control and citral groups were performed with the same amount of bacterial suspension but placed in an incubator at 9 °C. An aliquot of 100 µL was withdrawn at 0, 2, 5, 10, 20, 30, and 60 min, and these aliquots were plated onto TSA supplemented with 3% NaCl, followed by incubation at 37 °C for 24 h and counting.

2.6. Antibacterial Effect of LED Combined with Citral against V. parahaemolyticus on Shrimp

One hundred fresh shrimps were collected from a retail market, frozen, and stored in a −20 °C refrigerator. Individual shrimp had an average weight of 15.0 g and a length of 13.0 cm. The difference of shrimp length and weight of all experimental samples did not exceed ±10%. Briefly, shrimp with head and shell were washed with sterile water and immersed in 0.02% (*v*/*v*) NaClO disinfectant for 10 min under aseptic conditions. Then, residual NaClO was removed from shrimp by washing twice with sterile water and the surface of the samples was wiped with a sterilized paper towel. Bacterial suspension of *V. parahaemolyticus* strains ATCC 17802, 240, and 245 was prepared according to the method in Section 2.5. Citral was dissolved in DMSO, then 50 µL of citral solution was added into the bacterial solution of the LED plus citral group and the citral group. The concentration of citral in the bacterial solution of both groups was 0.1 mg/mL. The same dose of DMSO was added to the control group and the LED treatment. The shrimp samples were then immersed into bacterial suspensions and mixed, followed by being placed in sterile petri dishes. The dishes were placed under LED illumination at 4 °C, while the treatments without illumination were set at 9 °C to offset the rise in temperature generated by LED irradiation. Samples were withdrawn at 0, 5, 10, 20, 60, and 120 min post-inoculation. After vortexing for 2 min in PBS solution, aliquots of 100 µL of the dilution series were plated on TSA supplemented with 3% NaCl medium and incubated at 37 °C for 24 h.

2.7. Sensory Evaluation for Fresh Shrimp by Trained Panel

Fresh shrimp samples were prepared as described in Section 2.6. Shrimps of each group were treated with 405 nm LED, 0.1 mg/mL of citral, and 405 nm LED plus 0.1 mg/mL of citral for 120 min, respectively. Then, the sensory quality of shrimp samples was evaluated as described by Jeyasekaran et al. [34] with some modifications, as shown in Table S1. The 10 trained sensory assessors carried out sensory evaluation in terms of the smell, appearance, and texture of the samples, respectively. Then, the 3 parameters were added together as the overall acceptance. The total scores were between 18 points (extremely fresh) and 3 points (totally corrupted).

2.8. Bacterial Morphology

The cell morphology of *V. parahaemolyticus* ATCC 17802 was observed and recorded by FESEM (S-4800; Hitachi, Tokyo, Japan). The bacterial suspension of the four groups (control, LED-illuminated, 0.1 mg/mL citral, and LED-illuminated +0.1 mg/mL citral) was washed

twice with PBS buffer and added with 2.5% (*v*/*v*) glutaraldehyde solution (prepared with PBS buffer), sealed with plastic film, and fixed for 10 h at 4 °C. Suspension was washed with PBS solution and sterile water, then added with 1% osmium acid, followed by fixing for 5 h. The bacteria were gradient eluted with 30%, 50%, 70%, 80%, and 90% ethanol, followed by dissolving in ethanol. The droplets of the final suspension were added on the sterilized round cover slides and transferred into a centrifugal tube for air-drying. The slides were dried in a high vacuum, coated with gold, and observed at 20 kV.

2.9. Determination of Bacterial Outer Membrane Integrity

To elucidate the antimicrobial mechanism of LED illumination and citral against *V. parahaemolyticus*, bacterial outer membrane integrity was performed in accordance with the method of Shi et al. [29], with minor modifications. LIVE/DEAD® BacLight Viability Kit L-7007 (Molecular Probes, Eugene, OR, USA) was used, which encompassed SYTO®9 (green fluorescent dye) and PI (propidium iodide, red fluorescent dye). When bacterial suspension was incubated with these nucleic acid dyes, green fluorescence was produced from the viable bacteria having intact cellular membranes, whereas red fluorescence was produced from the dead bacteria with compromised membranes. Briefly, the overnight culture of *V. parahaemolyticus* ATCC 17802 was collected and resuspended using 0.85% NaCl. For harvesting of live and dead cells, 1 mL of bacteria suspension was added separately into 20 mL of 0.85% NaCl and 20 mL of 70% isopropyl alcohol. After incubating at 25 °C for 1 h, the optical density of both samples was adjusted at 600 nm to 0.5. Bacterial suspensions were formulated by mixing varying percentages of viable cells (0, 10%, 50%, 90%, and 100%) with non-viable cells, and the standard curve was plotted. Cells treated with 405 nm LED and 0.1 mg/mL of citral for 30 min were centrifuged, followed by pipetting 100 µL of samples into 96-well black, opaque microtiter plates. Each well was pipetted with 100 µL aliquots of the 2× working staining solution, and thorough mixing proceeded. The mixture was incubated at 25 °C for 10 min in the dark. Dyes trapped inside the cells were immediately measured using InfiniteTM M200 PRO (TECAN, Mannedorf, Switzerland), and set of fluorochrome filters: excitation wavelength (485 nm), emission wavelength SYTO®9 (542 nm), and PI (610 nm).

2.10. Comet Assay

Bacterial suspensions of *V. parahaemolyticus* ATCC 17802 were prepared according to the method of Kim et al. [12] with a slight modification, using the Comet Assay Kit (Abcam ab238544, Shanghai, China). Here, 75 µL of the aliquot was pipetted on comet slides, then slides were placed at 4 °C for 15 min to fix the agarose. Thereafter, a 1 h immersion of the comet slides was accomplished in pH 10 Lysis Buffer under dark conditions at 4 °C, and then a further 30 min immersion proceeded in alkaline solution for the slides under the same conditions. Electrophoresis was performed for 20 min (12 V, 100 mA) using alkaline electrophoresis buffer. The slides were then subjected sequentially to three washings with distilled water, each for 2 min, a 10 min dehydration using 70% (*v*/*v*) chilled ethanol, drying in air, and subsequent staining with 100 µL of Vista Green DNA Dye staining solution for each well. A Leica DM6 B epifluorescent microscope (Wetzlar, Germany) was utilized in conjunction with Vista Green DNA Dye (WB, 450–480 nm) for acquisition of micrographs at a magnification of 1000×.

2.11. DNA Fragmentation Analysis

V. parahaemolyticus ATCC 17802 DNA fragmentation following the combination of 405 nm LED treatment and 0.1 mg/mL of citral was analyzed according to the method of Kim et al. [12] with a slight modification, using the TaKaRa MiniBEST Bacteria Genomic DNA Extraction Kit (TAKARA BIO INC). The purified DNA was dissolved in 150 µL of Elution Buffer. The 40 mL 1% (*w*/*v*) agarose gel solution was boiled 3 times, cooled for a moment, and added with 4 µL of GelRed nucleic acid dye. Samples with loading buffer

(5:1, v/v) were electrophoresed at 120 V for 30 min. The gel was visualized with GELDOC XR+ (Bio-Rad Laboratories, Co., Ltd., Shanghai, China).

2.12. Statistical Analysis

Significant differences in the mean value were calculated at the 95% confidence interval ($p < 0.05$) using one-way analysis of variance (ANOVA). The Kruskal–Wallis test was used for a comparison of sensory scores. All statistical analysis was performed using the IBM SPSS statistical software (version 19.0; SPSS Inc., Chicago, IL, USA). Data were expressed as mean ± standard deviation (SD) ($n = 6$).

3. Results

3.1. Bacterial Inactivation by Combination of LED Illumination and Citral in PBS

The inactivation effects of 405 nm LED and 0.1 mg/mL of citral against *V. parahaemolyticus* in PBS were investigated and the results are shown in Table 1. The population of non-illuminated cells in the control group remained stable within 1 h, at 3.16×10^6 CFU/mL. The population of citral-treated cells showed a 1.5 log (CFU/mL) reduction after 1 h. The inactivation of *V. parahaemolyticus* treated with the LED illumination and 0.1 mg/mL of citral was most effective compared to the other treatments, producing a severe reduction of 6.5 log after 5 min. The number of viable cells was lower than the detectable limit after 10 and 5 min of LED treatment and LED combined with citral treatment, respectively.

Table 1. Inactivation of *Vibrio parahaemolyticus* by combination of 405 nm LED illumination and citral in PBS.

Time (min)	*Vibrio parahemolyticus* (log CFU/mL)			
	Control	LED	Citral	LED + Citral
0	6.56 ± 0.08 ^{a}	6.56 ± 0.08 ^{a}	6.56 ± 0.08 ^{a}	6.56 ± 0.08 ^{a}
2	6.61 ± 0.10 ^{a}	5.54 ± 0.12 ^{a}	6.71 ± 0.10 ^{a}	2.70 ± 0.01 ^{a}
5	6.49 ± 0.23 ^{a}	4.51 ± 0.19 ^{b}	6.15 ± 0.33 ^{a}	ND ^{c}
10	6.28 ± 0.27 ^{a}	ND ^{c}	6.03 ± 0.25 ^{b}	ND ^{c}
20	6.37 ± 0.12 ^{a}	ND ^{c}	5.58 ± 0.22 ^{b}	ND ^{c}
30	6.52 ± 0.41 ^{a}	ND ^{b}	5.54 ± 0.27 ^{a}	ND ^{b}
60	6.26 ± 0.22 ^{a}	ND ^{c}	5.03 ± 0.30 ^{b}	ND ^{c}

ND: Not detected. Different letters indicate significant ($p < 0.05$) differences.

3.2. Bacterial Inactivation by Combination of LED Illumination and Citral on Shrimp

Shrimp were inoculated with bacterial suspension and observed for 2 h, as shown in Table 2. After 2 h of LED illumination, the bacterial population reduced about 3 log (CFU/mL). Additionally, the presence of 0.1 mg/mL of citral led to a 2 log reduction in the population of *V. parahaemolyticus* on shrimp. The inactivation of *V. parahaemolyticus* through LED illumination treatment in combination with 0.1 mg/mL of citral was most effective, and the number of bacteria decreased to 3.5 log (CFU/mL) within 20 min and fell below the detection limit (10 CFU/mL) after 2 h.

Table 2. Inactivation of *Vibrio parahaemolyticus* by combination of 405 nm LED illumination and citral on shrimp.

Time (min)	*Vibrio parahemolyticus* (log CFU/mL)			
	Control	LED	Citral	LED + Citral
0	6.02 ± 0.18 ^{a}	6.02 ± 0.18 ^{a}	6.02 ± 0.18 ^{a}	6.02 ± 0.18 ^{a}
5	6.02 ± 0.18 ^{a}	4.63 ± 0.25 ^{ab}	5.83 ± 0.23 ^{b}	4.65 ± 0.38 ^{b}
10	5.84 ± 0.26 ^{a}	4.43 ± 0.19 ^{a}	5.76 ± 0.22 ^{b}	4.30 ± 0.15 ^{b}
20	5.81 ± 0.19 ^{a}	3.12 ± 0.09 ^{a}	5.60 ± 0.24 ^{b}	2.45 ± 0.10 ^{b}
60	6.07 ± 0.10 ^{a}	2.75 ± 0.09 ^{a}	5.28 ± 0.07 ^{b}	1.78 ± 0.33 ^{c}
120	5.90 ± 0.18 ^{a}	2.53 ± 0.02 ^{b}	4.35 ± 0.21 ^{c}	ND ^{d}

ND: Not detected. Different letters indicate significant ($p < 0.05$) differences.

3.3. Sensory Evaluation for Shrimp

The effect of 405 nm LED and 0.1 mg/mL of citral on shrimp is shown in Figure 1. The overall sensory scores of shrimp with difference treatments are shown in Table 3. The statistical analysis of the overall acceptance showed no significant difference ($p > 0.05$) between samples. Although the combination of LED and the citral treatment sample had obtained lower scores for the odor attribute (5.0 ± 0.4), the overall acceptance of all shrimp samples was higher than 15 points with all treatments, indicating that the three treatments did not affect the overall sensory quality of the raw shrimp.

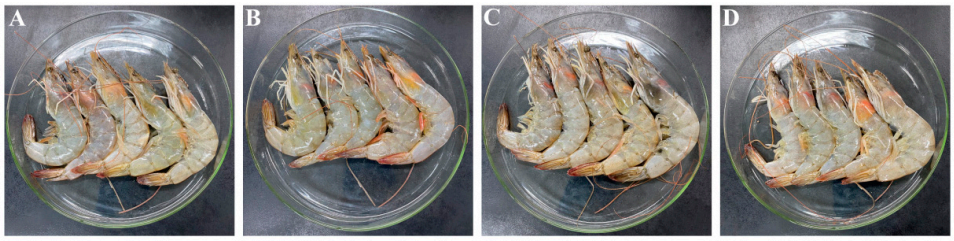

Figure 1. Effect of combination of 405 nm LED and 0.1 mg/mL of citral on sensory evaluation of shrimp. (**A**) Untreated, (**B**) treated with 405 nm LED irradiation for 120 min, (**C**) treated with 0.1 mg/mL of citral for 120 min, and (**D**) LED treatment combined with 0.1 mg/mL of citral for 120 min.

Table 3. Sensory evaluation of fresh shrimp with LED illumination, 0.1 mg/mL of citral, and LED plus 0.1 mg/mL of citral treatment for 120 min.

Treatments	Odor	Appearance	Texture	Overall Acceptance
Control	5.3 ± 0.6^{a}	5.3 ± 0.5^{a}	5.3 ± 0.8^{a}	15.9 ± 1.3^{a}
LED	5.5 ± 0.5^{a}	5.3 ± 0.6^{a}	5.2 ± 0.7^{a}	16.0 ± 1.3^{a}
Citral	5.6 ± 0.5^{a}	5.0 ± 0.8^{a}	5.2 ± 0.6^{a}	15.8 ± 1.4^{a}
LED + Citral	5.0 ± 0.4^{a}	5.3 ± 0.6^{a}	5.6 ± 0.5^{a}	15.9 ± 1.0^{a}

Mean ± standard deviation ($n = 10$). Same letters indicate no significant differences ($p > 0.05$).

3.4. FESEM Observations

As shown in Figure 2, the shape of untreated cells was rod-shaped and smooth, while LED-treated cells were ruptured after 10 min of exposure (Figure 2B). Cells showed shrinkage with the presence of 0.1 mg/mL of citral (Figure 2C). When cells were treated with LED and citral, cells showed significant shrinkage, with some cells breaking into pieces (Figure 2D).

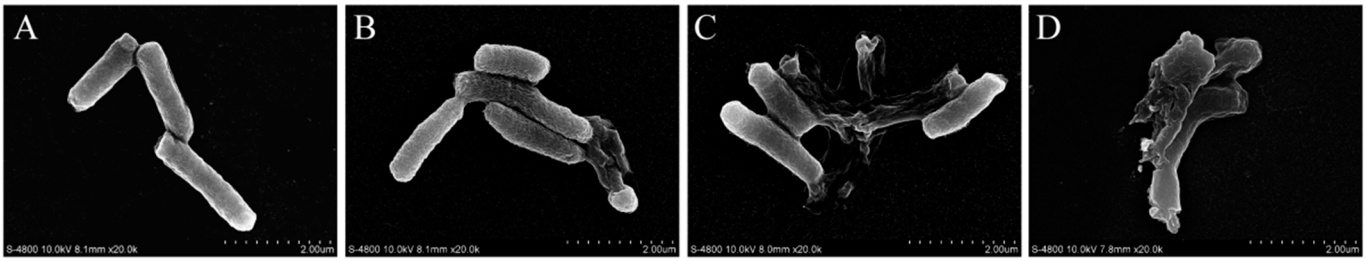

Figure 2. Scanning electron micrographs of *Vibrio parahaemolyticus.* (**A**) Untreated, (**B**) treated with 405 nm LED irradiation for 10 min, (**C**) treated with 0.1 mg/mL of citral for 10 min, and (**D**) LED treatment combined with 0.1 mg/mL of citral for 10 min.

3.5. Effect of 405 nm LED Illumination and Citral on Outer Membrane Integrity

The bacterial suspensions were prepared by mixing 0%, 10%, 50%, 90%, and 100% of the volume of live bacteria with the dead bacteria, respectively. The standard curve was set

properly. As shown in Figure 3, LED illumination and 0.1 mg/mL of citral treatment had certain effects on the cell membrane permeability of *V. parahaemolyticus*. The relative intensity of red fluorescence of the citral group was 175 ± 9.6 (A.U), while the relative intensity of red fluorescence of the LED group was 261 ± 7.3 (A.U), and the relative red fluorescence intensity of LED and 0.1 mg/mL of citral was 385 ± 4.3 (A.U). After being treated with LED illumination combined with citral, the proportion of dead bacteria reached 100%.

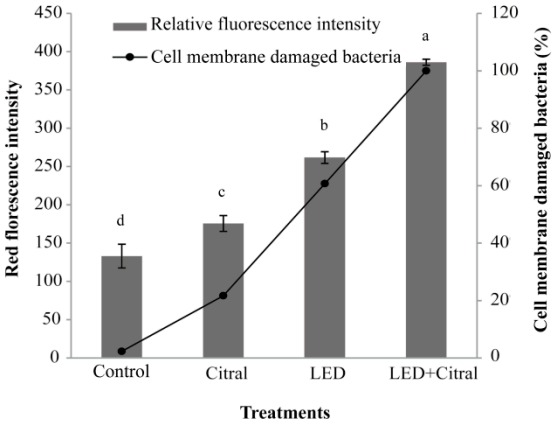

Figure 3. Effect of 405 nm LED illumination and 0.1 mg/mL of citral on outer membrane integrity of *Vibrio parahaemolyticus* for 30 min. Means marked with different lower-case letters are statistically different ($p < 0.05$).

3.6. Comet Assay

The comet assay was adopted for determining whether 405 nm LED irradiation and 0.1 mg/mL of citral addition would lead to DNA degradation. As shown in Figure 4, only clear heads were found in both LED-treated and untreated cells, suggesting that LED irradiation did not cause DNA breakage. Similarly, no tails (comets) were observed in citral and the LED combined with citral treatments. All single-cell electrophoresis photos observed by microscopy presented clear zones of the nucleus in cells without DNA tails.

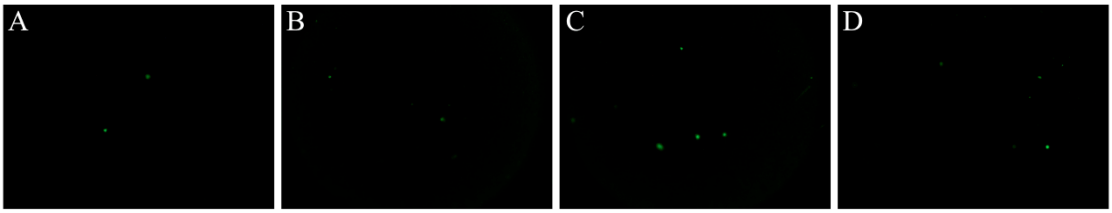

Figure 4. Comet assay of DNA extracted from *V. parahaemolyticus* ATCC 17802 from different treatments. (**A**) Untreated, (**B**) treated with 0.1 mg/mL of citral for 30 min, (**C**) treated with LED irradiation for 30 min, and (**D**) LED treatment combined with 0.1 mg/mL of citral for 30 min.

3.7. DNA Fragmentation Analysis

There was only one positive band present at 2000 bp in all DNA ladder profiles (Figure 5). No DNA fragments were observed, and the DNA migration bands of all samples were the same, indicating that no differences were observed in total genomic DNA among untreated, LED illumination, 0.1 mg/mL citral treatment, and the combination of LED and citral treatment cells. These results indicated that the three sterilization treatments did not induce DNA breakage in *V. parahaemolyticus*.

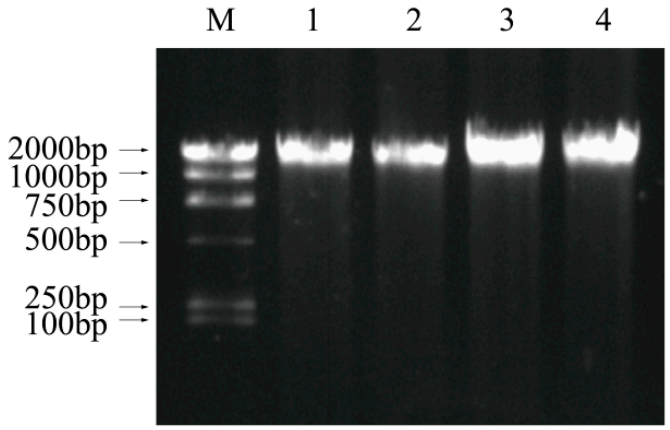

Figure 5. DNA fragmentation profiles of DNA extracted from *Vibrio parahaemolyticus*. Lane: M, λ/HindIII DNA marker; 1, untreated; 2, treated with 405 nm LED irradiation for 30 min; 3, treated with 0.1 mg/mL of citral for 30 min; 4, LED treatment combined with 0.1 mg/mL of citral for 30 min.

4. Discussion

The present study detected the effectiveness of 405 nm LED combined with 0.1 mg/mL of citral in inactivating *V. parahaemolyticus* on the shrimp surface to see if the LED technology has a potential to be applied to seafood preservation. Moreover, the bacterial membrane damage and DNA breakage of *V. parahaemolyticus* were determined to reveal the mechanism of the inactivation by 405 nm LED and citral.

LED with a specific wavelength (405 nm) has been proven to have a microbial inactivation effect [10,35,36]. The optimized LED sterilizing device in this study has a power of 20 W, a wavelength of 405 ± 5 nm, and was sterilized at 4 °C to simulate a practical food storage condition. Citral is a kind of edible plant-derived bacteriostatic agent whose antimicrobial action against some common pathogens has been demonstrated. Somolinos et al. [37] showed that citral at 0.2 μL/mL caused more than a 5 log CFU/mL *E. coli* cells' reduction at pH 4.0 for 24 h. Citral also showed antimicrobial activity against *L. monocytogenes*, *C. sakazakii,* and *V. parahaemolyticus* at relatively low concentrations. The MICs of citral against *L. monocytogenes* strains ranged from 60 to 300 μg/mL [38]. The MIC of citral against *C. sakazakii* strains was 0.6 μL/mL [37]. In Guo's study, the MICs of citral against *V. parahaemolyticus* ATCC 17802 was 0.1 mg/mL [38]. For this reason, we chose 0.1 mg/mL as an effective concentration of citral in this study. In the present study, 405 nm LED illumination combined with 0.1 mg/mL of citral inactivated 6 log CFU/mL of the populations of *V. parahaemolyticus* at 4 °C for 5 min, which could improve the efficiency of sterilization and significantly shorten the sterilization time. Additionally, the LED illumination treatment produced a severe reduction of 6 log in the population of bacteria. Similarly, Maclean et al. [10] reported that a 5 log reduction of *S. aureus* was conducted by 405 nm LED irradiation at a total dose of 36 J/cm^2. Endarko et al. [39] also showed that *L. monocytogenes* was decreased by about 5 log during the 405 nm LED irradiation at a dose of 185 J/cm^2. However, Endarko et al. [39] demonstrated that only slight reductions were observed in the population of *S. Enteritidis* by 1.36 log at a total dose of 739 J/cm^2, indicating that the antibacterial efficacy of 405 nm LED might be strain-dependent.

In the present study, 405 nm LED inactivated about 3 log CFU/mL of the population of *V. parahaemolyticus* for 2 h on shrimp. It was noticed that the population of *V. parahaemolyticus* was reduced to below the detection limit from 10^6 CFU/mL in LED, synergistic with 0.1 mg/mL of citral treatment for 2 h on the shrimp sample. It was more efficient to inactivate the bacteria on the shrimp surface than that of LED or citral alone. The effectiveness of 460 nm LED was also shown by Zheng et al. [33], where *C. sakazakii* was inactivated in powder infant milk with the concentration decreased from 8 to 1 log CFU/g. However, 460 nm LED illumination only led to significant bacterial inactivation in PBS, and did not decrease *L. monocytogenes* populations surviving on salmon [18]. The differences of

temperature, acidity, and polysaccharides' content in food matrices are probably the factors affecting the sterilization efficiency of LED and plant-derived natural components [16]. For sensory evaluation, LED illumination combined with 0.1 mg/mL of citral treatment did not affect the appearance, texture, odor, and acceptance of the shrimp sample. In terms of food quality parameters, whether LED combined with citral can be directly applied in other foods needs to be further studied.

As a selective permeation barrier around bacteria, the cell outer membrane protects bacteria from harmful substances, but allows nutrients to enter to maintain growth [40]. The results of SEM showed that *V. parahaemolyticus* cells shrink and rupture severely after 10 min treatment by LED illumination and 0.1 mg/mL of citral (Figure 2). In the LIVE/DEAD® BacLight™ assay, LED combined with 0.1 mg/mL of citral treatment made the cell grinding rupture ratio 100%, eventually (Figure 3). In the present study, some cells treated with citral alone showed obvious shrinkage without cell disintegration, suggesting that citral may bind to the cell surface [41]. Consistent with a previous investigation, Shi et al. showed that citral changes the bacteria cell morphology, and affects the bacteria cell membrane by decreased intracellular ATP concentration and reduced intracellular pH and cell membrane hyperpolarization. Compared with citral treatment, LED illumination caused more severe outer membrane damage in *V. parahaemolyticus*. Maclean et al. [10] found that the molecular conformation of partial proteins and lipids in the outer cellular membranes was altered by 405 nm light, which could gradually disrupt such membranes, progressively. The membrane lipids, being one of the chief ROS targets in the oxidative stress context, can be used to explain the LED illumination-elicited disruption of cellular membranes [42]. In our postulation, the ROS generated by LED-illuminated bacteria probably interact with the unsaturated fatty acids in the bacterial membranes directly to alter the membrane components, which facilitates better penetration of the outer cellular membranes by citral, ultimately to attain a synergistic bactericidal effect.

Genomic DNA is a critical ROS target generated upon oxidative stress, such as ultraviolet light irradiation and ionizing radiation. Through generation of oxidized derivatives (e.g., 8-hydroxy-deoxyguanosine) and damage of guanine bases, the ROS may result in the DNA breakage [43]. The comet assay and DNA ladder analysis were performed to investigate whether ROS generated by 405 nm LED irradiation would lead to DNA degradation, as well as determine the effect of 0.1 mg/mL of citral on DNA breakage. In this work, no DNA tailing was observed in the comet assay, and the overall assessment of thge genomic DNA ladder revealed no difference among untreated, LED-illuminated, and 0.1 mg/mL of citral treatment cells, implying that the 405 nm LED or 0.1 mg/mL of citral probably do not lead to rupture of bacterial DNA. Similarly, Nitzan and Ashkenazi [43] also found no breakage of DNA in *E. coli* after visible light irradiation with different wavelengths (400–450, 480–550, and 600–700 nm), while cytoplasmic membrane damage was observed. Kim et al. [12,20] also reported that the illumination with 405 ± 5 nm LED did not lead to DNA breakage in *B. cereus*, *E. coli* O157:H7, *L. monocytogenes*, *S. aureus*, *S. Typhimurium*, and *S. sonnei*. Most likely, the low concentration of ROS generated by *V. parahaemolyticus* treated with LED irradiation was not sufficient to induce breakage of bacterial DNA. It might only oxidize other cellular components, such as proteins and lipids. Furthermore, the effects of LED illumination and citral on plasmid DNA in *V. parahaemolyticus* need to be confirmed in the future.

5. Conclusions

In conclusion, the present study evidenced the antibacterial effect of 405 nm LED combined with citral on *V. parahaemolyticus* under refrigerated conditions. The results reveal that a 405 nm LED illumination combined with 0.1 mg/mL of citral could effectively reduce the number of *V. parahaemolyticus* in both PBS and fresh shrimp than either treatment individually. Besides, the findings indicate that 405 nm LED and 0.1 mg/mL of citral treatment had no significant effect on the sensory quality of the food sample, destroyed the cell outer membrane morphology of *V. parahaemolyticus*, and damaged the outer membrane

integrity. In addition, neither LED nor citral induced genomic DNA fragmentation in *V. parahaemolyticus*. Thus, 405 nm LED in combination with 0.1 mg/mL of citral might be a promising technology in eliminating *V. parahaemolyticus* in stored shrimp. The present study suggests the potential for using 405 nm LED combined with citral as a non-thermal and green technology for the control of pathogenic bacteria in the food matrix. In the future, studies are expected to better simulate a practical scenario with LED illumination and citral treatment in different food matrices.

Supplementary Materials: The following are available online at https://www.mdpi.com/article/10.3390/foods11142008/s1, Figure S1: Light-emitting diode (LED) illumination system. Table S1: The grading standard for fresh shrimp sensory evaluation.

Author Contributions: Conceptualization, X.X. and Y.Z.; methodology, S.W.; software, D.G.; validation, Z.L. and J.G.; formal analysis, X.Z.; investigation, S.W.; resources, Y.W., C.S. and X.X.; data curation, S.W.; writing—original draft preparation, Y.Z.; writing—review and editing, Y.Z.; supervision, X.X.; project administration, X.X.; funding acquisition, C.S. and X.X. All authors have read and agreed to the published version of the manuscript.

Funding: This work was supported by the National Natural Science Foundation of China (31801659), the class General Financial Grant from the Shaanxi Postdoctoral Science Foundation (2018BSHEDZZ150), the Key Research and Development Program of Shaanxi Province, China (2021NY-125), and the Science and Technology Program of Shaanxi Province, China (2022JM-111).

Institutional Review Board Statement: Not applicable.

Informed Consent Statement: Not applicable.

Data Availability Statement: The data presented in this study are available upon request from the corresponding author.

Conflicts of Interest: The authors declare no conflict of interest.

References

1. Baker-Austin, C.; Trinanes, J.; Gonzalez-Escalona, N.; Martinez-Urtaza, J. Non-Cholera Vibrios: The Microbial Barometer of Climate Change. *Trends Microbiol.* **2017**, *25*, 76–84. [CrossRef]
2. Baker-Austin, C.; Oliver, J.; Alam, M.; Ali, A.; Waldor, M.; Qadri, F.; Martinez-Urtaza, J. *Vibrio* spp. infections. *Nat. Rev. Dis. Primers* **2018**, *4*, 8. [CrossRef]
3. Kang, C.-H.; Shin, Y.; Yu, H.; Kim, S.; So, J.-S. Antibiotic and heavy-metal resistance of *Vibrio parahaemolyticus* isolated from oysters in Korea. *Mar. Pollut. Bull.* **2018**, *135*, 69–74. [CrossRef] [PubMed]
4. Yang, Y.; Xie, J.; Li, H.; Tan, S.; Chen, Y.; Yu, H. Prevalence, Antibiotic Susceptibility and Diversity of *Vibrio parahaemolyticus* Isolates in Seafood from South China. *Front. Microbiol.* **2017**, *8*, 2566. [CrossRef] [PubMed]
5. Wan Norhana, M.N.; Poole, S.E.; Deeth, H.C.; Dykes, G.A. Prevalence, persistence and control of *Salmonella* and *Listeria* in shrimp and shrimp products: A review. *Food Control* **2010**, *21*, 343–361. [CrossRef]
6. Chaiyakosa, S.; Charernjiratragul, W.; Umsakul, K.; Vuddhakul, V. Comparing the efficiency of chitosan with chlorine for reducing *Vibrio parahaemolyticus* in shrimp. *Food Control* **2007**, *18*, 1031–1035. [CrossRef]
7. Henneberger, P.K.; Olin, A.-C.; Andersson, E.; Hagberg, S.; Torén, K. The Incidence of Respiratory Symptoms and Diseases Among Pulp Mill Workers with Peak Exposures to Ozone and Other Irritant Gases. *Chest* **2005**, *128*, 3028–3037. [CrossRef]
8. Kumar, A.; Ghate, V.; Kim, M.J.; Zhou, W.; Khoo, G.H.; Yuk, H.G. Inactivation and changes in metabolic profile of selected foodborne bacteria by 460 nm LED illumination. *Food Microbiol.* **2017**, *63*, 12–21. [CrossRef]
9. Prasad, A.; Du, L.; Zubair, M.; Subedi, S.; Ullah, A.; Roopesh, M.S. Applications of Light-Emitting Diodes (LEDs) in Food Processing and Water Treatment. *Food Eng. Rev.* **2020**, *12*, 268–289. [CrossRef]
10. Maclean, M.; MacGregor, S.J.; Anderson, J.; Woolsey, G. Inactivation of Bacterial Pathogens following Exposure to Light from a 405-Nanometer Light-Emitting Diode Array. *Appl. Environ. Microbiol.* **2009**, *75*, 1932–1937. [CrossRef]
11. Murdoch, L.E.; Maclean, M.; MacGregor, S.J.; Anderson, J.G. Inactivation of *Campylobacter jejuni* by exposure to high-intensity 405-nm visible light. *Foodborne Pathog. Dis.* **2010**, *7*, 1211–1216. [CrossRef] [PubMed]
12. Kim, M.-J.; Mikš-Krajnik, M.; Kumar, A.; Yuk, H.-G. Inactivation by 405 ± 5 nm light emitting diode on *Escherichia coli* O157:H7, *Salmonella Typhimurium*, and *Shigella sonnei* under refrigerated condition might be due to the loss of membrane integrity. *Food Control* **2016**, *59*, 99–107. [CrossRef]
13. Ghate, V.S.; Ng, K.S.; Zhou, W.; Yang, H.; Khoo, G.H.; Yoon, W.-B.; Yuk, H.-G. Antibacterial effect of light emitting diodes of visible wavelengths on selected foodborne pathogens at different illumination temperatures. *Int. J. Food Microbiol.* **2013**, *166*, 399–406. [CrossRef] [PubMed]

14. Kumar, A.; Ghate, V.; Kim, M.J.; Zhou, W.; Khoo, G.H.; Yuk, H.G. Antibacterial efficacy of 405, 460 and 520 nm light emitting diodes on *Lactobacillus plantarum*, *Staphylococcus aureus* and *Vibrio parahaemolyticus*. *J. Appl. Microbiol.* **2016**, *120*, 49–56. [CrossRef] [PubMed]
15. Kim, M.-J.; Bang, W.S.; Yuk, H.-G. 405 ± 5 nm light emitting diode illumination causes photodynamic inactivation of *Salmonella* spp. on fresh-cut papaya without deterioration. *Food Microbiol.* **2017**, *62*, 124–132. [CrossRef]
16. Kim, M.J.; Tang, C.H.; Bang, W.S.; Yuk, H.G. Antibacterial effect of 405 ± 5 nm light emitting diode illumination against *Escherichia coli O157:H7*, *Listeria monocytogenes*, and *Salmonella* on the surface of fresh-cut mango and its influence on fruit quality. *Int. J. Food Microbiol.* **2017**, *244*, 82–89. [CrossRef]
17. Li, X.; Kim, M.-J.; Yuk, H.-G. Influence of 405 nm light-emitting diode illumination on the inactivation of *Listeria monocytogenes* and *Salmonella* spp. on ready-to-eat fresh salmon surface at chilling storage for 8 h and their susceptibility to simulated gastric fluid. *Food Control* **2018**, *88*, 61–68. [CrossRef]
18. Kim, M.J.; Yuk, H.G. Antibacterial Mechanism of 405-Nanometer Light-Emitting Diode against *Salmonella* at Refrigeration Temperature. *Appl. Env. Microbiol.* **2017**, *83*, e02582-16. [CrossRef]
19. Luksienė, Z.; Zukauskas, A. Prospects of photosensitization in control of pathogenic and harmful micro-organisms. *J. Appl. Microbiol.* **2009**, *107*, 1415–1424. [CrossRef]
20. Kim, M.-J.; Mikš-Krajnik, M.; Kumar, A.; Ghate, V.; Yuk, H.-G. Antibacterial effect and mechanism of high-intensity 405 ± 5 nm light emitting diode on *Bacillus cereus*, *Listeria monocytogenes*, and *Staphylococcus aureus* under refrigerated condition. *J. Photochem. Photobiol. B Biol.* **2015**, *153*, 33–39. [CrossRef]
21. Josewin, S.W.; Ghate, V.; Kim, M.-J.; Yuk, H.-G. Antibacterial effect of 460 nm light-emitting diode in combination with riboflavin against *Listeria monocytogenes* on smoked salmon. *Food Control* **2018**, *84*, 354–361. [CrossRef]
22. Tajkarimi, M.M.; Ibrahim, S.A.; Cliver, D.O. Antimicrobial herb and spice compounds in food. *Food Control* **2010**, *21*, 1199–1218. [CrossRef]
23. Tiwari, B.K.; Valdramidis, V.P.; O'Donnell, C.P.; Muthukumarappan, K.; Bourke, P.; Cullen, P.J. Application of natural antimicrobials for food preservation. *J. Agric. Food Chem.* **2009**, *57*, 5987–6000. [CrossRef] [PubMed]
24. Hyldgaard, M.; Mygind, T.; Meyer, R.L. Essential oils in food preservation: Mode of action, synergies, and interactions with food matrix components. *Front. Microbiol.* **2012**, *3*, 12. [CrossRef] [PubMed]
25. National Food Safety Standard for Uses of Food Additives (GB 2760-2011). Available online: www.nhc.gov.cn (accessed on 9 December 2020).
26. Food and Drug Administration (2005). GRAS Notifications. Available online: www.fda.gov (accessed on 5 December 2020).
27. Fisher, K.; Phillips, C.A. The effect of lemon, orange and bergamot essential oils and their components on the survival of *Campylobacter jejuni*, *Escherichia coli O157*, *Listeria monocytogenes*, *Bacillus cereus* and *Staphylococcus aureus* In Vitro and in food systems. *J. Appl. Microbiol.* **2006**, *101*, 1232–1240. [CrossRef]
28. Kawacka, I.; Olejnik-Schmidt, A.; Schmidt, M.; Sip, A. Natural Plant-Derived Chemical Compounds as *Listeria monocytogenes* Inhibitors In Vitro and in Food Model Systems. *Pathogens* **2021**, *10*, 12. [CrossRef]
29. Shi, C.; Song, K.; Zhang, X.; Sun, Y.; Sui, Y.; Chen, Y.; Jia, Z.; Sun, H.; Sun, Z.; Xia, X. Antimicrobial Activity and Possible Mechanism of Action of Citral against *Cronobacter sakazakii*. *PLoS ONE* **2016**, *11*, e0159006. [CrossRef]
30. Somolinos, M.; García, D.; Condón, S.; Mackey, B.; Pagán, R. Inactivation of *Escherichia coli* by citral. *J. Appl. Microbiol.* **2010**, *108*, 1928–1939. [CrossRef]
31. Korenblum, E.; Regina de Vasconcelos Goulart, F.; de Almeida Rodrigues, I.; Abreu, F.; Lins, U.; Alves, P.B.; Blank, A.F.; Valoni, É.; Sebastián, G.V.; Alviano, D.S.; et al. Antimicrobial action and anti-corrosion effect against sulfate reducing bacteria by lemongrass (*Cymbopogon citratus*) essential oil and its major component, the citral. *AMB Express* **2013**, *3*, 44. [CrossRef]
32. Ortiz, M.I.; González-García, M.P.; Ponce-Monter, H.A.; Castañeda-Hernández, G.; Aguilar-Robles, P. Synergistic effect of the interaction between naproxen and citral on inflammation in rats. *Phytomedicine Int. J. Phytother. Phytopharm.* **2010**, *18*, 74–79. [CrossRef]
33. Zheng, Z.; Xie, Y.; Ma, S.; Tu, J.; Li, J.; Liang, S.; Xu, Y.; Shi, C. Effect of 405-nm light-emitting diode on environmental tolerance of *Cronobacter sakazakii* in powdered infant formula. *Food Res. Int.* **2021**, *144*, 110343. [CrossRef] [PubMed]
34. Jeyasekaran, G.; Ganesan, P.; Anandaraj, R.; Jeya Shakila, R.; Sukumar, D. Quantitative and qualitative studies on the bacteriological quality of Indian white shrimp (*Penaeus indicus*) stored in dry ice. *Food Microbiol.* **2006**, *23*, 526–533. [CrossRef] [PubMed]
35. Maclean, M.; MacGregor, S.J.; Anderson, J.; Woolsey, G. High- intensity narrow-spectrum light inactivation and wavelength Sensitivity of *Staphylococcus aureus*. *FEMS Microbiol. Lett.* **2008**, *285*, 227–232. [CrossRef] [PubMed]
36. Murdoch, L.E.; Maclean, M.; Endarko, E.; MacGregor, S.J.; Anderson, J.G. Bactericidal effects of 405 nm light exposure demonstrated by inactivation of *Escherichia*, *Salmonella*, *Shigella*, *Listeria*, and *Mycobacterium* species in liquid suspensions and on exposed surfaces. *Sci. World J.* **2012**, *2012*, 137805. [CrossRef] [PubMed]
37. Yang, Y.; Ma, S.; Guo, K.; Guo, D.; Li, J.; Wang, M.; Wang, Y.; Zhang, C.; Xia, X.; Shi, C. Efficacy of 405-nm LED illumination and citral used alone and in combination for the inactivation of *Cronobacter sakazakii* in reconstituted powdered infant formula. *Food Res. Int.* **2022**, *154*, 111027. [CrossRef]
38. Guo, D.; Sun, H.; Sun, Z.; Xia, X.; Shi, C. Antimicrobial activity of citral against *Vibrio parahaemolyticus*. *Food Sci.* **2019**, *40*, 113–120. [CrossRef]

39. Endarko, E.; Maclean, M.; Timoshkin, I.V.; MacGregor, S.J.; Anderson, J.G. High-Intensity 405 nm Light Inactivation of *Listeria monocytogenes*. *Photochem. Photobiol.* **2012**, *88*, 1280–1286. [CrossRef]
40. Guo, D.; Wang, S.; Li, J.; Bai, F.; Yang, Y.; Xu, Y.; Liang, S.; Xia, X.; Wang, X.; Shi, C. The antimicrobial activity of coenzyme Q(0) against planktonic and biofilm forms of *Cronobacter sakazakii*. *Food Microbiol.* **2020**, *86*, 103337. [CrossRef]
41. Bajpai, V.K.; Sharma, A.; Baek, K.-H. Antibacterial mode of action of *Cudrania tricuspidata* fruit essential oil, affecting membrane permeability and surface characteristics of food-borne pathogens. *Food Control* **2013**, *32*, 582–590. [CrossRef]
42. Cabiscol, E.; Tamarit, J.; Ros, J. Oxidative stress in bacteria and protein damage by reactive oxygen species. *Int. Microbiol. Off. J. Span. Soc. Microbiol.* **2000**, *3*, 3–8.
43. Nitzan, Y.; Ashkenazi, H. Photoinactivation of *Acinetobacter baumannii* and *Escherichia coli* B by a Cationic Hydrophilic Porphyrin at Various Light Wavelengths. *Curr. Microbiol.* **2001**, *42*, 408–414. [CrossRef] [PubMed]

foods

MDPI

Review

Radio Frequency Treatment of Food: A Review on Pasteurization and Disinfestation

Daniela Bermudez-Aguirre * and Brendan A. Niemira

Food Safety and Intervention Technologies, ERRC, ARS, USDA, 600 E Mermaid Lane, Wyndmoor, PA 19038, USA; brendan.niemira@usda.gov

* Correspondence: daniela.bermudez@usda.gov

Abstract: Radio frequency (RF) is a novel technology with several food processing and preservation applications. It is based on the volumetric heating generated from the product's dielectric properties. The dielectric properties of each material are unique and a function of several factors (i.e., temperature, moisture content). This review presents a list of dielectric properties of several foods and describes the use of RF as an innovative technology for the food industry. This paper includes several examples of pasteurization, fungi inactivation, and disinfestation in selected food products. The aim of this review is to present the potential applications of RF in pasteurization and disinfestation and research needs that should be addressed. RF has been successfully applied in the inactivation of pathogens such as *Salmonella* spp., *Listeria monocytogenes*, and *Escherichia coli* in low- and high-moisture food. The disinfestation of crops is possible using RF because of selective heating. This process inactivates the insects first because of the different dielectric properties between the pests and the food. The products' final quality can be considerably better than conventional thermal processes. The processing time is reduced compared to traditional heating, and thermal damage to the food is minimized. The main drawback of the technology is the lack of uniform heating, mainly when the product is surrounded by a packaging material with different dielectric properties from the food.

Keywords: radio frequency; thermal processing; volumetric heating; pasteurization; disinfestation; dielectric properties

1. Introduction

For several decades, conventional thermal processing has been the preferred technology to pasteurize and sterilize food. It is based on applying heat from an external source, such as water, steam, or air. However, the heat can degrade the nutritional quality and affect the product's sensory characteristics. Regarding energy and cost, it is highly desirable to reduce the processing time. From the microbiological point of view, pasteurization and sterilization are needed to provide a safe product. Both thermal technologies ensure the microbial quality of the product, but both processes adversely affect the food's bioactive compounds and sensory attributes.

On the other hand, foodborne outbreaks become more common every year. Primary pathogens such as *Salmonella* spp., *Escherichia coli* O157:H7, and *Listeria monocytogenes* are frequently associated with these outbreaks. The Centers for Disease Control and Prevention [1] reports a list of outbreaks involving a diverse number of food products yearly. Some microorganisms, such as *Salmonella* spp., have been resistant to different food environments, such as refrigeration temperature, low moisture content, and low- and high-acid foods. It is possible to find this microorganism in foods, such as flour, baby formula, produce, peanut butter, spices, juices, eggs and poultry products, and fish, and the list is endless. Many pathogens have built resistance to conventional technologies, and they have become adaptable to stress factors such as extreme pH, temperature, and water activity conditions, to mention a few [2,3]. Then, any food could be a good vehicle for pathogens if safety precautions are not taken during food processing.

Emerging technologies surged as an option to improve food quality but also to ensure the microbial safety of the product. Most of the novel technologies offer faster microbial inactivation preserving the sensory and nutritional attributes of the food. In the area of emerging thermal processing technologies, radio frequency (RF), microwave, and ohmic heating are just a few examples. Radio frequency (RF) is energy that belongs to the electromagnetic spectrum and, as a novel thermal technology, uses the intrinsic properties of food for heating. Unlike conventional thermal processing, RF generates heat inside the product, and because of that, the volumetric heating is quick, and the required time to inactivate microorganisms is considerably less. This short processing time allows for maintaining the nutritional and sensory properties of the product almost without change. It also provides a more efficient technology from the energy and cost points of view. RF has also been tested for other applications in food processing, such as disinfestation of products, processing aid during drying, thawing and baking, cooking, tempering, and roasting [4,5]. This manuscript reviews this technology as an option for food pasteurization and disinfestation, highlighting the advantages of RF but also those research gaps that need to be researched in the next coming years.

2. Basic Principles

RF is a novel thermal technology based on the volumetric heating of the product. This technology uses the dielectric and thermal properties of the food to generate heat from inside the product. The range of frequencies in the electromagnetic spectrum for radio frequency extends from 1 to 300 MHz. However, there are specific frequencies for Industrial, Scientific, and Medical (ISM) uses. The Federal Communications Commission (FCC) allowed for the use of radio frequencies for heating at 13.56 MHz, 27.12 MHz, and 40.68 MHz [4,5]. These restrictions in using specific frequencies avoid interference with other radio frequency areas, such as cellphone telecommunications.

When a material is in contact with an alternating electric field, the thermal and electrical properties of the product will react to this interaction. The ions in the material will attempt to migrate to the opposite pole of the electric field; in other words, positive ions will move close to the negative pole of the electromagnetic field and vice versa [4,5]. This is called ionic migration or conduction (Figure 1a). Furthermore, the rotation of dipole molecules, such as water, aligning to the electromagnetic field will generate heat because of friction effects. In an oscillating magnetic field, these movements are reversed thousands of times every second. The heating effect of radio frequency is the consequence of the collision of ions inside the food and the friction between dipole molecules (Figure 1b, c). These physical phenomena are in some way similar to microwave heating and are illustrated in Figure 1.

2.1. Dielectric Properties

The dielectric properties of food are critical during volumetric heating because they will determine how uniformly and how quickly a product will heat when exposed to an oscillating electric field [6]. In other words, the dielectric properties of food quantify how the energy from the radio frequency wave is reflected, stored, or utilized [7].

The dielectric properties are related to the relative permittivity (ε), which determines the ability of a material to interact with an electromagnetic field, as shown in Equation (1) as follows:

$$\varepsilon = \varepsilon' - j\varepsilon'' \quad (1)$$

where ε' is the material's dielectric constant, and ε'' is the dielectric loss factor.

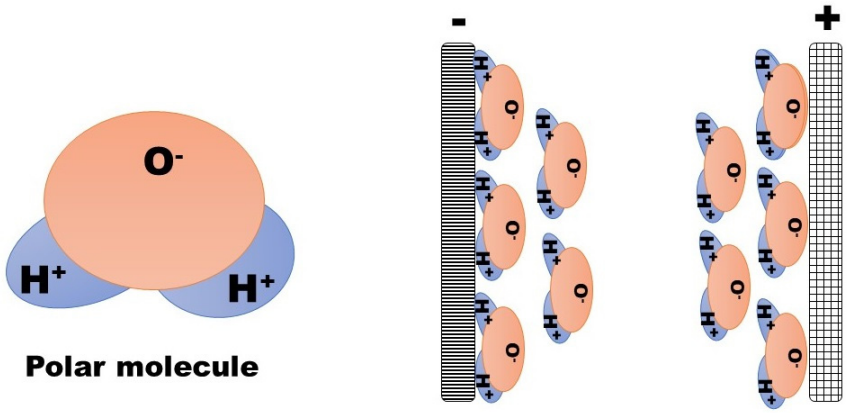

(**a**)

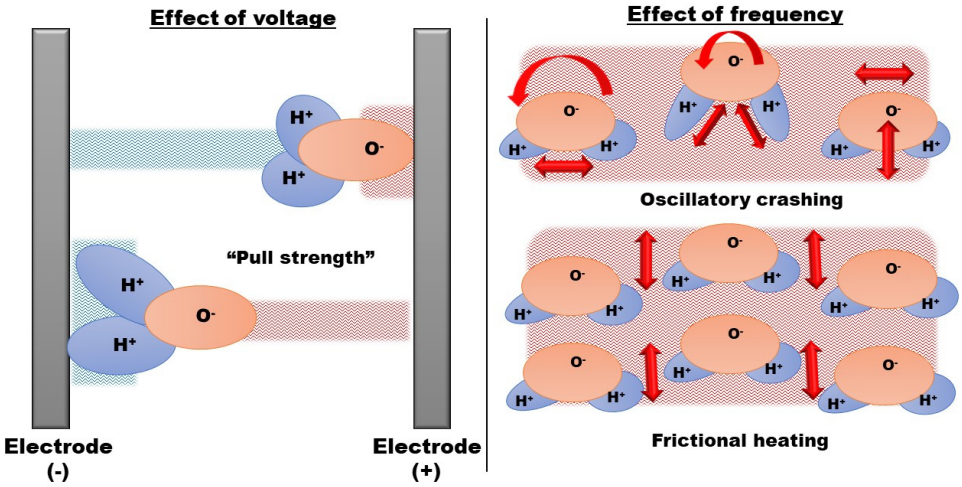

(**b**)

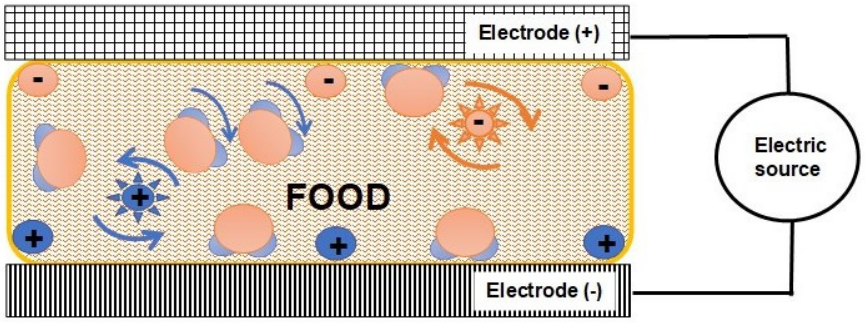

(**c**)

Figure 1. Schematic representation of polar molecules and radio frequency heating. (**a**) A polar molecule (i.e., water) aligns against electrodes, (**b**) the effect of the electric field has a "pulling strength" on the polar molecules; the effect of frequency produces oscillatory crashing and frictional heating, (**c**) dielectric heating in foods is based on the collision of ions aligning to the electric field and the friction between molecules because of the dipole rotation.

The dielectric constant ε' is a measurement of the material or food to absorb, transmit, or reflect electromagnetic energy. The loss factor ε'' provides information about the ability of a material to dissipate energy during heating. It gives a measurement of the energy lost from the electric field. A low value of ε'' means the material absorbs less energy and does not heat appropriately with RF [4]. The penetration depth (d_p) is the distance below the surface at which the power is reduced to $1/e$ (e = 2.718) or 36.9% of its original value [8]. It can be calculated as follows with Equation (2):

$$d_P = \frac{c}{2\pi f \sqrt{2\varepsilon' \left[\sqrt{1 + \left(\frac{\varepsilon''}{\varepsilon'}\right)^2} - 1\right]}} \quad (2)$$

where c is the speed of light (3×10^8 m/s), and f is the working frequency of the RF equipment [7]. RF shows a better penetration depth compared to microwaves. This characteristic makes RF ideal for processing large unpackaged products [9]. All these properties are a function of temperature, frequency, density, moisture content, and food composition. Other important properties of food when working with RF are the electrical conductivity (S/m), the thermal conductivity (W/m K), and the specific heat capacity (J/kg K).

The dielectric properties of food can be adjusted to specific values to improve the heating of the product. These modifications are made when the product's composition is changed (i.e., adding salt, modifying the water content, or changing the water state).

There are several methods to quantify the dielectric properties of food, including the following:

a. Open-ended coaxial probe (OCP). This method allows for the quantification of the permittivity in semisolids and liquids. The sample preparation is easy, and the results have high accuracy. The probe of the equipment works by flashing signals; in solids, the probe touches a flat surface of the material, and in liquids, the probe plunges inside the product. The main drawback is the presence of air gaps that can provide erroneous measurements.
b. Transmission line method (TLM). This methodology has high accuracy and sensitivity for solids and liquids, though the main limitations are the restricted range of frequencies (<100 MHz) and the time-consuming sample preparation. The dielectric properties are quantified via the phase and amplitude of a microwave signal reflected from a material sample placed by the end of a transmission line.
c. Resonant cavity method. This method is suitable for high-temperature solid materials and is the most accurate. The sample is placed in the middle of a waveguide, and changes in frequency are recorded. This method is quick, and sample preparation is easy (non-destructive). However, the analysis of data can become complex.
d. Parallel plates. The sample is placed between two electrodes, and an alternate current is applied. The sample needs to be added as a flat sheet. It is an inexpensive and highly accurate method but with limited frequency (20 Hz–1 GHz).
e. Free space. In this method, the solid sample is placed between two antennas to apply energy together with a vector network analyzer. Samples are analyzed in the microwave range, a non-contact, non-destructive technique.

The easiest method is the first one. It does not damage the sample, provides measurements in broadband, and does not require specific containers. The other methods are more accurate but are time-consuming, and the measurements are limited to particular frequencies [10].

2.1.1. Effect of Moisture Content

Water is found in food as free water or bound water. Free water is available for microbial growth; bound water is part of the food components attached to proteins, carbohydrates, and other molecules. The water molecule has a high polarity, and when water

molecules are exposed to an electric field, the molecules rotate, aligning to the electric field, generating heat (see Figure 1). The free water in food has similar dielectric properties to liquid water; bound water has dielectric properties like ice. As the moisture content of the product increases, the dielectric properties increase too. However, the dielectric properties depend on the temperature of low-moisture food. If the temperature increases, the dielectric properties increase [10]. Table 1 shows a clear example of the effect of moisture content on the dielectric properties. Comparing two products, Red Delicious apples (87% moisture content) to dried apricots (24.6% moisture content), at 20 °C, the dielectric constant is about two times higher for apples, regardless of the frequency.

Table 1. Dielectric properties of fruits and vegetables at selected temperatures in the radio frequency range (27.12 and 40.68 MHz).

Product	Temperature (°C)	Moisture Content (%)	Dielectric Constant (ε')		Loss Factor (ε'')		Penetration Depth (m)		Reference
			27.12 MHz	40.68 MHz	27.12 MHz	40.68 MHz	27.12 MHz	40.68 MHz	
Golden Delicious apple (pulp)	20	-	63.58	-	67.88	-	-	-	[11]
Red Delicious apple (pulp)	20	-	62.38	-	67.37	-	-	-	[11]
Red Delicious apple	20	87	74.6	74.7	92.0	61.1	0.189	-	[12]
	40		70.6	70.8	130.7	87.5			
	60		66.8	66.8	178.6	119.9			
Apple juice	25	-	81.9	79.9	135.5	88.7	-	-	[13]
	55		74.7	71.5	224.3	146.5			
	85		68.9	64.4	314.8	205.4			
Apricots (dried)	20	24.6	33.9	32.3	11.8	10.6	88.8×10^{-2}	64.9×10^{-2}	[14]
	40		37.4	35.7	19.9	16.2	56.3×10^{-2}	45.0×10^{-2}	
	60		40.8	38.9	37.4	28.9	32.8×10^{-2}	27.4×10^{-2}	
Avocado (pulp)	20	-	146.73	-	574.71	-	-	-	[11]
Avocado	20	-	115.7	92.7	699.6	477.2	5.1×10^{-2}	-	[15]
	40		131.6	100.0	951.6	648.6			
	60		140.5	105.4	1422.0	965.1			
Cherimoya	20	-	71.5		68.6		9.4×10^{-2}	-	[15]
	40		68.4	-	64.5	-			
	60		70.0		65.4				
Dates	20	19.7	27.2	25.5	10.1	9.0	93.0×10^{-2}	68.2×10^{-2}	[14]
	40		31.0	28.9	15.0	12.2	67.5×10^{-2}	53.9×10^{-2}	
	60		35.0	32.9	26.9	20.0	41.4×10^{-2}	35.7×10^{-2}	
Figs (dried)	20	27.3	37.7	35.7	14.4	13.1	76.7×10^{-2}	55.5×10^{-2}	[14]
	40		42.3	40.1	23.8	19.2	50.0×10^{-2}	40.5×10^{-2}	
	60		46.5	44.2	42.2	32.7	31.0×10^{-2}	25.7×10^{-2}	
Grape juice	25	-	81.3	79.1	209.1	136.7	-	-	[13]
	55		74.6	70.9	339.8	221.6			
	85		68.8	63.5	507.2	330.7			
Grapefruit (pulp)	20	-	99.42	-	245.7	-	-	-	[11]
Kiwi slices (airdried)	20	59.5	81.49	74.12	332.14	235.17	7.71×10^{-2}	6.42×10^{-2}	[16]
	80		90.68	82.98	777.66	546.03	4.73×10^{-2}	3.89×10^{-2}	
	20	70	97.53	88.62	407.45	284.32	6.94×10^{-2}	5.83×10^{-2}	
	80		96.74	86.06	808.19	576.96	4.64×10^{-2}	3.78×10^{-2}	
Kiwi slices (osmotic dehydrated)	20	60.5	73.15	67.46	291.92	201.50	8.25×10^{-2}	7.01×10^{-2}	[16]
	80		82.00	75.91	703.63	494.31	4.97×10^{-2}	4.10×10^{-2}	
	20	70.2	91.28	82.48	371.19	258.78	7.30×10^{-2}	6.14×10^{-2}	
	80		89.71	80.76	757.67	545.84	4.80×10^{-2}	3.89×10^{-2}	
Longan	20	-	75.2	73.8	230.1	156.5	9.7×10^{-2}	-	[15]
	40		71.6	69.5	326.4	221.9			
	60		67.5	65.0	431.4	293.3			
Orange juice	25	-	83.5	81.1	222.1	144.9	-	-	[13]
	55		76.4	72.6	372.4	242.5			
	85		65.4	60.3	522.5	340.0			
Orange, navel (pulp)	20	-	84.57	-	222.48	-	-	-	[11]
Orange, Valencia (pulp)	20	-	85.29	-	240.09	-	-	-	[11]
Passion fruit	20	-	82.7	73.5	264.1	179.7	9.0×10^{-2}	-	[15]
	40		88.1	74.7	373.6	254.1			
	60		96.6	77.7	523.9	356.3			
Peach (pulp)	20	-	90.09	-	269.5	-	-	-	[11]
Pear juice	25	-	80.9	79.7	182.2	119.1	-	-	[13]
	55		71.2	69.4	300.5	196.0			
	85		61.9	59.8	435.8	284.2			

Table 1. *Cont.*

Product	Temperature (°C)	Moisture Content (%)	Dielectric Constant (ε')		Loss Factor (ε'')		Penetration Depth (m)		Reference
			27.12 MHz	40.68 MHz	27.12 MHz	40.68 MHz	27.12 MHz	40.68 MHz	
Persimmon	20	-	76.0	73.6	258.6	176.0	10.5×10^{-2}	-	[15]
	40		75.5	72.2	369.9	251.3			
	60		69.1	64.9	470.8	319.4			
Pineapple juice	25	-	84.9	81.2	276.8	180.7	-	-	[13]
	55		75.1	69.4	436.2	284.5			
	85		65.5	58.1	586.2	382.3			
Potatoes	20	83.3	48.7		293.5		-	-	[17]
	40	79.8	57.2	-	623.4	-			
	60	73.3	118.2		693.0				
Potatoes, mashed (0.8% NaCl)	20	84.7	88.6	82.4	297.5	203.6	84.0×10^{-3}	72.1×10^{-3}	[18]
	60		89.9	79.5	541.0	367.9	58.4×10^{-3}	49.0×10^{-3}	
	120		102.8	81.6	1153.8	782.4	38.5×10^{-3}	31.8×10^{-3}	
Potatoes, mashed (1.8% NaCl)	20	85.9	78.2	71.4	713.3	480.5	49.5×10^{-3}	41.5×10^{-3}	[18]
	60		79.9	68.6	1306.7	878.2	35.7×10^{-3}	29.6×10^{-3}	
	120		112.2	84.3	3152.2	2104.4	22.8×10^{-3}	18.8×10^{-3}	
Prunes (dried)	20	30.2	40.6	38.7	17.2	15.7	66.9×10^{-2}	48.3×10^{-2}	[14]
	40		44.4	42.7	25.4	20.6	48.1×10^{-2}	38.9×10^{-2}	
	60		48.9	47.2	47.8	38.4	28.4×10^{-2}	22.9×10^{-2}	
Raisins	20	15	21.9	20.2	8.1	7.4	103.7×10^{-2}	74.0×10^{-2}	[14]
	40		28	26.1	9.8	9.0	96.9×10^{-2}	68.7×10^{-2}	
	60		33.8	31.9	11.4	10.6	91.3×10^{-2}	64.4×10^{-2}	
White sapote	20	-	76.0	73.6	258.6	176.0	9.0×10^{-2}	-	[15]
	40		75.5	72.2	369.9	251.3			
	60		69.1	64.9	470.8	319.4			

Another example is presented in Table 2 for milk. The dielectric constant for raw milk (88.20% moisture content) is 90.4 (27.12 MHz, 20 °C). The dielectric constant for whole milk powder (1.8% moisture content) is 1.51 at the same frequency and temperature. Table 2 presents a compilation of dielectric properties for animal food products and the effect of the moisture content. Meanwhile, Table 3 shows several examples of low-moisture food like flour, spices, and nuts; these products have a low dielectric constant.

Table 2. Dielectric properties of animal food products at selected temperatures in the radio frequency range (27.12 and 40.68 MHz).

Product	Temperature (°C)	Moisture Content (%)	Dielectric Constant (ε')		Loss Factor (ε'')		Penetration Depth (m)		Reference
			27.12 MHz	40.69 MHz	27.12 MHz	40.68 MHz	27.12 MHz	40.68 MHz	
Meat									
Beef meatball	20	66.9	68.8	56.6	474.4	323.9	61.7×10^{-3}	51.1×10^{-3}	[19]
	60		79.1	69.1	922.0	625.4	43.0×10^{-3}	35.6×10^{-3}	
	100		95.8	79.0	1557.5	1054.1	32.7×10^{-3}	27.0×10^{-3}	
Beef (lean)	Heating	71.5	70.5	-	418.7	-	0.132	-	[20]
Lamb (lean)	Heating	73	77.9	-	387.2	-	0.140	-	[20]
Pork (lean)	Heating	73.9	69.6	-	392.0	-	0.137	-	[20]
Pork (fat)	Heating	19.0	12.5	-	13.1	-	1.054	-	[20]
Lean beef (11.8% fat content)	5	67.8	74	-	290	-	0.100	-	[21]
	10		72		310		0.100		
Beef (50:50, 36.1% fat content)	5	48.2	42	-	110	-	0.260	-	[21]
	10		40		120		0.220		
Fatty beef (65.7% fat content)	5	26.3	19	-	20	-	0.580	-	[21]
	10		18		18		0.620		
Poultry									
Chicken breast	20	75.1	91.64	83.50	332.33	227.34	78.55×10^{-3}	66.96×10^{-3}	[22]
	60		109.18	94.59	567.21	388.57	57.74×10^{-3}	48.27×10^{-3}	
	100		126.03	106.28	618.96	427.76	55.57×10^{-3}	46.12×10^{-3}	

Table 2. *Cont.*

Product	Temperature (°C)	Moisture Content (%)	Dielectric Constant (ε')		Loss Factor (ε'')		Penetration Depth (m)		Reference
			27.12 MHz	**40.69 MHz**	**27.12 MHz**	**40.68 MHz**	**27.12 MHz**	**40.68 MHz**	
Chicken (lean)	Heating	73.6	75.0	-	480.8	-	0.123	-	[20]
Turkey (lean)	Heating	74.5	73.5	-	458.4	-	0.126	-	[20]
Eggs									
Liquid egg whites	20	85	84.6	76.6	427.0	256.4	-	-	[23]
	60		81.3	68.0	646.4	427.7			
	100		118.1	88.9	1242.3	784.3			
Pre-cooked egg whites	20	-	89.3	81.9	411.8	256.3	-	-	[23]
	60		92.5	82.3	732.1	460.0			
	100		106.8	88.2	1145.0	698.9			
Liquid whole egg	20	73.7	76.3	68.8	335.9	208.4	-	-	[23]
	60		77.4	66.0	612.0	377.1			
	100		96.9	77.5	956.4	589.8			
Pre-cooked whole eggs	20	-	79.6	71.0	336.8	209.5	-	-	[23]
	60		85.2	72.1	594.1	367.4			
	100		94.2	75.4	874.1	539.5			
Egg albumen	24	87.8	89	81	507	362	-	-	[24]
Egg yolk	24	52.1	56	51	200	145	-	-	[24]
Dairy									
Mozzarella cheese	20	59.1	55.6	49.4	358.5	245.5	71.3×10^{-3}	59.5×10^{-3}	[19]
	60		74.6	63.0	853.6	579.9	44.7×10^{-3}	37.0×10^{-3}	
	100		82.2	66.1	1266.9	858.9	36.3×10^{-3}	29.9×10^{-3}	
Raw milk	20	88.20	90.4	83.3	299.8	203.6	0.098	0.076	[25]
	60		93.3	80.0	562.6	379.8	0.068	0.048	
	120		109.3	84.5	979.8	661.9	0.050	0.038	
Skimmed milk	20	90.44	89.7	84.5	310.0	209.4	0.096	0.072	[25]
	60		91.1	80.6	590.6	399.0	0.065	0.048	
	120		102.0	83.3	1020.2	690.1	0.040	0.036	
Whole milk powder	20	1.8	1.51		0.007				[26]
	50		2.09	-	0.100	-	-	-	
	90		4.46		2.511				
Non-fat milk powder	20	4.8	1.12		0.004				[26]
	50		2.00	-	0.100	-	-	-	
	90		3.16		1.580				
Concentrated non-fat milk (35%)	20	65.45	99.1	87.5	536.8	365.6	0.069	0.052	[25]
	60		119.6	99.0	1121.6	760.0	0.048	0.032	
	120		152.9	117.6	1953.5	1319.2	0.038	0.028	
Concentrated milk									
70%	22	-	76.4	-	233.8	-	0.142	-	[27]
85%			76.3		266.4		-		
100%			75.8		282.1		0.130		
Fish and seafood									
Salmon	20	75.7	77.61	-	462.66	-	63.10×10^{-3}	-	[22]
	60		96.84		809.98		46.61×10^{-3}		
	100		116.37		1185.56		38.11×10^{-3}		
Salted (2.3%) salmon caviar	20	-	129.8	-	1349.4	-	3.7×10^{-2}	-	[28]
	50		121.5		1501.1		3.4×10^{-2}		
	80		182.0		2614.5		2.6×10^{-2}		
Unsalted (0.8%) salmon caviar	20	-	70.7	-	470.8	-	6.3×10^{-2}	-	[28]
	50		46.4		375.9		7.2×10^{-2}		
	80		59.6		642.7		5.5×10^{-2}		
Salted (3.3%) sturgeon caviar	20	-	81.5	-	1004.0	-	4.2×10^{-2}	-	[28]
	50		111.5		1769.5		3.1×10^{-2}		
	80		202.8		2873.3		2.5×10^{-2}		
Unsalted (0.2%) sturgeon caviar	20	-	61.0	-	105.5	-	16.0×10^{-2}	-	[28]
	50		77.4		210.8		11.0×10^{-2}		
	80		92.5		352.2		7.80×10^{-2}		
Trout	20	72.8	83.64	-	343.83	-	76.02×10^{-3}	-	[22]
	60		103.55		645.04		53.30×10^{-3}		
	100		100.34		806.62		46.82×10^{-3}		

Table 3. Dielectric properties of miscellaneous food products at selected temperatures in the radio frequency range (13.56 and 27.12 MHz).

Product	Temperature (°C)	Moisture Content (%)	Dielectric Constant (ε')		Loss Factor (ε'')		Penetration Depth (m)		Reference
			13.56 MHz	27.12 MHz	13.56 MHz	27.12 MHz	13.56 MHz	27.12 MHz	
Flour, starch, bread									
Chestnut flour (compressed)	20	45.3	-	31.2	-	45.9	-	0.280	[29]
	40			38.8		77.9		0.190	
	60			57.7		158.1		0.130	
Chickpea flour	20	7.9	-	2.99	-	0.16	-	17.92	[30,31]
	50			3.44		0.19		-	
	90			11.20		4.27		13.6	
Chickpea flour	20	20.9	-	4.50	-	0.81	-	44.9	[29,30]
	50			11.43		7.85		-	
	90			71.59		248.25		0.088	
Green pea flour	20	21.6	-	7	-	1.4	-	3.61	[31]
	60			28		20		0.52	
	90			85		180		0.146	
Lentil flour	20	21.5	-	5.5	-	1	-	4.31	[31]
	60			30		25		0.42	
	90			100		200		0.12	
Potato starch	-	-	5.72	5.56	0.14	0.1	1.08	0.55	[32]
Soybean flour	20	19.9	-	6	-	1.5	-	2.70	[31]
	60			20		20		0.39	
	90			70		200		0.09	
Tapioca flour	-	-	4.07	3.91	0.13	0.09	1.31	0.67	[32]
Wheat flour	25	12.56	-	5.61	-	5.42	-	-	[33]
	55			6.58		6.25			
	85			23.50		20.47			
Wheat flour with 10% bran content	25	12.56	-	0.54	-	0.54	-	-	[33]
	55			0.62		0.60			
	85			9.74		9.39			
Wheat germ	25	7.05	2.78	2.64	0.30	0.29	-	-	[34]
	55		3.46	3.37	0.43	0.39			
	85		5.39	5.14	0.68	0.62			
White bread	25	34.6	2.76	2.35	4.56	2.32	2.105	0.1283	[35]
	55		3.37	2.80	10.70	5.09	1.206	0.721	
	85		4.22	3.45	26.55	11.98	0.710	0.417	
Nuts									
Almonds (ground shells)	20	6	-	2.07	-	0.10	-	24.82	[36]
	50			2.18		0.12		-	
	90			4.42		1.35		2.78	
Almonds (ground shells)	20	36	-	8.96	-	12.43	-	0.496	[36]
	50			13.41		38.48		-	
	90			26.91		92.30		0.150	
Almonds (ground shells)	25	12	-	9.3	-	5.7	-	98.9×10^{-2}	[36]
	60			11.1		11.0		58.6×10^{-2}	
	100			13.8		26.0		31.5×10^{-2}	
Macadamia nuts	25	24	-	20.6	-	47.5	-	22.3×10^{-2}	[37]
	60			22.9		81.0		15.9×10^{-2}	
	100			29.2		173.5		10.3×10^{-2}	
Peanut kernels	25	10	-	6.2	-	0.8	-	5.24	[38]
	85			7		1.15		3.79	
Peanut kernels	25	30	-	25	-	50	-	0.22	[38]
	85			35		125		0.12	
Pecan kernels (no salt)	25	15	-	8.97	-	3.35	-	6.07	[39]
	65			20.01		15.19		1.29	
Pecan kernels (light salt)	25	15	-	11.46	-	8.58	-	69.95	[39]
	65			23.71		27.02		29.54	
Pecan kernels (medium salt)	25	15	-	13.97	-	14.96	-	51.69	[39]
	65			27.43		34.83		22.79	
Pecan kernels (heavy salt)	25	15	-	15.48	-	24.26	-	42.69	[39]
	65			29.37		47.96		13.76	
Pistachio (non-salted)	24	3.5	-	10.37	-	5.33	-	0.53	[40]
Pistachio (100 mg sodium/serving)	24	4.08	-	15.34	-	15.83	-	0.31	[40]
Pistachio (330 mg sodium/serving)	24	3.75	-	23.78	-	42.83	-	0.19	[40]
Pistachio kernels: non-salted	25	15	-	11.85	-	5.99	-	104.27×10^{-2}	[41]
	85			17.74		23.09		36.93×10^{-2}	

Table 3. *Cont.*

Product	Temperature (°C)	Moisture Content (%)	Dielectric Constant (ε')		Loss Factor (ε'')		Penetration Depth (m)		Reference
			13.56 MHz	27.12 MHz	13.56 MHz	27.12 MHz	13.56 MHz	27.12 MHz	
Pistachio kernels: light salted	25 85	15	-	15.73 24.65	-	15.65 63.36	-	49.06×10^{-2} 18.92×10^{-2}	[41]
Pistachio kernels: medium salted	25 85	15	-	21.41 32.55	-	24.92 82.66	-	36.85×10^{-2} 16.60×10^{-2}	[41]
Pistachio kernels: strong salted	25 85	15	-	22.15 31.42	-	44.82 133.21	-	23.60×10^{-2} 12.13×10^{-2}	[41]
Species									
Chili powder	-	-	7.22	6.85	0.61	0.39	0.95	0.49	[32]
Cumin	-	9.6	2.1	2.0	-	-	-	-	[42]
Curry	-	8.3	2.1	2.0	0.01	0	-	-	[42]
Garlic	-	3.1	1.8	1.7	-	-	-	-	[42]
Onion powder	-	-	2.22	2.18	-	-	-	-	[32]
Paprika	-	12.3	3.6	3.4	0.20	0.18	-	-	[42]
Black pepper	-	10.4	3.0	2.8	0.10	0.05	-	-	[42]
Red pepper	-	11.5	2.8	2.2	0.1	0.07	-	-	[42]
Red pepper powder	25 35 55 85	17.6	-	6.63 7.55 9.83 23.28	-	2.00 2.80 5.76 50.69	-	3.00	[43]
White pepper	-	10.2	3.6	3.4	0.18	0.12	-	-	[42]
Turmeric	23	9.5	2.8	2.6	0.12	0.09	-	-	[42]
Others									
Black-eyed pea	20 40 60	16.8	-	3.64 4.18 6.67	-	0.40 0.60 1.67	-	8.42 6.03 2.76	[44]
Broccoli powder	20 40 60 80	9.1	4.66 5.78 8.75 12.48	4.21 5.58 8.22 11.35	0.17 0.28 0.81 2.1	0.12 0.19 0.54 1.34	12.48 7.95 3.43 1.88	8.86 5.17 2.48 1.27	[32]
Edible fungi powder (*Pleurotus eryngii*)	25 55 85	12.0	4 7 26	-	1 3 36	-	4.30 2.42 0.29	-	[45]
Edible fungi powder (*Pleurotus eryngii*)	25 55 85	21.2	8 30 70	-	0.001 50 460	-	2.19 0.24 0.072	-	[45]
Edible fungi powder (*Pleurotus eryngii*)	25 55 85	30.9	20 60 142	-	10 180 740	-	0.430 0.110 0.051	-	[45]
Honey (Jujube)	25	17.5	-	30.70	-	8.06	-	-	[46]
Honey (Yellow-locust)	25	18.1	-	32.45	-	8.74	-	-	[46]
Honey (Milk vetch)	25	17.1	-	30.98	-	8.27	-	-	[46]
Lasagna sauce	20 60 100	92.0	-	86.2 77.7 85.6	-	1045.3 1862.1 3043.7	-	40.3×10^{-3} 29.6×10^{-3} 23.0×10^{-3}	[19]
Lasagna noodles	20 60 100	60.7	-	92.5 85.2 85.1	-	516.8 943.3 1496.6	-	60.1×10^{-3} 42.6×10^{-3} 33.2×10^{-3}	[19]
Mung bean	20 40 60	14.4	-	4.21 4.50 6.07	-	0.43 0.54 1.11	-	8.44 6.93 3.93	[44]

2.1.2. Effect of Temperature

The effect of temperature on the dielectric properties is a complex relationship. In general, when the temperature increases, the dielectric constant also increases. However, the changes are a function of the frequency of the loss factor. For instance, at low frequencies, the loss factor will increase as the temperature rises, and it is because of ionic conductance. As previously defined in Section 2.1, the loss factor provides information about how easily the material can dissipate energy during heating. At high frequencies, the loss factor decreases as the temperature rises because of free-water dispersion [10]. Table 2 presents the effect of temperature on the dielectric constant (ε') of chicken breast. At 27.12 MHz, ε' is 91.64 when the temperature is 20 °C, but ε' is increased to 109.18 when the temperature

reaches 60 °C. For chickpea flour, the dielectric constant reported at 20 °C is 2.99, and this constant at 90 °C is 11.20, with both values at the same moisture content (7.9%) and same frequency (27.12 MHz), as presented in Table 3.

2.1.3. Effect of Food Composition

Some food components, such as salt or fat content, can affect the dielectric properties of the product. For example, the presence of salt can change the dielectric constant of the food because of ionic conduction. The material's loss factor (ε'') will increase in a product with high salt content as the temperature and frequency increase [4]. This fact can be observed in Table 2 for fish and seafood. The example of salmon caviar, containing 2.3% salt, has a loss factor (ε'') of 1349.4 at 20 °C. Comparing the same product at the same temperature and frequency but with low salt content (0.8%), the loss factor decreased to 470.8. Another example is presented in Table 3 with pecan kernels with no salt (ε'' 3.35), light salt (ε'' 8.58), medium salt (ε'' 14.96), and heavy salt (ε'' 24.26).

The ash content of food can also impact the dielectric properties. The minerals present in foods and those non-organic components represent the ash content. Ashes can bind some water ions reducing the functionality of these volumetric heaters. Products with low ash content, such as fruits and vegetables, do not significantly affect the dielectric properties. Products with higher ash content are expected to have a lower dielectric constant and higher loss factor [10].

The effect of fat content in food has also been studied during RF heating. One study by Farag et al. [47] using beef (lean, fatty, 50:50 mixture) showed that fat does not allow for the proper heating of the product. The three products showed an initial temperature increase when the radio frequency heating started, but the fatty product showed a quick decrease in the temperature. A specific example is presented in Table 2 for pork. The dielectric constant of lean pork is 69.6 (27.12 MHz) and decreases to 12.5 when the pork has high-fat content.

2.1.4. Other Effects

In the case of heterogeneous mixtures, such as granular or particulate materials, the product's bulk density will impact the food's dielectric properties. This is important when processing grains, seeds, and spices [6,10]. During processing grains or seeds, there are void spaces in the bulk material. These spaces are filled with air. Then, the dielectric properties of air must be considered during the evaluation.

Studies of the dielectric properties of diverse food and materials have been widely reported. Since the knowledge of these properties represents the foundation for developing radio frequency treatments and equipment, quantifying these properties has been extensively reported in the literature. Tables 1–3 present a compilation of some of the electrical properties reported for fruits and vegetables, animal products, and miscellaneous food. The values in the tables belong to the most common frequency used for food applications (13.56, 27.12, and 40.68 MHz). Also, the values are presented at different temperatures and, in some cases, at additional moisture content. Specific values at a particular temperature or processing conditions are available in some literature reports.

3. Equipment

The most basic RF equipment consists of a couple of electrodes connected to a radio frequency source. The food is placed between two electrodes to apply the electric field. The gap between the electrodes can be modified to adjust the intensity of the treatment. Figure 2a is a schematic representation of a simple RF semi-continuous equipment. This piece consists of two parallel electrodes connected to the alternating radio frequency energy source. The chamber is loaded with food on the left and the processed product leaves on the right. The system can operate semi-continuously if a conveyor belt is added to move the product. Another electrode configuration is the stray field (fringe field), which consists of a series of electrodes with specific shapes, such as bars, rods, or narrow plates. Depending on the thickness of the food, different electrode arrangements can be used for processing.

For example, the staggered through field electrodes are preferred for regular products with a thickness of about 6 mm, and these are the best choice for thawing. The stray-field electrodes are selected for products like sheets with thicknesses less than 1 mm. Meanwhile, parallel plate electrodes are the best option for bulk, thicker and large products [48]. Some RF systems are equipped with an auxiliary hot air system. This air will help maintain the product's temperature and increase the process's lethality [49].

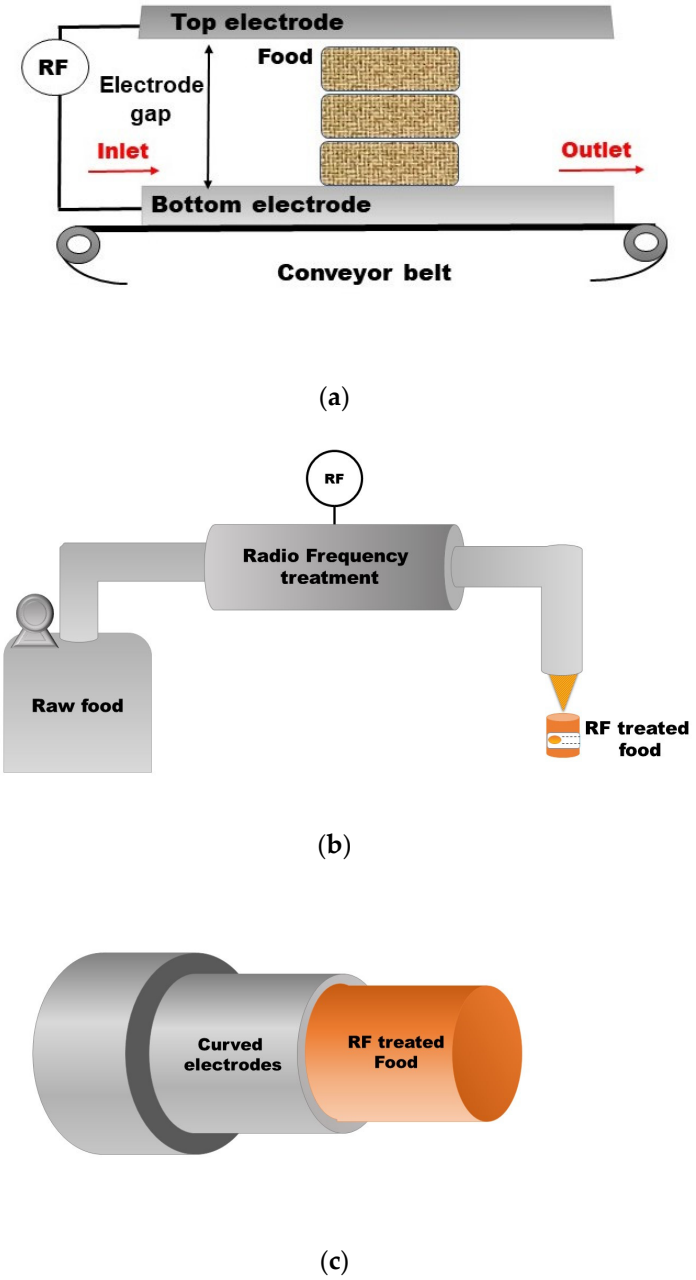

Figure 2. Schematic representation of radio frequency equipment (**a**) Semi-continuous mode for solid food in which the system uses a parallel plate array of electrodes; (**b**) continuous mode for liquid pumpable food; (**c**) curved electrodes inside of a tubular RF system.

For liquid and pumpable products, the RF systems consist of tubular sections. The product is pumped through a tube with curved electrodes attached to the system. The liquid receives the treatment, and the heating results from the dielectric properties. This equipment has been tested for some salt solutions and milk [48]. A schematic representation of a liquid RF system is presented in Figure 2b,c.

In Figure 3, there is a representation of an RF system explicitly developed to pasteurize in-shell eggs. In this system, the eggs are rotated during the processing to allow for more uniform heating and reduce the problem of hotspots. The cooling water nozzle is used to spray cold water during the process and reduce the shell's temperature to protect the albumen from thermal damage. The active and ground electrode are conductive brushes to transfer the energy into the product. This system has been successfully adapted for use in combination with hot water immersion (HWI), hot water spraying (HWS), or hot air (HA) to reduce processing time [50–52]. A schematic diagram of the egg and the electrodes is shown in Figure 3a. The former electrodes of the existing RF system are shown in Figure 3b.

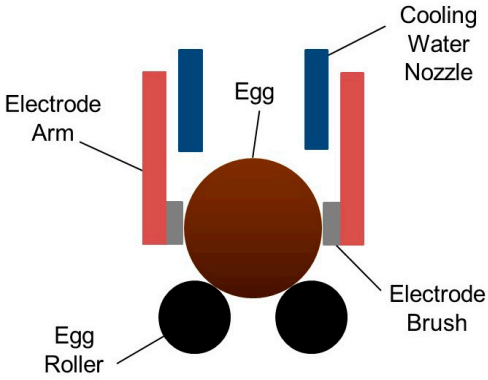

(**a**)

(**b**)

Figure 3. RF equipment to pasteurize in-shell eggs with a parallel plate array of electrodes, (**a**) Schematic representation [52]; (**b**) actual view of the system (Photo credit: USDA ARS ERRC).

Some critical factors during RF processing are the size, shape, orientation, homogeneity, and food location inside the equipment [49]. Zuo et al. [53] studied the effect of different sizes and densities of walnuts during RF treatments (27.12 MHz, 6 kW). Samples were placed in containers, and the thickness was measured. Whole and half walnut kernels were used, as well as cracking pieces. The heating rate was higher as the sample was thicker, but the heating uniformity was worse. However, as the heating rate decreased because the electrode gap was bigger, the uniformity was improved.

There is a mathematical equation to express the uniformity of RF heating, and it is called the RF heating uniformity index (λ), and it is described as follows in Equation (3):

$$\lambda = \frac{\sqrt{\sigma^2 - \sigma_0^2}}{\mu - \mu_0} \quad (3)$$

where σ_0 and σ are the initial and final standard deviation of the food temperature before and after processing, and m and m_0 are the final and initial temperature of the food. The lower the value λ, the better the heating uniformity [53,54]. The heating uniformity index (λ) increased as the kernel size in the previous study related to walnut kernels increased, but λ was decreased when the density of the kernels was increased. It was observed that mixing kernels (whole, halves, and cracking pieces) improved λ [53].

One of the main challenges today is the heating uniformity of the product when scaling up the technology. Some factors that affect the process's uniformity are the product's size and shape and the position between the electrodes. Several attempts have been made to improve the uniformity of the process, such as the rotation of the product or using a conveyor system to move the product inside the equipment, water immersion of the product, stirring/mixing, hot water preheating, hot air assistance, changes in the composition of the product, changes in electrode shapes, and adding some dielectric material to the product, among others [9,14,49,54–58]. Hao et al. [54] tested using a rotation device with sample mixing during RF heating of some granular products. Several variables were evaluated, such as the rotation speed, the product's moisture content, and the product size. The products included mung bean, coix seed, peanut kernel, and almond kernel. The authors concluded that the lowest value λ was for mung beans because of their small size and moisture content (8.15%).

It is also clear today that the heating uniformity of the product is affected by the dielectric properties and the density of the surrounding medium, often the packaging material [56]. In packaged food using rectangular containers, the main problem during RF is edge overheating. This is because of the higher energy absorption by the edges and corners of the packaged product. This different energy absorption is due to the differences in dielectric properties between the food and the packaging material [56]. Furthermore, some studies have indicated that the area of better heating when a product is placed between two electrodes is the central layer of the product. Also, when comparing the product's central point and edges, the latter seems to be better heated with RF [58]. Ideally, the packaging material should have a low density or a close value to the product treated with RF. If dielectric properties are similar between the food and the packaging material, the nonuniform heating will be reduced drastically, as the computer simulation experiments show [59].

RF is not only a quick and accessible technology to apply to food products. Besides the remarkable improvement in sensory and nutritional attributes of the treated product compared to conventional thermal processing, there are significant savings in energy and costs. RF can be considered a green, non-contact, waterless, and energy-efficient technology [9,60]. Some energy calculations were conducted in a detailed study to scale up an RF system. For a continuous system used for the disinfestation of walnuts, the energy or heating efficiency had an average value of 79.5%. This value was greatly improved by mixing the product, moving the product in a conveyor belt, and adding hot air to the processing [49].

4. Food Pasteurization

Pasteurization is a thermal process applied to food to inactivate pathogens, spoilage microorganisms, and enzymes, extending the product's shelf life. Food is usually heated at temperatures below 100 °C for several seconds or minutes [61]. Some inactivated pathogens via pasteurization are *Salmonella*, *L. monocytogenes*, *E. coli*, *Staphylococcus aureus*, and *Cronobacter sakazakii.* Pasteurization aims to reduce at least 5-log or 99.999% of the pathogen of concern in the product. However, to achieve this log-reduction, the processing time is long enough to degrade some nutrients such as vitamins and negatively affect sensory attributes like color or texture. Then, the need for an alternative for pasteurization using shorter processing times but ensuring the microbial quality of food brought radio frequency as an option. RF can achieve pasteurization standards in food products [57,61], and microbial inactivation is often higher than in conventional pasteurization [48].

The microbial inactivation because of RF is attributed to thermal effects on the cells [8]. The effects of the thermal treatment on microbial cells are mainly in the ribosomal DNA and the exhaustion of Mg^{+}, which are vital for metabolic processes. Protein coagulation has also been reported as one of the lethal effects of heat [62]. The thermal inactivation of the microorganisms occurs when the cell generates heat faster than the surrounding media. It is affected by the composition of the media but also by the organism itself. It is believed that there is a mechanical disruption of the cells when subjected to RF because of the continuous, rapid oscillation when re-aligning to the oscillating electric field. This constant realignment breaks the cellular membranes when the elastic limit of the cell is exceeded, leading to cellular death [63]. However, today, there is still controversy about the main inactivation factor during RF. Perhaps, it is likely correct to believe that the inactivation of microorganisms is due to a synergistic effect between thermal and mechanical effects of the radio frequency energy in the cell membrane and intercellular structures.

This novel thermal technology has been tested with successful results in the pasteurization of milk, meat, spices, nuts, flour, and eggs [9]. RF pasteurization can be an attractive option for those products with low moisture content, such as nuts. Conventional methods require very long processing times to ensure heat transfer in the product. Also, pathogens are more resistant to inactivation in low-moisture products [48]. RF offers the advantage of the product's internal heating, reducing the processing time considerably. A comprehensive list of pasteurized products using RF is presented in Table 4. These references belong to those experiments that showed at least a 5-log reduction of the pathogen in the food product. However, several references report pathogen inactivation at a lower degree. Some of these studies present possible improvements in the equipment and/or the processing conditions to enhance microbial inactivation.

Most of the current research shows hurdle technology as an option, combining several factors with RF to increase microbial death [64,65]. A few examples are presented in Table 4, for example, sesame and flaxseed seeds during the inactivation of S. Montevideo and S. Typhimurium. Xu et al. [64] treated the seeds with plant essential oils and RF to increase cell inactivation. These authors tested cinnamon vapor oil and oregano oil vapor. The best result was obtained with RF heating at 80 and 85 °C for 5 min and 0.83 μL/mL of cinnamon vapor oil for three days. This combination achieved more than a 5-log reduction of *Salmonella* cells.

RF can potentially be used in products involved in foodborne outbreaks reported recently. For example, a recent foodborne outbreak in 2022 in infant formula involved *C. sakazakii* or the presence of *E. coli* in cake mixes in the 2021 outbreak [1]. Several reports have also mentioned the presence of *Salmonella* spp. in flour. These products and microorganisms have been studied successfully, as shown in Table 4. RF can also be a valuable tool to treat spices that often contain high microbial loads if other interventions are unavailable or not practical. These high microbial concentrations in spices can limit the development of new products in the food industry and promote cross-contamination during the food production chain.

Table 4. Examples of pasteurization and fungi inactivation in food products using radio frequency.

Pasteurization *				
Product	**Microorganism**	**Processing Conditions**	**Log Reduction**	**Reference**
Corn flour	*Salmonella enterica* Enteritidis PT30	27.12 MHz, 6 kW, 85 °C, 10 min, followed by −20 °C 48 h	6.6	[66]
Wheat flour	*Salmonella* Enteritidis PT30	27.12 MHz, 6 kW, 30 min	>5	[67]
Liquid whole egg (LWE) and liquid egg yolk (LEY)	*Salmonella Enteritidis*	27.12 MHz, 12 kW, 180–285 s	5.6 (LWE) 5.3 (LEY)	[68]
Cumin seeds	*Salmonella enterica*	27.12 MHz, 6 kW, 90–106 s	>5.8	[69]
Sesame seeds	*Salmonella* Montevideo and *Salmonella* Typhimurium	27.12 MHz, 6 kW, 80 °C, 5 min, plus 0.83 µL/mL Cinnamon Vapor Oil	>5	[64]
Flaxseed seeds	*Salmonella* Montevideo and *Salmonella* Typhimurium	27.12 MHz, 6 kW, 85 °C, 5 min, plus 0.83 µL/mL Cinnamon Vapor Oil	>5	[64]
Ground black pepper	*Salmonella* spp.	27.12 MHz, 6 kW, 130 s	5.98	[70]
Paprika	*Salmonella* spp.	27.12 MHz, 6 kW, 80 °C, 5 min	>6	[71]
Shell egg	*Salmonella* Typhimurium	27.12 MHz, 1 kW, 56.7 °C, 21 min	>6.1	[52]
Black pepper kernels	*Salmonella* Typhimurium ATCC 14028	27.12 MHz, 12 kW, 100 °C, 8 min	>6	[72]
Basil leaves	*Salmonella* spp. and *Enterobacter faecium*	27.12 MHz, 6 W, 65 s	>6.5	[73]
Buckwheat kernels	*Salmonella* Typhimurium, *Escherichia coli* ATCC 25922, *Cronobacter sakazakii*	27.12 MHz, 6 kW, 85 °C, 5 min	≈5	[74]
Cocoa powder	*Enterobacter faecium* NRRL B-2354	27.12 MHz, 6 kW, 75 °C, 48 min	5.5	[75]
Almonds (in-shell)	*Escherichia coli* ATCC 25922	27.12 MHz, 6 kW, 55 °C, 1.5 min	5	[76]
Eggshell	*Escherichia coli* ATCC 35218	27.12 MHz, 3.5 min, 35 °C and hot water (56.7 °C) for 20 min	6.5	[77]
Chunky peanut butter cracker sandwiches	*Escherichia coli* O157:H7	27.12 MHz, 9 kW, 90 s	5.3	[78]
Dried red pepper	*Escherichia coli* O157:H7	27.12 MHz, 9 kW, 50 s	>5	[79]
Black pepper kernels	*Escherichia coli* O157:H7	27.12 MHz, 12 kW, 90 °C, 7 min	>6	[72]
Ground beef	*Escherichia coli* (non-pathogenic cocktail)	27.12 MHz, 6 kW, 55 °C	5	[80]
Infant formula	*Cronobacter sakazakii*	27.12 MHz, 6 kW, 116.5 min, 70 °C (Dry heat)	5	[81]
Salmon caviar	*Listeria innocua*	27.12 MHz, 6 kW, 65 °C, 500 IU/mL nisin	>7	[82]
Fungi Inactivation				
Product	**Microorganism**	**Processing Conditions**	**Log Reduction**	**Reference**
Peanut kernels	*Aspergillus flavus*	27.12 MHz, 6 kW, and hot air (65 °C—9 min, 0.735 a_w/70 °C—15 min, 0.876 a_w)	3.0 and 3.4, respectively	[60]
Wheat seeds	*Aspergillus flavus*	27.12 MHz, 12 kW, and hot air (65 °C—10 min)	2 (when moisture content of seeds was 12%), 3 (when moisture content of seeds was 15%)	[83]
Corn seeds	*Aspergillus flavus*	27.12 MHz, 12 kW, and hot air (65 °C—10 min)	3 (when moisture content of seeds was 12%), 4 (when moisture content of seeds was 15%)	[83]
Corn grains	*Aspergillus parasiticus*	27.12 MHz, 6 kW, and hot air (70 °C—12 min)	5–6	[84]
Enriched white bread	*Penicillium citrinum*	27.12 MHz, 6 kW, and hot air (58 °C—5 min)	4	[85]
Chestnuts	*Penicillium crustosum*	27.12 MHz, 6 kW, and hot air (60 °C)	4	[86]

* Listed by microorganism.

Awuah et al. [87] tested RF to inactivate surrogate microorganisms in milk. The experiment involved strains of *L. innocua* and *E. coli* K12 inoculated in pasteurized whole milk. The treatment was conducted at 27.12 MHz, 2 kW, 65 °C, and 55 s. After processing the milk inside a piece of tubular equipment with a laminar flow, the inactivation was about 5 and 7 log-reduction for *L. innocua* and *E. coli,* respectively.

Eggs have been tested in different presentations using RF. *Salmonella* spp. is the leading pathogen of concern in this product [52]. In-shell eggs, liquid whole egg, egg white powder, liquid egg yolk, and liquid egg white are some examples evaluated under dielectric heating [51,52,68,88]. Table 4 shows some examples of the successful inactivation of microorganisms with RF in different egg products. Geveke et al. [52,77] were able to pasteurize shell eggs using radio frequency, inactivating *S.* Typhimurium and *E. coli* without changes in egg quality. This research group improved the process to reduce the processing time further. The combination of RF plus hot water immersion and RF plus hot water spraying decreased processing time to 19.5 and 24.5 min, ensuring the five log-reduction of the *Salmonella* strain. The processes did not affect the quality and functionality of the egg [50].

In Table 4, there is a list of some examples in which RF has been effective in the inactivation of fungi. *Aspergillus* spp. and *Penicillium* spp. are some of the most studied microorganisms. Together with *Fusarium* and *Alternaria*, these species are responsible for forming mycotoxins. These secondary metabolites can be present in food and represent a high risk for human health [89]. Some products with a short shelf life because of fungi spores can be treated with RF without altering the quality attributes but decreasing the spore count. The inactivation of *Aspergillus* spp. and *Penicillium* spp. presented in Table 4 shows that the longest processing time was 15 min. *Monilinia* spp. is a fungi specie that causes significant crop losses, such as peaches and nectarines, and it was studied under RF. Brown rot is a postharvest disease caused by *Monilinia laxa* Honey and *M. fructicola* Honey. Sisquella et al. [90] studied the use of RF (27.12 MHz, 15 kW, 40 °C, 4.5 min) in peaches and nectarines inoculated with *M. fruticola.* After the treatment, the brown rot disease was reduced to less than 10%.

5. Disinfestation

Pest control is essential in the production chain of nuts, cereals, grains, legumes, and seeds. Insects are responsible for damaging these products because of web forming and direct feeding. The most common pests are the codling moth (*Cydia pomonella*), navel orangeworm (*Amyelois transitella*), Indianmeal moth (*Plodia interpunctella*), and red flour beetle (*Tribolium castaneum*) [91,92].

Chemicals to control food pests have been used during postharvest activities because they are cheap, fast, and accessible. Some of these chemicals, such as phosphine, are highly toxic to humans, representing a serious health risk, even if found in small food traces. Releasing some of these compounds into the atmosphere after being used for pest disinfestation also has adverse environmental effects. Other food practices to control insect pests include heat, which usually involves a long processing time.

RF has been reported as a successful technology inactivating insects as a postharvest intervention in food products. The first reports of the technology to control pests in food date almost 90 years ago [93]. In the last 20 years, much work has been conducted in this area with successful results and fundamental advances in equipment development.

The RF energy inactivates insects because of thermal damage to the insect structure's carbohydrates, proteins, DNA, RNA, and lipids [8]. This technology has been successfully tested for the disinfestation of fresh fruits like nectarine, peach, plum, cherries, apples, oranges, and persimmons; grains such as rice and wheat; legumes such as lentils, black-eyed peas, mung beans, soybeans; dried fruits and nuts such as chestnuts, walnuts, almonds, raisins, dates, apricots, figs, and prunes [8,9].

The use of RF offers a green alternative to eliminating insects in foods. The technology is contactless, chemical, and residue-free and an efficient option in disinfestation. Several

reports about the use of RF in insect control are available, showing the elimination of codling moths in cherries and apples, Mexican fruit flies in persimmons, rice weevil (*Sitophilus oryzae*) in milled rice, orangeworm (*Amyelois transitella*) in almonds, among others [94,95]. In Table 5, there are additional examples of insect disinfestation in food products; in all cases, the disinfestation was complete (100%).

Table 5. Examples of disinfestation in food products using radio frequency.

Product	Organism	Processing conditions	Disinfestation Level	Reference
Rapeseeds	Red flour beetle (*Tribolium castaneum*)	27.12 MHz, 1.5 kW, 80 °C	100%	[96]
Milled, rough, and brown rice	Rice weevil (*Sitophilus oryzae*)	27.12 MHz, 12 kW, 50 °C, 5 min	100%	[97]
Rough, brown, and milled rice	*Rhyzopertha dominica* (Fabricius)	27.12 MHz, 15 kW, 54 °C, 11 min	100%	[98]
Walnuts	Rice moth larvae (*Corcyra cephalonica* L.)	6.78 MHz, 13.56 MHz, 27.12 MHz, 40.68 MHz, 2 kW, 70–76 °C, 20 min	100%	[99]

As a technology for pest control, the main highlight of RF is the feasibility of using selective or differential heating [95]. As previously mentioned, RF uses dielectric heating to increase the temperature of the product. The two main mechanisms involved in this heating are ionic polarization and dipole rotation. However, selective heating increases the insects' temperature until they reach a fatal value but maintains moderate heating of the host material or food. This fact considerably reduces any thermal degradation effect on the food quality [93].

Wang et al. [100] studied the use of RF to disinfest in-shell walnuts. The main pests found in this product are the codling moth, Indianmeal moth, and navel orangeworm. The RF processing of in-shell walnuts was a short treatment of only 5 min (6 kW, 27.12 MHz, 55 °C) that was able to kill 100% of the most heat-resistant pest, the navel orangeworm. This study also included the analysis of rancidity, sensory attributes, and shell characteristics. There were no changes between the control sample and the RF-processed samples. This is a clear example of how RF can inactivate the pests but protect and preserve the quality of the product because of selective heating. RF also promotes more uniform heating for in-shell products like walnuts. During conventional heating processes, the shell produces an isolation effect on the kernel extending the processing time. In the case of RF, the heating is generated in the shell and the kernel simultaneously, reducing the processing time and allowing a more uniform treatment.

6. Food Quality

As previously mentioned, RF surged as an alternative to conventional thermal treatment to reduce the undesirable effects on quality. Most studies conducted with this novel technology included a detailed examination of quality attributes after processing. The quality of the product is not impacted during RF because of the different approaches used during processing, such as the movement of the development, change in electrodes, and change in packaging materials, among others. Some of these are summarized in this section.

Dragon fruit or pitaya was treated with RF, and several quality attributes were studied after processing and during the shelf life. Shen et al.'s [101] primary goal was to identify the best treatment regarding the gaps between the electrode plates of the system that had the minimum impact on the quality of dragon fruit slices. The treatment (6 kW, 27.12 MHz, 10 min, 70 °C) delayed some biochemical reactions and microbial growth for 2–3 days during storage. This product has a high moisture content (82.63%) which increases the rate of enzymatic activity and microbial growth. Some changes were observed in color. However, as in many other novel technologies, some bioactive compounds were increased after the treatment. In the case of dragon fruit, the total phenolics were increased after RF.

The main reason could be the new structure of the product after processing that allows for a more straightforward quantification of the phenolics, releasing these compounds from intercellular structures. A similar fact was observed when kiwi puree was treated with RF treatments (27.12 MHz, 10 kW). The process delayed microbial growth and improved the quality of the product. A higher concentration of vitamin C, total phenolic compounds, and antioxidant capacity was found after RF processing. The panelists preferred the RF-treated product rather than the thermal process in terms of sensory quality. The color was also better during seven weeks of storage for the RF-treated food [102].

A study is mentioned in Table 4 about the pasteurization of peanut butter sandwiches, a potentially challenging RTE product, because of its complex, heterogeneous nature. In this research, the inactivation of pathogens was conducted in chunky and creamy peanut butter cracker sandwiches using RF. However, there was also a comprehensive evaluation of the product after processing. The color was evaluated in peanut butter and the cracker surface after the longest processing time (27.12 MHz, 9 kW, 90 s), and no changes were detected using analytical techniques. Furthermore, a sensory panel was conducted with the control and processed samples to evaluate any possible flavor, texture, and overall acceptability changes. The results showed no significant differences between the control and RF-processed samples [78].

Liao et al. [103] studied RF as a processing aid to stabilize wheat germ. This product is a rich ingredient in proteins, carbohydrates, fatty acids, and tocopherols that needs to be stabilized to extend the shelf life. The main problems during storage are oxidative and hydrolytic enzymatic reactions. During the RF processing (12 kW, 27.12 MHz), lipase, peroxidase, polyphenol oxidase, and lipoxygenase were inactivated. The extracted oils showed peroxide and acid values stable during the first three days of storage (25 °C), and no changes were detected in the α-tocopherol, amino acid, or fatty acid content. The process was better when the wheat germ was processed with an initial moisture content of about 15%.

A similar study was conducted by Xu et al. [74] on buckwheat. The main goal was to inactivate the natural flora in this product using RF (27.12 MHz, 6 kW). The tested temperature was 70 to 90 °C, and the processing time did not exceed 20 min. The natural flora composed of mesophiles, *Enterobacteriaceae*, yeasts, and molds showed a high initial value (>6 logs). The RF treatment was able to inactivate about three log reductions of natural microflora. Buckwheat was also inoculated with pathogens (*S.* Typhimurium, *E. coli*, *C. sakazakii*, *B. cereus*), and the treatment also inactivated about four log-reduction of pathogens. The quality studies showed that color was not affected after the RF treatment, using the strongest temperature conditions, and nutrient loss was not detected in the product compared to control samples.

Ling et al. [104] improved the efficiency of RF equipment to disinfest pistachios. This research team was able to inactivate 100% of the Indianmeal moth in the product. They used an RF system (27.12 MHz, 6 kW) that could kill all the insects in just a few minutes. For the in-shell pistachios in a 1.8 kg bag, the disinfestation was achieved in 5.6 min. Meanwhile, for the pistachios, shelled in a 2 kg bag, the time was only 5.5 min. These processes were more efficient than conventional hot air processing, which took 82 and 117 min, respectively. The authors evaluated the stability of the product during the storage, and there were no significant differences between control and RF-treated samples. The evaluated parameters were weight loss, peroxide values, fatty acid composition, and kernel color. In a similar study with the same pest but in-shell walnuts, RF processing (27.12 MHz, 25 kW, 52 °C) could fully disinfest the product after 5 min. Two kinds of products were used, the unwashed and the air-dried walnuts packaged in a polyethylene container. Walnuts were studied over storage for 20 days at 35 °C, and no changes were observed in kernel color, peroxide, or fatty acid values. This storage under temperature abuse conditions is equivalent to 2 years of commercial storage at 4 °C [100].

RF can also be used to change the functionality of some biomolecules with a specific goal. These changes can be later used for novel product development or to improve the

functionality of some products during food processing. A detailed study on RF on soy protein isolate (SPI) dispersion observed some changes in the protein structure after processing. The treatment applied at 6 kW, 27.12 MHz, and 90 °C changed the hydrophobicity of the SPI, reducing its hydration. Studies showed that the tertiary and secondary structures were changed, but the primary structure remained intact. The SPI was self-reassembled from the coil to a β-sheet structure, modifying its functionality [105].

In general terms, RF is a technology with several uses in the food industry. The advantages of this novel thermal technology are numerous compared to the conventional thermal process, as has been mentioned in the text. Other emerging technologies such as microwave, ohmic heating, or induction heating are also potential technologies to replace the conventional thermal process in the future. Although the description of these technologies is out of the scope of this manuscript, it is worth mentioning that each technology has specific uses for certain food products. For example, RF and microwave follow a similar heating mechanism at different frequencies, but the penetration depth in the product is a decision point to choose between technologies.

7. Conclusions

RF has been widely studied in recent decades, offering an alternative to conventional thermal processing. Knowledge about the dielectric properties of very diverse products has been published. Without a doubt, as of today, the main hurdle in using this technology is the nonuniformity of the product. Poor uniform heating can reduce product quality and create a safety risk from the microbial point of view. Much research is now focused on improving processing equipment and process optimization to address this hurdle. The constant work together with packaging scientists is also filling those gaps that will allow processing the food using RF in pre-packed containers. Like other novel technologies, each food represents a diverse and complex material to study and characterize because of its shape, size, composition, and structure. Numerical simulation has become a powerful tool in studying and developing processes and equipment. The regulatory aspects of RF related to pasteurization need to be carefully reviewed to be approved as an official technology for this sole purpose. RF is a green technology for pasteurization and disinfestation that can achieve food safety targets without changing product quality.

Author Contributions: D.B.-A.: Conceptualization, investigation, writing the original draft. B.A.N.: Conceptualization, supervision, project administration, writing review, and editing. All authors have read and agreed to the published version of the manuscript.

Funding: This research has been funded through the project USDA-ARS CRIS 8072-41420-025, "Validation and Commercialization of Innovative Processing Technologies".

Institutional Review Board Statement: Not applicable.

Informed Consent Statement: Not applicable.

Data Availability Statement: Data is contained within the article.

Conflicts of Interest: The authors declare no conflict of interest.

Statement: The mention of trade names or commercial products in this article is solely for the purpose of providing specific information. It does not imply a recommendation or endorsement by the U.S. Department of Agriculture. USDA is an equal opportunity provider and employer.

References

1. C.D.C. Centers for Disease Control and Prevention. Available online: www.cdc.gov (accessed on 1 July 2022).
2. Liao, X.; Ma, Y.; Daliri, E.B.M.; Koseki, S.; Wei, S.; Liu, D.; Ye, X.; Chen, S.; Ding, T. Interplay of antibiotic resistance and food-associated stress tolerance in foodborne pathogens. *Trends Food Sci. Technol.* **2020**, *95*, 97–106. [CrossRef]
3. Valdramidis, V.P.; Geeraerd, A.H.; Bernaerts, K.; Van Impe, J.F. Microbial dynamics versus mathematical model dynamics: The case of microbial heat resistance induction. *Innov. Food Sci. Emerg.* **2006**, *7*, 80–87. [CrossRef]
4. Di Rosa, A.R.; Bressan, F.; Leone, F.; Falqui, L.; Chiofalo, V. Radio frequency heating on food of animal origin: A review. *Eur. Food Res. Technol.* **2019**, *245*, 1787–1797. [CrossRef]

5. Datta, A.K.; Davidson, P.M. Microwave and radio frequency processing. *J. Food Sci.* **2011**, *65* (Suppl. 8), 32–41. [CrossRef]
6. Nelson, S.O.; Trabelsi, S. Factors influencing the dielectric properties of agricultural and food products. *J. Microw. Power Electromagn. Energy* **2012**, *46*, 93–107. [CrossRef]
7. Mao, Y.; Wang, S. Recent developments in radio frequency drying for food and agricultural products using a multi-stage strategy: A review. *Crit. Rev. Food Sci.* **2023**, *63*, 2654–2671. [CrossRef]
8. Jiao, S.; Salazar, E.; Wang, S. Radiofrequency. In *Electromagnetic Technologies in Food Science*; Gomez-Lopez, V.M., Bhat, R., Eds.; John Wiley & Sons, Ltd.: West Sussex, UK, 2022; pp. 272–297. [CrossRef]
9. Chen, J.; Lau, S.K.; Chen, L.; Wang, S.; Subbiah, J. Modeling radio frequency heating of food moving on a conveyor belt. *Food Bioprod Process.* **2017**, *102*, 307–319. [CrossRef]
10. Al-Faruq, A.; Zhang, M.; Bhandari, B.; Azam, S.M.R.; Khatun, M.H.A. New understandings on how dielectric properties of fruit and vegetables are affected by heat-induced dehydration: A review. *Dry. Technol.* **2019**, *37*, 1780–1792. [CrossRef]
11. Birla, S.I.; Wang, S.; Tang, J.; Tiwari, G. Characterization of radio frequency heating of fresh fruits influenced by dielectric properties. *J. Food Eng.* **2008**, *89*, 390–398. [CrossRef]
12. Wang, S.; Tang, J.; Johnson, J.A.; Mitcham, E.; Hansen, J.D.; Hallman, G.; Drake, S.R.; Wang, Y. Dielectric properties of foods and insect pests as related to radio frequency and microwave treatments. *Biosyst. Eng.* **2003**, *85*, 201–212. [CrossRef]
13. Zhu, X.; Guo, W.; Wu, X. Frequency- and temperature-dependent dielectric properties of fruit juices associated with pasteurization by dielectric heating. *J. Food Eng.* **2012**, *109*, 258–266. [CrossRef]
14. Alfaifi, B.; Wang, S.; Tang, J.; Rasco, B.; Sablani, S.; Jiao, Y. Radio frequency disinfection treatments for dried fruit: Dielectric properties. *LWT–Food Sci. Technol.* **2013**, *50*, 746–754. [CrossRef]
15. Wang, S.; Monzon, M.; Gazit, Y.; Tang, J.; Mitcham, E.J.; Armstrong, J.W. Temperature dependent dielectric properties of selected subtropical and tropical fruits and associated insect pests. *Trans. ASAE* **2005**, *48*, 1–9. [CrossRef]
16. Zhou, X.; Li, R.; Lyng, J.G.; Wang, S. Dielectric properties of kiwifruit associated with a combined radio frequency vacuum and osmotic drying. *J. Food Eng.* **2018**, *239*, 72–82. [CrossRef]
17. Ferrari-John, R.S.; Katrib, J.; Palade, P.; Batchelor, A.R.; Dodds, C.; Kingman, S.W. A tool for predicting heating uniformity in industrial radio frequency processing. *Food Bioprocess Technol.* **2016**, *9*, 1865–1873. [CrossRef]
18. Guan, D.; Cheng, M.; Wang, Y.; Tang, J. Dielectric properties of mashed potatoes relevant to microwave and radio-frequency pasteurization and sterilization process. *J. Food Sci.* **2004**, *69*, FEP30–FEP37. [CrossRef]
19. Wang, J.; Luechapattanaporn, K.; Wang, Y.; Tang, J. Radio-frequency heating of heterogenous food- Meat lasagna. *J. Food Eng.* **2012**, *108*, 183–193. [CrossRef]
20. Lyng, J.G.; Zhang, L.; Bruton, N.P. A survey on the dielectric properties of meats and ingredients used in meat product manufacture. *Meat Sci.* **2005**, *69*, 589–602. [CrossRef]
21. Farag, K.W.; Lyng, J.G.; Morgan, D.J.; Cronin, D.A. Dielectric and thermophysical properties of different beef meat blends over a temperature range of −18 to +10 °C. *Meat Sci.* **2008**, *79*, 740–747. [CrossRef]
22. Basaran, P.; Basaran-Akgul, N.; Rasco, B.A. Dielectric properties of chicken and fish muscle treated with microbial transglutaminase. *Food Chem.* **2010**, *120*, 361–370. [CrossRef]
23. Wang, J.; Tang, J.; Wang, Y.; Swanson, B. Dielectric properties of egg whites and whole eggs as influenced by thermal treatments. *LWT–Food Sci. Technol.* **2009**, *42*, 1204–1212. [CrossRef]
24. Guo, W.; Trabelsi, S.; Nelson, S.O.; Jones, D.R. Storage effects on dielectric properties of eggs from 10 to 1800 MHz. *J. Food Sci.* **2007**, *72*, E335–E340. [CrossRef]
25. Muñoz, I.; Gou, P.; Picouet, P.A.; Barlabé, A.; Felipe, X. Dielectric properties of milk during ultra-heat treatment. *J. Food Eng.* **2018**, *219*, 137–146. [CrossRef]
26. Dag, D.; Singh, R.K.; Kong, F. Dielectric properties, effect of geometry, and quality changes of whole, nonfat milk powder and their mixtures associated with radio frequency heating. *J. Food Eng.* **2019**, *261*, 40–50. [CrossRef]
27. Guo, W.; Zhu, X.; Liu, H.; Yue, R.; Wang, S. Effects of milk concentration and freshness on microwave dielectric properties. *J. Food Eng.* **2010**, *99*, 344–350. [CrossRef]
28. Al-Holy, M.; Wang, Y.; Tang, J.; Rasco, B. Dielectric properties of salmon (*Oncorhynchus keta*) and sturgeon (*Acipenser transmontanus*) caviar at radio frequency (RF) and microwave (MW) pasteurization frequencies. *J. Food Eng.* **2005**, *70*, 564–570. [CrossRef]
29. Guo, W.; Xu, X.; Zhu, X.; Wang, S. Temperature-dependent dielectric properties of chestnut and chestnut weevil from 10 to 4500 MHz. *Biosyst. Eng.* **2011**, *110*, 340–347. [CrossRef]
30. Guo, W.; Tiwari, G.; Tang, J.; Wang, S. Frequency, moisture and temperature dependent dielectric properties of chickpea flour. *Biosyst. Eng.* **2008**, *101*, 217–224. [CrossRef]
31. Guo, W.; Wang, S.; Tiwari, G.; Johnson, J.A.; Tang, J. Temperature and moisture dependent dielectric properties of legume flour associated with dielectric heating. *LWT–Food Sci. Technol.* **2010**, *43*, 193–201. [CrossRef]
32. Ozturk, S.; Kong, F.; Trabelsi, S.; Singh, R.K. Dielectric properties of dried vegetable powders and their temperature profile during radio frequency heating. *J. Food Eng.* **2016**, *169*, 91–100. [CrossRef]
33. Lin, B.; Wang, S. Dielectric properties, heating rate, and heating uniformity of wheat flour with added bran associated with radio frequency treatments. *Innov. Food Sci. Emerg.* **2020**, *60*, 102290. [CrossRef]
34. Ling, B.; Lyng, J.G.; Wang, S. Radio-frequency treatment for stabilization of wheat germ: Dielectric properties and heating uniformity. *Innov. Food Sci. Emerg.* **2018**, *48*, 66–74. [CrossRef]

35. Liu, Y.; Tang, J.; Mao, Z. Analysis of bread dielectric properties using mixture equations. *J. Food Eng.* **2009**, *93*, 72–79. [CrossRef]
36. Gao, M.; Tang, J.; Johnson, J.A.; Wang, S. Dielectric properties of ground almond shells in the development of radio frequency and microwave pasteurization. *J. Food Eng.* **2012**, *112*, 282–287. [CrossRef]
37. Wang, Y.; Zhang, L.; Gao, M.; Tang, J.; Wang, S. Temperature- and moisture-dependent dielectric properties of Macadamia Nut Kernels. *Food Bioprocess Technol.* **2013**, *6*, 2165–2176. [CrossRef]
38. Zhang, S.; Zhou, L.; Ling, B.; Wang, S. Dielectric properties of peanuts kernels associated with microwave and radio frequency drying. *Biosyst. Eng.* **2016**, *145*, 108–117. [CrossRef]
39. Zhang, J.; Li, M.; Cheng, J.; Wang, J.; Ding, Z.; Yuan, X.; Zhou, S.; Liu, X. Effects of moisture, temperature, and salt content on the dielectric properties of pecan kernels during microwave and radio frequency drying processes. *Foods* **2019**, *8*, 385. [CrossRef]
40. Jeong, S.G.; Ryu, S.; Kang, D.H. Salt content dependent dielectric properties of pistachios relevant to radio-frequency pasteurization. *Sci. Rep.* **2019**, *9*, 2400. [CrossRef]
41. Ling, B.; Guo, X.; Hou, L.; Li, R.; Wang, S. The dielectric properties of pistachio kernels are influenced by frequency, temperature, moisture and salt content. *Food Bioprocess Technol.* **2015**, *8*, 420–430. [CrossRef]
42. Ozturk, S.; Kong, F.; Singh, R.K.; Kuzy, J.D.; Li, C.; Trabelsi, S. Dielectric properties, heating rate, and heating uniformity of various seasoning spices and their mixtures with radio frequency heating. *J. Food Eng.* **2018**, *228*, 128–141. [CrossRef]
43. Guo, W.; Zhu, X. Dielectric properties of red pepper powder related to radio frequency and microwave drying. *Food Bioprocess Technol.* **2014**, *7*, 3591–3601. [CrossRef]
44. Jiao, S.; Johnson, J.A.; Tang, J.; Tiwari, G.; Wang, S. Dielectric properties of cowpea weevil, black-eyed peas and mung beans with respect to the development of radio frequency heat treatments. *Biosyst. Eng.* **2011**, *108*, 280–291. [CrossRef]
45. Qi, S.; Han, J.; Lagnika, C.; Jiang, N.; Qian, C.; Liu, C.; Li, D.; Tao, Y.; Yu, Z.; Wang, L.; et al. Dielectric properties of edible fungi powder related to microwave and radio frequency drying. *Food Prod. Process. Nutr.* **2021**, *3*, 15. [CrossRef]
46. Guo, W.; Liu, Y.; Zhu, X.; Wang, S. Dielectric properties of honey adulterated with sucrose syrup. *J. Food Eng.* **2011**, *107*, 1–7. [CrossRef]
47. Farag, K.W.; Marra, F.; Lyng, J.G.; Morgan, D.J.; Cronin, D.A. Temperature changes and power consumption during radio frequency tempering of beef lean/fat formulations. *Food Bioprocess Technol.* **2010**, *3*, 732–740. [CrossRef]
48. Wang, S.; Llave, Y.; Kong, F.; Marra, F.; Erdoğdu, F. Update on emerging technologies including novel applications: Radio frequency. In *Food Engineering Innovations Across the Food Supply Chain*; Juliano, P., Buckow, R., Nguyen, M.H., Knoerzer, K., Sellahewa, J., Eds.; Academic Press: London, UK, 2022; pp. 163–186. [CrossRef]
49. Wang, S.; Monzon, M.; Johnson, J.A.; Mitcham, E.J.; Tang, J. Industrial scale-radio frequency treatments for insect control in walnuts I: Heating uniformity and energy efficiency. *Postharvest Biol. Technol.* **2007**, *45*, 240–246. [CrossRef]
50. Yang, Y.; Geveke, D.J. Shell egg pasteurization using radio frequency in combination with hot air or hot water. *Food Microbiol.* **2020**, *85*, 103281. [CrossRef]
51. Yang, Y.; Geveke, D.J.; Brunkhorst, C.D.; Sites, J.E.; Geveke, N.J.; Tilman, E.D. Optimization of the radio frequency power, time and cooling water temperature for pasteurization of *Salmonella* Typhimurium in shell eggs. *J. Food Eng.* **2019**, *247*, 130–135. [CrossRef]
52. Geveke, D.J.; Bigley, A.B.W.; Brunkhorst, C.D.; Jones, D.R.; Tilman, E.D. Improvement in the radio frequency method to pasteurize shell eggs by automation and cost reduction. *Int. J. Food Sci. Technol.* **2018**, *53*, 2500–2508. [CrossRef]
53. Zuo, Y.; Zhou, B.; Wang, S.; Hou, K. Heating uniformity in radio frequency treated walnut kernels with different size and density. *Innov. Food Sci. Emerg.* **2022**, *75*, 102899. [CrossRef]
54. Hao, Y.; Mao, Y.; Hou, L.; Wang, S. Developing a rotation device in radio frequency systems for improving the heating uniformity in granular foods. *Innov. Food Sci. Emerg.* **2021**, *72*, 102751. [CrossRef]
55. Guan, X.; Lin, B.; Xu, Y.; Yang, G.; Xu, J.; Zhang, S.; Li, R.; Wang, S. Recent developments in pasteurizing seeds and their products using radio frequency heating. *Int. J. Food Sci. Technol.* **2022**, *57*, 3223–3243. [CrossRef]
56. Huang, Z.; Marra, F.; Wang, S. A novel strategy for improving radio frequency heating uniformity of dry food products using computational modeling. *Innov. Food Sci. Emerg.* **2016**, *34*, 100–111. [CrossRef]
57. Jiao, Y.; Tang, J.; Wang, S. A new strategy to improve heating uniformity of low moisture foods in radio frequency treatment for pathogen control. *J. Food Eng.* **2014**, *141*, 128–138. [CrossRef]
58. Wang, Y.; Zhang, L.; Gao, M.; Tang, J.; Wang, S. Evaluating radio frequency heating uniformity using polyurethane foams. *J. Food Eng.* **2014**, *136*, 28–33. [CrossRef]
59. Huang, Z.; Zhu, H.; Yan, R.; Wang, S. Simulation and prediction of radio frequency heating in dry soybeans. *Biosyst. Eng.* **2015**, *129*, 34–47. [CrossRef]
60. Fellows, P.J. *Food Processing Technology*, 3rd ed.; Woodhead Publishing: Cambridge, UK, 2009; pp. 381–395. [CrossRef]
61. Zhang, S.; Lan, R.; Zhang, L.; Wang, S. Computational modelling of survival of *Aspergillus flavus* in peanut kernels during hot air-assisted radio frequency pasteurization. *Food Microbiol.* **2021**, *95*, 103682. [CrossRef]
62. Marx, G.; Moody, A.; Bermudez-Aguirre, D. A comparative study on the structure of *Saccharomyces cerevisiae* under nonthermal technologies: High hydrostatic pressure, pulsed electric field and thermo-sonication. *Int. J. Food Microbiol.* **2011**, *151*, 327–337. [CrossRef]

63. Akhila, P.P.; Sunooj, K.V.; Aaliya, B.; Navaf, M.; Sudheesh, C.; Sabu, S.; Sasidharan, A.; Mir, S.A.; George, J.; Khaneghah, A.M. Application of electromagnetic radiations for decontamination of fungi and mycotoxins in food products: A comprehensive review. *Trends Food Sci. Technol.* **2021**, *114*, 399–409. [CrossRef]
64. Xu, Y.; Li, R.; Li, K.; Yu, J.; Bai, J.; Wang, S. Inactivation of inoculated *Salmonella* and natural microflora on two kinds of edible seeds by radio frequency heating combined with cinnamon oil vapor. *LWT–Food Sci. Technol.* **2022**, *154*, 112603. [CrossRef]
65. Xu, Y.; Xu, J.; Yang, G.; Quan, X.; Li, R.; Wang, S. Combined effects of intermittent radio frequency heating with cinnamon oil vapor on microbial control and quality changes of alfalfa seeds. *Int. J. Food Microbiol.* **2022**, *367*, 109586. [CrossRef]
66. Ozturk, S.; Liu, S.; Xu, J.; Tang, J.; Chen, J.; Singh, R.K.; Kong, F. Inactivation of *Salmonella Enteritidis* and *Enterococcus faecium* NRRL B-2354 in corn flour by radio frequency heating with subsequent freezing. *LWT Food Sci. Technol.* **2019**, *111*, 782–789. [CrossRef]
67. Liu, S.; Ozturk, S.; Xu, J.; Kong, F.; Gray, P.; Zhu, M.J.; Sablani, S.S.; Tang, J. Microbial validation of radio frequency pasteurization of wheat flour by inoculated pack studies. *J. Food Eng.* **2018**, *217*, 68–74. [CrossRef]
68. Zhu, X.; Cui, Y.; Jiao, S.; Shi, X. Development of a pasteurization method based on radio frequency heating to ensure microbial safety of liquid egg. *Food Control* **2021**, *123*, 107035. [CrossRef]
69. Chen, L.; Wei, X.; Irmak, S.; Chaves, B.D.; Subbiah, J. Inactivation of *Salmonella enterica* and *Enterococcus faecium* NRRL B-2354 in cumin seeds by radiofrequency heating. *Food Control* **2019**, *103*, 59–69. [CrossRef]
70. Wei, X.; Lau, S.K.; Stratton, J.; Irmak, S.; Subbiah, J. Radiofrequency pasteurization process for inactivation of *Salmonella* spp. and *Enterococcus faecium* NRRL B-2354 on ground black pepper. *Food Microbiol.* **2019**, *82*, 388–397. [CrossRef]
71. Ozturk, S.; Kong, F.; Singh, R.K. Evaluation of *Enterococcus faecium* NRRL B-2354 as a potential surrogate of *Salmonella* in packaged paprika, white pepper and cumin powder during radio frequency heating. *Food Control* **2020**, *10*, 106833. [CrossRef]
72. Tong, T.; Wang, P.; Shi, H.; Li, F.; Jiao, Y. Radio frequency inactivation of *E. coli* O157: H7 and *Salmonella Typhimurium* ATCC 14028 in black pepper (*piper nigrum*) kernels: Thermal inactivation kinetic study and quality evaluation. *Food Control* **2022**, *132*, 108553. [CrossRef]
73. Verma, T.; Chaves, B.D.; Irmak, S.; Subbiah, J. Pasteurization of dried basil leaves using radio frequency heating: A microbial challenge study and quality analysis. *Food Control* **2021**, *124*, 107932. [CrossRef]
74. Xu, Y.; Yang, G.; Li, R.; Xu, Y.; Lin, B.; Wang, S. Effects of radio frequency heating on microbial populations and physiochemical properties of buckwheat. *Int. J. Food Microbiol.* **2022**, *363*, 109500. [CrossRef]
75. Ballom, K.; Dhowlaghar, N.; Tsai, H.C.; Yang, R.; Tang, J.; Zhu, M.J. Radiofrequency pasteurization against *Salmonella* and *Listeria monocytogenes* in cocoa powder. *LWT–Food Sci. Technol.* **2021**, *145*, 111490. [CrossRef]
76. Li, R.; Kou, X.; Cheng, T.; Zheng, A.; Wang, S. Verification of radio frequency pasteurization process for in-shell almonds. *J. Food Eng.* **2017**, *192*, 103–110. [CrossRef]
77. Geveke, D.J.; Bigley, A.B.W.; Brunkhorst, C.D. Pasteurization of shell eggs using radio frequency heating. *J. Food Eng.* **2017**, *193*, 53–57. [CrossRef]
78. Ha, J.W.; Kim, S.Y.; Ryu, S.R.; Kang, D.H. Inactivation of *Salmonella enterica* serovar Typhimurium and *Escherichia coli* O157:H7 in peanut butter cracker sandwiches by radio frequency heating. *Food Microbiol.* **2013**, *34*, 145–150. [CrossRef]
79. Kim, S.Y.; Sagong, H.G.; Choi, S.H.; Ryu, S.; Kang, D.H. Radio frequency heating to inactivate *Salmonella* Typhimurium and *Escherichia coli* O157:H7 on black and red pepper spice. *Int. J. Food Microbiol.* **2012**, *153*, 171–175. [CrossRef]
80. Nagaraj, G.; Purohit, A.; Harrison, M.; Singh, R.; Hung, Y.C.; Mohan, A. Radiofrequency pasteurization of inoculated ground beef homogenate. *Food Control* **2016**, *59*, 59–67. [CrossRef]
81. Zhang, Y.; Xie, Y.; Chen, Y.; Pandiselvam, R.; Liu, Y. Surface free fat bridging contributes to the stickiness of powdered infant formula milk pasteurized by radio frequency dry heat treatment. *J. Food Eng.* **2022**, *323*, 111001. [CrossRef]
82. Al-Holy, M.; Ruiter, J.; Lin, M.; Kang, D.H.; Rasco, B. Inactivation of *Listeria innocua* in nisin- treated salmon (*Oncorhynchus keta*) and Sturgeon (*Acipenser transmontanus*) caviar heated by radio frequency. *J. Food Prot.* **2004**, *67*, 1848–1854. [CrossRef]
83. Jiao, S.; Zhong, Y.; Deng, Y. Hot air-assisted radio frequency heating effects on wheat and corn seeds: Quality change and fungi inhibition. *J. Stored Prod. Res.* **2016**, *69*, 265–271. [CrossRef]
84. Zheng, A.; Zhang, L.; Wang, S. Verification of radio frequency pasteurization treatment for controlling *Aspergillus parasiticus* on corn grain. *Int. J. Food Microbiol.* **2017**, *249*, 27–34. [CrossRef]
85. Liu, Y.; Tang, J.; Mao, Z.; Mah, J.H.; Jiao, S.; Wang, S. Quality and mold control of enriched white bread by combined radio frequency and hot air treatment. *J. Food Eng.* **2011**, *104*, 492–498. [CrossRef]
86. Hou, L.; Kou, X.; Li, R.; Wang, S. Thermal inactivation of fungal in chestnuts by hot air assisted radio frequency treatments. *Food Control* **2018**, *93*, 297–304. [CrossRef]
87. Awuah, G.B.; Ramaswamy, H.S.; Economides, A.; Mallikarjunan, K. Inactivation of *Escherichia coli* K12 and *Listeria innocua* in milk using radio frequency heating. *Innov. Food Sci. Emerg.* **2005**, *6*, 396–402. [CrossRef]
88. Boreddy, S.R.; Subbiah, J. Temperature and moisture dependent dielectric properties of egg white powder. *J. Food Eng.* **2016**, *168*, 60–67. [CrossRef]
89. Deng, L.Z.; Sutar, P.P.; Mujumdar, A.S.; Tao, Y.; Pan, Z.; Liu, Y.H.; Xiao, H.W. Thermal decontamination technologies for microorganisms and mycotoxins in low-moisture foods. *Annu. Rev. Food Sci. Technol.* **2021**, *12*, 287–305. [CrossRef]
90. Sisquella, M.; Viñas, I.; Picouet, P.; Torres, R.; Usall, J. Effect of host and *Monilinia* spp. variables on the efficacy of radio frequency treatment on peaches. *Postharvest Biol. Technol.* **2014**, *87*, 6–12. [CrossRef]

91. Martinez-Sastre, R.; Peña, R.; González-Ibáñez, A.; García, D.; Miñarro, M. Top-down and bottom-up regulation of codling moth populations in cider apple orchards. *Crop Prot.* **2021**, *143*, 105545. [CrossRef]
92. Gao, M.; Tang, J.; Wang, Y.; Powers, J.; Wang, S. Almond quality as influenced by radio frequency heat treatments for disinfestation. *Postharvest Biol. Technol.* **2010**, *58*, 225–231. [CrossRef]
93. Macana, R.J.; Baik, O.D. Disinfestation of insect pests in stored agricultural materials using microwave and radio-frequency heating: A review. *Food Res. Int.* **2018**, *34*, 483–510. [CrossRef]
94. Zhou, L.; Ling, B.; Zheng, A.; Zhang, B.; Wang, S. Developing radio frequency technology for postharvest insect control in milled rice. *J. Stored Prod. Res.* **2015**, *62*, 22–31. [CrossRef]
95. Wang, S.; Tang, J.; Johnson, J.A.; Cavalieri, R.P. Heating uniformity and differential heating of insects in almonds associated with radio frequency energy. *J. Stored Prod. Res.* **2013**, *55*, 15–20. [CrossRef]
96. Yu, D.; Shrestha, B.; Baik, O.D. Radio frequency (RF) control of red flour beetle (*Tribolium castaneum*) in store rapeseeds (*Brassica napus* L.). *Biosyst. Eng.* **2016**, *151*, 248–260. [CrossRef]
97. Jiao, S.; Sun, W.; Yang, T.; Zou, Y.; Zhu, X.; Zhao, Y. Investigation of the feasibility of radio frequency energy for controlling insects in milled rice. *Food Bioprocess Technol.* **2017**, *10*, 781–788. [CrossRef]
98. Hou, L.; Liu, Q.; Wang, S. Efficiency of industrial-scale radio frequency treatments to control *Rhyzopertha dominica* (Fabricius) in rough, brown and milled rice. *Biosyst. Eng.* **2019**, *186*, 246–258. [CrossRef]
99. Mao, Y.; Wang, P.; Wu, Y.; Hou, L.; Wang, S. Effects of various radio frequencies on combined drying and disinfestation treatments for in-shell walnuts. *LWT–Food Sci. Technol.* **2021**, *144*, 111246. [CrossRef]
100. Wang, S.; Monzon, M.; Johnson, J.A.; Mitcham, E.J.; Tang, J. Industrial scale-radio frequency treatments for insect control in walnuts II: Insect mortality and product quality. *Postharvest Biol. Technol.* **2007**, *45*, 247–253. [CrossRef]
101. Shen, Y.; Zheng, L.; Gou, M.; Xia, T.; Li, N.; Song, X.; Jiang, H. Characteristics of pitaya after radio frequency treating: Structure, phenolic compounds, antioxidant, and antiproliferative activity. *Food Bioprocess Technol.* **2020**, *13*, 180–186. [CrossRef]
102. Lyu, X.; Peng, X.; Wang, S.; Yang, B.; Wang, X.; Yang, H.; Xiao, Y.; Baloch, A.B.; Xia, X. Quality and consumer acceptance of radio frequency and traditional heat pasteurized kiwi puree during storage. *Int. J. Food Sci. Technol.* **2018**, *53*, 209–218. [CrossRef]
103. Liao, N.; Damayanti, W.; Zhao, Y.; Xu, X.; Zheng, Y.; Wu, J.; Jiao, J. Hot air-assisted radio frequency treatment effects on physicochemical properties, enzyme activities and nutritional quality of wheat germ. *Food Bioprocess Technol.* **2020**, *13*, 901–910. [CrossRef]
104. Ling, B.; Hou, L.; Li, R.; Wang, S. Storage stability of pistachios as influenced by radio frequency treatments for postharvest disinfestation. *Innov. Food Sci. Emerg.* **2016**, *33*, 357–364. [CrossRef]
105. Guo, C.; Zhang, Z.; Chen, J.; Fu, H.; Subbiah, J.; Chen, X.; Wang, Y. Effects of radio frequency heating treatment on structure changes of soy protein isolate for protein modification. *Food Bioprocess Technol.* **2017**, *10*, 1574–1583. [CrossRef]

MDPI AG
Grosspeteranlage 5
4052 Basel
Switzerland
Tel.: +41 61 683 77 34

Foods Editorial Office
E-mail: foods@mdpi.com
www.mdpi.com/journal/foods

Academic Open
Access Publishing

mdpi.com

ISBN 978-3-7258-4344-2